

**I. SYNTHESIS, REACTIVITY, STRUCTURE AND APPLICATION OF
SPIROEPOXY- β -LACTONES: STUDIES TOWARD (-)-MACULALACTONE A
II. METAL MEDIATED COUPLINGS OF DICHLOROOLEFINS APPLICABLE
TO THE HATERUMALIDES**

A Dissertation

by

RICHARD JEFFREY DUFFY

Submitted to the Office of Graduate Studies of
Texas A&M University
in partial fulfillment of the requirements for the degree of

DOCTOR OF PHILOSOPHY

December 2007

Major Subject: Chemistry

**I. SYNTHESIS, REACTIVITY, STRUCTURE AND APPLICATION OF
SPIROEPOXY- β -LACTONES: STUDIES TOWARD (-)-MACULALACTONE A
II. METAL MEDIATED COUPLINGS OF DICHLOROOLEFINS APPLICABLE
TO THE HATERUMALIDES**

A Dissertation

by

RICHARD JEFFREY DUFFY

Submitted to the Office of Graduate Studies of
Texas A&M University
in partial fulfillment of the requirements for the degree of

DOCTOR OF PHILOSOPHY

Approved by:

Chair of Committee,	Daniel Romo
Committee Members,	David Bergbreiter
	Brian Connell
	Stephen Safe
Head of Department,	David Russell

December 2007

Major Subject: Chemistry

ABSTRACT

I. Synthesis, Reactivity Structure and Application of Spiroepoxy- β -lactones: Studies
Toward (-)-Maculalactone A II. Metal Mediated Couplings of Dichloroolefins

Applicable to the Haterumalides. (December 2007)

Richard Jeffrey Duffy, B. S.; B. S., University of Oklahoma

Chair of Advisory Committee: Dr. Daniel Romo

Marine natural products have continued to be a source of compounds with interesting structures and biological activities. Two such compounds are maculalactone A and haterumalide NA. In the process of exploring a route to the synthesis of haterumalide NA, the novel ring system, spiroepoxy- β -lactones were discovered. Spiroepoxy- β -lactones were synthesized by the oxidation of ketene-homo dimers with dimethyldioxirane (DMDO). After a synthetic route to this ring system was obtained we next explored the varied reactivity of spiroepoxy- β -lactones, and it was apparent that they might be applied to the synthesis of maculalactone A.

Also with the aim of the total synthesis of the haterumalides, a palladium catalyzed cross coupling was developed. This reaction couples a 1,1-dichloroolefin with an alkyl zinc reagent. It was found that this reaction necessitates a heteroatom on the zinc reagent in order to proceed.

DEDICATION

In Memory of my Father

ACKNOWLEDGEMENTS

I would like to thank my advisor Professor Daniel Romo, for his guidance and giving me a project that has continually kept me on my toes.

I would like to thank Professor David Bergbeiter for his insightful lectures during my first year. I would also like to thank Professors Brian Connell and Stephen Safe for their time and graciously serving on my committee.

I would like to thank all Romo group members past and present. I would especially like to thank, Andy Mitchell, Kay Morris, and Changsuk Lee for their helpful discussions and being a continual source of support throughout my graduate career. I would like to thank Henry Nguyen for his late night discussions of chemistry, continual laughter, and for his friendship. I would also like to thank Karine Poullenec for helpful insights and fun times even when she is across the Pond. For my best friend Aurore Loudet who if it were not for graduate school I would have not met such a fun, and supportive person. Also I would like to thank Carré Zalma and Joe Grill for the late night games of Monopoly and making my stay in College Station all the more enjoyable.

Finally, I would like to thank my mom, my sisters Kerri and Erin and my brother Greg for their undying support in all my endeavors. Without them it would have made this journey all the more difficult.

TABLE OF CONTENTS

	Page
ABSTRACT	iii
DEDICATION	iv
ACKNOWLEDGEMENTS	v
TABLE OF CONTENTS	vi
LIST OF FIGURES.....	ix
LIST OF TABLES	x
 CHAPTER	
I INTRODUCTION: THE SYNTHESIS OF UNUSUAL STRAINED SPIRO RING SYSTEMS AND THEIR EXPLOITS IN SYNTHESIS	1
Oxaspiro[2.2]pentanes	1
1,4-Dioxaspiro[2.2]pentanes	15
1-Oxaspiro[2.3]hexanes	25
4-Oxaspiro[2.3]hexanes	33
1,5-Dioxaspiro[3.2]hexanes	36
II STUDIES TOWARD THE HATERUMALIDES: THE SYNTHESIS AND STRUCTURE OF SPIROEPOXY- β -LACTONES	41
Isolation and Biological Activity of the Haterumalides.....	41
Previous Syntheses of Haterumalide NA	42
Retrosynthetic Analysis of the Haterumalides	49
Model Studies Toward the Oxidation of Ketene-Homo Dimers.....	51
Conclusions	56

CHAPTER	Page
III	A SURVEY OF THE REACTIVITY OF SPIROEPOXY- β -
	LACTONES AND STUDIES TOWARD MACULALACTONE A .. 58
	Introduction 58
	Isolation and Biological Activity of the Maculalactones 68
	Previous Syntheses of Maculalactone A 69
	Retrosynthesis of Maculalactone A..... 71
	Coupling Route to Maculalactone A..... 71
IV	TRANS-SELECTIVE CROSS COUPLING OF 1,1-
	DICHLOROALKENES 74
	Introduction 74
	Optimization of the Coupling..... 76
	Attempted Synthesis of Diene 2.52..... 83
	Alternate Retrosynthesis of Diene 2.52..... 85
	Synthesis of Diene 2.52..... 86
	Synthesis of a Model Coupling Partner..... 86
	Conclusions 88
V	CONCLUSIONS 89
	REFERENCES..... 91
	APPENDIX A EXPERIMENTAL PROCEDURES AND SELECTED
	SPECTRA 99
	APPENDIX B SINGLE CRYSTAL X-RAY DATA FOR
	β -LACTONE 2.64a 192
	APPENDIX C SINGLE CRYSTAL X-RAY STRUCTURE OF
	TETRONATE 3.20 204
	APPENDIX D SINGLE CRYSTAL X-RAY STRUCTURE OF
	TRIFLATE 3.55 210

	Page
APPENDIX E SINGLE CRYSTAL X-RAY STRUCTURE OF	
DIOL 4.22	219
VITA	227

LIST OF FIGURES

	Page
Figure 1.1 Structure of equilenin (1.46)	11
Figure 2.1 Structures of the haterumalides	41
Figure 3.1 ^{13}C NMR spectral expansion of carbinol region of α -hydroxy ketone 3.12	62
Figure 3.2 Structures of maculalactones A-M (3.32-3.44)	69
Figure 4.1 Structure of Z-chloro-dialkyl-alkene containing natural products.....	75
Figure 4.2 X-ray structure of diol 4.29	85

LIST OF TABLES

	Page
Table 2.1 Exploration of Epoxidation Conditions of Ketene-Homo Dimers....	52
Table 2.2 Substrate Scope of the Epoxidation of Ketene-Homo Dimers.....	53
Table 2.3 X-ray Structure of Spiroepoxy- β -Lactone 2.64a and Selected Bond Lengths	54
Table 2.4 Observed and Calculated Bond Lengths (\AA) for Spiroepoxy- β -Lactone 2.64a and Related Ring Systems	55
Table 4.1 Optimization of Reaction Temperature for Coupling of 4.8 and 4.10	79
Table 4.2 Optimization of Reaction Time for Coupling of 4.8 and 4.10 by Microwave Heating	79
Table 4.3 Varying the Equivalents of Zinc Reagent for the Coupling of 4.8 and 4.10 by Microwave Heating	80
Table 4.4 Scope of the Coupling of Model 1,1-Dichloroolefins 4.12 and 4.8 with Various Alkyl Zinc Reagents	82

CHAPTER I

INTRODUCTION: THE SYNTHESIS OF UNUSUAL STRAINED SPIRO RING SYSTEMS AND THEIR EXPLOITS IN SYNTHESIS

Small ring compounds have continually fascinated chemists due to their unusual structures, and the reactions that are made possible due to the inherent ring strain of these compounds. Isolated small strained carbocyclic and heterocyclic rings have been known for quite some time, as of late there have been a number of new spiro-heterocycles described. Specifically, the utility of oxa- and dioxo-spiropentanes and spirohexanes has been demonstrated for the synthesis of natural and unnatural products. These ring systems investigated have shown varied and interesting reactivity due to the unique physical properties of these small rings. The aim of this review is to provide an overview of the synthesis and reactivity of small strained spiro-heterocycles and to illustrate their applications in synthesis. This review will be restricted to spiro-ring systems since other strained systems have been reviewed previously.^{1, 2}

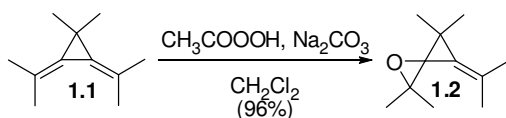
Oxaspiro[2.2]pentanes

The first and simplest of these spirocycles, oxaspiro[2.2]pentanes, is also the oldest in the group with confirmed syntheses dating back to 1968.³ These spiro systems were initially synthesized by the action of peracetic acid on unsaturated cyclopropane derivative **1.1** to give oxaspiro[2.2]pentane **1.2** (Scheme 1.1). This method proved to be quite general, as the substrate can be made by olefination of the corresponding carbonyl compounds with cyclopropyl phosphonium ylides. However, this method suffers from

This dissertation follows the style of *Journal of the American Chemical Society*.

only modest selectivity requiring an appropriate directing group (*i.e.* ether).⁴ After this first synthesis, several other methods were devised for the synthesis of oxaspiro[2.2]pentanes. These methods include addition of lithiated bromocyclopropanes,⁵ and diazocompounds to ketones,⁶ reaction of singlet oxygen with bicyclopopylidene,^{7, 8} selenone additions to ketones,⁹ and the addition of cyclopropyl sulfur ylides to carbonyl compounds.^{10, 11}

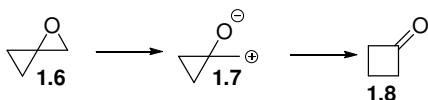
Scheme 1.1. First Synthesis of an Oxaspiro[2.2]pentane.



By far the most widely used and arguably the most selective synthesis of oxaspiro[2.2]pentanes remains to be the addition of cyclopropyl sulfoxonium ylides to carbonyl compounds. This particular method has several advantages over the previously developed methods in that the reaction conditions are relatively mild and the addition is quite diastereoselective.¹² Through a series of elegant studies it was determined that the ylide addition proceeds *via* equatorial attack at the carbonyl carbon, in cyclic compounds. While this process is highly diastereoselective, there has yet to be an enantioselective process developed. Johnson reported chiral sulfoximine ylide additions to α,β -unsaturated carbonyl compounds, however the racemic counterpart performed poorly with simple carbonyl compounds such as the reaction of cyclohexanone **1.3** with sulfoximine ylide **1.4** to yield oxaspiro[2.2]pentane **1.5** and thus the chiral series was not attempted (Scheme 1.2).¹³

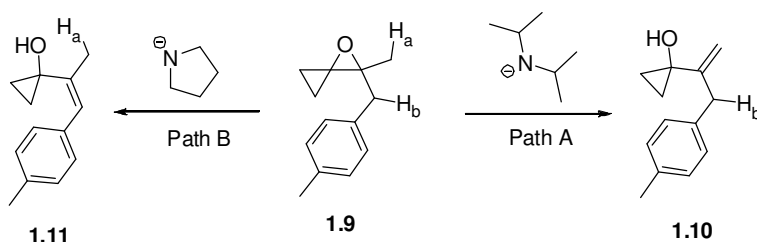
Scheme 1.2. Reaction of Sulfoximines with Cyclohexanone.

Oxaspiro[2.2]pentanes display two primary modes of reactivity. One mode, leading to a cyclobutanone, appears to be driven by the release of the strain energy of the ring system (Scheme 1.3).¹² However, this is not entirely satisfactory, as cyclobutanes possess essentially the same amount of strain energy as cyclopropanes, 26 kcal/mol and 28 kcal/mol respectively, due to the eclipsing interactions of the substituents of a cyclobutane.¹⁴ Alternatively, the ring expansion of a cyclopropane to a cyclobutane proceeds when appropriate functionalization is present, such as with oxaspiro[2.2]pentanes **1.6**. Ionization of the epoxide, either by addition of a Lewis acid or thermally induced, would yield a highly stabilized intermediate cyclopropylcarbinyl cation **1.7**. This type of cation is uniquely stabilized due to the π -character of the σ -bonds in cyclopropanes, and consequently they undergo a pinacol like rearrangement to cyclobutanone **1.8**. This process is favorable due to the release of ring strain of the starting epoxide and cyclopropane in addition to the formation of a C=O bond.

Scheme 1.3. Rearrangement of Oxaspiro[2.2]pentane to Cyclobutanone.

The second major mode of reactivity of oxaspiro[2.2]pentanes is their base induced elimination to form vinyl cyclopropanes. This particular transformation is driven by the relief of ring strain upon opening of the epoxide. Trost developed conditions allowing access to both regioisomeric products **1.10** and **1.11** from spiroepoxide **1.9** (Scheme 1.4).^{15, 16} Use of the more hindered base, lithium diisopropylamide, led to deprotonation of oxaspiro[2.2]pentane **1.9** at the more accessible H_a (Path A) to yield olefine **1.10**. Use of the less sterically demanding lithium amide of pyrrolidine leads to deprotonation of less sterically accessible H_b (Path B) which gave the more substituted and conjugated olefin **1.11**.

Scheme 1.4. Base Induced Elimination of a Oxaspiro[2.2]pentane to form Vinyl Cyclopropanes.

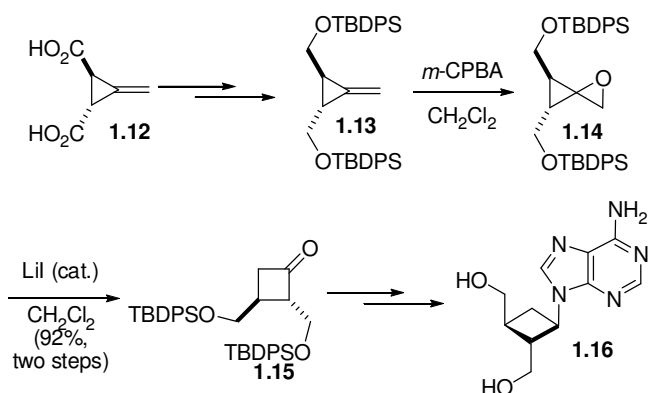


This ring system has proven to be a useful intermediate in a number of syntheses of natural and unnatural products. Since their last review¹² oxaspiro[2.2]pentanes have continued to be valuable in the synthesis of other complex architectures. This ring system has proved to be valuable for both the synthesis of new ligands, natural and unnatural products.

The first application of oxaspiro[2.2]pentanes is in the synthesis of carbocyclic analogues of the antibiotic/antiviral natural product oxetanocin (Scheme 1.5).¹⁷ Hsiao's synthesis hinges on the construction of an optically active cyclobutanone **1.15**. Their

approach to this ring system hinges on building an appropriate oxaspiro[2.2]pentane and its subsequent rearrangement to the corresponding cyclobutanone. The synthesis begins with Feist's acid **1.12** which is resolved utilizing quinine. After resolution and a series of standard manipulations, they are able to obtain methylene cyclopropane **1.13** in good overall yield. The substrate is now setup for the key oxidation/rearrangement sequence. This is accomplished by exposing methylene cyclopropane **1.13** to *meta*-chloroperbenzoic acid (*m*-CPBA) and then subsequent rearrangement of the oxaspiro[2.2]pentane **1.14** with catalytic lithium iodide to give key cyclobutanone **1.15** in excellent yield over the two steps. By use of a C₂ symmetric substrate selectivity issues are bypassed in the oxidation step. Cyclobutanone **1.15** could then be transformed into carbocyclic oxetanocin analogue **1.16**.

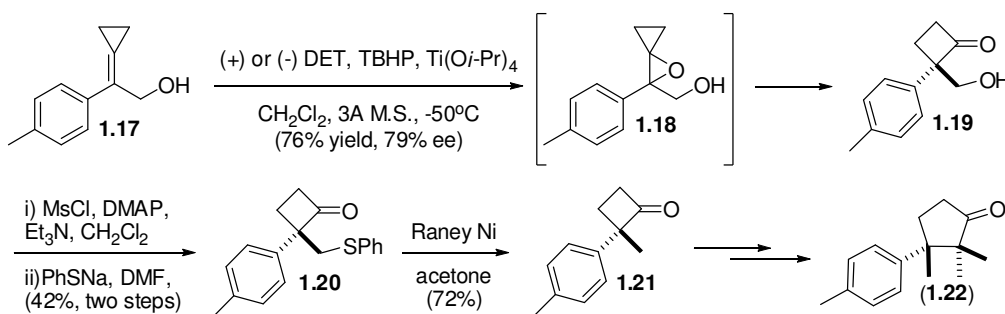
Scheme 1.5. Synthesis of a Carbocyclic Oxetanocin Analogue.



In addition to diastereoselective methods, enantioselective epoxidation methods have also proven to be effective in yielding optically active oxaspiro[2.2]pentanes in some cases. This was applicable to the synthesis of both enantiomers of the sesquiterpene natural product α -cuparenone (Scheme 1.6).¹⁸ The synthesis of either

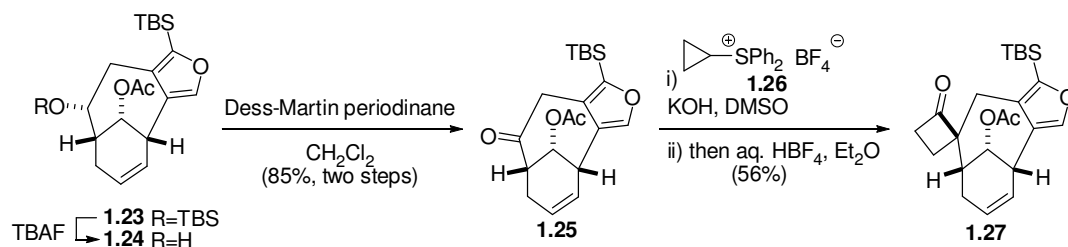
enantiomer of α -cuparenone begins with epoxidation of cyclopropene **1.17** under Sharpless conditions resulting in an aryl substituted oxaspiro[2.2]pentane **1.18** that rearranges to cyclobutanone **1.19** in modest yield and enantiomeric excess. The primary alcohol is then converted to phenylsulfide **1.20** utilizing a two step protocol. The cyclobutanone **1.20** is then desulfurated by the action of Raney nickel in acetone to yield methyl-cyclobutanone **1.21** in good yield. This represents a formal total synthesis of α -cuparenone (**1.22**) as this is a common intermediate in a previous synthesis.¹⁹

Scheme 1.6 Synthesis of α -Cuparenone.



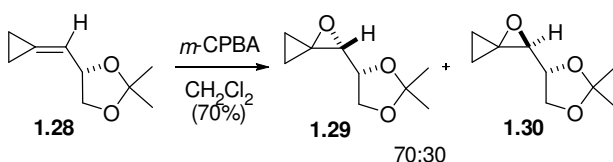
Perhaps one of the more complex uses of a oxaspiro[2.2]pentane is an elegant model study toward the synthesis of the architecturally intriguing natural products CP-225,917 and CP-263,114.^{20, 21} After several steps cyclohexenone can be transformed into the advanced furan intermediate **1.23**, which then undergoes silyl-deprotection to alcohol **1.24** and subsequent oxidation to ketone **1.25** (Scheme 1.7). Ketone **1.25** provides a springboard to cyclobutanone **1.27** through the addition of cyclopropyl sulfonium tetrafluoroborate **1.26** and rearrangement to the cyclobutanone **1.27** under acidic conditions. This sequence depicts one of the most complicated substrates utilized in the Trost cyclobutanone synthesis.

Scheme 1.7. Model Studies Toward the Synthesis of CP-225,917 and CP-263,114.



The diastereoselective synthesis of both the acetogenin natural product muricatacin and the pheromone japonilure have also been accomplished by the utilization of an oxaspiro[2.2]pentane as one of the intermediates.²² The first key reaction is the oxidation of methylene cyclopropane **1.28** to the corresponding oxaspiro[2.2]pentanes **1.29** and **1.30**. The diastereoselectivity of this reaction proves to only be modest giving a 70:30 mixture of diastereomers (Scheme 1.8).

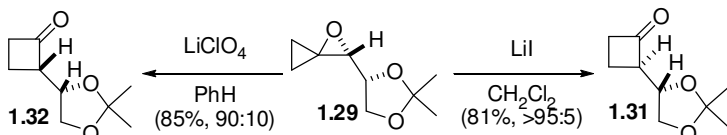
Scheme 1.8. Diastereoselective Oxidation of Methylene Cyclopropane **1.28**.



With oxaspiro[2.2]pentane **1.29** in hand, the next key reaction was the rearrangement to the cyclobutanone **1.31** (Scheme 1.9). This reaction proved to be challenging, in that the identity of the Lewis acid proved to be key for the selectivity of the outcome of the reaction as has been previously noted.²³ However, under the optimized conditions of lithium iodide in dichloromethane the reaction proved to be essentially selective for the desired diastereomer. Interestingly, the other undesired

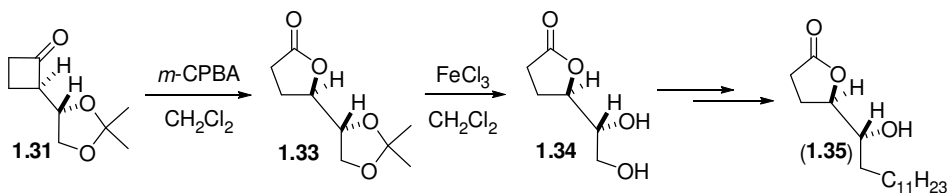
diastereomer **1.32** could be obtained in good selectivity by using lithium perchlorate in place of lithium iodide hinting at a change in mechanism when lithium perchlorate is used.

Scheme 1.9. Rearrangement of Oxaspiro[2.2]pentane **1.29**.

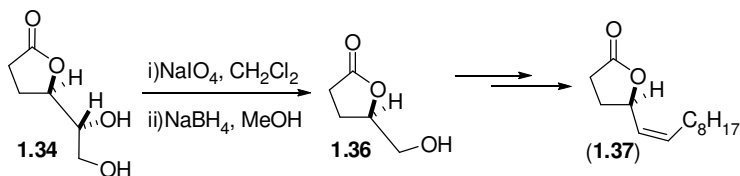


After having accomplished the key oxidation-rearrangement reaction sequence, the subsequent steps toward the formal syntheses of muricatacin and japonilure are rather straightforward (Scheme 1.10). Baeyer-Villiger oxidation of the cyclobutanone **1.31** to the corresponding γ -lactone **1.33** followed by deprotection of the acetonide to give diol **1.34**, provided a common intermediate in two syntheses of muricatacin (**1.35**).^{24, 25}

Scheme 1.10. Formal Synthesis of Muricatacin.

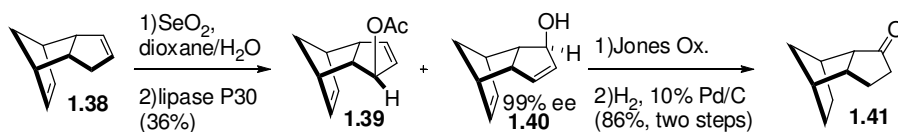


Alternatively, diol **1.34** can be oxidatively cleaved to the aldehyde (Scheme 1.11). This unstable aldehyde is then reduced to the alcohol **1.36**. This represents a formal synthesis of japonilure (**1.37**).²⁶

Scheme 1.11. Formal Synthesis of Japonilure.

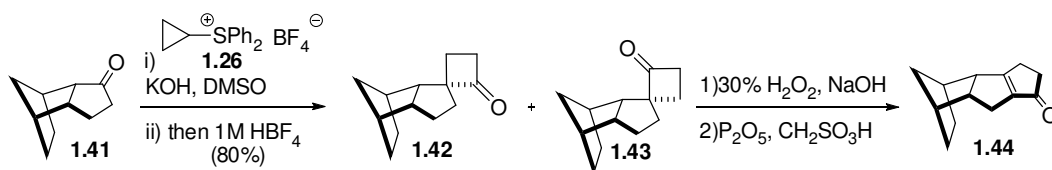
Not only have oxaspiro[2.2]pentanes found application in synthesis of natural and unnatural products but they have found application in the synthesis of structurally interesting compounds, *i.e.* polyspiranes, and ligands for catalysis. While polyspiranes have been the subject of previous reviews² and will therefore not be discussed, the later has not been included. Although only an isolated synthesis exists, it illustrates the broad ranging applicability of this ring system and will be mentioned.

Paquette showed that oxaspiro[2.2]pentanes can be applied in different arenas besides total synthesis. This is exemplified in its utilization in the synthesis of a new set of chiral cyclopentadienide ligands.²⁷ Paquette's synthesis of these new chiral cyclopentadienide ligands begins with dicyclopentadiene **1.38**, first by oxidation with selenium dioxide and then resolution with lipase P30 to give alcohol **1.40** along with acetate **1.39** in high optical purity. This is followed by Jones oxidation of the alcohol to the corresponding α,β -ketone and subsequent reduction to the saturated ketone **1.41** (Scheme 1.12).

Scheme 1.12. Synthesis of Ketone **1.41**.

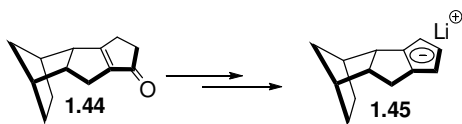
Ketone **1.41** is then subjected to the Trost cyclobutanone synthesis conditions by exposure to cyclopropyl diphenyl sulfoxonium tetrafluoroborate **1.26** under basic conditions (Scheme 1.13). Subsequent rearrangement with aqueous acid yields an inconsequential mixture of cyclobutanones **1.42** and **1.43**. The mixture of cyclobutanones **1.42** and **1.43** are then oxidized to the γ -lactones and exposed to the combination of phosphorous pentoxide and methane sulfonic acid to yield the α,β -unsaturated ketone **1.44**.

Scheme 1.13. Synthesis of Ketone **1.44**.



The completed synthesis of the cyclopentadienide ligand was accomplished in three steps (Scheme 1.14). The first step was the reduction ketone **1.44** to the alcohol. This was then eliminated under acidic conditions to yield a cyclopentadiene, which can then be deprotonated with *n*-butyl lithium to yield the desired cyclopentadienide **1.45**.

Scheme 1.14. Synthesis of Cyclopentadienide **1.45**.



The formal total synthesis of the steroid (+)-equilenin (**1.46**) was also accomplished utilizing oxaspiro[2.2]pentanes (Figure 1).^{28, 29} Ihara's synthesis of equilenin (**1.46**) began with a naphthalene derivative **1.47**, which was epoxidized under Jacobsen conditions in moderate yield and enantiomeric excess (ee) to yield the desired cyclobutanone **1.49** directly due to the oxaspiro[2.2]pentane's **1.48** instability to the reaction conditions (Scheme 1.15).

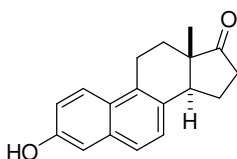
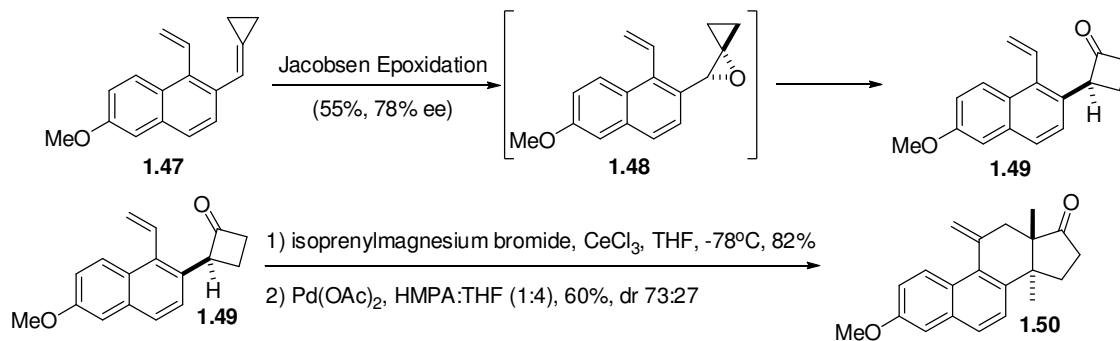


Figure 1.1. Structure of equilenin (**1.46**).

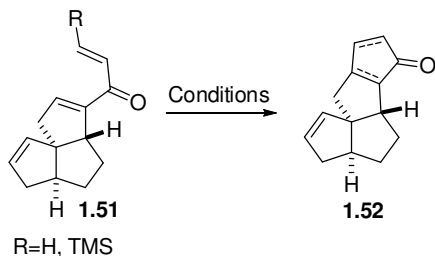
Attempts to improve the optical purity of the cyclobutanone through the utilization of other epoxidation methods did not yield better results. Shi epoxidation utilizing the fructose derived catalyst also resulted in low optical purity. Attempts to improve this, through a variety of solvents and using the 'catalyst' in superstoichiometric amounts, did not improve the optical purities to sufficient levels. This observed reduction of enantioselectivity is presumably due to the stabilization of the potential benzylic cation by the methoxy substituent leading to an unselective rearrangement to the cyclobutanone as optical purities increase drastically when the methoxy substituent is replaced by hydrogen, up to 93% ee. The isoperenyl group was installed on the cyclobutanone **1.49** with cerium trichloride to give the precursor to the key cascade ring expansion reaction which took place with a full equivalent of palladium acetate to give

cyclopentanone **1.50** which could then be transformed to (+)-equilenin (**1.46**) after a few further transformations.

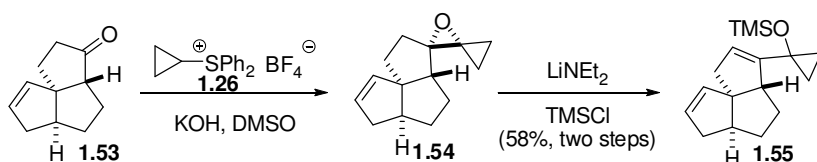
Scheme 1.15. Total Synthesis of (+)-equilenin.



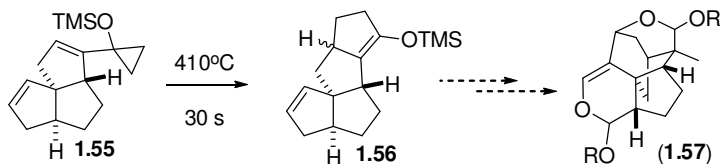
Paquette's studies toward the synthesis of the trikingolides illustrate the power of small rings in synthesis due to failure of the original plan to construct the cyclopentenone ring intermediate **1.52** through a Nazarov type cyclization. Once the divinyl ketone **1.51** for the Nazarov cyclization was completed, it was found that cyclization under a variety of conditions did not lead to the desired cyclopentenone in sufficient yields to be synthetically useful. Even the assistance of a silicon atom in the β -position only led to low yields or mixtures of stereoisomers at the ring fusion (Scheme 1.16).

Scheme 1.16. Attempted Nazarov Cyclization.

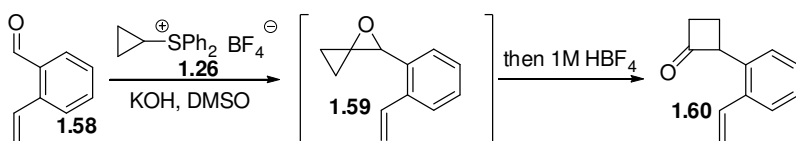
With these failures of more standard conditions, they next turned their attention to the construction of the cyclopentenone, *via* Trost's annulation procedure, using an oxaspiro[2.2]pentane as an intermediate. This protocol begins with ketone **1.53** condensation with cyclopropyl sulfoxonium ylide **1.26** leading to oxaspiro[2.2]pentane derivative **1.54**, which was used in the elimination step without purification to yield cyclopropane **1.55** (Scheme 1.17).

Scheme 1.17. Cyclopentenone Annulation *via* 1-Oxaspiro[2.2]pentane **1.54**.

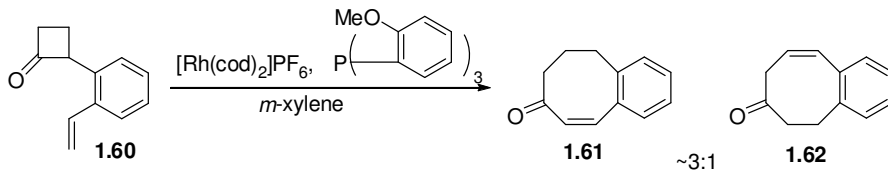
To complete the annulation cyclopropane **1.55** was flash vacuum pyrolyzed to yield the desired cyclopentanone as its silylenol ether **1.56** in excellent yield (Scheme 1.18). Unfortunately, attempts to utilize this strategy toward an ultimate synthesis of the trikingolides (**1.57**) did not result in a complete synthesis.

Scheme 1.18. Completion of Trost Cyclopentenone Annulation Protocol.

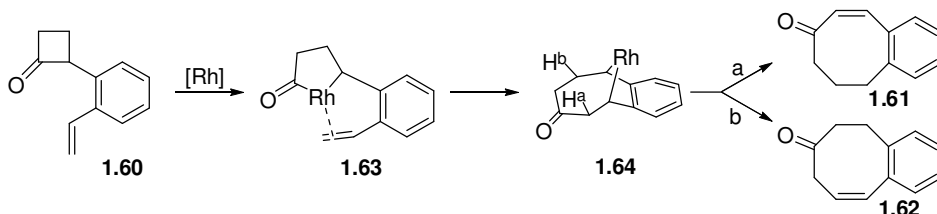
In addition to access to numerous natural products and the synthesis of new chiral ligands, oxaspiro[2.2]pentanes have also provided access to substrates for interesting transformations. An example substrate transformation is the rhodium catalyzed eight-membered ring synthesis developed by Murakami (Scheme 1.19).³⁰ In this transformation the desired *o*-styryl-cyclobutanones **1.60** were synthesized utilizing Trost's cyclopropyl sulfoxonium ylide **1.26** procedure to generate the desired oxaspiro[2.2]pentane **1.59** which were subsequently rearranged under protic conditions to yield the desired cyclobutanone **1.60**.

Scheme 1.19. Synthesis of *o*-Styryl-Cyclobutanones.

Cyclobutanone **1.60** was then exposed to a rhodium alkene complex in the presence of a phosphine ligand in refluxing *m*-xylene resulting in cyclooctenones **1.61** and **1.62** (Scheme 1.20). No reaction was observed with substitution on the vinyl group, however, substitution of the phenyl ring was tolerated with similar results.

Scheme 1.20. Rhodium Catalyzed Synthesis of Eight-Membered Rings.

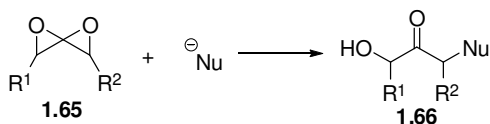
The reaction proceeded by oxidative addition of the rhodium (I) catalyst to the cyclobutanone **1.60** to yield an acylrhodium intermediate **1.63** (Scheme 1.21). The acylrhodium then went migratory insertion into the adjacent vinyl group to yield a rhodium bicycle **1.64** which has two potential options for β -elimination to yield the observed products.

Scheme 1.21. Proposed Mechanism for Eight Member Ring Synthesis.

1, 4-Dioxaspiro[2.2]pentanes

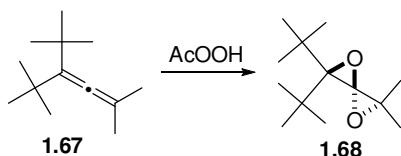
Like the oxaspiro[2.2]pentanes, the more oxidized 1,4-dioxaspiro[2.2]pentanes **1.65** display one primary mode of reactivity. The reactivity of this the smallest example of a spiro-acetal, hinges on the relief of the strain energy contained in both epoxide rings to give α -nucleophile substituted α' -hydroxy ketones **1.66** as products (Scheme 1.22). These nucleophile additions are broad in scope and can be both intra- and inter-molecular in nature.

Scheme 1.22. General Reactivity of 1, 4-Dioxaspiro[2.2]pentanes.



This interesting member of the spiro-acetals was first synthesized by Crandall in 1966 and regained the interest of synthetic chemists in recent years.^{31, 32} Crandall found that exposure of tetramethylallene to peracetic acid resulted in the formation of several oxidized products. Although 1,4-dioxaspiro[2.2]pentane was not directly detected, several of the reaction products pointed to its formation, because it underwent an acid or thermal mediated rearrangement to give the observed products. It was not until 1968 that Crandall succeeded in isolating a 1,4-dioxaspiro[2.2]pentane **1.68** by careful distillation of the oxidation products of allene **1.67** (Scheme 1.23).³³

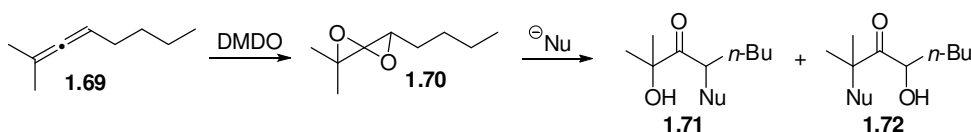
Scheme 1.23. First Isolation of a 1,4-Dioxaspiro[2.2]pentane.



It was still two decades before 1,4-dioxaspiro[2.2]pentanes found their way into more synthetically useful scenarios.³⁴⁻³⁶ This time gap was due to the lack of an efficient neutral and mild oxidizing reagent to effect this transformation. This role was filled by the advent of dimethyldioxirane (DMDO) by Murray and co-workers.³⁷ With a more general synthesis of 1,4-dioxaspiro[2.2]pentanes available, synthetic transformations

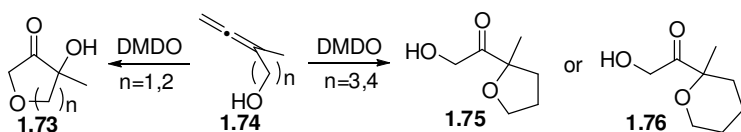
could be explored (Scheme 1.24). It was found that exposure of diepoxide **1.70**, available from allene **1.69**, to various nucleophiles typically yielded substituted ketones of type **1.71** and **1.72** depending on the steric demands of the nucleophile used, and whether the conditions were Lewis acidic in nature. The more sterically demanding nucleophiles react to give preference for the formation of ketone **1.71** compared to less sterically demanding nucleophiles which yielded mixtures of both substituted ketones **1.71** and **1.72**. Under acidic conditions preference was for the initial formation of ketone **1.72**.

Scheme 1.24. Nucleophile Additions to 1,4-Dioxaspiro[2.2]pentanes



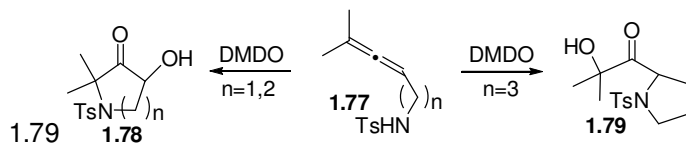
Crandall and co-workers also found that intramolecular cyclizations were also possible with an appropriate pendant nucleophile (Scheme 1.25).^{35, 38} Thus, oxidation of allenic alcohols **1.74** containing one or two carbon atom tethers yielded tetrahydrofuranones **1.73**. The reaction proceeds by attack at the distal epoxide C-O bond with the alcohol to form the observed products. When the tether is extended to three or four carbon atoms nucleophilic addition favors the proximal epoxide C-O bond to form tetrahydrofurans **1.75** and tetrahydropyrans **1.76**, respectively.

Scheme 1.25. Synthesis of Cyclic Ethers *via* 1,4-Dioxaspiro[2.2]pentanes.

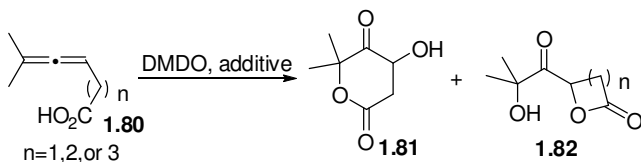


In analogy to allenyl alcohols, protected amines also give cyclic heterocycles as products (Scheme 1.26). Exposure of a tosyl protected allenyl amine **1.77** with a one or two carbon tether yielded amino-ketones **1.78** where nucleophilic attack of the amine occurred at the distal epoxide C-O bond. Conversely, when the tether was lengthened to three carbon atoms **1.79**, again in analogy to the alcoholic series, nucleophilic attack instead occurred at the proximal epoxide C-O bond. Contrary to what was observed with the alcoholic substrates the amine substrates suffered from lower yields, 52% vs. 87%, due to competing oxidation at the nitrogen atom to give further oxidized by-products.

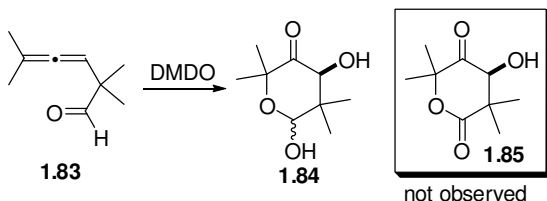
Scheme 1.26. Synthesis of Cyclic Amines from 1,4-Dioxaspiro[2.2]pentanes.



Similarly, when allenic carboxylic acids **1.80** were employed as substrates the corresponding lactones were obtained as products (Scheme 1.27).^{39, 40} When the tether length was only one carbon atom δ -lactones **1.81** were obtained as the major product. Interestingly, when the tether was one carbon atom and sodium bicarbonate was added to the reaction to form the sodium carboxylate a β -lactone **1.82** and δ -lactone **1.81** were observed. When acid was added the reaction gave the δ -lactone **1.81** as the major product.

Scheme 1.27. Synthesis of Lactones Utilizing 1,4-Dioxaspiro[2.2]pentanes.

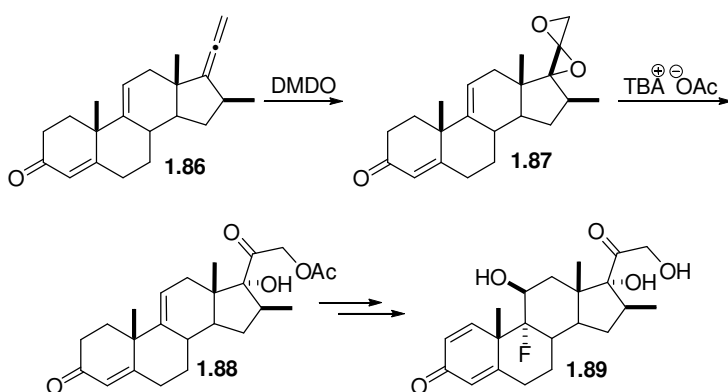
Allenyl aldehydes were also explored as substrates in oxidative cyclizations as an alternate to carboxylic acids as it is known that DMDO will oxidize aldehydes to the corresponding carboxylic acids (Scheme 1.28).^{37, 41} However, with these substrates epoxidation proved to be competitive with oxidation of the aldehyde. With this scenario, intramolecular cyclization becomes competitive with intermolecular oxidation of the aldehyde. Thus, after oxidation of the aldehyde **1.83** the observed product is not the expected keto-lactone **1.85**, but is in fact the acetal **1.84**. Utilizing scrupulously dry DMDO in the presence of a suitable alcohol an alkyl acetal can be obtained.

Scheme 1.28. Oxidative cyclization of Allenyl Aldehydes.

Even though this ring system has been known since 1966, and several investigations into their reactivity with various nucleophiles have been conducted, it was thirty years until it was applied in the synthesis of a complex molecule. The synthesis of betamethosone by Andrews and co-workers demonstrated the practicality of 1,4-

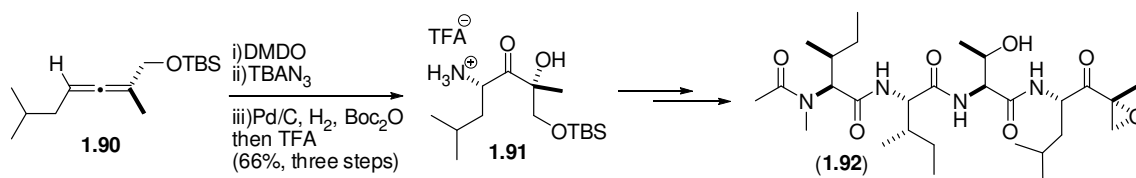
dioxaspiro[2.2]pentanes (Scheme 1.29).⁴² Starting from allene **1.86** derived from 9 α -hydroxyandrost-4-ene-3,17-dione, oxidation with DMDO provided 1,4-dioxaspiro[2.2]pentane derivative **1.87** which upon subjection to tetrabutylammonium acetate yielded acetate substituted ketone **1.88**. This could then be converted to betamethosone **1.89** by known conditions.⁴³

Scheme 1.29. Use of 1,4-Dioxaspiro[2.2]pentanes in Corticosteroid Synthesis.



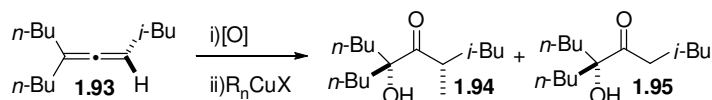
The utility of this ring system is also highlighted in Williams' modular synthesis of the selective proteasome inhibitor epoxomicin (**1.92**) (Scheme 1.30).⁴⁴ Beginning with allene **1.90**, which is derived from isovaleraldehyde, a successive sequence of oxidation with DMDO, azide addition and reduction of the unstable azido-ketone delivered the stable amino-ketone **1.91**. This route was chosen due to the low yield or instability of other amino-ketones derived from alternate nitrogen sources. The completion of the synthesis was accomplished by successive peptide coupling, followed by the transformation of the tertiary alcohol into the requisite epoxide to produce epoxomicin (**1.92**). This sequence proceeded in excellent overall yield of 20% for all steps.

Scheme 1.30. Synthesis of Epoxomicin.

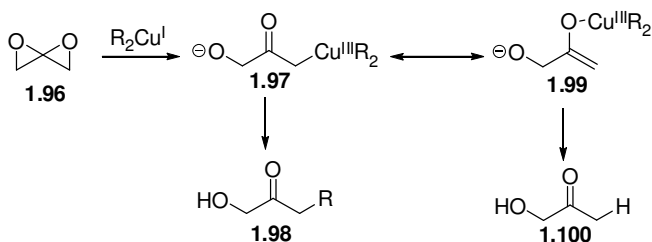


Nucleophilic additions to 1,4-dioxaspiro[2.2]pentanes are not limited to heteroatoms; carbon based nucleophiles can also provide substituted ketone products. The addition of cuprates to this ring system proved difficult at first, but could be made effective with the appropriate choice of reagent (Scheme 1.31).⁴⁵

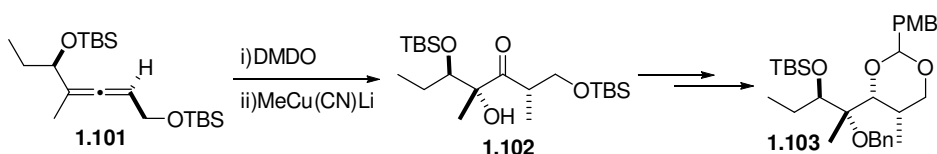
Scheme 1.31. Addition of Cuprates to 1,4-Dioxaspiro[2.2]pentanes.



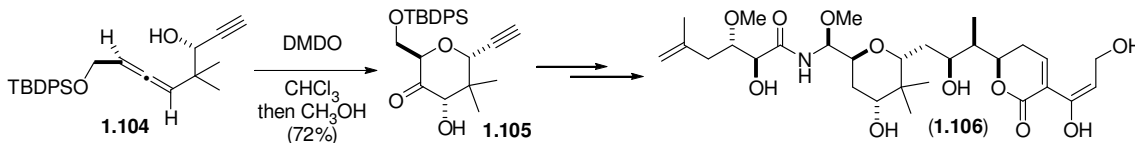
The choice of typical dialkyl cuprates derived from alkyl lithiums provided some of the desired addition product **1.94** along with ketone **1.95** as the major product. The production of hydroxyl-ketone **1.94** proved to be surprising but not unfounded.⁴⁶ This reaction presumably occurred through oxidative addition of the Cu(I) species to the epoxide **1.96**, to give an intermediate α -Cu(III) ketone **1.97** and which provided two divergent reaction pathways (Scheme 1.32). First, ‘normal’ reductive elimination yielded the desired substituted product **1.98**. Whereas, isomerization to the corresponding enolate **1.99** would lead to observed ketone **1.100**. The second reaction manifold was avoided by the use of alkylcyano cuprates.

Scheme 1.32. Two Reaction Pathways for Cuprate Addition.

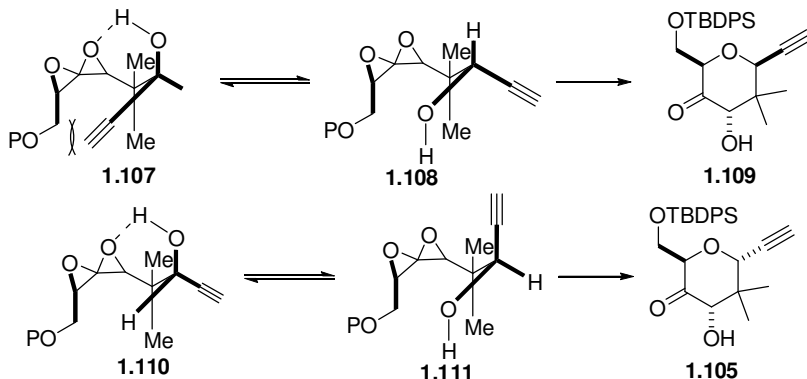
With this methodology in hand, it was then applied to the synthesis of a precursor towards the antibiotic erythromycin (Scheme 1.33). Oxidation of allene **1.101** with subsequent exposure to methylcyanocuprate yielded ketone **1.102** in good diastereoselectivity, 8:1. This was then transformed to the known protected tetrol **1.103** by standard methods.⁴⁷

Scheme 1.33. Synthesis of a Precursor to Erythromycin.

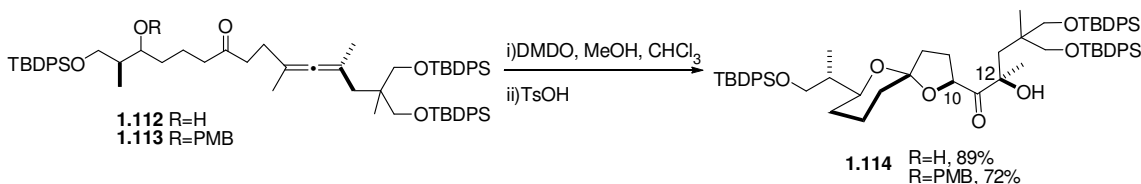
In 2004, the selective anti-tumor agent psymberin was isolated from a sponge off the coast of Papua New Guinea.⁴⁸ The tetrahydropyran of this natural product lends itself to be constructed utilizing Crandall's methodology (Scheme 1.34). Advanced allene **1.104** was subjected to oxidation, in the presence of DMDO, to give the intermediate 1,4-dioxaspiro[2.2]pentane which cyclized to dihydropyranone **1.105** upon the addition of methanol. The dihydropyranone **1.105** could then be transformed into a known intermediate in the synthesis of psymberin (**1.106**).

Scheme 1.34. Synthesis of the Dihydropyran of Psymberin.

The unusual necessity of methanol to bring about cyclization can be explained by looking at the conformations of the 1,4-dioxaspiro[2.2]pentane and its diastereomer (Scheme 1.35). If the opposite stereochemistry of the alcohol was used in the oxidative cyclization, it spontaneously cyclized to give the *cis*-dihydropyranone. This is due to the destabilization of the unproductive hydrogen-bonded conformation **1.107** due to steric interactions, which promotes the formation of the productive conformation **1.108** and leads to *cis*-dihydropyranone **1.109**. Conversely, the other diastereomer forms a stable hydrogen-bonded complex **1.110**, due to a lack of the destabilizing interactions. The productive conformation **1.111** is destabilized due to interactions between the alkyne and the epoxide. In order to break up this stable hydrogen-bonded complex, a protic solvent is added which drives the formation of conformer **1.111** and thus formation of the desired *trans*-dihydropyran **1.105**.

Scheme 1.35. Conformational Analysis Leading to the Two Diastereomeric Pyrans.

A very elegant synthesis of the A-B ring system of pectenotoxin 4 by Williams was also devised using a 1,4-dioxaspiro[2.2]pentane as a key intermediate (Scheme 1.36).⁴⁹ Keto-allene **1.112** is oxidized by DMDO to the *bis*-epoxide, which is then captured by the pendant ketone and generates an oxocarbenium ion. This cation is then captured by the alcohol to give the A-B ring system of pectenotoxin 4 **1.114** in good yield. Additionally, the diastereoselectivities for both oxidations is good, >20:1 for the C12 alcohol and 7:1 for the C10 center. This cascade reaction sequence could be extended by a further reaction by the use of PMB protected alcohol **1.113**, in that DMDO also can be used to remove the PMB group.

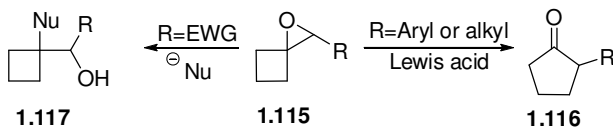
Scheme 1.36. Synthesis of the A-B ring System of Pectenotoxin 4.

1-Oxaspiro[2.3]hexanes

Similarly to the previously described ring systems, the construction of 1-oxaspiro[2.3]hexanes is analogous. Although many methods exist, oxidation of methylene cyclobutanes by agents such as DMDO or peracids are the most prevalent. This ring system has also been constructed by the addition of α -lithio selenocyclobutanes to carbonyl compounds,^{50, 51} addition of sulfur ylides to cyclobutanones,⁵² oxidation of methylene cyclobutanes with *N*-bromosuccinimide in water,⁵³ transition metal mediated epoxidations of cyclobutenes,⁵⁴ and oxidation of methylenecyclobutanes with chiral versions of DMDO.^{55, 56}

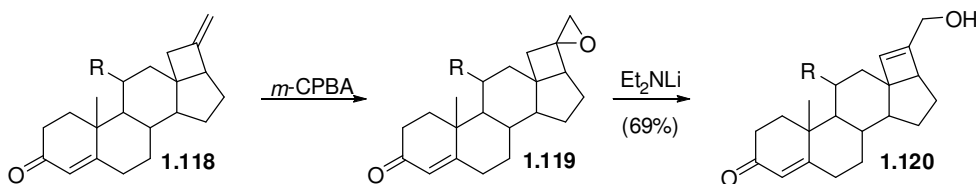
Oxaspiro[2.2]pentanes and 1-oxaspiro[2.3]hexanes **1.115** have similar reactivity patterns (Scheme 1.37). When the ring system was functionalized with an aryl or alkyl group, it underwent a facile ring expansion to cyclopentanones **1.116** under Lewis acidic conditions exhibited similarly with oxaspiro[2.2]pentanes.^{52, 57} Likewise this ring expansion was driven by the release of the strain energy of both rings, and the presence of an aryl group would likely stabilize the forming carbocation necessary for the rearrangement. Conversely, nucleophiles were added to make substituted cyclobutanes **1.117** when the ring system was functionalized with an appropriate electron withdrawing group. This was presumably due to the destabilization of the cation, which was necessary for the rearrangement and preference of reaction at the distal cyclobutyl C-O bond.

Scheme 1.37. General Reactivity of 1-Oxaspiro[2.3]hexanes.



The first application of 1-oxaspiro[2.3]hexane in synthesis was the attempted construction of an aldosterone derivative (Scheme 1.38).⁵⁸ Steroid **1.118**, which was obtained after several steps from pregnenolone acetate, was oxidized by the action of *m*-CPBA to give 1-oxaspiro[2.3]hexane **1.119**. The 1-oxaspiro[2.3]hexane **1.119**, was then eliminated with lithium diethylamide to give cyclobutene **1.120**. This reaction sequence worked well when R=H, however when R≠H the elimination essentially did not proceed. With these disappointing results this route was abandoned for a more productive pathway.

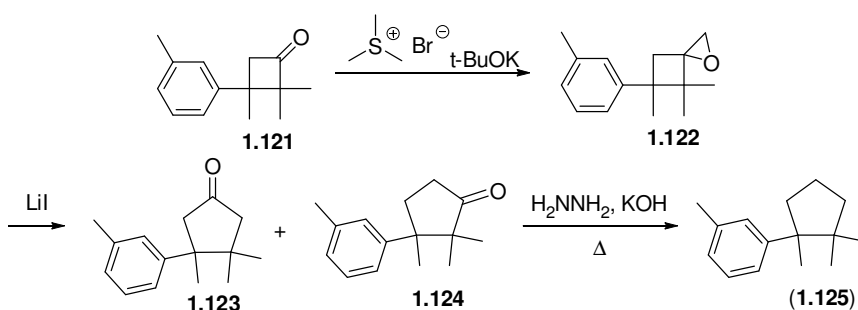
Scheme 1.38. Application of 1-Oxaspiro[2.3]hexanes Toward an Aldosterone.



The aromatic sesquiterpene natural product herbertene, isolated from the liverwort *Herberta adunca*, is another early example of the use of 1-oxaspiro[2.3]hexanes in natural product synthesis (Scheme 1.39).⁵² The synthesis of the key 1-oxaspiro[2.3]hexane **1.122** begins with cyclobutanone **1.121**; this was made from a toluene derivative and dimethyl ketene *via* thermal cyclization. Cyclobutanone **1.121** is

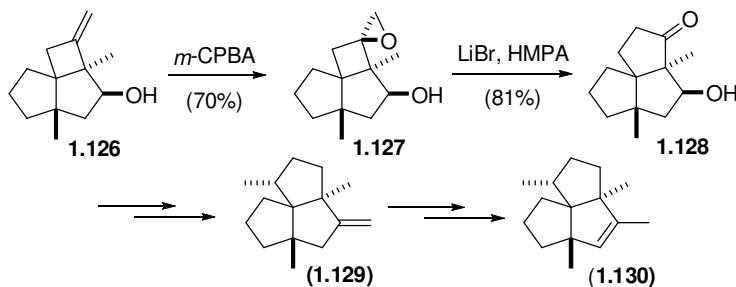
then condensed with trimethylsulfonium bromide, under basic conditions, to yield the desired spirosystem **1.122**. Upon exposure to catalytic lithium iodide, this spirosystem rearranges to an inconsequential mixture of carbonyl isomers **1.123** and **1.124**. The synthesis is completed by reduction of the carbonyl to the methylene in herbertene (**1.125**) by the Huang-Minlon reduction.⁵⁹ This concise synthesis of herbertene (**1.125**) proves to be efficient with an overall yield of ~30%.

Scheme 1.39. Synthesis of Herbertene.



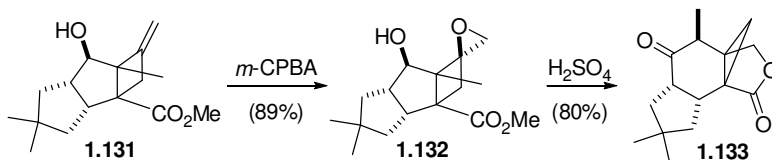
Triquinane natural products have been a long standing proving ground for methodology as is also the case with 1-oxaspiro[2.3]hexanes. Both isocomene and β-isocomene could be synthesized from a common 1-oxaspiro[2.3]hexane (Scheme 1.40).⁶⁰ The synthesis of key 1-oxaspiro[2.3]hexane **1.127** derives from cyclobutene **1.126** by hydroxyl directed epoxidation with *m*-CPBA to give a single epoxide **1.127** in good yield. Rearrangement gave cyclopentanone **1.128**, by the action of lithium bromide with hexamethylphosphoramide (HMPA), gave a single regioisomer again in good yield. This cyclopentanone **1.128** was then transformed into β-isocomene (**1.129**) after several steps to isocomene (**1.130**).

Scheme 1.40. Synthesis of Isocomene and β -Isocomene *via* an 1-Oxaspiro[2.3]hexane.



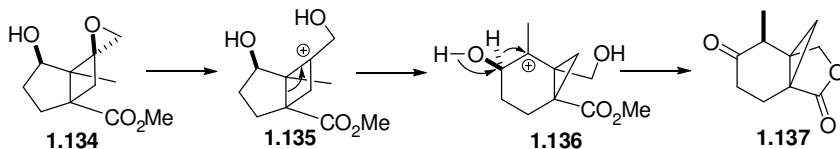
A particularly elegant use of a 1-oxaspiro[2.3]hexane is Tobe's synthesis of marasmic acid (Scheme 1.41).^{61, 62} In this synthesis cyclobutene **1.131** is oxidized with *m*-CPBA to give the epoxide **1.132**. Epoxide **1.132** then undergoes a cascade rearrangement with sulfuric acid to give lactone **1.133**, which is a precursor to marasmic acid.

Scheme 1.41. Use of a Cyclobutyl-Cyclopropylcarbinyl Rearrangement in the Synthesis of Marasmic Acid.



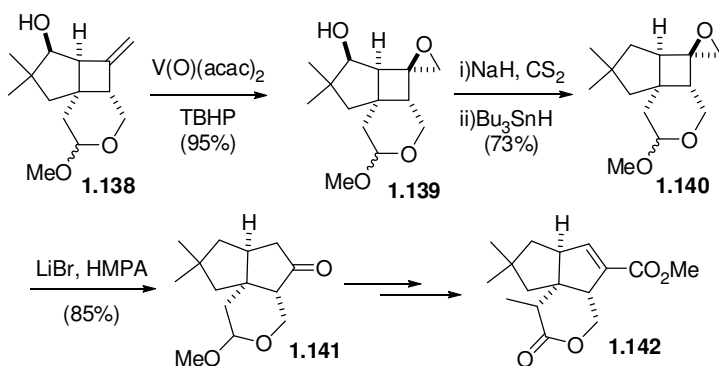
The mechanism of this cascade rearrangement is depicted in simplified version, the cyclopentane was omitted for clarity, in Scheme 1.42. Protonation of epoxide **1.134** leads to the formation of cyclobutyl cation **1.135**, which then underwent a bond migration that gave the new cyclopropylcarbinyl cation **1.136**. This cation then underwent a 1,2-hydride shift that gave the observed product after lactonization **1.137**.

Scheme 1.42. Mechanism for the Cascade Rearrangement of the Epoxide **1.134** to Lactone **1.137**.



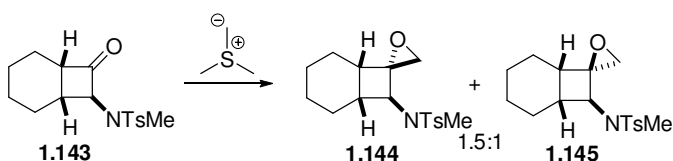
The use of 1-oxaspiro[2.3]hexane ring expansion also proved to be particularly effective for the synthesis of pentalenolactone E and G methyl esters (Scheme 1.43).⁵⁴ Cyclobutene **1.138** was constructed by a photo [2+2] cycloaddition from the corresponding allene and enone. Alkene **1.138** was then epoxidized in a hydroxyl directed fashion by the use of $V(O)(acac)_2$ in the presence of *tert*-butylhydroperoxide (TBHP) to give epoxide **1.139** in excellent yield and selectivity. Alcohol **1.139** was then deoxygenated using the Barton protocol.⁶³ Next, epoxide **1.140** underwent ring expansion to give cyclopentanone **1.141** in near complete regioselectivity. Cyclopentanone **1.141** could then be converted to pentalenolactone E methyl ester **1.142** after a few additional steps. Pentalenolactone G methyl ester was also accessed utilizing a similar strategy.

Scheme 1.43. Synthesis of Pentalenolactone E Methyl Ester.

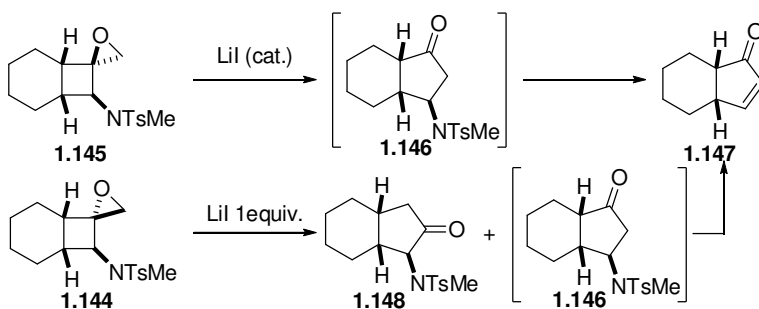


Amino-substituted 1-oxaspiro[2.3]hexanes are also accessible via a two step process in good optical purities (Scheme 1.44).^{64, 65} The amino-cyclobutanones **1.143** are available directly from the [2+2] cycloaddition of keteniminium salts and disubstituted olefins. These cyclobutanones **1.143** can then be condensed with sulfur ylides to yield the corresponding epoxide **1.144** and **1.145** in good yield and poor diastereoselectivities.

Scheme 1.44. Synthesis of Aminosubstituted 1-Oxaspiro[2.3]hexanes.

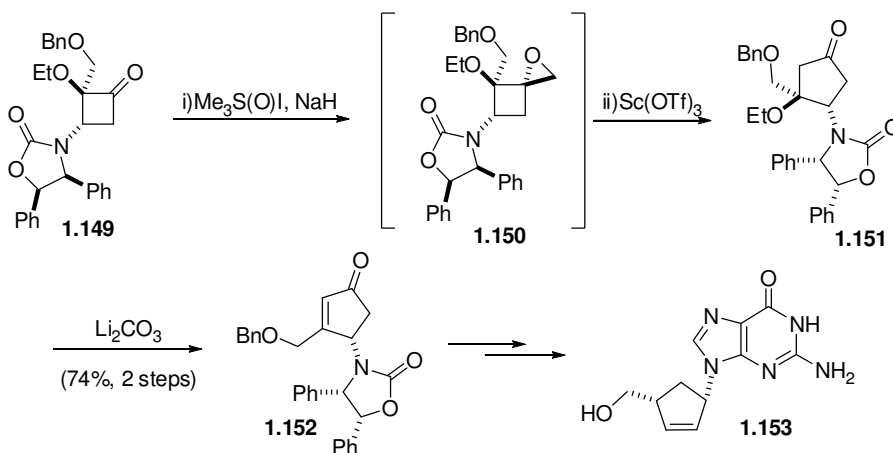


These amino-substituted 1-oxaspiro[2.3]hexanes could then be converted to the subsequent cyclopentenones by exposure to either a catalytic or stoichiometric amount of lithium iodide (Scheme 1.45). The *exo*-isomer **1.145** underwent a more facile rearrangement as only a catalytic amount of lithium iodide is necessary. However, the *endo*-isomer required more forcing conditions demanding a full equivalent of lithium iodide. Both isomers presumably gave the same intermediate β -amino cyclopentanone **1.146**, but under the reaction conditions β -aminocyclopentanone **1.146** eliminated to give the observed cyclopentenone **1.147**. The regioselectivity of the rearrangement of the *endo*-isomer **1.144** was not as selective as the *exo*-isomer **1.145**. This resulted in the formation of two products, α -aminocyclopentanone **1.148** and cyclopentenone **1.147**. This process proved, in most cases, to preserve the optical purity of the starting epoxide in all of the products as the enantiomeric excess was preserved in all products.

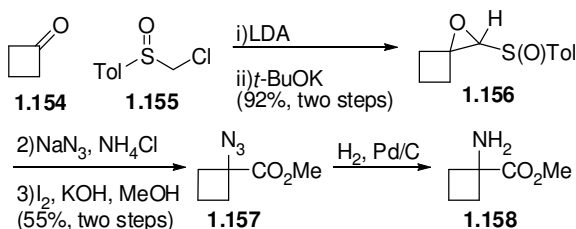
Scheme 1.45. Rearrangement to form Cyclopentenones.

One of the main advantages of 1-oxaspiro[2.3]hexanes is their facile rearrangement to the corresponding cyclopentanones. Addition of diazomethane to cyclobutanones can give the same products, however they are often as a mixture of regioisomers. An example of the use of this ring system to bring about a more selective rearrangement compared to a similar reaction with diazomethane is the synthesis of carbovir **1.153** by Hegedus and co-workers (Scheme 1.46).⁶⁶ The substrate cyclobutanone **1.149**, for the rearrangement, was constructed using a photolytic reaction of a chromium carbene with an ene-carbamate. Upon reaction with dimethylsulfoxonium methylide the intermediate 1-oxaspiro[2.3]hexane **1.150** was formed, and then exposed to scandium triflate triggers a rearrangement to cyclopentanone **1.151**. Other Lewis acids brought about elimination of the β -ethoxy group in addition to rearrangement. In a second step, the ethoxy group was eliminated under basic conditions to give cyclopentenone **1.152** which was then transformed to carbovir **1.153** after several steps.

Scheme 1.46. Synthesis of the Antiviral Agent (+)-Carbovir.

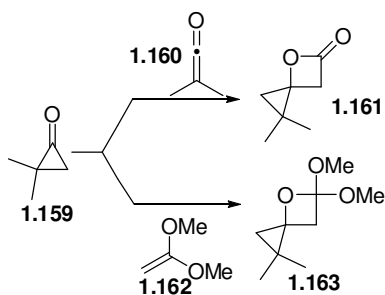


The propensity of 1-oxaspiro[2.3]hexanes to open to cyclobutylcarbinyl cations under Lewis acid conditions, and subsequent rearrangement, can be thwarted with the attachment of an appropriate electron withdrawing group. The two step protocol to generate sulfoxyl substituted epoxides is an example of a synthesis of this type of substrate (Scheme 1.47).^{67, 68} Cyclobutanone **1.154** reacted with chloromethyl substituted sulfoxide **1.155** under the action of LDA to give an intermediate alcohol that could be cyclized to the corresponding epoxide **1.156**. Nucleophiles, such as azide, could be added to the distal carbon of the epoxide **1.156** would gave an azido-aldehyde, which was directly oxidized to the methyl ester **1.158** by the use of basic iodine in methanol. The azido ester **1.157** could then be reduced to the corresponding amine by catalytic hydrogenation. While this procedure proved effective in the racemic sense for a variety of substrates the analogous process with a chiral sulfoxide was only demonstrated for a select few substrates.

Scheme 1.47. Synthesis of α -Quaternary Amino Acids Using Ketones.**4-Oxaspiro[2.3]hexanes**

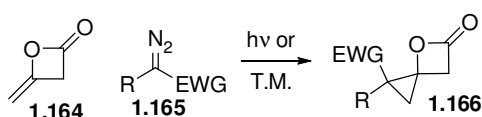
Even though 4-oxaspiro[2.3]hexanes have been the subject of several syntheses, their application to the synthesis of natural and unnatural products has yet to be envisioned. Presumably due to the lack of scope in their syntheses, very few applications have been undertaken, and their synthesis will only be covered in brief.

The first construction of this ring system was by Turro in the late 1960's (Scheme 1.48).^{69, 70} While the cycloaddition between cyclopropanone **1.159** and ketene **1.160** proceeded in modest yields of cycopropane **1.161**, it proceeded in excellent yield for the dimethyl acetal of ketene **1.162** to give orthoester **1.163**, 90%. It still suffered from the lack of adequate syntheses of the requisite cyclopropanones to be broadly applicable.

Scheme 1.48. Thermal [2+2] Cycloaddition of Cyclopropanone and Alkenes.

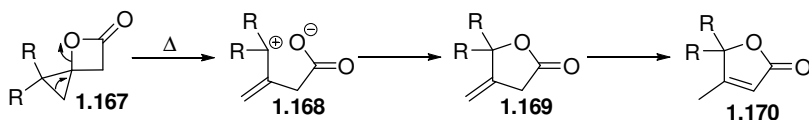
Perhaps one of the more broadly applicable syntheses of 4-oxaspiro[2.3]hexanes is the decomposition of diazo-compounds in the presence of diketene **1.164** (Scheme 1.49).⁷¹⁻⁷⁴ A variety of diazocompounds **1.165** bearing an electron withdrawing group in the form of a phosphonate or ester did give the 4-oxaspiro[2.3]hexanes **1.166** with varying degrees of success. The identity of the substituents appears to be crucial to the outcome of the reaction. However, both light mediated and transition metal mediated decomposition of the diazocompounds gave similar results.

Scheme 1.49. Diazo Decomposition to Form Cyclopropyl- β -Lactones.



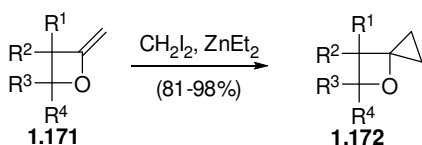
One of the major reactions of this highly strained system is the thermal rearrangement to give furanones of type **1.169** or **1.170** as the products (Scheme 1.50). It is thought that this reaction proceeds *via* cleavage of one of the cyclopropyl C-C bond and the C-O bond of the β -lactone to give a zwitterion intermediate **1.168**. This, then undergoes ring closure to give the initial product **1.169** which partially or completely isomerizes to furanone **1.170**, under the reaction conditions.

Scheme 1.50. Thermal Rearrangement of 4-Dioxaspiro[2.3]hexanes.

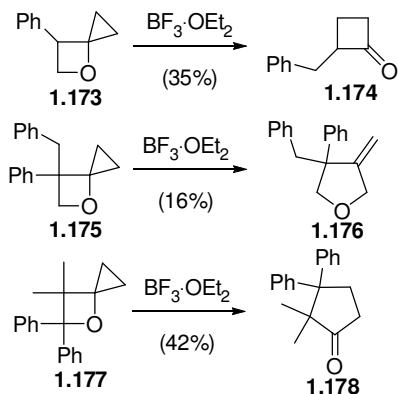


The most general synthesis to date is that of cyclopropanation of 2-methylene oxetanes. 2-Methylene oxetanes **1.171**, which are available from the corresponding β -lactones by the method of Howell⁷⁵, underwent a Simmons-Smith cyclopropanation to give 4-diaoxaspiro[2.3]hexanes **1.172** (Scheme 1.51). The only accessible structural variation is where the substituents are on the oxetane ring. Cyclopropanation does proceed in good yields for a variety of substrates.

Scheme 1.51. Use of Simmons-Smith Reaction for the Construction of 4-Oxaspiro[2.3]hexanes.



With a more general synthesis in hand, attention could be turned to the reactivity of the ring system (Scheme 1.52). Depending on the substrate, exposure to Lewis acid gave a variety of different structures, unfortunately the yields for these reactions were very moderate, limiting their potential in synthesis.

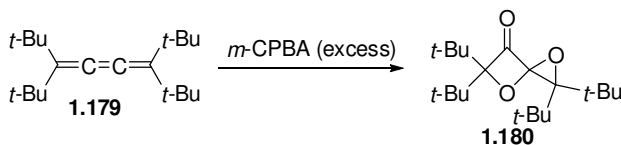
Scheme 1.52. Lewis Acid Mediated Rearrangements.

In addition to the above described procedures, 4-oxaspiro[2.3]hexanes have been observed as products, by-products or intermediates in several other more exotic reactions. This ring system was isolated in low yields from photochemical reaction between carbonyl compounds and olefins.^{76, 77} They have also been constructed by cyclopropanation of alkylidene oxetanes with dichlorocarbene.⁷⁸ 4-Oxaspiro[2.3]hexanes are also an intermediate in the synthesis of a polyspirane,⁷⁹ but the most current example of their synthesis is an isolated report of the fragmentation of a benzylidene acetal to yield a 4-oxaspiro[2.3]hexane.⁸⁰

1,5-Dioxaspiro[3.2]hexanes

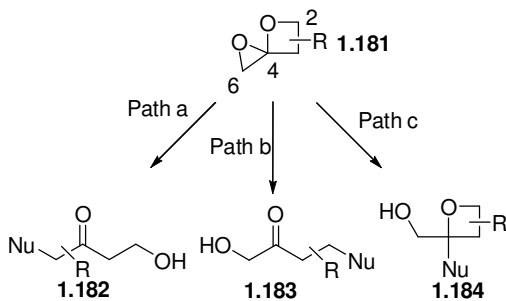
The first example of 1,5-dioxaspiro[3.2]hexanes was initially synthesized by chance.⁸¹ In an exploration of the oxidation of cumulene with peracids, Crandall found that exposure of cumulene **1.179** to an excess of *m*-CPBA yielded several products, one of them was 1,5-dioxaspiro[3.2]hexane **1.180** (Scheme 1.53).

Scheme 1.53. Oxidation of a Cumulene to Yield a 1,5-Dioxaspiro[3.2]hexane.



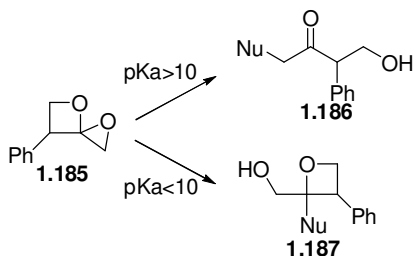
While this type of reaction did provide the desired ring system; it was not synthetically practical given the starting material. However, a synthetically viable route was not developed until more than a decade later that. Howell and co-workers have shown that methyleneoxetanes can yield 1,5-dioxaspiro[3.2]hexanes in good yields and modest to good diastereoselectivity in most cases.⁸² Additionally, the methyleneoxetanes can be readily accessed from β -lactones, which in turn can be made by a variety of methods. This particular method is also tolerant of a variety of functional groups which should prove useful in the synthetic arena.

In contrast to the previously described heterocycles, 1,5-dioxaspiro[3.2]hexanes **1.181** display varied reactivity depending on conditions employed (Scheme 1.54). Given the ring system, there are three possible modes of reactivity. Most probable reaction is path 'a', because nucleophilic attack is at the least hindered C6 that completely unravels the entire ring system with relief of all ring strain, to yield α -substituted ketones **1.182**. The next most probable is reaction pathway 'b', which is attack at C2, to relieve all ring strain yielding β -substituted ketones **1.183**. Finally, the least probable reaction pathway 'c', in which a nucleophile adds to C4 to give substituted oxetanes **1.184** as products. Pathway 'a' seemed the most likely due to the unsterically hindered attack of a nucleophile. Pathway 'c' was initially precluded due to the increased basicity of the oxetane oxygen over the epoxide oxygen, which would increase its lability.

Scheme 1.54. Reactivity of 1,5-Dioxaspiro[3.2]hexanes Towards Nucleophiles.

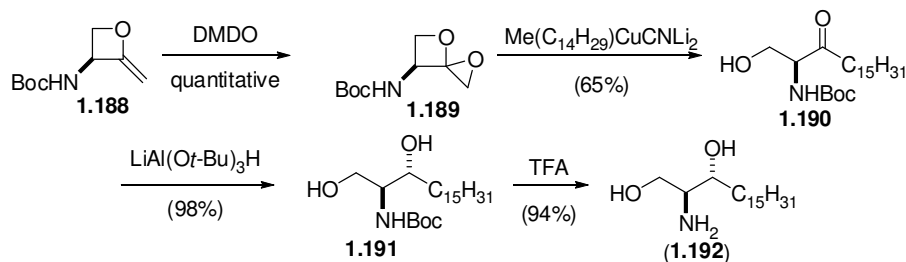
Howell and co-workers discovered many interesting things during their initial investigation of the reactivity of this poorly studied ring system.^{83, 84} Initially, most nucleophiles would add to the least hindered C6 position and follow reaction pathway ‘a’ to yield α -substituted ketones. These nucleophiles were quite diverse and included examples such as alcohols, acetate and sodium thiophenoxide. Contrary to these results, when DIBAL-H, Me_3Al , or TMSN_3 were utilized as nucleophiles the major product observed switched to that from addition to C4 yielding substituted oxetane products. This was initially attributed, to the Lewis acidic aluminum or silicon atom which facilitated the ring opening of the epoxide. Later it was found that heterocyclic nucleophiles, with acidic protons that have a pK_a of greater than 10 would yield the α -substituted ketones as products **1.186**, while those below a pK_a of ~ 10 , would yield the same substituted oxetanes **1.187** as product (Scheme 1.55).

Scheme 1.55. Influence of Acidity on the Reactivity of 1,5-Dioxaspiro[3.2]hexanes.



Computational analysis was also performed on these reaction pathways. It was found that with anionic nucleophiles there is a small preference for attack at C6. This mode of attack then results in a highly exothermic, 59.9 kcal/mol, unraveling of both rings to yield the observed product. Conversely, when in an acidic solution there is no preference for protonation at the oxetane or the epoxide oxygen, rather it is the stabilities of the generated oxonium ion. Obviously, the preference at this stage is for opening of the epoxide ring with generation of an oxetane oxonium, which is more stable than the corresponding epoxide oxonium by 18.8 kcal/mol.

In synthesis, the 1,5-dioxaspiro[3.2]hexane ring system proved to be a versatile building block toward the cell signaling and immunomodulatory molecules dihydrosphingosines, sphingosines, and phytosphingosines.⁸⁵⁻⁸⁷ Scheme 1.54 was illustrative of this versatility by the synthesis of *D-erythro*-sphinganine. Methylene oxetane **1.188** derived from serine was first oxidized to the 1,5-dioxaspiro[3.2]hexane **1.189** by DMDO in quantitative yield. The ring system is then exposed to a higher order cuprate to yield ketone **1.190** in good yield. The ketone **1.190** was selectively reduced by the action of lithium tri-*t*-butoxy aluminum hydride in excellent yields to give the alcohol **1.191**. The synthesis was completed by deprotection of the Boc-group with trifluoroacetic acid to afford *D-erythro*-sphinganine (**1.192**).

Scheme 1.54. Synthesis of D-Erythro-Sphinganine.

With the recent advances in the synthesis of small rings, there has been several new spiro-heterocycles that have been accessed. The construction of these ring systems allowed access to not only molecules of theoretical interest but also synthons for a variety of natural and unnatural products. These ring systems have also proven useful as they can undergo rearrangements with high selectivity, while the more traditional methods have proven to be less selective. With the combination of reactivity and selectivity there is no doubt that there will be continued interest in these spiro-heterocycles for a long time to come.

CHAPTER II

STUDIES TOWARD THE HATERUMALIDES: THE SYNTHESIS AND STRUCTURE OF SPIROEPOXY- β -LACTONES⁸⁸

Isolation and Biological Activity of the Haterumalides

Chemical entities derived from natural sources have been a continual source of novel structures and biological activities. Natural products have also been the mainstay for drug development as more than half of the current chemical entities from 1981-2002 have been derived in some fashion from natural products.⁸⁹ In particular, marine sources have been a continual pool of architecturally intriguing and potent molecular structures. Such a group of natural products that proves to be both structurally and biologically interesting are the haterumalides (Figure 2.1)

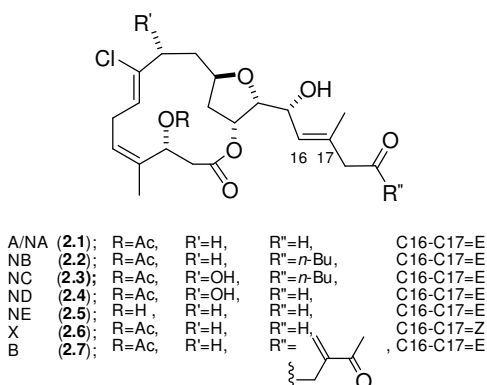


Figure 2.1. Structures of the haterumalides.

Haterumalides NA-NE (2.1-2.5) belong to a class of natural products that have been isolated from a marine sponge *Ircinia* sp. the source of haterumalides NA-NE (2.1-2.5)⁹⁰ and the source of haterumalide B (2.7) was identified as a marine ascidian

Lissoclinium sp.⁹¹ One additional haterumalide, X (**2.6**), along with haterumalides NA (**2.1**), B (**2.7**), and NE (**2.5**) were isolated from the soil bacterium *Serratia liquefaciens*.⁹² The haterumalides contain several interesting structural features which make them attractive targets for total synthesis. First is their *trans*-tri-substituted tetrahydrofuran ring, and second is the skipped diene containing a *Z*-chloro-alkene moiety. It should also be noted that the initially proposed stereostructures were corrected as a result of total syntheses.⁹³⁻⁹⁶

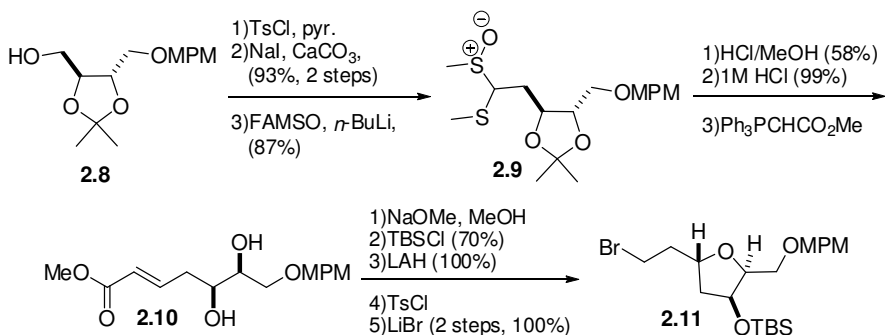
In addition, to their interesting structures the haterumalides display a variety of interesting biological activities including varying degrees of cytotoxicity with haterumalide NA (**2.1**) displaying an IC₅₀ value of 68 nM against the leukemia cancer cell line P388.⁹⁰ Haterumalide B inhibits the first division of fertilized sea urchin egg cell at concentrations as low as 18 pM.⁹¹

Previous Syntheses of Haterumalide NA

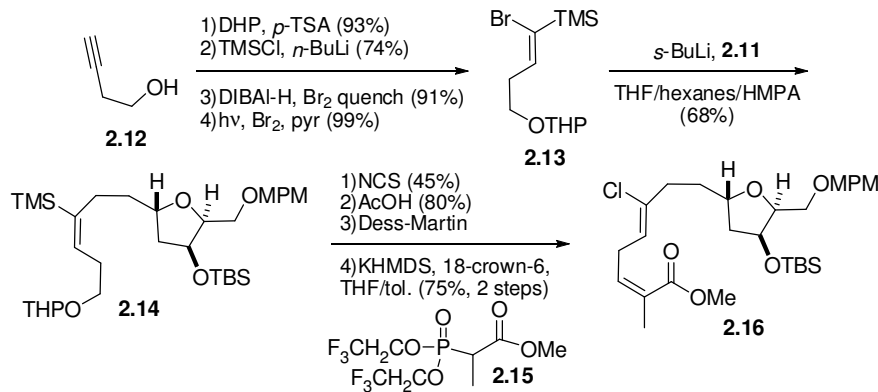
There have been two previously reported syntheses of *ent*-haterumalide NA (**2.1**) and one synthesis of the natural enantiomer. Kigoshi and co-workers published the first synthesis of the enantiomer of the methyl ester of *ent*-haterumalide NA (**2.1**).⁹³ The synthesis of the tetrahydrofuran core began with a threitol derivative **2.8**, the primary alcohol was converted to the iodide *via* a two step procedure (Scheme 2.1). The iodide was then homologated by one carbon by the use of the anion generated from FAMSO, methyl methylsulfinylmethyl sulfide, to give acetal **2.9**. After a two step deprotection of both the 1,2-diol and the aldehyde, a Wittig reaction gave α,β -unsaturated ester **2.10**. The tetrahydrofuran (THF) ring was then constructed by a Michael addition of the free alcohol to the α,β -unsaturated ester. The remaining alcohol was protected as its TBS

ether, and the ester was completely reduced to the alcohol. Conversion of the primary alcohol to the bromide *via* the tosylate gave THF **2.11**.

Scheme 2.1. Kigoshi's Synthesis of the Tetrahydrofuran Core of Haterumalide NA.

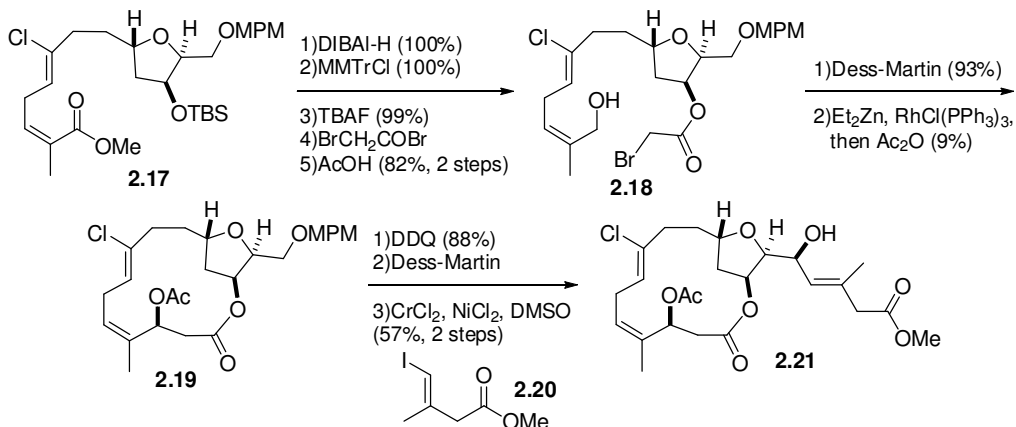


With the THF core **2.11** in hand, Kigoshi next moved toward the coupling of the skipped diene fragment and THF **2.11** (Scheme 2.2). The synthesis of the western hemisphere fragment began with protection of the primary alcohol of 3-butyn-1-ol **2.12** as the THP acetal and protection of the acetylenic position with a trimethylsilyl group. Alkyne hydroalumination with bromine quench gave the corresponding (*E*)-alkenyl bromide which was then photoisomerized to give (*Z*)-alkene **2.13** which is ready for coupling. Treatment of alkene **2.13** with *sec*-butyl lithium afforded the corresponding vinyl lithium reagent which was added to bromide **2.11** to give olefin **2.14**. The silyl group was then exchanged for chlorine by the action of *N*-chlorosuccinimide concurrent with isomerization of the alkene to the desired *Z*-alkene geometry. After deprotection and oxidation of the alcohol, a Still modified Horner-Wadsworth-Emmons olefination with phosphonate **2.15** was employed to give diene **2.16**.

Scheme 2.2. Coupling of the Western Hemisphere to the THF Core **2.11**.

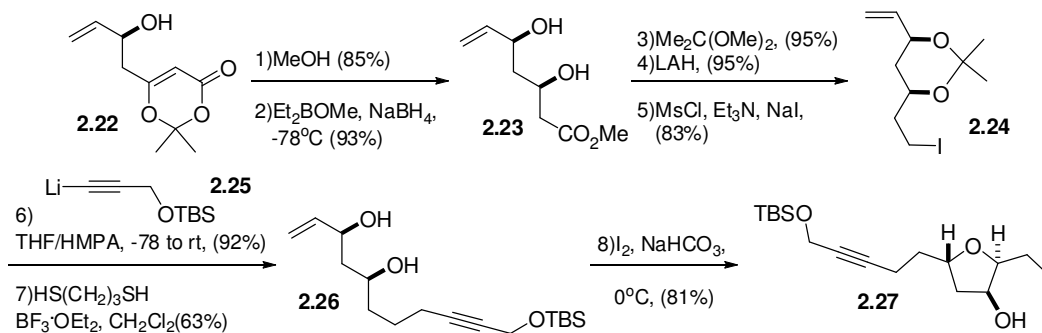
The next key step was a Reformatsky-type reaction to provide the macrocycle (Scheme 2.3). The macrocyclization precursor was made in several straightforward steps from ester **2.17**. Reduction of the ester to the alcohol and temporary trityl protection followed by deprotection and acylation with bromoacetyl bromide gave macrocycle precursor **2.18**. Allylic alcohol oxidation and then submission to Reformatsky-type reaction conditions gave macrocycle **2.19** in very poor yield. The yield of this reaction could not be improved under a variety of conditions that were explored due to olefin isomerization. The MPM group is then removed and the alcohol oxidation to the aldehyde which was utilized in a Nozaki-Hiyama-Kishi reaction to append on the side chain **2.20**, thus completing the first synthesis of the enantiomer of haterumalide NA as its methyl ester **2.21**.

Scheme 2.3. Completion of the Synthesis of *ent*-Haterumalide NA.



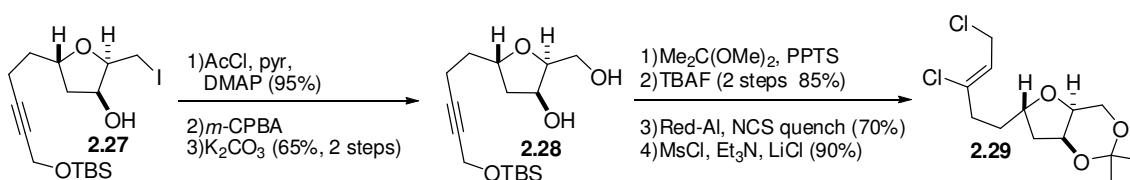
The second synthesis of *ent*-haterumalide NA (2.1) was accomplished later that year by Snider and co-workers.⁹⁴ Their synthesis of the THF core begins with allylic alcohol **2.22** which can be obtained through a vinylogous aldol reaction (Scheme 2.4). Alcohol **2.22** was first deprotected to unveil the ketone which was reduced to give diol **2.23**. Diol **2.23** was then protected as its acetonide and the ester was completely reduced to the alcohol. This primary alcohol was converted to iodide **2.24** *via* the mesylate. Lithio-acetylene **2.25** was then coupled and following deprotection of the acetonide gave diol **2.26**. Finally, an iodo-etherification procedure gave THF **2.27** in good yield.

Scheme 2.4. Snider's Route to the THF Core of Haterumalide NA.



The alcohol of THF **2.27** was then acylated and the iodide oxidized to the corresponding iodoso compound (Scheme 2.5). Potassium carbonate hydrolyzed both the iodoso and the ester functionalities to give diol **2.28**. The two alcohols were protected as their acetonide and the TBS group was removed with fluoride. Hydroalumination of the intermediate alcohol with Red-Al and the oxidation of alkenyl aluminium by *N*-chlorosuccinimide provided the chloro-alkene. The allylic alcohol was then transformed into allyl chloride **2.29** by the use of mesyl chloride in conjunction with lithium chloride.

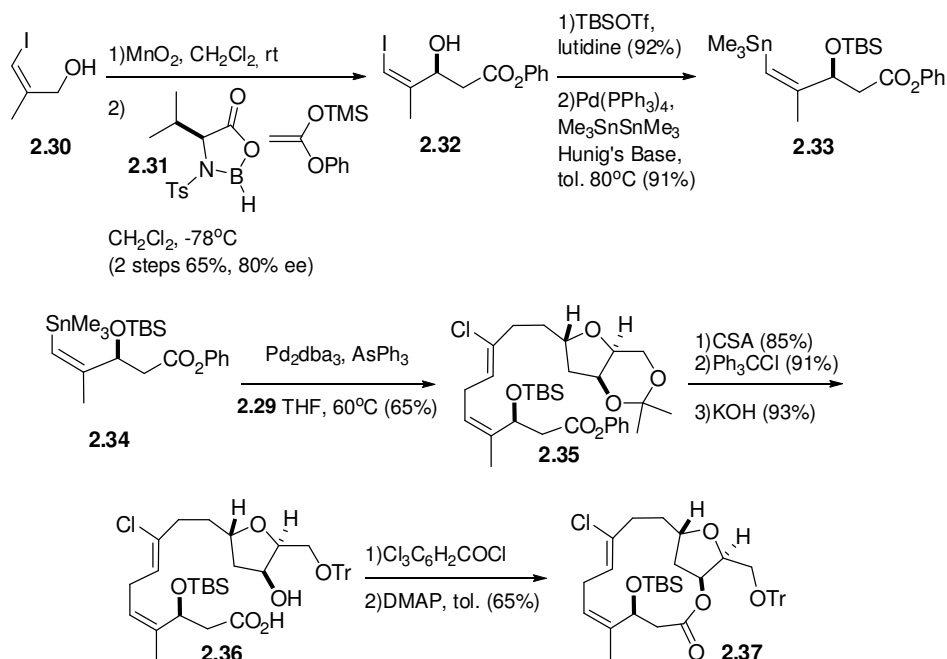
Scheme 2.5. Synthesis of Allyl Chloride **2.29**.



Synthesis of the Stille coupling partner for allyl chloride **2.29** began with known alcohol **2.30**, which was oxidized to the aldehyde and then underwent an aldol reaction in the presence of chiral Lewis acid **2.31** to give alcohol **2.32** (Scheme 2.6). Alcohol **2.32** was protected as its TBS ether, and the iodine was exchanged for a trimethylstannyl group under palladium catalysis to give vinyl stannane **2.33**. With both coupling partners in hand, the Stille coupling between vinyl stannane **2.33** and allyl chloride **2.29** was undertaken to give THF **2.35** in good yield. Next deprotection of the acetonide under acidic conditions followed by trityl protection of the primary alcohol and basic hydrolysis of the phenolic ester gave acid **2.36** ready for macrocyclization. Macrocyclization is accomplished using a two step Yamaguchi protocol to afford macrocycle **2.37**.

Completion of the synthesis of haterumalide NA methyl ester is brought about by deprotection of the hydroxyl at C3 and acylation followed by coupling with the side chain by the method developed by Kigoshi.

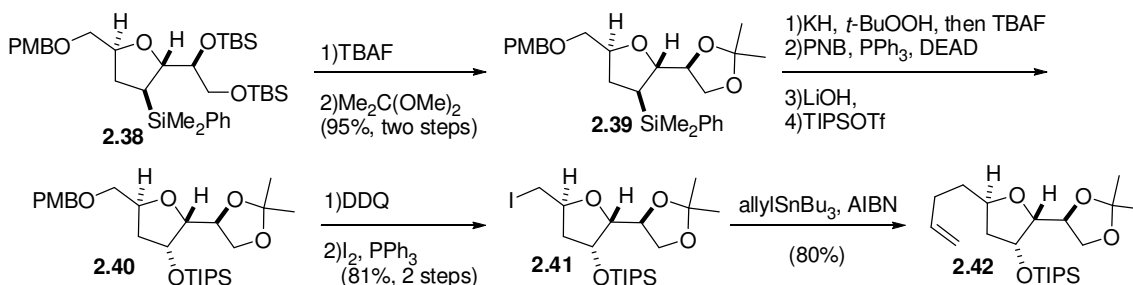
Scheme 2.6. End Game of Snider's Synthesis of *ent*-Haterumalide NA Methyl Ester.



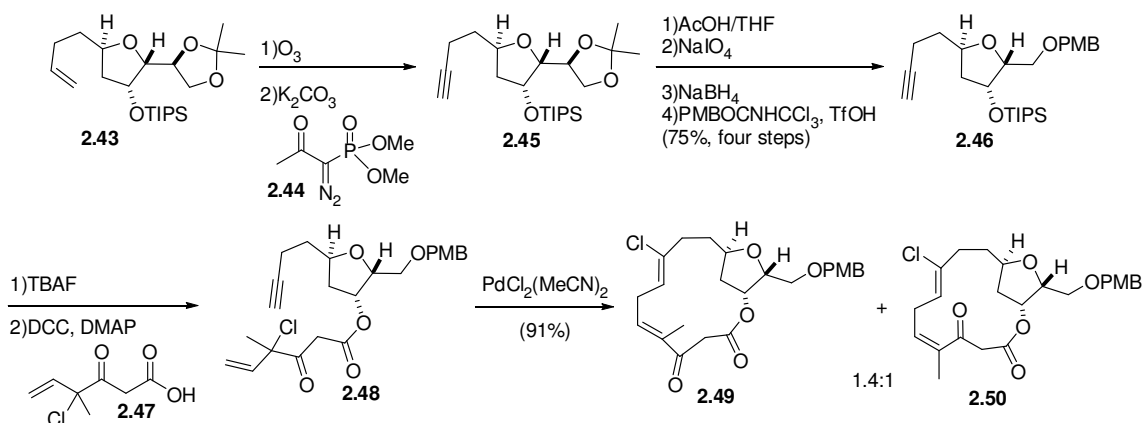
The only synthesis of the correct enantiomer of haterumalide NA (**2.1**) was carried out by Hoyer and co-workers.⁹⁵ Hoyer's synthesis began with advanced silane **2.38** which was available in several steps by methodology developed by Roush and Micalizio (Scheme 2.7).⁹⁷ A protecting group switch from silyl ether **2.38** to acetonide **2.39** was uneventfully accomplished in two steps. Tamao-Fleming oxidation of the silane **2.39** to the alcohol and subsequent inversion using the Mitsunobu protocol yielded acetonide **2.40** after hydrolysis and protection as the silyl ether. DDQ removal of the PMB group followed by exposure to iodine in the presence of triphenylphosphine

gave iodide **2.41**. Homologation of iodide **2.41** by three carbon atoms was accomplished by a radical process to give alkene **2.42**.

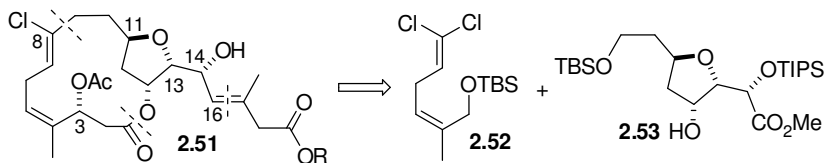
Scheme 2.7. Synthesis of THF **2.42**.



Alkene **2.42** was then converted to the corresponding alkyne by a two step procedure. First, ozonolysis of the alkene to the aldehyde and then alkynylation with diazophosphonate **2.44** gave alkyne **2.45** (Scheme 2.8). The acetonide of alkyne **2.45** was removed under acidic conditions and the resulting diol was oxidatively cleaved to the aldehyde. This aldehyde was then reduced with sodium borohydride and the resulting alcohol was then protected to give alkyne **2.46**. Next, the TIPS group was removed by the action of fluoride and coupling with acid **2.47** which gave ester **2.48**. The key alkyne haloallylation reaction was carried out by reaction of alkyne **2.48** with a palladium catalyst to obtain the macrocycle in good overall yield as a 1.4 to 1 mixture of geometrical isomers and unfortunately, the desired (*Z*)-olefin was the minor product **2.50**. This macrocycle however was carried forward in a similar sequence to that of Kigoshi and Snider to finish the synthesis of the natural enantiomer of haterumalide NA (**2.1**).

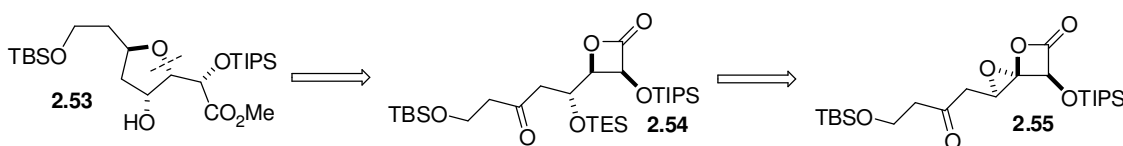
Scheme 2.8. Completion of the Synthesis of (-)-Hateumalide NA.**Retrosynthetic Analysis of the Haterumalides**

The combination of interesting structure and biological activity initially drew our attention to this class of natural products. In our original retrosynthesis, we envisioned that haterumalide NA could be constructed *via* three major disconnections (Scheme 2.9). We envisioned that the C8-C9 bond could be constructed through a transition metal catalyzed coupling. The macrolactone could be formed from a β -lactone derived from diene **2.52** as the hydroxyl at C12 is somewhat hindered and would require a reactive acylating agent.^{93, 98} Finally, the side chain could be appended by an appropriate olefination reaction with the aldehyde derived from ester **2.53**.

Scheme 2.9. Retrosynthetic Analysis of Haterumalide NA.

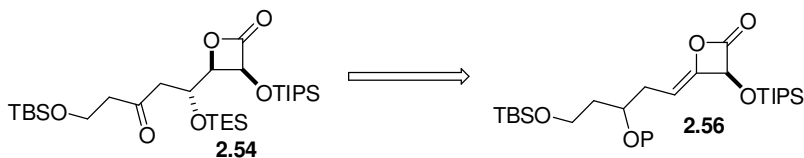
We next envisioned that the tetrahydrofuran core **2.53** of the haterumalides could be prepared from an appropriately functionalized *cis*- β -lactone such as **2.54** (Scheme 2.10). This β -lactone would give rise to the desired tetrahydrofuran **2.53** by a Lewis acid mediated cyclization developed by Mead.⁹⁹ Reduction of the intermediate oxocarbenium ion is predicted to give the *trans*-tetrahydrofuran using the model developed by Woerpel for similar substrates.¹⁰⁰ While the construction of *cis*- β -lactones are well documented¹⁰¹, γ -siloxy-*cis*- β -lactones have not been previously described. The lack of routes to γ -siloxy-*cis*- β -lactone such as β -lactone **2.54** led us to consider the development of methods for their preparation and in particular we were attracted to studying the potential for regio- and diastereoselective reduction of spiroepoxy- β -lactones **2.55**.

Scheme 2.10. Retrosynthesis of THF **2.53**.



Calter demonstrated that ketene homo-dimers can be prepared by cinchona alkaloid catalyzed dimerizations in good yields and with high enantioselectivities.¹⁰² This method could potentially be applied to the construction of β -lactone **2.54** by oxidation of the olefin present in hetero-ketene dimer **2.56** (Scheme 2.11). We predicted that oxidation of the olefin would take place opposite to the α -substituent due to steric interactions between the oxidant and the substituent. To explore the viability of this route we set out to explore a model study using ketene-homo dimers as substrates.

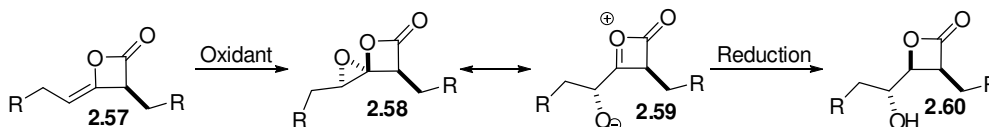
Scheme 2.11. Retrosynthesis of β -Lactone **2.54**.



Model Studies Toward the Oxidation of Ketene-Homo Dimers

Our attention focused on developing appropriate oxidation conditions that would provide the desired γ -oxygenation while leaving the β -lactone nucleus intact (Scheme 2.12).¹⁰³ It was assumed that epoxidation would result in an intermediate spiroepoxy- β -lactone **2.58** that might be highly unstable and therefore be reduced *in situ* to the desired β -lactone **2.60**. Reduction would favor formation of an oxocarbenium ion such as **2.59** over that generated from the epoxide based on ring strain considerations.

Scheme 2.12. Epoxidation and Reduction of Ketene-Homo Dimers.



We next set out to explore oxidation conditions and the first oxidant that was explored was *m*-CPBA. Not surprisingly acidic *m*-CPBA even with buffering conditions gave multiple products. It was obvious from this result that the oxidation would necessitate milder conditions. The next oxidant chosen to fit these requirements was DMDO, a mild non-nucleophilic and neutral oxidant.³⁷ However, exposure of dimer **2.61** to DMDO at low temperatures lead to no reaction (Table 2.1, entry 2). We were

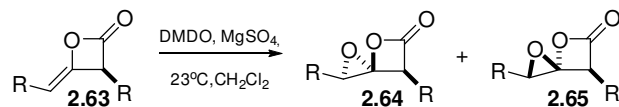
pleased to find that exposure of dimer **2.61** to freshly prepared DMDO at ambient temperature led to the production of a single product. Secure assignment of the structure of this compound as spiroepoxy- β -lactone **2.62** was delayed stability to silica gel chromatography but tentatively assigned at this point based on NMR, MS, and IR.

Table 2.1. Exploration of Epoxidation Conditions of Ketene-Homo Dimers.

Reaction scheme: Ketene-homo dimer **2.61** (a molecule with a ketene group and a lactone ring) reacts under 'Conditions' to form spiroepoxy- β -lactone **2.62** (where the ketene group has been converted to an epoxide ring fused to the lactone).

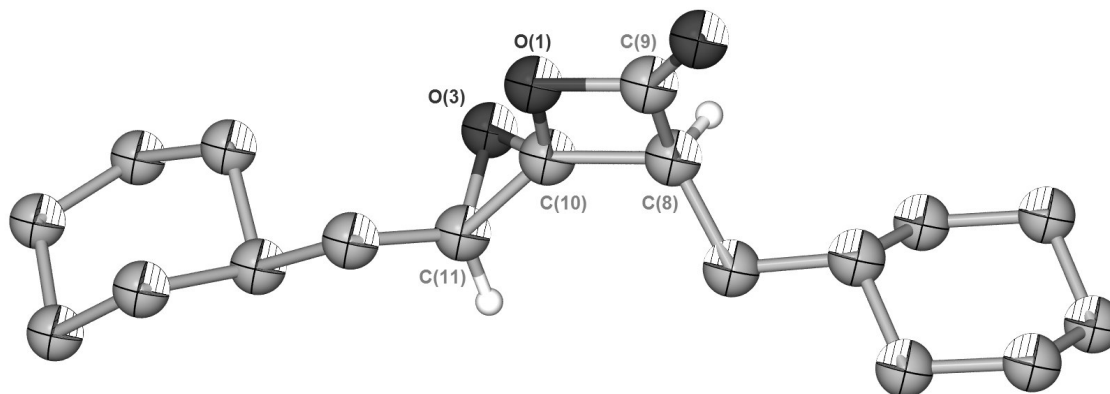
Entry	Conditions	Outcome
1	<i>m</i> -CPBA, NaHCO ₃ , CH ₂ Cl ₂ , 0°C	Multiple products
2	DMDO, CH ₂ Cl ₂ , -78°C	No reaction
3	DMDO, CH ₂ Cl ₂ , 23°C	Single stable product

To give further support to the structural assignment of the oxidation product structure as that of spiroepoxy- β -lactone **2.62**, we explored the scope of this oxidation (Table 2.2). Both straight chain alkyl substituents **2.62** and carbocycles **2.64a** were tolerated with good yields and diastereoselectivities (entries 1 and 2). Aromatic groups **2.64b** were also tolerated but with reduced yields. Additional functionality in the form of protected alcohols **2.64c** was also tolerated but with reduced yield but high diastereoselectivity. Finally an azido functionality in adduct **2.64d** was also tolerated in moderate yield and good diastereoselectivity (entry 5).

Table 2.2. Substrate Scope of the Epoxidation of Ketene-Homo Dimers.

Entry	Dimer	Yield	dr (2.64 : 2.65)	Product
1	<i>n</i> -Bu	80	14:1	2.62
2	CyCH ₂	76	10:1	2.64a
3	PhCH ₂	57	24:1	2.64b
4	TIPSO(CH ₂) ₄	40	17:1	2.64c
5	N ₃ (CH ₂) ₄	61	16:1	2.64d

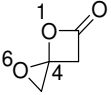
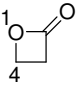

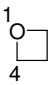
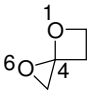
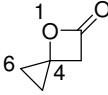
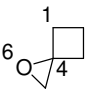
During this exploration of substrate scope, we were pleased to find that spiroepoxy- β -lactone **2.64a** was a crystalline solid suitable for X-ray diffraction analysis. The X-ray structure of spiroepoxy- β -lactone **2.64a** revealed several interesting physical features (Table 2.3). First, the C11-O3 bond is slightly lengthened to 1.486 Å when compared to the average bond length from crystallographic data that was deposited with the Cambridge Crystallographic Data Center, from a more typical length of 1.446 Å.¹⁰⁴ Additionally, the C10-O3 bond of the epoxide spiro-center has been significantly shortened to the observed 1.380 Å from the average of 1.446 Å. Finally the C10-O1 bond is slightly shortened to 1.448 Å from the more typical 1.492 Å. Taken together this data could have two possible explanations for the observed bond lengths.

Table 2.3. X-ray Structure of Spiroepoxy- β -Lactone **2.64a** and Selected Bond Lengths.

Entry	Bond	Observed Length	Average Length
1	C11-O3	1.486	1.446
2	C10-O3	1.380	1.446
3	C10-O1	1.448	1.492

One explanation is due to the unusual bonding observed with small rings. Due to the increased strain associated with three and four membered rings the hybridization at the atoms within the ring have an increased p-orbital character to help alleviate some of this strain. With this increase in p-orbital character within the ring there is an increase in s-orbital character in the exocyclic bonds and thus an associated shortening.¹⁰⁵ To address the possibility that the observed shortening is due to hybridization effects the optimized structures of this and related ring systems were calculated at the B3LYP/6-31+G**+zpe level of theory.¹⁰⁶ As can be seen from Table 2.4, the hybridization effects do account for some of the shortening observed in the ring system. However, based on calculations hybridization effects do not account for all of the observed bond shortening.

Table 2.4. Observed and Calculated Bond Lengths (Å) for Spiroepoxy- β -Lactone **2.64a** and Related Ring Systems.

Ring System Bond							
X1-C4	1.448 ^a	1.492 ^b	-	1.452 ^b	1.415 ^c	1.458 ^c	1.531 ^c
C4-X6	1.380 ^a	-	1.446 ^b	-	1.399 ^c	1.487 ^c	1.423 ^c
C4-C5	1.437 ^a	-	1.466 ^b	-	1.461 ^c	1.487 ^c	1.467 ^c
C5-X6	1.486 ^a	-	-	-	1.464 ^c	1.527 ^c	1.445 ^c

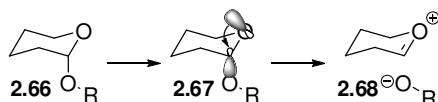
^aObserved bond lengths for spiroepoxy- β -lactone **2.63a**. ^bAveraged bond lengths from those available in the Cambridge Crystallographic Data Centre.¹⁰⁴ ^cCalculated bond lengths for optimized structures.

Since the observed bond shortening cannot be accounted for by hybridization effects alone another phenomenon must also be present to explain these results. Given that this ring system is an acetal, one such phenomenon that could explain these results is the anomeric effect.

The anomeric effect is a phenomenon that is observed in systems in which one of the carbon atoms bears two heteroatoms, typically oxygen but most heteroatoms will participate to varying degrees.¹⁰⁷ Due to the lone pairs of electrons on the heteroatom and the polarization of the other carbon-heteroatom bond, there is a donation of the non-bonding lone pair of electrons into the σ^* anti-bonding orbital of the geminal carbon-heteroatom bond. The result of this donation of electron density is simplistically depicted in Scheme 2.13 structure **2.68**. Namely, there is a pronounced increase in double bond

character in the first carbon heteroatom bond and thus a bond shortening is observed. The other carbon-heteroatom bond is weakened due to donation into the anti-bonding orbital resulting in an observed bond lengthening.

Scheme 2.13. Depiction of the Anomeric Effect.



We considered whether simple anomeric effects could account for the observed differences in the bond lengths seen in the crystal structure of spiroepoxy- β -lactone **2.64a**. First, a distinct bond shortening of the C10-O3 bond would be expected concurrently with a bond lengthening of the C10-O1 bond. However, this still does not explain the observed results as the C10-O3 bond is shortened, but the C10-O1 bond is not lengthened but rather shortened to some degree, 0.044 Å. Therefore, the best description of this ring system is one in which there is not one anomeric effect but in fact two anomeric effects. This would explain the observed bond shortening of the C10-O3 bond and the bond shortening of the C10-O1 bond. This is surprising given the increased strain that would be accompanied by the increase in double bond character of the epoxide ring. This effect may be a consequence of the constrained geometry of the ring system which leads to the observed anomeric effects.

Conclusions

In conclusion, we oxidized ketene-homo dimers to their corresponding spiroepoxy- β -lactones. Oxidation was accomplished by using the mild, neutral, and non-

nucleophilic oxidizing agent DMDO in moderate to good yields for a variety of functionalized substrates. We obtained a crystal structure of this novel ring system and several interesting physical characteristics were gleaned from analysis of the structure and comparison to related spiro ring systems. Finally, through the use of calculations, we determined that this ring system likely possesses a double anomeric effect which would account for the observed physical features observed in the crystal structure. The observed physical data hints at the possible reactivities that will be observed.

CHAPTER III

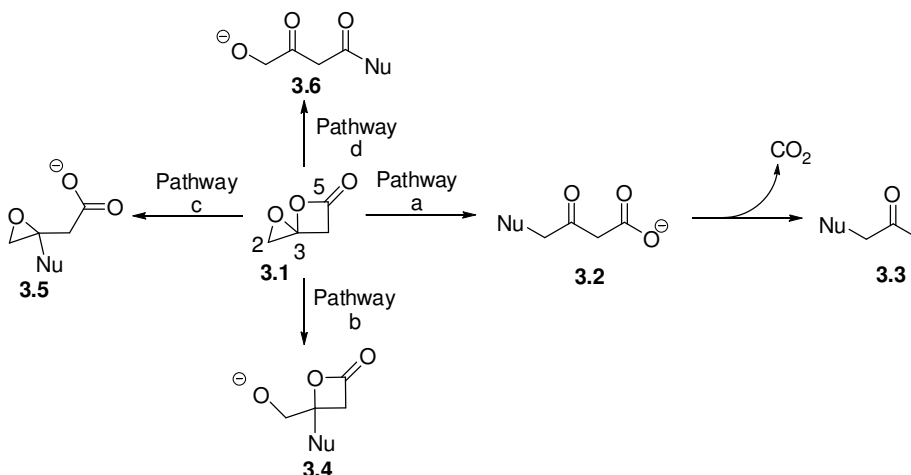
A SURVEY OF THE REACTIVITY OF SPIROEPOXY- β -LACTONES AND STUDIES TOWARD MACULALACTONE A⁸⁸

Introduction

Several other spiro-acetals have been recently shown to have an interesting and varied reactivity profile (See chapter I). This inspired us to conduct a similar investigation into the reactivity of the novel ring system 1,4-dioxaspiro[2.3]hexanone **3.1** ring system. Considering the functionalities present in this ring system there are four possible modes of reactivity with a nucleophile that were envisioned (Scheme 3.1). The first mode is addition to the distal epoxide C-O bond, pathway 'a'. This mode of addition would lead to a γ -substituted β -keto-carboxylate **3.2** as an initial product. This product would likely undergo a facile decarboxylation to yield α -substituted ketones **3.3** as the ultimate product. The second mode involves addition to an oxocarbenium derived from cleavage of the epoxide ring at the spirocenter. This would result in a γ -hydroxy- β -lactone **3.4** which was the initially desired reaction manifold to obtain the requisite β -lactone for haterumalide synthesis. Alternatively, a nucleophile could add to an oxocarbenium derived from cleavage of the β -lactone ring at the spirocenter instead of the epoxide (pathway 'c'). This cleavage would result in the formation of an epoxy-acid **3.5** as the product. The final mode involves nucleophilic addition at the β -lactone carbonyl leading to acylation and cleavage of both rings to initially yield a γ -hydroxy- β -keto-acid **3.6**. With these possible reaction manifolds in mind we set out to explore a variety of nucleophiles and reaction conditions to ascertain the preferred reaction

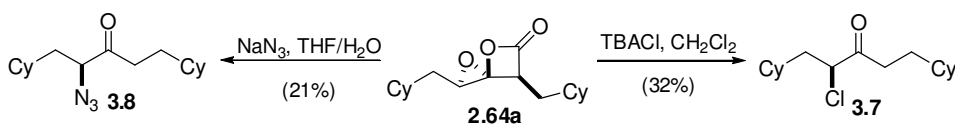
pathways for a given nucleophile. Ultimately we expected to apply discovered conditions leading to reaction manifold type 'b' to the synthesis of the tetrahydrofuran of the haterumalides.

Scheme 3.1. Modes of Nucleophilic Addition to 1,4-Dioxaspiro[2.3]hexanones.



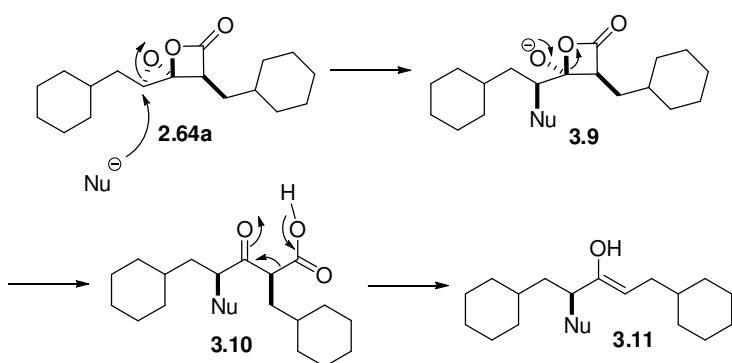
When spiroepoxy- β -lactone **2.64a** was exposed to tetrabutylammonium chloride, the major isolated product was α -chloroketone **3.7** in low yield. Similarly, when the same spirocompound was exposed to sodium azide in a THF/H₂O mixture α -azidoketone **3.8** was obtained in low yield. These reactions are examples of nucleophilic addition by pathway 'a'.

Scheme 3.2. Nucleophilic Additions to Spiroepoxy- β -Lactone **2.64a** (Pathway 'a').



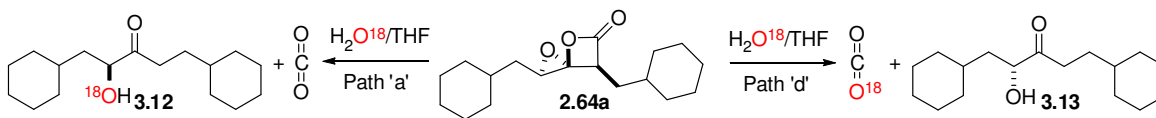
The proposed mechanism for these additions is outlined in Scheme 3.3. Attack of the nucleophile to the distal epoxide C-O bond would result in hemiketal **3.9** which would collapse to give the intermediate keto-carboxylate **3.10**. This intermediate likely undergoes facile decarboxylation to yield enolate **3.11** and ultimately ketone **3.7** after protonation.

Scheme 3.3. Proposed Mechanism of Chloride and Azide Addition.



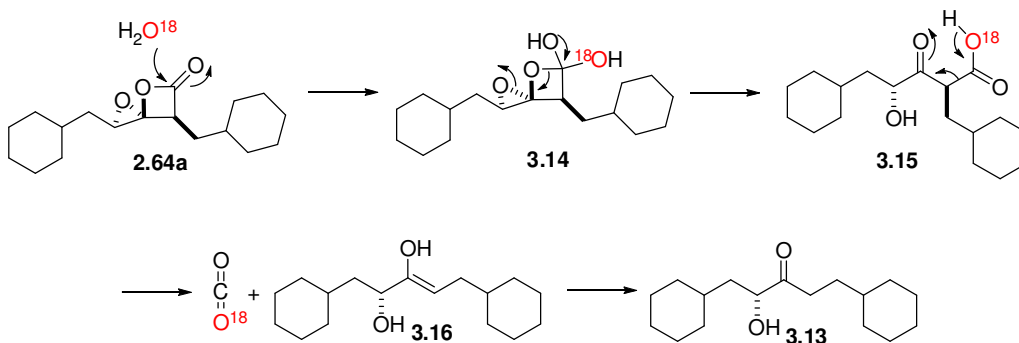
The reaction of spiroepoxy-β-lactone **2.64a** with water over protracted periods of time led to α-hydroxy ketone **3.12**. Mechanistically, there are two routes that could provide the same ketone product. In an effort to distinguish between these two different reaction pathways, the reaction was repeated with isotopically enriched water containing 90% O¹⁸. The two reaction pathways are: (1) addition through reaction pathway ‘a’ which would result in the product incorporating and retaining the oxygen-18 isotope, ketone **3.12** (Scheme 3.4) (2) addition to the β-lactone carbonyl (pathway ‘d’), which would result in the incorporation of the oxygen-18 into the carbon dioxide derived from decarboxylation and thus no isotope incorporation into ketone **3.11** (Scheme 3.4).

Scheme 3.4. Possible Pathways for Addition of Water to Spiroepoxy- β -Lactone **2.64a**.



Pathway 'd' would result in loss of labeled carbon dioxide by a process outlined in Scheme 3.5. Addition of labeled water to the carbonyl of the β -lactone ring of **2.64a** would result in tetrahedral intermediate **3.14** which would then undergo cleavage of both rings to generate keto-acid **3.15**. Keto-acid **3.15** can then lose carbon dioxide, containing the label, and yield enol **3.16** which tautomerizes to ketone **3.13**.

Scheme 3.5. Mechanism involving Acyl Addition/Decarboxylation (pathway 'd').



After conducting this reaction it was necessary to analyze the outcome *via* two methods, namely mass spectrometry by electrospray ionization and ^{13}C NMR. Although mass spectrometry did show an increase of two amu over the control experiment for the ketone **3.12**, ^{13}C NMR would ensure the position of the label as it is well-known that oxygen can be incorporated into ketones through exchange with water molecules under

both acid and base catalysis.^{108, 109} ^{13}C NMR studies were undertaken to determine the site of oxygen-18 incorporation by observation of the slight shielding effect of the ^{18}O isotope versus ^{16}O on a ^{13}C atom.¹¹⁰

Analysis of this shielding effect by ^{13}C NMR would distinguish incorporation of ^{18}O at the alcohol carbon or the carbonyl carbon. As seen in Figure 3.1a, an upfield shift is observed for the labeled α -hydroxyl bearing ^{13}C with a small shoulder corresponding to residual H_2^{16}O incorporation. A ~1:1 mixture of ^{13}C derived from addition of a ~1:1 mixture of ^{18}O enriched and normal water confirms the labeling of this position (Figure 3.1b). Expansion of the carbonyl region did not show shift differences expected for incorporation of ^{18}O at the carbonyl carbon.

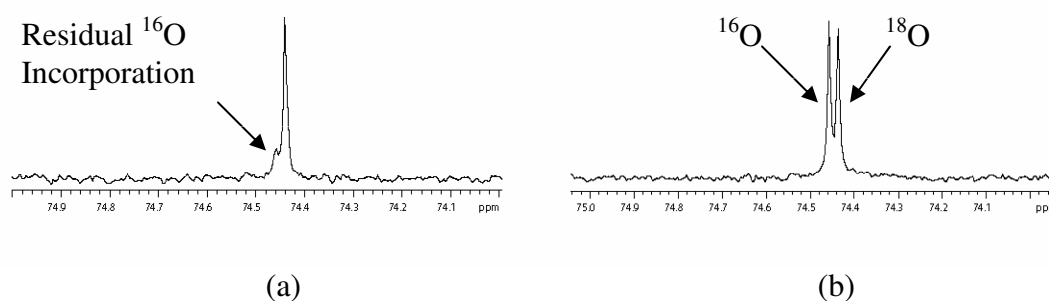
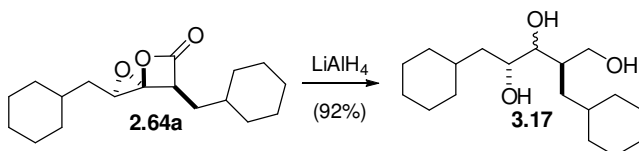


Figure 3.1. ^{13}C NMR spectral expansion of carbinol region of α -hydroxy ketone **3.12** following: (a,) reaction with 90% atom H_2^{18}O . (b) reaction with ~1:1 mixture of ^{18}O enriched and normal H_2^{16}O water above in Figure.

Reduction of the spiroepoxy- β -lactone **2.64a** with lithium aluminum hydride gave the corresponding triol **3.17** in excellent yield (Scheme 3.6). The nucleophilic addition of hydride is a result of initial addition to the carbonyl carbon, (pathway 'd') since no

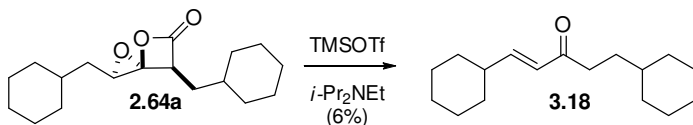
deoxygenation is observed at C4 or C5 and this is also consistent with reduction of β -lactones with metal hydrides leading to acyl C-O versus C-O alkyl cleavage. Also, the product reduction of the β -lactone carbonyl reveals an α -hydroxy ketone which is then reduced to the observed triol **3.17**. Attempts to effect the desired reduction for haterumalide under Lewis acidic conditions, ZnCl_2 , $\text{BF}_3\cdot\text{OEt}_2$, etc. in combination with reducing agents led to either no reaction or complex mixtures of products.

Scheme 3.6. Metal Hydride Reduction of Spiroepoxy- β -Lactone **2.64a**.



Spiroepoxy- β -lactone **2.64a** also reacts with base in the presence of Lewis acid to provide a small amount of α,β -unsaturated ketone **3.18** in low yield (Scheme 3.7). This reaction represents a different reaction pathway than those outlined in Scheme 3.1, but not uncommon to similar systems (*cf.* Chapter I).

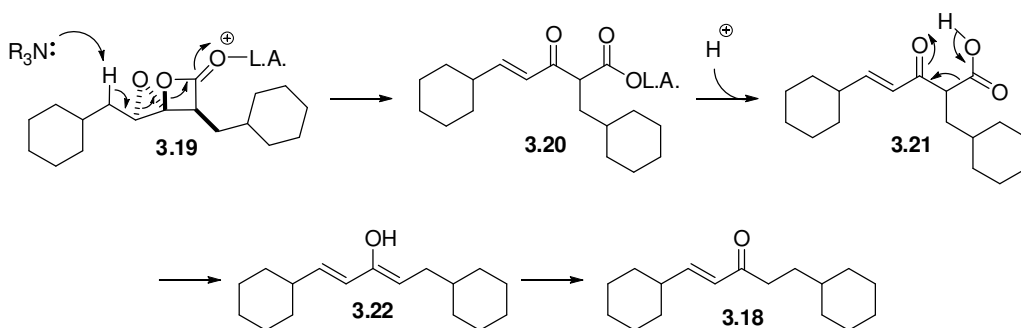
Scheme 3.7. Elimination of Spiroepoxy- β -Lactone **2.64a**.



The proposed mechanism for this elimination is outlined Scheme 3.8. Activation of the carbonyl of the β -lactone ring, such as Lewis acid complex **3.19**, leads to

deprotonation with the amine present and loss of both rings to yield keto-carboxylate **3.20**. Upon workup the carboxylate is protonated to give keto-acid **3.21** which decarboxylates to yield enol **3.22**. Tautomerization of enol **3.22** leads to the observed α,β -unsaturated ketone **3.18**.

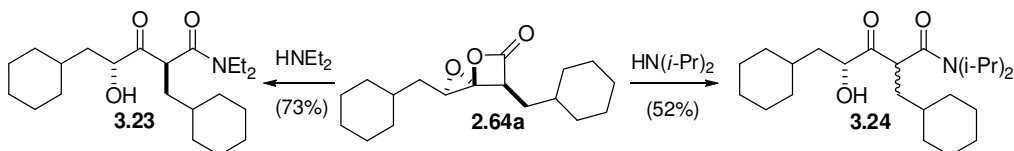
Scheme 3.8. Mechanism of Lewis Acid Induced Elimination of Spiroepoxy- β -Lactone **2.64a**.



Exposure of a single diastereomer of spiroepoxy- β -lactone **2.64a** to two different amines two different reaction manifolds were observed. Reaction with the less sterically hindered diethylamine resulted in a single diastereomer of a β -keto-amide **3.23** resulting from simple nucleophilic addition through pathway 'd' (Scheme 3.8). However, when spiroepoxy- β -lactone **2.64a** was exposed to a more sterically hindered amine, diisopropylamine, it surprisingly resulted in an essentially 1:1 mixture of diastereomeric keto-amides **3.24**. While this initial result was intriguing our only viable initial hypothesis was that the reaction had to proceed through an intermediate in which the α -stereocenter was lost prior to or as a result of nucleophilic addition of the amine. This was assumed due to $A^{1,3}$ strain which severely retard the epimerization of α -substituted β -

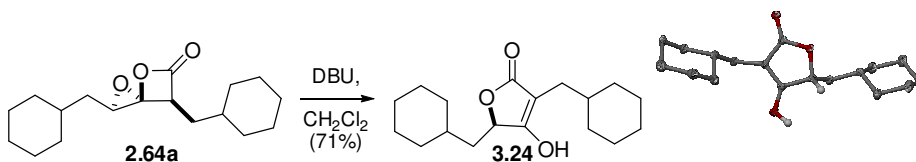
ketoamides.¹¹¹ In fact it was found that exposure of a single diastereomer of diethyl amide **3.23** to deuterated diisopropylamine led to no incorporation of deuterium suggestive of no epimerization of that center over 4 h.

Scheme 3.8. Reaction of Spiroepoxy- β -Lactone **2.64a** with Amines.



Interestingly, when spiroepoxy- β -lactone **2.64a** was exposed to the tertiary base diazabicycloundecane (DBU), the tetronic acid derivative **3.24** was obtained as the sole product (Scheme 3.9). The structure was confirmed by X-ray structure. This result inconjunction with the previous results with secondary amines intrigued us and required a mechanistic rationale.

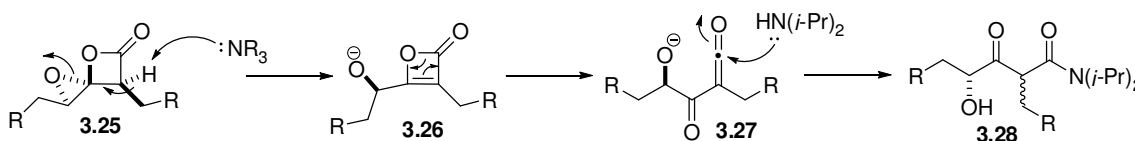
Scheme 3.9. Base-Induced Rearrangement of Spiroepoxy- β -Lactones.



With these results in hand, we considered two possible explanations for the observed results. The first possibility is that the amine directly deprotonates spiroepoxy- β -lactone **3.25** with loss of the epoxide ring to form oxet-3-en-2-one intermediate **3.26**

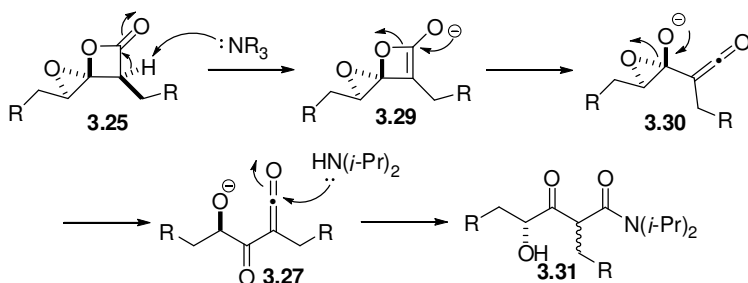
(Scheme 3.10) which may undergo a retro[2+2] reaction to form keto-ketene intermediate **3.27**. The formation of keto-ketene **3.27** rationalizes the loss of relative stereochemistry which is observed during generation of tertiary amide **3.28**.

Scheme 3.10. One Possible Mechanism for the Observed Outcomes.



An alternative mechanism involves deprotonation at the α -position of the β -lactone leading to the formation of enolate **3.29**, which then undergoes ring cleavage to form tetrahedral intermediate **3.30** (Scheme 3.11). Subsequent epoxide ring cleavage would yield the previously described keto-ketene intermediate **3.27** which ultimately leads to β -keto-amide **3.31** with loss of the stereochemistry at the α -carbon.

Scheme 3.11. Alternative Mechanism Leading to Amide **3.24**.



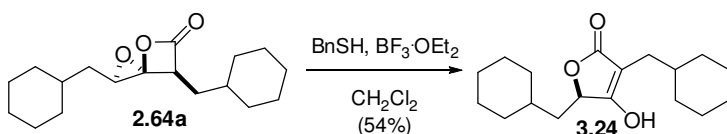
In order to provide support for one of these mechanistic possibilities, we set out to study this reaction by *in situ* IR since ketenes produce a very easily discriminated absorption band in the infrared spectrum, at 2100 cm^{-1} . Unfortunately, we were unable to

observe this intermediate at ambient or low temperatures which does not exclude the possibility of a ketene intermediate as it may simply be a short-lived intermediate and thus not readily detected by IR.

An alternative method to provide evidence for a keto-ketene **3.27** as an intermediate is through direct trapping of a putative ketene intermediate with reagents known to react rapidly with ketenes such as TEMPO which leads to esters containing two TEMPO molecules.¹¹² However, it should be noted that we recognized that this would be challenging as we were attempting to trap an intermediate in an intermolecular fashion which must be competitive with intramolecular cyclization of the same ketene intermediate. Several attempts led only to the expected rearrangement to a butenolide and the production of small quantities of α -hydroxy ketone **3.12** due to residual water in TEMPO.

We were interested in exploring nucleophiles that might add to alkyl C-O bonds in these systems which led us to study sulfur nucleophiles. When spiroepoxy- β -lactone **2.64a** was treated with benzyl thiol at low temperatures, $-78 \rightarrow -20$ °C, no reaction was observed and no change was observed when warmed to room temperature, 23 °C, for protracted time periods. However, when exposed to a combination of benzyl thiol and boron trifluoride diethyl etherate at -78 °C a reaction ensued which was completed in 30 min to give a moderate yield of tetronic acid **3.24** (Scheme 3.12).

Scheme 3.12. Reaction of **2.64a** with Thiol and Lewis Acid.



Having found this dichotomy between the reactivity of thiols with and without Lewis acid we set out to explore this further. A control experiment with only boron trifluoride diethyl etherate also gave tetronic acid **3.24** in good yield (79%) indicating that Lewis acid was responsible for the rearrangement. Other Lewis acids, $\text{Zn}(\text{OTf})_2$, $\text{Sn}(\text{OTf})_2$, and $\text{In}(\text{OTf})_3$ gave similar results. While the mechanism is unclear at this time it presumably involves cleavage of one of the spiro C-O bond to form an oxycarbenium intermediate which then drives the rearrangement to the tetronic acid.

The facile production of tetronic acid derivatives from these spiroepoxy- β -lactones led us to explore the possibility that this ring system might provide facile access to tetronic acid derivatives or butenolide motifs, which are common motifs in natural products.¹¹³ This led us to consider the natural product maculalactone A which possesses an interesting tribenzyl tetronic acid-like structure that might be accessible *via* a spiroepoxy- β -lactone.

Isolation and Biological Activity of the Maculalactones

Maculalactones A-M (**3.32-3.44**) were isolated from the marine cyanobacterium *Kyrtuthrix maculans* (Figure 3.2) and are a group of γ -lactone containing natural products with maculalactone A (**3.32**) being the simplest member of the family with complexity increasing in the more oxidized versions such as maculalactone K (**3.42**).¹¹⁴⁻
¹¹⁷ Of all of the members, only maculalactone A (**3.32**) has shown any significant biological activity. Maculalactone A (**3.32**) has been shown to inhibit the growth of marine bivalves on rock surfaces where *Kyrtuthrix maculans* grows. Due to this biological activity it is being explored as an additive to paints as an anti-fouling agent.

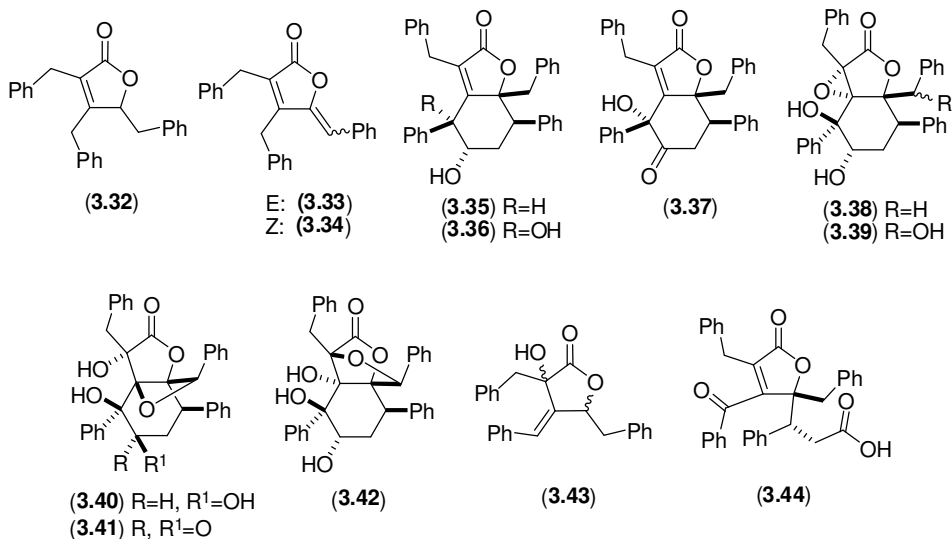
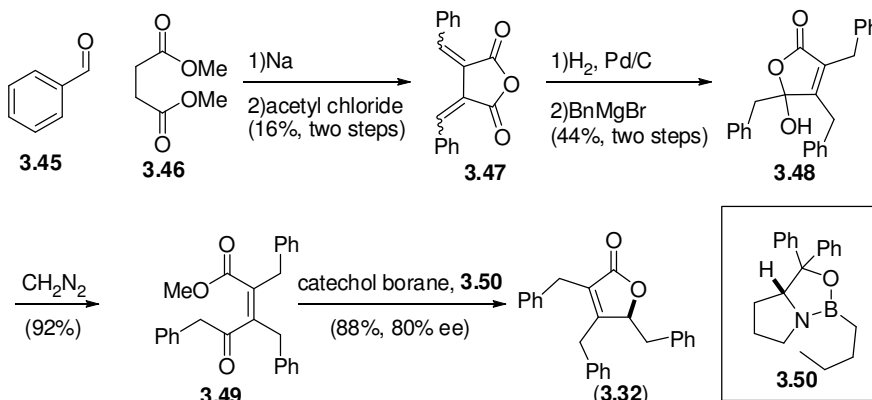


Figure 3.2. Structures of maculalactones A-M (3.32-3.44).

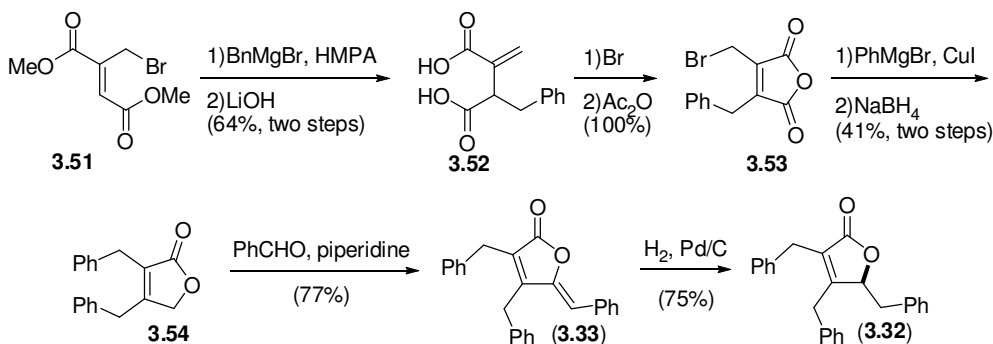
Previous Syntheses of Maculalactone A

Maculalactones A-C (3.32-3.34) has also attracted the attention of synthetic and to date there have been two syntheses of each of these natural products, including one enantioselective synthesis of maculalactone A (3.32).

The first synthesis by Brown began with Stobbe condensation of benzylaldehyde 3.45 and ester 3.46 followed by anhydride formation to give dienoate 3.47 in poor yield over the two steps (Scheme 3.13).¹¹⁸ This route was chosen due to its amenability to large scale in spite of the poor yield. Hydrogenation of anhydride 3.47 followed by addition of a benzyl Grignard reagent led to the production of alcohol 3.48. Exposure of alcohol 3.48 to diazomethane leads to ring opening and the formation of ketone 3.49 which was then reduced with catachol borane in the presence of chiral Lewis acid 3.50 in good yields and good enantiomeric excess.

Scheme 3.13. Brown's Synthesis of Maculalactone A (**3.32**).

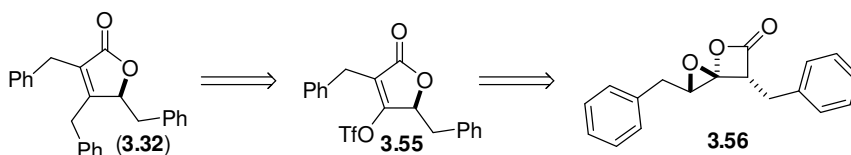
Argade's synthesis of maculalactones A (**3.32**) and B (**3.33**) begins with bromide **3.51** which is derived from citraconic anhydride (Scheme 3.14).¹¹⁹ Addition of a benzyl group in a 1,4 fashion lead to diacid **3.52** after hydrolysis of both esters. The alkene was then brominated and the anhydride **3.53** was formed by use of acetic anhydride. The bromide was then displaced with phenyl cuprate followed by complete reduction of the carbonyl to the corresponding methylene to give γ -lactone **3.54**. Following condensation with benzaldehyde to yield maculalactone B (**3.33**) was obtained. Finally, catalytic hydrogenation of maculalactone B (**3.33**) then gave racemic maculalactone A (**3.32**).

Scheme 3.14. Argade's Synthesis of Maculalactone A and B.

Retrosynthesis of Maculalactone A

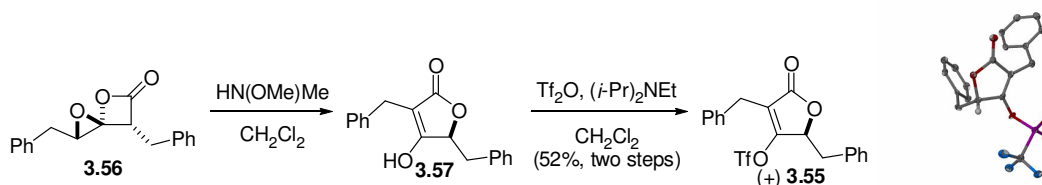
Our retrosynthesis of maculalactone A (**3.32**) begins with disconnection of the C4 benzyl group, which could be accomplished with the aid of a transition metal coupling from enol triflate **3.55** (Scheme 3.15). This triflate **3.55** could in turn be made from the corresponding tetronic acid derivative which would be derived from optically active spiroepoxy- β -lactone **3.56**.

Scheme 3.15. Retrosynthesis of Maculalactone A (**3.27**).



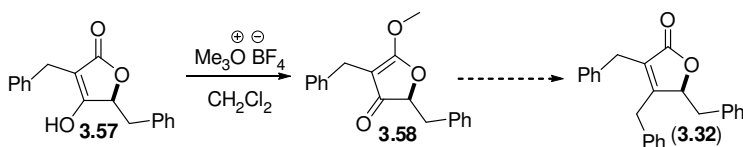
Coupling Route to Maculalactone A

Our synthesis of the required triflate **3.55** begins with optically active spiroepoxy- β -lactone **3.56**, obtained from the optically active dimer synthesized with TMSO-quinine.^{120, 121} Rearrangement with *N,O*-dimethylhydroxyamine gave the tetronic acid **3.57** (Scheme 3.16). *N,O*-dimethylhydroxyamine was used in the rearrangement as it seemed that tetronic acid **3.57** could be prone to epimerization. Due to the difficulty in purifying tetronic acid **3.57** the crude reaction mixture was then converted to the triflate **3.55** in modest yield over two steps. The position of the triflate was also confirmed by X-ray analysis.

Scheme 3.16. Synthesis of Triflate **3.55**.

Unfortunately, the coupling reaction necessary to finish the synthesis proved to be quite difficult. Attempts to couple triflate **3.55** with hypervalent tin reagents, which have been shown to be effective in sterically hindered settings, only resulted in hydrolysis of the triflate.¹²² Attempts using other transition metal catalysts, such as copper or iron, also met with failure.

As tetronic acids are veiled β -keto-lactones it was expected that revealing this functionality would be a more viable route maculalactone A (**3.32**) (Scheme 3.17). To accomplish the tetronic acid **3.57** was converted to enol ether **3.58**.¹²³ This ketone was then treated with a variety of different benzyl-metal reagents, including lithium, magnesium, cerium, however these all returned starting material. This may be due to deprotonation to form a furan type intermediate, which would not react further.

Scheme 3.17. Alternate route to Maculalactone A (**3.32**).

In conclusion we explored the reactivity of spiroepoxy- β -lactones under a variety of conditions. Out of the four possible reaction manifolds considered, it appears that the

majority of nucleophiles react through pathways 'a' or 'd' involving acyl C-O or distal epoxide C-O bond cleavage respectively. We have also shown that under basic conditions, an achiral intermediate is likely formed, possibly a keto-ketene intermediate which however could not be detected, but can undergo an intramolecular cyclization to form tetronic acid derivatives. Additionally, Lewis acid also led to tetronic acid derivatives through cleavage of one of the spiro C-O bonds to form an oxycarbenium intermediate which then rearranges to give the observed product. Finally, we have attempted to make the marine natural product maculalactone A by taking advantage of these reactivities.

CHAPTER IV

TRANS-SELECTIVE COUPLINGS OF 1,1-DICHLOROALKENES

Introduction

The stereoselective synthesis of trisubstituted alkenes under mild conditions remains a challenging problem in synthesis. Further difficulty is added when one of the three substituents is a halogen atom. In pursuit of a solution to this problem, methods have been developed for the synthesis of bromo and iodo alkenes utilizing either a trans-selective cross coupling in the case of 1,1-dibromo-alkenes¹²⁴ or modified Wittig reactions (e.g. Stork-Zhao olefination¹²⁵). However, few highly stereoselective methods exist for the corresponding reaction incorporating chlorine which would be useful due to the presence of vinyl chloride moieties in a variety of recently isolated natural products including pinnaic acid (**4.1**), taupinnaic acid (**4.2**)¹²⁶, the auranosides (**4.3**)¹²⁶ (e.g. auranoside A), halichlorine (**4.4**)¹²⁷, and the haterumalides (**2.1**)⁹⁰ (e.g. haterumalide NA) (Figure 4.1).

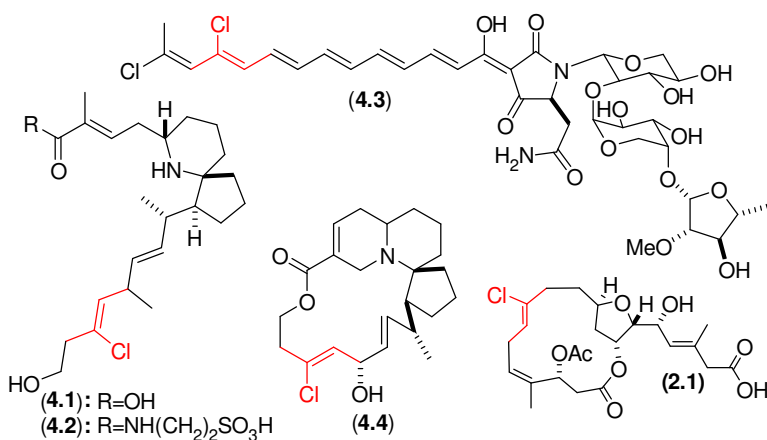
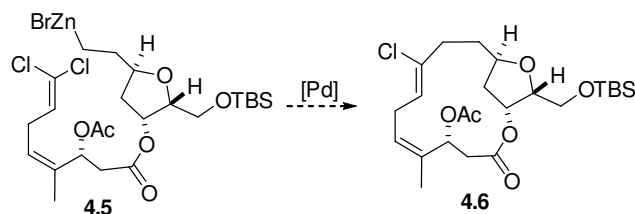


Figure 4.1. Structure of Z-chloro-dialkyl-alkene containing natural products.

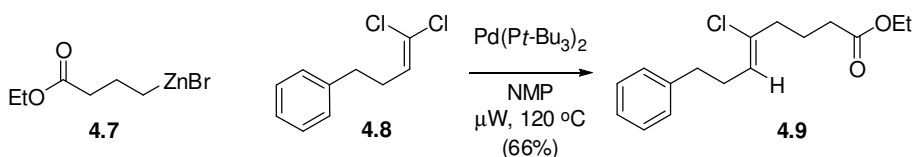
All of these natural products contain a trisubstituted alkene incorporating a chlorine atom as one of the substituents. Additionally the two alkyl groups bear a *trans* relationship to one another. This re-occurring motif led us to explore the feasibility of a trans-selective cross-coupling between a suitable nucleophile and a 1,1-dichloro-alkene under palladium catalysis. We hoped that this coupling could be used in a macrocyclization toward haterumalide NA (Scheme 4.1). Such that intramolecular coupling of skipped diene **4.5** to give macrocycle **4.6**. At the onset of our endeavor there was only one paper detailing a similar reaction.¹²⁸ However, recently there have been a few reports detailing an isolated coupling and two papers have recently appeared that explore the type of coupling in a broader context.^{129, 130}

Scheme 4.1 Proposed Coupling for Haterumalide NA.



Encouraged by the fact that great strides have recently been made with palladium catalysis as applied to a variety of very challenging substrates, *i.e.* aryl chlorides. These studies have led to the development of cross-coupling conditions employing a multitude of new catalysts and conditions.^{131, 132} We therefore embarked on screening catalysts for their ability to promote cross-coupling of dichloroolefins with nucleophiles. After screening several phosphine ligands we were very pleased to find that bis-(tri-*tert*-butylphosphine) palladium (0), recently utilized for cross-coupling with aryl chlorides, provided an initial hit for this reaction by coupling dichloroolefine **4.8** with alkyl zinc reagent **4.7** to give olefin **4.9**.¹³³

Scheme 4.2 Initial successful coupling of dichloroolefin **4.8** with zincate **4.7**.



Optimization of the Coupling

These initial studies with bis-(tri-*tert*-butylphosphine) palladium (0) coupling of 1,1-dichloroolefin and a zinc reagent derived from *tert*-butyl 4-bromobutanoate required optimization of the conditions to improve the yield of this process. Our interest in

applying this coupling in the arena of natural product synthesis dictated several requirements for this reaction. The first was that the zinc reagent used in the reaction had to be formed under mild conditions to allow for the complex functionality present in possible natural product total synthesis schemes. Additionally, we hoped to minimize the reaction times necessary since as coupling reactions especially with deactivated systems like 1,1-dichloroolefins are known to have protracted reaction times. The geminal chlorine has a deactivating effect on the initial insertion step into the C-Cl bond and subsequently the trisubstituted olefin has greater reactivity, devoid of the geminal chloride, this causing double substitution a potential problem in the process.¹²⁹ With these requirements and challenges in mind, we set out to find a procedure that would be amenable to complex settings.

Addressing the first requirement was relatively easy as there are a number of very efficient and mild protocols that have been developed for the synthesis of alkyl zinc reagents from alkyl bromides.¹³⁴ One procedure for the mild conversion of alkyl bromides to alkyl zincs and that was applied to a similar coupling employed recently by Fu involves a modified Knochel procedure, using the highly polar solvent *N,N*-dimethylacetamide. Use of this solvent is thought to facilitate insertion of metallic zinc into a carbon bromine or iodine bond at 80 °C and room temperature respectively.¹³⁵ Given that the reaction temperature and time are relatively mild we decided this would fit our requirements. Additionally, it was very attractive to use a direct metal insertion, as transmetalation conditions typically use excesses reactive lithium reagents which are not compatible with a number of functional groups that might be present in a total synthesis.

With the requirement of a functional group friendly method for generation of the zinc reagent we next turned our attention to minimize the duration of the reaction.

The advent of the microwave oven and its drastic reduction in the time it takes to cook foods, intrigued chemists for its use as a potential alternative to other heating methods including oil baths and heating mantles. However, it was not until 1986 that the first microwave assisted reaction was reported.¹³⁶ Since that time there has been an explosion of literature using microwaves to heat reactions.¹³⁶ The vast majority of these reactions exhibit an increased rate of reaction and thus significant shortening of reaction times. With this precedent and given that microwave heating had been used in similar context, the use of microwave heating was considered for the planned coupling of 1,1-dichloroolefins and alkyl zinc reagents.¹³⁷ Initially, optimization of the temperature of the reaction was studied for the coupling of dichloroolefin **4.8** and alkyl zinc **4.10** and as can be seen, at lower temperature the conversion is minimal (Table 4.1, entries 1 and 2). However there is sharp increase in conversion when the reaction is run at 100 °C, and then a decrease when the temperature is further increased to 120 °C. These results are suggestive that the optimal temperature is ~100 °C and possibly reactions above this temperature result in rapid catalyst or reagent decomposition.

Table 4.1. Optimization of Reaction Temperature for Coupling of **4.8** and **4.10**.

Entry	Temperature (°C)	Conversion ^a
1	80	5%
2	90	10%
3	100	50%
4	120	18%

^aConversion was monitored by ¹H NMR.

We next explored the reaction time and found that with only 15 minutes of heating only 14% conversion was observed (Table 4.2). However when the reaction time was increased to 2 h 52% conversion was obtained.

Table 4.2. Optimization of Reaction Time for Coupling of **4.8** and **4.10** by Microwave Heating.

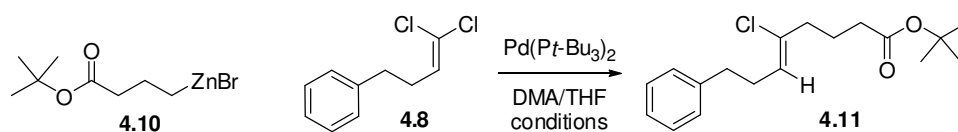
Entry	Time	Conversion ^a
1	15 minutes	14%
2	1 hour	19%
3	2 hours	52%

^aConversion was monitored by ¹H NMR.

The remaining variable to be explored was the number of equivalent of zinc reagent necessary for the reaction. It was found that the utilization of 1.5-2.5 equivalents of zinc reagent led to relatively poor conversions (entries 1-3, Table 4.3). Interestingly,

an increase to 3.0 equivalents of zinc reagent led to complete conversion. The need for a large excess of zinc reagent is unclear. The quality of the zinc reagent appeared good as ^1H NMR showed complete conversion to the alkyl zinc reagents and reaction with iodine confirmed this, the necessity of excess zinc reagent was reproducible with different batches of zinc reagent.

Table 4.3. Varying the Equivalents of Zinc Reagent for the Coupling of **4.8** and **4.10** by Microwave Heating.



Entry	Equivalents	Conversion ^a
1	1.5	18%
2	2	29%
3	2.5	35%
4	3	100%

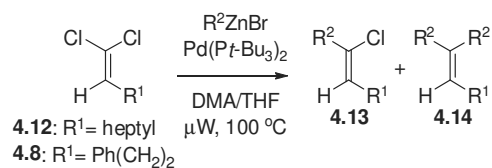
^aConversion was monitored by ^1H NMR.

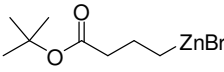
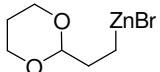
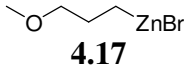
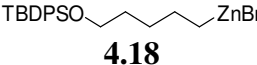
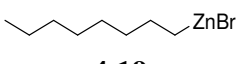
We then set out to explore the scope of the reaction using our optimized conditions described above (Table 4.4). With alkyl zinc reagents that contain a heteroatom that is 4-5 atoms away from the Zn species, the coupling reaction proceeds in moderate yield to give the monocoupled products using the standardized conditions (entries 1-4). However, when the heteroatom is absent or protected with a bulky protecting group that would prevent chelation, the reaction does not provide coupled adduct (entries 5-6). This may suggest the requirement for chelation leading to stabilization of the alkyl zinc reagent at the conditions required for the reaction or leading to a more reactive zinc reagent. Another observation was made concerning the allowed

water content of *N,N*-dimethylacetamide employed as solvent. If the water content was >100 ppm, as determined by Karl-Fischer titration, no coupling was observed even though active zinc reagent was still present, as determined by reaction with iodine. This became a frequent problem as the water content of commercial (Aldrich) *N,N*-dimethylacetamide used in this study was often over 150 ppm. To overcome this problem double distillation of the *N,N*-dimethylacetamide from barium oxide at reduced pressures was required and proved effective.

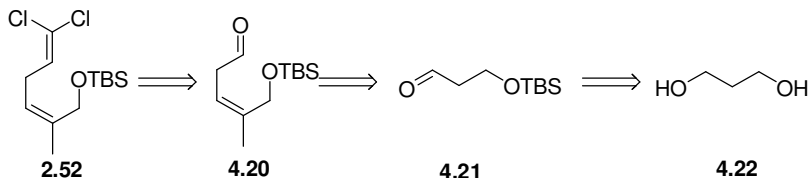
Having determined the optimal reaction conditions and briefly explored the reaction scope, we turned our attention back to our original goal of applying this reaction to natural product synthesis. As discussed in Chapter II, we planned to apply this methodology to the coupling of the western hemisphere and the THF fragment resulting in the C8-C9 bond of the haterumalides. Toward this goal, we considered various routes to diene **2.52**, which would be serviceable for an eventual total synthesis of haterumalide NA. After a survey of the literature, we found that the two most common methods for construction of the 1,1-dichloro-alkene motif were Corey-Fuchs reaction of an appropriate aldehyde with carbon tetrachloride in the presence of triphenyl phosphine¹³⁸, and reductive fragmentation of trichloromethyl group bearing an adjacent leaving group.¹³⁹ This led us to devise two retrosyntheses of diene **2.52** with the first employing aldehyde **4.20** using a Corey-Fuchs protocol. While this strategy was straight-forward since all proposed steps were precedented, there were two potential problems with this route. The first being the intermediacy of a volatile siloxy-aldehyde **4.21**¹⁴⁰ and the the other being the Corey-Fuchs reaction on an enolizable aldehyde. Ultimately consideration of these problems led to the exploration of an alternate one.¹³³

Table 4.4. Scope of the Coupling of a Model 1,1-Dichloroolefins **4.12** and **4.8** and Various Alkyl Zinc Reagents.

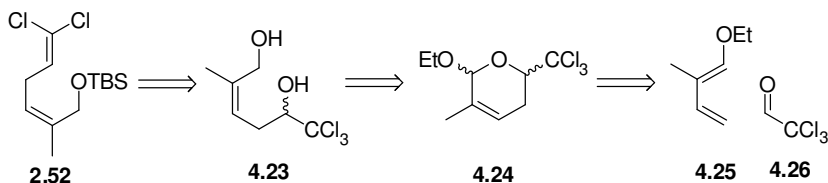


Entry	R ¹	R ²	Product/ Ratio	yield ^a
1	4.12	$\text{NC}-\text{CH}_2\text{CH}_2\text{CH}_2\text{ZnBr}$ 4.15	4.13a:4.14a 100:0	52%
2	4.8	 4.10	4.13b:4.14b 100:0	60%
3	4.12	 4.16	4.13c:4.14c 100:0	39%
4	4.8	 4.17	4.13d:4.14d 100:0	40%
5	4.8	 4.18	NR ^b	0%
6	4.12	 4.19	NR ^b	0%

^a Refers to isolated yields. ^b No reaction.

Scheme 4.3. First Retrosynthesis of Diene **2.52**

The second retrosynthesis considered for diene **2.52** would begin with a reductive fragmentation to yield the 1,1-dichloro-alkene and protection of the allylic alcohol to give diol **4.23**. This would be constructed by either reductive cleavage or hydrolysis of acetal **4.24** followed by reduction of the corresponding aldehyde and protection. Pyran **4.24** would be constructed from known ethoxy-diene **4.25** and chloral **4.26** in a hetero-Diels-Alder reaction.¹⁴¹

Scheme 4.4. Second Generation Retrosynthesis of Diene **2.52**.**Attempted Synthesis of Diene 2.52**

The synthesis of diene **2.52** began with the hetero-Diels-Alder reaction between ethoxy-diene **4.25**, available in two steps from tiglic aldehyde, and chloral **4.26** to give pyran **4.24** in moderate yields on gram scale.¹⁴¹ The use of toluene was crucial as other solvents led to very low yields.

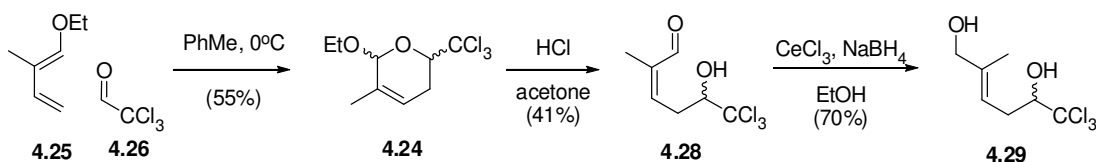
Attempts were made to directly cleave pyran **4.24** to give aldehyde **4.27** with a variety of metal reagents, such as Zn(0), Cr(II), and Pb/Cd, however all of these reagents led to no reaction. Due to this result we sought to utilize pyran **4.24** in an alternative route.

Scheme 4.5 Attempted reductive cleavage of pyran **4.24**.



We next considered hydrolysis of pyran **4.24** with aqueous HCl in acetone to provide the corresponding lactol. However, an aldehyde was obtained as the product which we initially assigned as aldehyde **4.28**. We rationalized the absence of the expected lactol on the basis of the attenuated nucleophilicity of the alcohol with the attached electron-withdrawing trichloromethyl group. Aldehyde **4.28** was then reduced under Luche conditions to the allylic alcohol **4.29** which enabled unambiguous assignment of the geometry of allylic alcohol **4.29** since it was a crystalline solid.

Scheme 4.6. Second Generation Synthesis of Diene **2.52**.



Based on X-ray analysis the olefin geometry was found to be the undesired (*E*)-allylic alcohol **4.29** (Figure 4.2). As it was not known whether the hydrolysis step or reduction steps were responsible for the isomerization, we choose to explore another route to diene **2.52**.

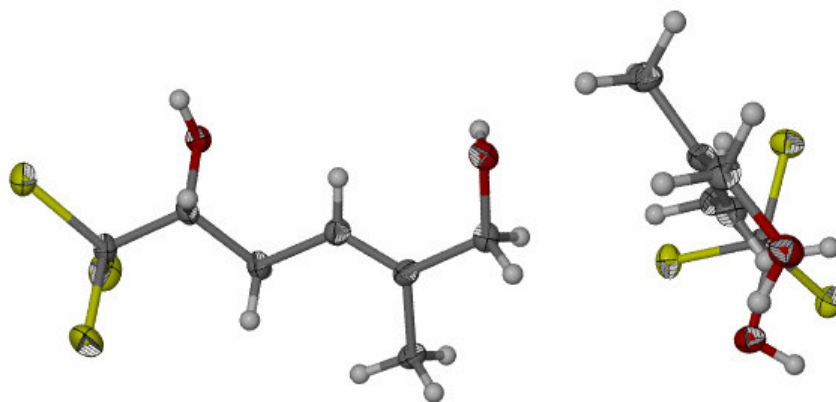
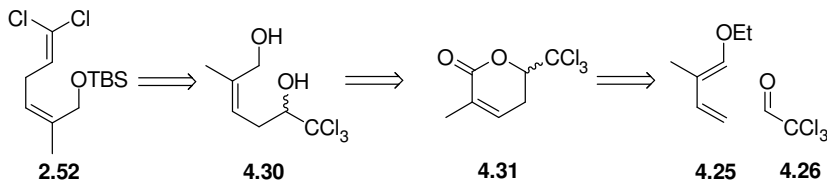


Figure 4.2. X-ray structure of diol **4.29**.

Alternate Retrosynthesis of Diene 2.52

In light of the olefin isomerization problem, we decided to take another look at the retrosynthesis of diene **2.52**. Taking a note from the literature, we choose to pursue a method used by Hale in his partial synthesis of bryostatin. Following the hetero-Diels-Alder reaction between ethoxy diene **4.25** and chloral **4.26**, the intermediate acetal would be oxidized with Jones reagent to give lactone **4.31**.^{142, 143}

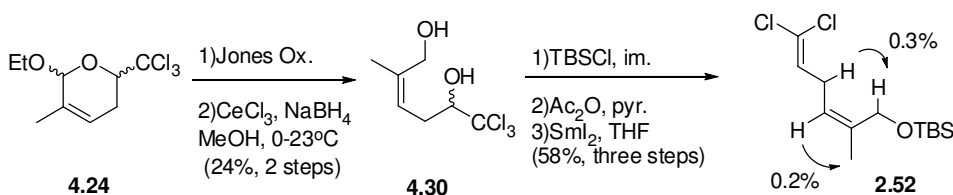
Scheme 4.4. Third Generation Retrosynthesis of Diene **2.52**.



Synthesis of Diene 2.52

The revised synthesis of diene **2.52** began from pyran **4.24** and Jones oxidation to the lactone and direct Luche reduction to the diol **4.30**, which proceeded in overall modes yield of 24% for the two steps. The primary alcohol was protected over the secondary and following exposure to samarium diiodide to effect the reductive fragmentation, the delivered the desired skipped diene **2.52** in good overall yield 58% for the 3 steps. The geometry of the olefin was confirmed by nOe experiments.

Scheme 4.5. Synthesis of Diene **2.52**.

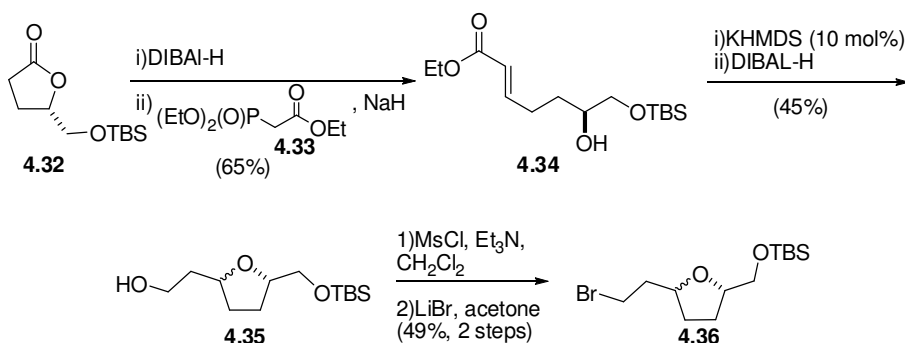


Synthesis of a Model Coupling Partner

With a viable synthesis of diene **2.52** in hand we next turned our attention to the synthesis of a coupling partner. To best model the desired coupling necessary for haterumalide, we set out to synthesize an appropriate alkyl zinc with a pendant THF which following our model studies, the appropriately placed heteroatom, *i. e.* oxygen of

the THF ring would be essential for successful coupling. The synthesis of an appropriate THF began with known lactone **4.32**,^{144, 145} which is available from glutamic acid by reduction and then Horner-Wadsworth-Emmons olefination with phosphonate **4.33**. This sequence gave α,β -unsaturated ester **4.34**¹⁴⁶ which was cyclized to the desired THF by a Michael reaction. The intermediate ester proved to be unstable to silica gel chromatography so the crude ester was reduced with DIBAL-H to alcohol **4.35**, which was then converted to the bromide using a two step procedure. Mesylation and then displacement with bromide to gave the alkyl zinc precursor **4.36** readied for coupling with the previously made skipped diene **2.52**.

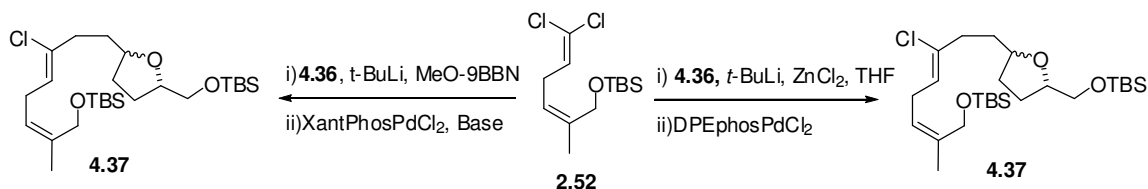
Scheme 4.6. Synthesis of Model THF.



With both fragments in hand, we decided to test the coupling with three available methods for dichloroolefins including our developed procedure (Scheme 4.7). Initial studies with the Negishi protocol for coupling skipped diene **2.52** with the corresponding zinc reagent derived from bromide **4.36** consistently gave no reaction for this system.¹²⁹ The Roulland procedure using an alkyl borane as the coupling partner led to several

products presumably due to partial or complete deprotection of the silyl groups and isomerization of the olefins.

Scheme 4.7 Alternate Methods for Coupling Diene **2.52**.



Conclusions

In conclusion, we were able to develop a coupling reaction between a 1,1-dichloro-alkene and an alkyl zinc reagent. We hope to apply this to a model study and eventually to the construction of the C8-C9 bond of the haterumalides. We were also able to determine that the coupling reaction necessitates a heteroatom incorporated in the zinc reagent. Finally, we have also been able to devise a synthesis of diene **2.52** which would be necessary in such a reaction.

CHAPTER V

CONCLUSIONS

Marine natural products have continued to inspire a great diversity of methodologies that are geared toward their synthesis. Two such natural products are haterumalide NA and maculalactone A. In fact it was the knowledge gained in trying to develop a strategy for the synthesis of haterumalide NA that ultimately led to the first synthesis of spiroepoxy- β -lactones and the pursuit of the synthesis of maculalactone A.

In our quest to devise a synthesis of a γ -silyloxy-*cis*- β -lactone for the construction of the tetrahydrofuran of haterumalide NA we discovered a novel class of spiro-heterocycles, namely spiroepoxy- β -lactones. These heterocycles exhibited interesting structural features that were gleaned from the x-ray structure of one example. Based on this x-ray structure and calculations we were able to determine that the unexpected stability of this ring system may be derived from a double anomeric effect. While these systems did not demonstrate the desired reactivity necessary for the synthesis of the tetrahydrofuran fragment found in haterumalide NA, they did demonstrate various interesting modes of reactivity. For example, this spiro ring system underwent an interesting rearrangement to butenolides in the presence of an appropriate base. It was this mode of reactivity that led to the potential utility of this ring system in a synthesis of maculalactone A. Unfortunately, this did not culminate in a successful total synthesis of this natural product.

Another key reaction for our proposed route to haterumalide NA was a palladium-catalyzed cross coupling between an alkyl zinc reagent and a 1,1-dichloro-alkene. An appropriate skipped diene substrate that bears the required dichloroolefin was prepared

using a hetero-Diels-Alder reaction followed by subsequent ring cleavage to deliver a Western fragment that is serviceable for the total synthesis of the haterumalides. We successfully demonstrated the utility of the coupling strategy for a variety of heteroatom substituted zinc reagents in the presence of the highly dipolar solvent *N,N*-dimethylacetamide and with the aid of microwave heating. We also sought to apply this coupling strategy to a functionalized tetrahydrofuran and the skipped diene substrate which constitutes a model study for the synthesis of haterumalide.

REFERENCES

1. Yang, H. W.; Romo, D. *Tetrahedron* **1999**, *55*, 6403.
2. de Meijere, A.; Kozhushkov, S. I. *Chem. Rev.* **2000**, *100*, 93.
3. Crandall, J. K.; Paulson, D. R. *J. Org. Chem.* **1968**, *33*, 991.
4. Bernard, A. M.; Floris, C.; Frongia, A.; Piras, P. P. *Tetrahedron* **2000**, *56*, 4555.
5. Hiyama, T.; Takehara, S.; Kitatani, K.; Nozaki, H. *Tetrahedron Lett.* **1974**, 3295.
6. Wiseman, J. R.; Chan, H.-F. *J. Am. Chem. Soc.* **1970**, *92*, 4749.
7. Erden, I.; De Meijere, A.; Rousseau, G.; Conia, J. M. *Tetrahedron Lett.* **1980**, *21*, 2501.
8. De Meijere, A.; Erden, I.; Weber, W.; Kaufmann, D. *J. Org. Chem.* **1988**, *53*, 152.
9. Krief, A.; Dumont, W.; Laboureur, J. L. *Tetrahedron Lett.* **1988**, *29*, 3265.
10. Trost, B. M.; LaRochelle, R.; Bogdanowicz, M. J. *Tetrahedron Lett.* **1970**, 3449.
11. Trost, B. M.; Bogdanowicz, M. J. *J. Am. Chem. Soc.* **1971**, *93*, 3773.
12. Trost, B. M. *Top. Curr. Chem.* **1986**, *133*, 3.
13. Johnson, C. R.; Katekar, G. F.; Huxol, R. F.; Janiga, E. R. *J. Am. Chem. Soc.* **1971**, *93*, 3771.
14. Pell, A. S.; Pilcher, G. *J. Chem. Soc., Faraday Trans.* **1965**, *61*, 71.
15. Rickborn, B.; Thummel, R. P. *J. Org. Chem.* **1969**, *34*, 3583.
16. Trost, B. M.; Bogdanowicz, M. J. *J. Am. Chem. Soc.* **1973**, *95*, 289.
17. Hsiao, C. N.; Hannick, S. M. *Tetrahedron Lett.* **1990**, *31*, 6609.
18. Nemoto, H.; Ishibashi, H.; Nagamochi, M.; Fukumoto, K. *J. Org. Chem.* **1992**, *57*, 1707.
19. Gadwood, R. C. *J. Org. Chem.* **1983**, *48*, 2098.
20. Kwon, O.; Su, D.-S.; Meng, D.; Deng, W.; D'Amico, D. C.; Danishefsky, S. J. *Angew. Chem. Int. Ed.* **1998**, *37*, 1877.

21. Kwon, O.; Su, D.-S.; Meng, D.; Deng, W.; D'Amico, D. C.; Danishefsky, S. J. *Angew. Chem. Int. Ed.* **1998**, *37*, 1880.
22. Bernard, A. M.; Frongia, A.; Piras, P. P.; Secci, F. *Org. Lett.* **2003**, *5*, 2923.
23. Trost, B. M.; Bogdanowicz, M. J. *J. Am. Chem. Soc.* **1973**, *95*, 5321.
24. Saniere, M.; Charvet, I.; Le Merrer, Y.; Depezay, J.-C. *Tetrahedron* **1995**, *51*, 1653.
25. Baylon, C.; Prestat, G.; Heck, M.-P.; Mioskowski, C. *Tetrahedron Lett.* **2000**, *41*, 3833.
26. Chattopadhyay, S.; Mamdapur, V. R.; Chadha, M. S. *Synth. Commun.* **1990**, *20*, 1299.
27. Sivik, M. R.; Bauer, W.; Schleyer, P. v. R.; Paquette, L. A. *Organometallics* **1996**, *15*, 5202.
28. Nemoto, H.; Yoshida, M.; Fukumoto, K.; Ihara, M. *Tetrahedron Lett.* **1999**, *40*, 907.
29. Yoshida, M.; Abdel-Hamid Ismail, M.; Nemoto, H.; Ihara, M. *J. Chem. Soc., Perkin Trans. 1* **2000**, 2629.
30. Matsuda, T.; Fujimoto, A.; Ishibashi, M.; Murakami, M. *Chem. Lett.* **2004**, *33*, 876.
31. Crandall, J. K.; Machleder, W. H. *Tetrahedron Lett.* **1966**, 6037.
32. Crandall, J. K.; Machleder, W. H. *J. Am. Chem. Soc.* **1968**, *90*, 7292.
33. Crandall, J. K.; Machleder, W. H.; Thomas, M. J. *J. Am. Chem. Soc.* **1968**, *90*, 7346.
34. Crandall, J. K.; Batal, D. J. *J. Org. Chem.* **1988**, *53*, 1338.
35. Crandall, J. K.; Batal, D. J. *Tetrahedron Lett.* **1988**, *29*, 4791.
36. Crandall, J. K.; Batal, D. J.; Sebesta, D. P.; Lin, F. *J. Org. Chem.* **1991**, *56*, 1153.
37. Murray, R. W.; Jeyaraman, R. *J. Org. Chem.* **1985**, *50*, 2847.
38. Crandall, J. K.; Batal, D. J.; Lin, F.; Reix, T.; Nadol, G. S.; Ng, R. A. *Tetrahedron* **1992**, *48*, 1427.

39. Crandall, J. K.; Rambo, E. *J. Org. Chem.* **1990**, *55*, 5929.
40. Crandall, J. K.; Rambo, E. *Tetrahedron* **2002**, *58*, 7027.
41. Crandall, J. K.; Rambo, E. *Tetrahedron Lett.* **1994**, *35*, 1489.
42. Andrews, D. R.; Giusto, R. A.; Sudhakar, A. R. *Tetrahedron Lett.* **1996**, *37*, 3417.
43. Charney, W.; Herzog, H. L., *Microbial Transformations of Steroids: A Handbook*. 1967; p 728 pp.
44. Katukojvala, S.; Barlett, K. N.; Lotesta, S. D.; Williams, L. J. *J. Am. Chem. Soc.* **2004**, *126*, 15348.
45. Ghosh, P.; Lotesta, S. D.; Williams, L. J. *J. Am. Chem. Soc.* **2007**, *129*, 2438.
46. Mitani, M.; Matsumoto, H.; Gouda, N.; Koyama, K. *J. Am. Chem. Soc.* **1990**, *112*, 1286.
47. Peng, Z.-H.; Woerpel, K. A. *J. Am. Chem. Soc.* **2003**, *125*, 6018.
48. Cichewicz, R. H.; Valeriote, F. A.; Crews, P. *Org. Lett.* **2004**, *6*, 1951.
49. Lotesta, S. D.; Hou, Y.; Williams, L. J. *Org. Lett.* **2007**, *9*, 869.
50. Halazy, S.; Krief, A. *Tetrahedron Lett.* **1980**, *21*, 1997.
51. Halazy, S.; Krief, A. *J. Chem. Soc., Chem. Commun.* **1982**, 1200.
52. Leriverend, M. L.; Leriverend, P. *C. R. Acad. Sci. Ser. C* **1975**, *280*, 791.
53. Razin, V. V.; Ulin, N. V. *Russ. J. Org. Chem.* **2003**, *39*, 33.
54. Pirrung, M. C.; Thomson, S. A. *J. Org. Chem.* **1988**, *53*, 227.
55. Shen, Y.-M.; Wang, B.; Shi, Y. *Angew. Chem. Int. Ed.* **2006**, *45*, 1429.
56. Shen, Y.-M.; Wang, B.; Shi, Y. *Tetrahedron Lett.* **2006**, *47*, 5455.
57. Leriverend, M. L. *C. R. Acad. Sci. Ser. C* **1974**, *279*, 755.
58. Miyano, M. *J. Org. Chem.* **1981**, *46*, 1846.
59. Huang, M. *J. Am. Chem. Soc.* **1946**, *68*, 2487.

60. Tobe, Y.; Yamashita, T.; Kakiuchi, K.; Odaira, Y. *J. Chem. Soc., Chem. Commun.* **1985**, 898.
61. Tobe, Y.; Sato, J.; Sorori, T.; Kakiuchi, K.; Odaira, Y. *Tetrahedron Lett.* **1986**, 27, 2905.
62. Tobe, Y.; Yamashita, D.; Takahashi, T.; Inata, M.; Sato, J.; Kakiuchi, K.; Kobihiro, K.; Odaira, Y. *J. Am. Chem. Soc.* **1990**, 112, 775.
63. Barton, D. H. R.; McCombie, S. W. *J. Chem. Soc., Perkin Trans. 1* **1975**, 1574.
64. Mahuteau-Betzer, F.; Ghosez, L. *Tetrahedron Lett.* **1999**, 40, 5183.
65. Mahuteau-Betzer, F.; Ghosez, L. *Tetrahedron* **2002**, 58, 6991.
66. Brown, B.; Hegedus, L. S. *J. Org. Chem.* **2000**, 65, 1865.
67. Satoh, T.; Hirano, M.; Kuroiwa, A. *Tetrahedron Lett.* **2005**, 46, 2659.
68. Satoh, T.; Hirano, M.; Kuroiwa, A.; Kaneko, Y. *Tetrahedron* **2006**, 62, 9268.
69. Turro, N. J.; Williams, J. R. *Tetrahedron Lett.* **1969**, 321.
70. Turro, N. J.; Edelson, S. S.; Williams, J. R.; Darling, T. R.; Hammond, W. B. *J. Am. Chem. Soc.* **1969**, 91, 2283.
71. Kato, T.; Katagiri, N.; Sato, R. *J. Org. Chem.* **1980**, 45, 2587.
72. Geraghty, N. W. A.; Murphy, P. A. *Tetrahedron Lett.* **1994**, 35, 6737.
73. Murphy, P. V.; O'Sullivan, T. J.; Geraghty, N. W. A. *J. Chem. Soc., Perkin Trans. 1* **2000**, 2109.
74. Kato, T.; Katagiri, N.; Sato, R. *Chem. Pharm. Bull.* **1981**, 29, 2361.
75. Dollinger, L. M.; Howell, A. R. *J. Org. Chem.* **1996**, 61, 7248.
76. Shimizu, N.; Ishikawa, M.; Ishikura, K.; Nishida, S. *J. Am. Chem. Soc.* **1974**, 96, 6456.
77. Funke, C. W.; Cerfontain, H. *J. Chem. Soc., Perkin Trans. 2* **1976**, 1902.
78. Marschall, H.; Muehlenkamp, W. B. *Chem. Ber.* **1976**, 109, 2785.
79. Fitjer, L.; Rissom, B.; Kanschik, A.; Egert, E. *Tetrahedron* **1994**, 50, 10879.

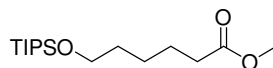
80. O'Neil, K. E.; Kingree, S. V.; Minbirole, K. P. C. *Org. Lett.* **2005**, 7, 515.
81. Crandall, J. K.; Salazar, G. E.; Watkins, R. J. *J. Am. Chem. Soc.* **1987**, 109, 4338.
82. Ndakala, A. J.; Howell, A. R. *J. Org. Chem.* **1998**, 63, 6098.
83. Howell, A. R.; Ndakala, A. J. *Org. Lett.* **1999**, 1, 825.
84. Taboada, R.; Ordonio, G. G.; Ndakala, A. J.; Howell, A. R.; Rablen, P. R. *J. Org. Chem.* **2003**, 68, 1480.
85. Ndakala, A. J.; Hashemzadeh, M.; So, R. C.; Howell, A. R. *Org. Lett.* **2002**, 4, 1719.
86. So, R. C.; Ndonge, R.; Izmirian, D. P.; Richardson, S. K.; Guerrero, R. L.; Howell, A. R. *J. Org. Chem.* **2004**, 69, 3233.
87. Howell, A. R.; So, R. C.; Richardson, S. K. *Tetrahedron* **2004**, 60, 11327.
88. Reproduced in part with permission from *J. Am. Chem. Soc.* Duffy, R. J.; Morris, K. A.; Romo, D. *J. Am. Chem. Soc.* **2005**, 127, 16754.
89. Newman, D. J.; Cragg, G. M.; Snader, K. M. *J. Nat. Prod.* **2003**, 66, 1022.
90. Takada, N.; Sato, H.; Suenaga, K.; Arimoto, H.; Yamada, K.; Ueda, K.; Uemura, D. *Tetrahedron Lett.* **1999**, 40, 6309.
91. Ueda, K.; Hu, Y. *Tetrahedron Lett.* **1999**, 40, 6305.
92. Levenfors, J. J.; Hedman, R.; Thaning, C.; Gerhardson, B.; Welch, C. J. *Soil Biol. Biochem.* **2004**, 36, 677.
93. Kigoshi, H.; Kita, M.; Ogawa, S.; Itoh, M.; Uemura, D. *Org. Lett.* **2003**, 5, 957.
94. Gu, Y.; Snider, B. B. *Org. Lett.* **2003**, 5, 4385.
95. Hoye, T. R.; Wang, J. *J. Am. Chem. Soc.* **2005**, 127, 6950.
96. Kigoshi, H.; Hayakawa, I. *Chem. Rec.* **2007**, 7, 254.
97. Micalizio, G. C.; Roush, W. R. *Org. Lett.* **2001**, 3, 1949.
98. In previous studies macrocyclization proved to be difficult.
99. Mead, K. T.; Pillai, S. K. *Tetrahedron Lett.* **1993**, 34, 6997.

100. Larsen, C. H.; Ridgway, B. H.; Shaw, J. T.; Woerpel, K. A. *J. Am. Chem. Soc.* **1999**, *121*, 12208.
101. Wang, Y.; Zhao, C.; Romo, D. *Org. Lett.* **1999**, *1*, 1197.
102. Calter, M. A.; Orr, R. K.; Song, W. *Org. Lett.* **2003**, *5*, 4745.
103. Sauer, J. C. *J. Am. Chem. Soc.* **1947**, *69*, 2444.
104. Allen, F. H.; Kennard, O.; Watson, D. G.; Brammer, L.; Orpen, A. G.; Taylor, R. *J. Chem. Soc., Perkin Trans. 2* **1987**, S1.
105. Eckert-Maksic, M.; Maksic, Z. B. *Theochem* **1982**, *3*, 325.
106. Calculations were done by Dr. Huda Henry.
107. Deslongchamps, P., *Organic Chemistry Series, Vol. 1: Stereoelectronic Effects in Organic Chemistry*. 1983; 390 pp.
108. Byrn, M.; Calvin, M. *J. Am. Chem. Soc.* **1966**, *88*, 1916.
109. Lawson, A. M.; Leemans, F. A.; McCloskey, J. A. *Steroids* **1969**, *14*, 603.
110. Diakur, J.; Nakashima, T. T.; Vederas, J. C. *Can. J. Chem* **1980**, *58*, 1311.
111. Evans, D. A.; Ennis, M. D.; Le, T.; Mandel, N.; Mandel, G. *J. Am. Chem. Soc.* **1984**, *106*, 1154.
112. Allen, A. D.; Cheng, B.; Fenwick, M. H.; Givhchi, B.; Henry-Riyad, H.; Nikolaev, V. A.; Shikhova, E. A.; Tahmassebi, D.; Tidwell, T. T.; Wang, S. J. *Org. Chem.* **2001**, *66*, 2611.
113. Zografos, A. L.; Georgiadis, D. *Synthesis* **2006**, 3157.
114. Lee, S.-C.; Williams, G. A.; Brown, G. D. *J. Nat. Prod.* **1998**, *61*, 29.
115. Lee, S.-C.; Williams, G. A.; Brown, G. D. *Phytochemistry* **1999**, *52*, 537.
116. Wong, H.-F.; Williams, G. A.; Brown, G. D. *Phytochemistry* **2002**, *60*, 425.
117. Brown, G. D.; Wong, H. F.; Hutchinson, N.; Lee, S. C.; Chan, B. K. K.; Williams, G. A. *Phytochem. Rev.* **2005**, *3*, 381.
118. Brown, G. D.; Wong, H.-F. *Tetrahedron* **2004**, *60*, 5439.
119. Kar, A.; Gogoi, S.; Argade, N. P. *Tetrahedron* **2005**, *61*, 5297.

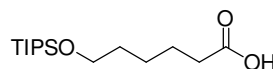
120. Calter, M. A.; Guo, X.; Liao, W. *Org. Lett.* **2001**, *3*, 1499.
121. Purohit, V. C.; Richardson, R. D.; Smith, J. W.; Romo, D. *J. Org. Chem.* **2006**, *71*, 4549.
122. Garcia Martinez, A.; Osio Barcina, J.; del Rosario Colorado Heras, M.; de Fresno Cerezo, A. *Organometallics* **2001**, *20*, 1020.
123. Kapferer, T.; Brueckner, R.; Herzig, A.; Koenig, W. A. *Chemistry--A European Journal* **2005**, *11*, 2154.
124. Roush, W. R.; Moriarty, K. J.; Brown, B. B. *Tetrahedron Lett.* **1990**, *31*, 6509.
125. Stork, G.; Zhao, K. *Tetrahedron Lett.* **1989**, *30*, 2173.
126. Chou, T.; Kuramoto, M.; Otani, Y.; Shikano, M.; Yazawa, K.; Uemura, D. *Tetrahedron Lett.* **1996**, *37*, 3871.
127. Kuramoto, M.; Tong, C.; Yamada, K.; Chiba, T.; Hayashi, Y.; Uemura, D. *Tetrahedron Lett.* **1996**, *37*, 3867.
128. Minato, A.; Suzuki, K.; Tamao, K. *J. Am. Chem. Soc.* **1987**, *109*, 1257.
129. Tan, Z.; Negishi, E.-i. *Angew. Chem. Int. Ed.* **2006**, *45*, 762.
130. Liron, F.; Fosse, C.; Pernolet, A.; Roulland, E. *J. Org. Chem.* **2007**, *72*, 2220.
131. Netherton, M. R.; Fu, G. C. *Topics in Organometallic Chemistry* **2005**, *14*, 85.
132. Nicolaou, K. C.; Bulger, P. G.; Sarlah, D. *Angew. Chem. Int. Ed.* **2005**, *44*, 4442.
133. Skauge, A. R. L. *Postdoctoral Report* **2005**.
134. Knochel, P.; Millot, N.; Rodriguez, A. L.; Tucker, C. E. *Organic Reactions (New York)* **2001**, *58*, 417.
135. Zhou, J.; Fu, G. C. *J. Am. Chem. Soc.* **2003**, *125*, 14726.
136. Kappe, C. O. *Angew. Chem. Int. Ed.* **2004**, *43*, 6250.
137. Appukkuttan, P.; Van der Eycken, E. *Top. Curr. Chem.* **2006**, *266*, 1.
138. Corey, E. J.; Fuchs, P. L. *Tetrahedron Lett.* **1972**, 3769.

139. Hatch, C. E., III; Baum, J. S.; Takashima, T.; Kondo, K. *J. Org. Chem.* **1980**, *45*, 3281.
140. Pirrung, M. C.; Webster, N. J. G. *J. Org. Chem.* **1987**, *52*, 3603.
141. Barbot, F.; Miginiac, P. *Helvetica Chimica Acta* **1979**, *62*, 1451.
142. Malanga, C.; Menicagli, R.; Dell'Innocenti, M.; Lardicci, L. *Tetrahedron Lett.* **1987**, *28*, 239.
143. Hale, K. J.; Hummersone, M. G.; Bhatia, G. S. *Org. Lett.* **2000**, *2*, 2189.
144. Taniguchi, M.; Koga, K.; Yamada, S. *Tetrahedron* **1974**, *30*, 3547.
145. Wrona, I. E.; Garbada, A. E.; Evano, G.; Panek, J. S. *J. Am. Chem. Soc.* **2005**, *127*, 15026.
146. Stangeland, E. L.; Sammakia, T. *J. Org. Chem.* **2004**, *69*, 2381.

APPENDIX A EXPERIMENTAL PROCEDURES AND SELECTED SPECTRA

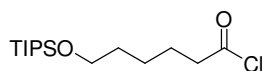


Methyl 6-(triisopropylsilyloxy)hexanoate. was prepared from methyl-6-hydroxy hexanoate (3.66 g, 25.0 mmol) by dissolving in DMF (30 mL) followed by the addition of imidazole (2.04 g, 30 mmol) and TIPSCl (5.80 g, 30.0 mmol). The colorless solution was stirred at 23 °C for 2 d. The reaction was quenched with brine (10 mL) and extracted with Et₂O (3 X 50 mL). The combined organic phase was back extracted with brine (2 X 5 mL) and then dried over Na₂SO₄. This crude oil was purified by flash chromatography (5:95 Et₂O/hexanes) to afford the methyl 6-(triisopropylsilyloxy)hexanoate (5.33 g, 70%). *R_f* 0.19 (5:95, Et₂O /hexanes); IR (thin film) ν_{max} 1737 cm⁻¹; ¹H NMR (500 MHz, benzene-d₆) δ 3.52 (t, *J* = 6.5 Hz, 2H), 3.31 (s, 3H), 2.07 (t, *J* = 7.5 Hz, 2H), 1.53 (pentet, *J* = 7.5 Hz, 2H), 1.41 (dt, *J* = 6.5, 15.0 Hz, 2H), 1.30-1.23 (m, 2H), 1.09-0.99 (m, 21H); ¹³C NMR (125 MHz, benzene-d₆) δ 173.2, 63.4, 50.9, 34.1, 33.0(2), 25.7, 18.3(6), 12.3(3); LRMS (ESI) Calcd. For C₁₆H₃₄O₃Si [M+Li] 309, found 309.

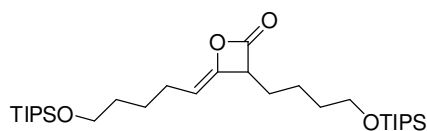


6-(triisopropylsilyloxy)hexanoic acid. 6-(triisopropylsilyloxy)hexanoic acid was prepared from methyl-6-(triisopropylsilyloxy)hexanoate. (5.33 g, 17.6 mmol) by dissolving in THF (200 mL) and adding LiOH (22.8 mL, 1 M) at 23 °C. Stirring was continued at the same temperature for 6.5 h. The reaction was acidified to pH 2 with dilute HCl. The solution was extracted with Et₂O (3 X 50 mL). The combined organic fractions were washed with brine (2 X 10 mL). The organic phase was dried over

MgSO₄ and concentrated. Purification by flash chromatography (1:9 to 1:4 Et₂O/hexanes) to afford the 6-(triisopropylsilyloxy)hexanoic acid (1.98 g, 39%) as a pale yellow oil. *R_f* 0.1 (1:4 Et₂O /hexanes); IR (thin film) ν_{\max} 1716 cm⁻¹; ¹H NMR (500 MHz, benzene-d₆) δ 3.50 (t, *J* = 6.5 Hz, 2H), 2.03 (t, *J* = 7.5 Hz, 2H), 1.45 (pentet, *J* = 7.5 Hz, 2H), 1.38 (app. pentet, *J* = 6.5 Hz, 2H), 1.22-1.19 (m, 2H), 1.17-0.95 (m, 21H); ¹³C NMR (125 MHz, benzene-d₆) δ 180.7, 63.2, 34.0, 32.8, 25.5, 24.6, 18.1(6), 12.2(3); LRMS (ESI) Calcd. for C₁₅H₃₂O₃Si [M-H] 287, found 287.

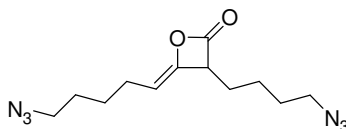


6-(Triisopropylsilyloxy)hexanoyl chloride. 6-(Triisopropylsilyloxy)hexanoyl chloride was prepared from 6-(triisopropylsilyloxy)hexanoic acid (1.37 g, 4.70 mmol) in CH₂Cl₂ (47 mL) by the addition of oxalyl chloride (783 mg, 6.15 mmol). This solution was stirred until gas evolution had stopped, 3.5 h. The solution was concentrated by rotary evaporation and then placed under vacuum to yield 6-(triisopropylsilyloxy)hexanoyl chloride (1.44 g, 100%) as a pale yellow oil. IR (thin film) ν_{\max} 1803 cm⁻¹; ¹H NMR (500 MHz, benzene-d₆) δ 3.44 (t, *J* = 6.5 Hz, 2H), 2.16 (t, *J* = 7.5 Hz, 2H), 1.27-1.18 (m, 4H), 1.10-0.97 (m, 26H); ¹³C NMR (125 MHz, benzene-d₆) δ 173.1, 63.0, 46.8, 32.5, 24.8, 24.8, 18.1(6), 12.2(3).



(Z)-3-(4-(triisopropylsilyloxy)butyl)-4-(5-(triisopropylsilyloxy)pentylidene)oxetan-2-one. To a solution of quinuclidine·HCl (83.1 mg, 0.52 mmol) and diisopropylethylamine (739 mg, 5.72 mmol) in CH₂Cl₂ (32 mL) at -78 °C was added a solution of 6-

(triisopropylsilyloxy)hexanoyl chloride (1.44g, 5.20 mmol) in CH_2Cl_2 (20 mL). This solution was slowly warmed to 23 °C over 5 h. The reaction mixture was concentrated to a third of its volume and the amine hydrochlorides were precipitated by the addition of pentane (50 mL). This solution was filtered to remove the salts and concentrated to an oil. Immediate purification by flash chromatography (5:95, Et_2O /hexanes) afforded (Z)-3-(4-(triisopropylsilyloxy)butyl)-4-(5-(triisopropylsilyloxy)pentylidene)oxetan-2-one (344 mg, 25%) as a colorless oil. R_f 0.29 (5:95 Et_2O /hexanes); IR (thin film) ν_{max} 1875, 1726 cm^{-1} ; ^1H NMR (500 MHz, benzene- d_6) δ 4.39 (dt, J = 1.5, 7.5 Hz, 1H), 3.63 (t, J = 6.0 Hz, 1H), 3.49 (t, J = 6.0 Hz, 2H), 3.28 (app. t, J = 7.5 Hz, 1H), 2.19-2.08 (m, 2H), 1.57-1.44 (m, 4H), 1.40-1.29 (m, 6H), 1.14-1.01 (m, 42 H); ^{13}C NMR (125 MHz, benzene- d_6) δ 168.8, 146.6, 101.0, 63.3, 63.1, 54.0, 32.7(2), 27.5, 26.2, 24.8, 23.2, 18.3(6), 18.2(6), 12.3(3), 12.3(3); LRMS (ESI) Calcd. for $\text{C}_{30}\text{H}_{60}\text{O}_4\text{Si}_2$ 541, found 541.



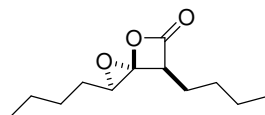
(Z)-3-(4-azidobutyl)-4-(5-azidopentylidene)oxetan-2-one. To a solution of quinuclidine·HCl (101 mg, 0.620 mmol) and diisopropylethylamine (881 mg, 6.80 mmol) in CH_2Cl_2 (40 mL) was added freshly prepared 6-azido-hexanoyl chloride (1.01 g, 6.20 mmol) at -78 °C. This solution was allowed to slowly warm to 23 °C over 10 h. The solution was concentrated to a third of its volume and the amine hydrochloride were precipitated by the addition of pentane (50 mL). The solution was filtered to remove the salts and concentrated to an oil. Immediate purification by flash chromatography (3:7 EtOAc/hexanes) afforded (Z)-3-(4-azidobutyl)-4-(5-azidopentylidene)oxetan-2-one (471 mg, 55%) as a yellow oil. R_f 0.4 (1:4 EtOAc/hexanes); IR (thin film) ν_{max} 2100, 1849

cm⁻¹; ¹H NMR (500 MHz, benzene-d₆) δ 4.16 (dt, *J* = 1.3, 7.0 Hz, 1H), 3.15 (app. dt, *J* = 1.0, 7.0 Hz, 1H), 2.65 (t, *J* = 6.5 Hz, 2H), 2.51 (t, *J* = 6.5 Hz, 2H), 1.88 (m, 2H), 1.18-0.9 (m, 10H); ¹³C NMR (125 MHz, benzene-d₆) δ 168.4, 146.4, 100.4, 53.6, 50.9, 50.6, 28.2, 28.2, 26.8, 26.4, 24.2, 23.5; LRMS (ESI) Calcd. for C₁₂H₁₈N₆O₂ 285, found 285 [M+Li].

General Procedure for the Preparation of Dimethyldioxirane (DMDO) in Acetone.

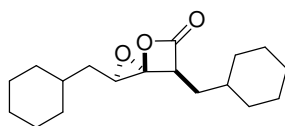
This procedure was adapted from the described by Murray and Singh. To a 2 L three neck round-bottom flask was added 350 mL of water, 146 g of sodium bicarbonate and 300 mL of acetone and were rapidly stirred. A flask containing 300 g of Oxone[®] was attached to the 2 L flask *via* flexible tubing. A jacketed condenser was attached to one neck and the third neck was stoppered. To the condenser was attached a glass U-tube followed by another glass condenser leading to a 100 mL round bottom flask that contained activated 4 Å molecular sieves and was vented to a water aspirator. This flask was cooled to -78 °C with a dry ice/acetone bath and Oxone[®] was added in three portions over 20 min. Upon complete addition of Oxone[®], the reaction apparatus was maintained under vacuum to collect the DMDO as a yellow solution in acetone for 15 min. This DMDO solution was determined to be 0.076 M by titration by the method of Murray and Singh. The DMDO solution was used immediately in the epoxidations as described.

Representative Procedure for Epoxidation of 4-Alkylidene-2-oxetanones as described for Spiroepoxy-β-Lactone (+/-) 2.61.

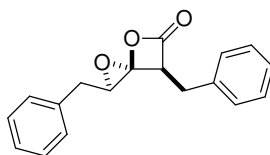


To a solution of (Z)-3-butyl-4-pentylideneoxetan-2-one (370 mg, 1.90 mmol) in CH₂Cl₂ (100 mL) at 0 °C was added MgSO₄ (100 mg, 0.83 mmol, ~0.5 equiv) and an acetone

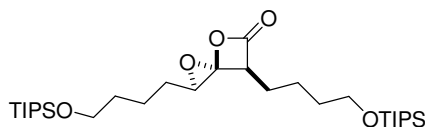
solution of DMDO (60 mL, 0.076 M, ~2.5 equiv) in one portion to give a pale yellow slurry which was warmed to 23 °C and stirred for 5 h. The reaction mixture was then filtered through a pad of MgSO₄ and the volatiles were removed by rotary evaporation. The colorless residue was purified by flash chromatography on SiO₂ (1:9 EtOAc/hexanes); *R_f* 0.4 (1:9 EtOAc/hexanes); IR (thin film) ν_{max} 1859 cm⁻¹; ¹H NMR (500 MHz, benzene-d₆) δ 3.18 (dd, *J* = 7.0, 7.8 Hz, 1H), 2.72 (dd, *J* = 5.5, 6.8 Hz, 1H), 1.62-1.56 (m, 1 H), 1.48-1.40 (m, 1H), 1.28-1.08 (m, 7H), 1.04-0.94 (m, 3H), 0.74 (t, *J* = 7.5 Hz, 3H), 0.68 (t, *J* = 6.5 Hz, 3H); ¹³C NMR (75 MHz, benzene-d₆) δ 167.2, 91.0, 58.8, 53.8, 28.6, 28.0, 27.8, 25.1, 22.5, 22.4, 13.9, 13.8; LRMS (ESI) Calcd. for C₁₂H₂₀O₃ [M+H] 213, found 213.



Spiroepoxy- β -lactone 2.63a. The spiroepoxy- β -lactone **2.63a** was prepared according to the general procedure from (Z)-4-(2-cyclohexylethylidene)-3-(cyclohexylmethyl)oxetan-2-one (174 mg, 0.63 mmol). Purification by flash chromatography (1:9, Et₂O/hexanes) afforded the spiroepoxy- β -lactone **2.63a** (140 mg, 76%, dr 10:1) as a clear oil, which crystallized upon storage at -20 °C. Recrystallization from pentane *via* slow evaporation at -20 °C afforded small white crystals, m.p. 64-65 °C (pentane). *R_f* 0.45 (1:9 Et₂O/hexanes); IR (thin film) ν_{max} 1854 cm⁻¹; ¹H NMR (500 NMR, benzene-d₆) δ 3.37 (dd, *J* = 6.6, 8.7 Hz, 1H), 2.95 (dd, *J* = 5.4, 6.9 Hz, 1H), 1.7-0.4 (m, 26 H); ¹³C NMR (125 MHz, benzene-d₆) δ 167.5, 91.5, 58.1, 52.0, 35.65, 35.63, 35.45, 35.44, 33.11, 33.08, 32.9, 32.7, 26.43, 26.40, 26.33, 26.26, 26.29, 26.17; LRMS (APCI) Calcd. for C₁₈H₂₈O₃ [M+H] 293, found 293.

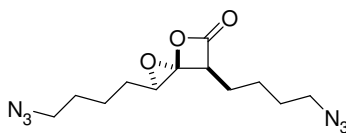


Spiroepoxy-β-lactone 2.63b. Spiroepoxy-β-lactone **2.63b** was prepared according to the general procedure from (Z)-3-benzyl-4-(2-phenylethylidene)oxetan-2-one¹²¹ (112 mg, 0.424 mmol). Purification by flash chromatography (1:5, Et₂O/hexanes) afforded spiroepoxy-β-lactone **2.63b** (68 mg, 57%, 24:1) as a clear oil. *R_f* 0.25 (1:5, Et₂O/hexanes); [α]_D²³ -26.6 (*c* = 1.0, CH₂Cl₂); IR (thin film) *v*_{max} 1854 cm⁻¹; ¹H NMR (500 MHz, benzene-*d*₆) δ 7.09-7.00 (m, 3H), 6.99-6.89 (m, 5H), 6.71-6.67 (m, 2H), 3.46 (dd, *J* = 6.5, 8.0 Hz, 1H), 2.87 (app. t, *J* = 6.5 Hz, 1H), 2.72 (dd, *J* = 6.5, 14.5 Hz, 1H), 2.55 (dd, *J* = 6.5, 14.5 Hz, 1H), 2.41 (dddd, *J* = 6.5, 8.0, 8.0, 15.5 Hz, 2H); ¹³C NMR (125 MHz, benzene-*d*₆) δ 166.5, 136.1, 136.0, 129.1, 129.0(2), 128.8, 128.6(2), 127.2(2), 127.2(2), 90.8, 59.2, 54.3, 34.6, 31.0; LRMS (APCI) Calcd. for C₁₈H₁₆O₃ [M+H] 281, found 281.

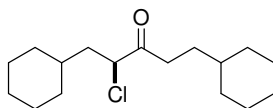


Spiroepoxy-β-lactone 2.63c. Spiroepoxy-β-lactone **2.63c** was prepared according to the general procedure from (Z)-3-(4-(triisopropylsilyloxy)butyl)-4-(5-(triisopropylsilyloxy)pentylidene)oxetan-2-one (158 mg, 0.118 mmol) with the exception of the reaction time of 2 h. Purification by flash chromatography (1:9, Et₂O/hexanes) afforded spiroepoxy-β-lactone **2.63c** (65 mg, 40%, dr 16.5:1) as a clear oil. *R_f* 0.33 (1:9 Et₂O/hexanes); IR (thin film) *v*_{max} 1854 cm⁻¹; ¹H NMR (500 MHz, benzene-*d*₆) δ 3.54 (t, *J* = 5.5 Hz, 2H), 3.46 (t, *J* = 5.5 Hz, 2H), 3.20 (t, *J* = 7.5 Hz, 1H), 2.85 (dd, *J* = 5.0, 7.0 Hz, 1H), 1.73-1.00 (m, 54H); ¹³C NMR (125 MHz, benzene-*d*₆) δ 167.1, 91.0, 63.1, 63.0,

59.0, 53.9, 32.7, 32.7, 28.0, 25.4, 23.1, 22.6, 18.3(6), 18.2(6), 12.28(3), 12.25(3); LRMS (ESI) Calcd. for $C_{30}H_{60}O_5Si_2$ $[M+Li]$ 563, found 563.

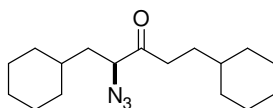


Spiroepoxy- β -lactone 2.63d. Spiroepoxy- β -lactone **2.63d** was prepared according to the general procedure from (Z)-3-(4-azidobutyl)-4-(5-azidopentylidene)oxetan-2-one (150 mg, 0.539 mmol). Purification by flash chromatography (3:10 EtOAc/hexanes) afforded spiroepoxy- β -lactone **2.63d** (97 mg, 61%, dr 16:1) as a pale yellow oil. R_f 0.33 (1:9 Et₂O/hexanes); IR (thin film) ν_{max} 1849 cm^{-1} ; 1H NMR (300 MHz, benzene- d_6) δ 3.09 (t, J = 6.3 Hz, 1H), 2.63 (dd, J = 5.4, 11.7 Hz, 1H), 2.56 (t, J = 4.2 Hz, 2H), 2.52 (t, J = 4.2 Hz, 2H), 1.50-0.85 (m, 12H); ^{13}C NMR (125 MHz, benzene- d_6) δ 166.8, 90.7, 58.4, 53.6, 50.8, 50.6, 28.4, 28.2, 27.5, 24.8, 23.5, 23.0; LRMS (APCI) Calcd. for $C_{12}H_{18}N_6O_3$ $[M+H]$ 295, found 295.

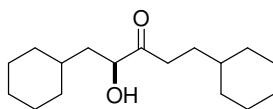


α -Chloroketone 3.6. To a solution of spiroepoxy- β -lactone **2.63a** (90.0 mg, 0.308 mmol) in CH_2Cl_2 (1.6 mL) was added tetra-*n*-butylammonium chloride (170 mg, 0.616 mmol) as a solution in CH_2Cl_2 (1.5 mL) and stirred at 23 $^{\circ}C$ for 14 h. The solution was concentrated and the residue was purified by flash chromatography (5:95 Et₂O/hexanes) to give chloroketone **3.6** (28.2 mg, 32%) as a colorless oil. R_f 0.63 (1:9 Et₂O/hexanes); IR (thin film) ν_{max} 1721, 1445 cm^{-1} ; 1H NMR (500 MHz, benzene- d_6) δ 4.14 (t, J = 7.5 Hz, 1H), 2.43 (dt, J = 7.5, 17.5 Hz, 1H), 2.41 (dt, J = 7.5, 17.5 Hz, 1H), 1.68, (t, J = 7.0

Hz, 2H), 1.64-1.41 (m, 14H), 1.18-0.95 (m, 8H), 0.81-0.57 (m, 4H); ^{13}C NMR (125 MHz, benzene- d_6) δ 204.4, 61.8, 41.1(2), 37.2, 35.9, 34.5, 33.5(2), 33.2(2), 31.3, 26.7, 26.50, 26.48, 26.3, 26.1; LRMS (ESI) Calcd. for $\text{C}_{17}\text{H}_{29}\text{ClO}$ [M+H] 285, found 285.

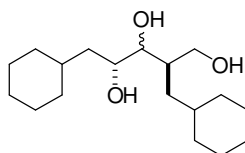


α -azidoketone 3.7. To a solution of spiroepoxy- β -lactone **2.63a** (61.1 mg, 0.209 mmol) in THF/ H_2O (2.5 mL, 4:1) was added sodium azide (33.5 mg, 0.515 mmol) and the homogenous solution was stirred at 23 $^\circ\text{C}$ for 38 h. The reaction mixture was dried over Na_2SO_4 and after washing with CH_2Cl_2 (3 X 5 mL), the combined organics were concentrated and the residue was purified by flash chromatography (1:4 Et_2O /hexanes) to give azidoketone **3.7** (12.5 mg, 21%) as a pale yellow oil. R_f 0.74 (1:4 Et_2O /hexanes); IR (thin film) ν_{max} 2100, 1726 cm^{-1} ; ^1H NMR (500 MHz, CDCl_3) δ 3.86 (app. t, J = 12 Hz, 1H), 2.56 (ddd, J = 6.0, 6.5, 18.0 Hz, 1H), 2.53 (ddd, J = 6.0, 6.5, 18.0 Hz, 1H), 1.87-1.13 (m, H), 1.07-0.84 (m, H); ^{13}C NMR (125 MHz, CDCl_3) δ 208.4, 65.7, 38.0, 37.2, 37.0, 34.4, 33.7, 33.07, 33.05, 32.2, 30.7, 26.5, 26.3, 26.2(2), 26.1, 25.9; LRMS (APCI) Calcd. for $\text{C}_{17}\text{H}_{29}\text{N}_3\text{O}$ [M+H] 292, found 292.



α -hydroxy-ketone 3.11. To a solution of spiroepoxy- β -lactone **2.63a** (46.5 mg, 0.159 mmol) in THF (1.45 mL) was added doubly distilled H_2O (0.25 mL, pH=6.5). The solution was allowed to stir for 19 h at 23 $^\circ\text{C}$. The reaction was then filtered through Na_2SO_4 and concentrated. The residue was purified by flash chromatography (1:4 Et_2O /hexanes) to give the α -hydroxy ketone **3.11** (9.9 mg, 53%) as a colorless oil. R_f

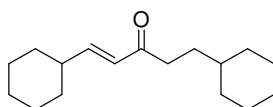
0.48 (1:4 Et₂O /hexanes); IR (thin film) ν_{max} 3475, 1709, 1446 cm⁻¹; ¹H NMR (500 MHz, benzene-d₆) δ 4.04 (ddd, J = 3.1, 5.0, 15.5 Hz, 1H), 3.55 (d, J = 5.0 Hz, 1H), 2.14 (ddd, J = 6.5, 26.0 Hz, 1H), 1.98 (ddd, J = 6.5, 26.0 Hz, 1H), 1.95-1.89 (m, 2H), 1.82-0.64 (m, 31H); ¹³C NMR (125 MHz, benzene-d₆) δ 213.8, 74.5, 41.6, 37.2, 35.3, 34.40, 33.97, 33.1, 33.0, 32.16, 31.2, 26.49, 26.46, 26.3, 26.2(2), 26.0; LRMS (ESI) Calcd. for C₁₇H₃₀O₂Li [M+Li] 273, found 273.



Triol 3.16. A solution of spiroepoxy- β -lactone **2.63a** (112.1 mg, 0.384 mmol) in Et₂O (0.9 mL) was added dropwise to a suspension of LiAlH₄ (18.5 mg, 0.768 mmol) in 2.6 mL of Et₂O at -20 °C. The reaction mixture was stirred for 8 min and then warmed to 0 °C for 0.75 h and then to 23 °C for 2 h. The reaction was quenched by dilution with 4 mL Et₂O and slow addition of 0.02 mL H₂O, followed by the addition of 0.02 mL 15% NaOH, and 0.06 mL H₂O. The reaction mixture was stirred vigorously until the all the gray color disappeared and K₂CO₃ was added and the solution was stirred for 15 min and then filtered through MgSO₄ and concentrated. The residue was purified by flash chromatography (1:1 Et₂O/hexanes) to yield the triol **3.16** (106 mg, 92%) as a milky oil as a mixture of diastereomers. R_f 0.40 (1:1 Et₂O/hexanes); IR (thin film) ν_{max} 3362, 1447 cm⁻¹; ¹H NMR (300 MHz, CDCl₃) δ 3.84-3.71 (m, 6H), 3.70-3.60 (m, 2H), 3.42-3.34 (m, 1H), 3.20-3.02 (br s, 1H), 2.84-2.64 (br s, 1H), 2.02-0.63 (m, 81H); ¹³C NMR (125 MHz, CDCl₃) δ 78.1, 77.5, 70.1, 69.9, 64.6, 63.5, 41.8, 41.0(2), 39.4, 38.0, 36.8, 35.1, 34.9, 34.7, 34.3, 34.00, 33.97, 33.8, 33.3, 32.7, 32.6, 32.5, 32.1, 29.7, 26.61, 26.55(2),

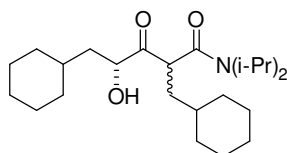
26.43(2), 26.35, 26.30, 26.2(2), 26.1(2); LRMS (APCI) Calcd. for $C_{18}H_{35}O_3$ [M+H] 299, found 299.

Experiment to Determine Site of Attack by H_2O . The reaction was run under identical conditions utilizing 90% H_2O^{18} to determine the site of incorporation of water into the spiroepoxy- β -lactone. Incorporation of a single ^{18}O was confirmed based on ^{13}C NMR which reflected a characteristic ~ 0.023 - 0.026 ppm upfield shift (δ 74.443; actual shift 0.014) due to the attached ^{18}O atom and a residual ^{16}O peak was observed at the chemical shift for the unlabelled compound (δ 74.457). Additionally, ESI-MS showed the incorporation of a single ^{18}O atom.

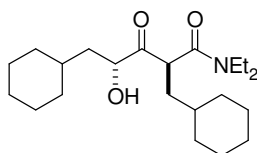


Enone 3.17. A solution of spiroepoxy- β -lactone **2.63a** (340mg, 1.17 mmol) in CH_2Cl_2 (9 mL) was cooled to -96 °C. To the solution was added diisopropylethylamine (0.59 mL, 2.0 M) followed directly by addition of trimethylsilyl triflate (0.45 mL, 2.6 M) both as solutions in CH_2Cl_2 . The solution was stirred for 0.5 h, then warmed to -78 °C for 2 h and then -40 °C for 2 h. The reaction was quenched by the addition of saturated $NaHCO_3$ (5 mL) at -40 °C. The solution was warmed to 23 °C, extracted with CH_2Cl_2 (4 X 5 mL), dried through $MgSO_4$, and concentrated. The residue was purified by flash chromatography (0:100 5:95 \rightarrow Et $_2$ O/hexanes) to afford enone **3.17** (18.6 mg, 6%) as a colorless oil. R_f 0.63 (1:4 Et $_2$ O/hexanes); IR (thin film) ν_{max} 1754, 1721, 1697, 1673, 1628, 1448 cm^{-1} ; 1H NMR (300 MHz, benzene- d_6) δ 6.72 (dd, J = 6.6, 15.9 Hz, 1H), 6.03 (d, J = 15.9 Hz, 1H), 2.35 (t, J = 7.5 Hz, 2H), 2.06-0.64 (m, 47H); ^{13}C NMR (125 MHz,

benzene-d₆) δ 199.1, 150.6, 128.2, 40.5, 37.9, 37.5, 33.3, 31.9, 31.8, 30.1(2), 26.8, 26.5(2), 26.0, 25.8(2); LRMS (ESI) Calcd. for C₁₇H₂₈OLi [M+Li] 255, found 255.

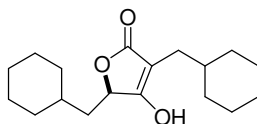


Diisopropyl amide 3.19. To a solution of spiroepoxy- β -lactone **2.63a** (39.9 mg, 0.136 mmol) in CH₂Cl₂ (3 mL) was added diisopropylamine (27.6 mg, 0.273 mmol) at 23 °C and stirred for 19 h. The solution was concentrated and the residue was purified by flash chromatography (1:1 Et₂O/hexanes) to give amide **3.19** as an inseparable mixture of diastereomers (27.7 mg, 52%, dr 1:1.14) as a clear oil. *R_f* 0.25 (1:1 Et₂O/hexanes); IR (thin film) ν_{max} 1716, 1639 cm⁻¹; ¹H NMR (500 MHz, benzene-d₆) δ 6.15 (t, *J* = 6.0 Hz, 1H), 6.03 (t, *J* = 5.5 Hz, 1H), 4.49-4.44 (m, 1H), 4.43-4.36 (m, 2H), 4.22 (d, *J* = 6.5 Hz, 1H), 4.09 (q, *J* = 7.5 Hz, 2H), 3.05 (app. septet, *J* = 6.5 Hz, 4H), 1.91-1.46 (m, 34H), 1.37-0.74 (m, 41H); ¹³C NMR (125 MHz, benzene-d₆) δ 212.6, 211.7, 168.8, 168.7, 75.9, 75.4, 54.6, 54.1, 41.9, 41.2, 39.64, 39.59, 38.9, 37.7, 36.1, 36.0, 34.6, 34.4, 34.3, 34.2, 33.7, 33.4, 33.3, 32.33, 32.31, 31.76, 26.84, 26.78, 26.70, 26.69, 26.65, 26.48, 26.44, 26.42, 26.40, 26.36, 20.21, 20.20, 13.8; LRMS (ESI) Calcd. for C₂₄H₄₃NO₃ [M+Li-CH₂CH₂] 372, found 372.

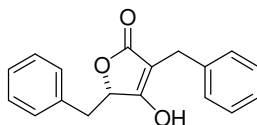


Diethyl amide 3.18. To a solution of spiroepoxy- β -lactone **2.63a** (47.2 mg, 0.160 mmol) in CH₂Cl₂ (2 mL) was added diethylamine (0.03 mL, 0.32 mmol) and stirred at 23 °C for 22 h. The solution was concentrated and the residue purified by flash chromatography

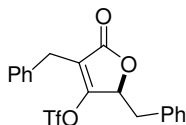
(1:1 Et₂O/hexanes) to give amide **3.18** (42.8 mg, 73%) as a white solid, m.p. 106-108 °C, which was recrystallized from CH₂Cl₂. *R_f* 0.19 (1:1 Et₂O/hexanes); IR (thin film) ν_{\max} 1721, 1609 cm⁻¹; ¹H NMR (500 MHz, CDCl₃) δ 4.30 (dd, *J* = 0.31, 10.5 Hz, 1H), 3.88 (dd, *J* = 5.5, 8.0 Hz, 1H), 3.43-3.32 (m, 4H), 2.04 (ddd, *J* = 5.5, 8.0, 13.5 Hz, 1H), 1.89 (br s, 1H), 1.86 (br s, 1H), 1.75-1.53 (m, 13 H), 1.38-1.09 (m, 15H), 1.01-0.82 (m, 4H); ¹³C NMR (125 MHz, CDCl₃) δ 169.1, 73.7, 50.9, 42.3, 41.7, 40.6, 36.3, 36.0, 34.4, 33.9, 33.6, 32.9, 32.0, 26.5, 26.4, 26.3, 26.1, 26.0, 14.5, 12.7; LRMS (ESI) Calcd. for C₂₂H₃₉NO₃ [M+Li] 372, found 372.



Butenolide 3.24. Butenolide **3.24** was prepared from spiroepoxy- β -lactone . To a solution of **2.64a** (34.9 mg, 0.119 mmol) in CH₂Cl₂ (1.5 mL) was added DBU (36.3 mg, 0.239 mmol) and the solution was stirred at 23 °C for 12 h. The reaction was quenched with saturated NH₄Cl and then extracted with EtOAc (5 X 10 mL) dried over Na₂SO₄ and concentrated. The residue was purified by flash chromatography (2:1 Et₂O/hexanes) to give butenolide **3.24** (24.8 mg, 71%) as a white solid m.p. 147-148 °C which was recrystallized from CH₂Cl₂. *R_f* 0.22 (6:3 Et₂O/hexanes); IR (thin film) ν_{\max} 1716, 1639 cm⁻¹; ¹H NMR (500 MHz, CD₃OD) δ 4.78 (dd, *J* = 2.8, 9 Hz, 1H), 2.03 (ddd, *J* = 6.5, 7.0, 13.5 Hz, 1H), 1.99 (ddd, *J* = 7.0, 7.0, 13.5, Hz, 1H), 1.90-1.64 (m, 12H), 1.60-1.45 (m, 2H), 1.42-1.15 (m, 9H), 1.08-0.87 (m, 6H); ¹³C NMR (125 MHz, CD₃OD) δ 177.2, 177.0, 99.2, 76.2, 39.8, 37.1, 34.4, 34.1, 32.99, 32.93, 32.8, 28.4, 26.4, 26.29, 26.26, 26.20(2), 26.1; LRMS (ESI) Calcd. for C₁₈H₂₈O₃ [M+H] 293, found 293.

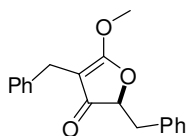


Benzyl Butenolide 3.57. To a solution of spiroepoxy- β -lactone **2.64b** (61.4 mg, 2.19 mmol) in CH_2Cl_2 (5 mL) was added *N,O*-dimethylhydroxylamine (20 mL, 0.219 mmol) and stirred at 23 °C for 6 h at which time the solution had copious amounts of white solid. The suspension was concentrate to give butenolide **3.57** (61.4 mg, 100%) as a white solid. Purification of butenolide **3.57** was not possible due to its instablity to silica gel. IR ν_{max} 1715, 1650 cm^{-1} ; ^1H NMR (500 MHz, CD_3OD) δ 7.25-7.20 (m, 5H), 7.13-7.05 (m, 3H), 6.76 (d, J = 7.5Hz, 2H), 5.05 (t, J = 4.3 Hz, 1H), 3.43-3.28 (obs, 2H), 3.01 (dd, J = 5.0, 14.5 Hz, 1H); ^{13}C NMR (125 MHz, CD_3OD) δ 176.3, 175.8, 138.8, 134.8, 129.8, 128.1(2), 128.0(2), 127.7, 126.9, 125.6, 100.5, 78.3, 36.8, 26.3; LRMS (ESI) Calcd. for $\text{C}_{18}\text{H}_{16}\text{O}_3$ 280, found 287 $[\text{M}+\text{Li}]$.

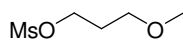


Triflate 3.55. To a solution of butenolide **3.52** (37.9 mg, 0.14 mmol) in CH_2Cl_2 (1.4 mL) was added Hunig's base (0.3 mL, 0.15 mmol) and Tf_2O (0.2 mL, 0.14 mmol) at -78 °C and stirred for 2 h. The reaction was quenched at -78 °C with pH 7 buffer and extracted with CH_2Cl_2 (3 X 5 mL) and dried with MgSO_4 and concentrated. The residue was purified by column chromatography (3:10 Et_2O /hexanes) to give triflate **3.50** (47.9 mg, 52%) as an oily solid. R_f 0.50 (3:7 Et_2O /hexanes); $[\alpha]_{\text{D}}^{23}$ +71 (c = 1.0, CH_2Cl_2); IR ν_{max} 1779 cm^{-1} ; ^1H NMR (500 MHz, benzene- d_6) δ 7.26-7.12 (m, 8H), 6.79-6.75 (m, 2H), 5.40 (t, J = 5.0 Hz, 1H), 3.51 (s, 2H), 3.41 (dd, J = 4.3, 14.5 Hz, 1H), 3.03 (dd, J = 4.3, 14.5 Hz, 1H); ^{13}C NMR (125 MHz, benzene- d_6) δ 167.8, 161.3, 135.2, 132.8, 129.7,

128.8, 128.7, 128.5, 128.2, 126.9, 77.6, 36.7, 28.3; LRMS (ESI) Calcd. for $C_{19}H_{15}O_5F_3S$ 412, found 419 [M+Li].

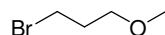


Enol Ether 3.53. To a solution of butenolide **3.52** in CH_2Cl_2 (2 mL) was added Me_3OBF_4 (38.7 mg, 0.248 mmol) and stirred at 23 °C for 24 h. Starting material was still present and an additional amount of Me_3OBF_4 (21.2 mg, 0.143 mmol) was added. The reaction was quenched with pH 7 buffer (2 mL) and extracted with CH_2Cl_2 (3 X 5 mL) to give enol ether **3.53** (23.6 mg, 97%) as a clear oil. Purification of enol ether **3.53** was not possible due to its instability to silica gel. IR ν_{max} 1729, 1658 cm^{-1} ; 1H NMR (500 MHz, benzene- d_6) δ 7.17 (d, J = 8.0 Hz, 2H), 7.07 (d, J = 8.0 Hz, 2H), 7.02-6.96 (m, 6H), 4.31 (dd, J = 4.1, 6.5 Hz, 1H), 3.47 (d, J = 15.5 Hz, 1H), 3.37 (d, J = 15.5 Hz, 1H), 3.00 (s, 3H), 3.00-2.97 (obs., 1H), 2.80 (dd, J = 6.5, 14.5 Hz, 1H); ^{13}C NMR (benzene- d_6) δ 195.6, 180.0, 140.8, 135.7, 129.7, 128.5, 128.46, 128.3, 128.2(2), 126.9, 126.0, 93.5, 81.4, 54.9, 36.8, 25.9; LRMS (APCI) Calcd. for $C_{19}H_{18}O_3$ [M+H] 295, found 295.



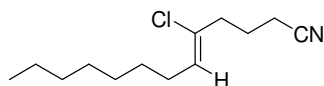
3-Methoxypropyl methanesulfonate. To a solution of 3-methoxypropanol in CH_2Cl_2 (200 mL) was added Et_3N (6.789 g, 67.1 mmol) and cooled to 0 °C. To this mixture was added methanesulfonyl chloride (7.042 g, 61.5 mmol) and stirred at this temperature for 2 h. The reaction of then quenched by the addition of pH 7 buffer (10 mL) and extracted with Et_2O (3 X 20 mL). The combined organic were then dried with Na_2SO_4 and concentrated to a light yellow oil. This oil was purified by flash chromatography (8:2,

Et₂O:hexanes) to give 3-methoxypropyl methansulfonate as a clear oil (8.85 g, 94%). *R_f* 0.35 (8:2 Et₂O/hexanes); IR (thin film) ν_{\max} 1650 cm⁻¹; ¹H NMR (500 MHz, CDCl₃) δ 4.35 (t, *J* = 6.5 Hz, 2H), 3.51 (t, *J* = 7.0 Hz, 2H), 3.36 (s, 3H), 3.03 (s, 3H), 2.02 (pentet, *J* = 6.0 Hz, 2H); ¹³C NMR (125 MHz, CDCl₃) δ 68.1, 67.6, 59.0, 37.4, 29.7; LRMS (CI) Calcd. for C₅H₁₂O₄S [M+H] 169, found 169.



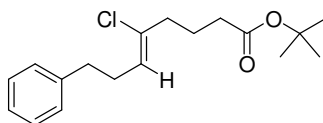
1-Bromo-3-methoxypropane. To a solution of 3-methoxypropyl methansulfonate (8.85 g, 52.6 mmol) in acetone was added lithium bromide (13.81 g, 157.8 mmol) and heated to reflux for 6 h. The reaction mixture was cooled and then concentrated. The residue was dissolved in water and extracted with CH₂Cl₂ (3 X 10 mL). The combined organics were dried with Na₂SO₄ and concentrated to give 1-bromo-3-methoxypropane as a pale yellow oil (4.81 g, 60%). IR (thin film) ν_{\max} 1116 cm⁻¹; ¹H NMR (500 MHz, CDCl₃) δ 3.52 (t, *J* = 6.5 Hz, 4H), 3.37 (s, 3H), 2.12 (pentet, *J* = 6.0 Hz, 2H); ¹³C NMR (125 MHz, CDCl₃) δ 70.3, 59.0, 33.0, 30.8; LRMS (CI) Calcd. for C₄H₉BrO [M+H] 153.9, found 153.9.

General Procedure for the formation of zincates. To an oven dried flask containing zinc powder (1.702 g, 26.0 mmol) was added DMA (12.8 mL) and iodine (0.325 g, 1.28 mmol). This slurry was stirred at 60 °C until the brown color of the iodine had disappeared. The alkyl bromide (2.500 g, 12.8 mmol) was then added to this slurry and heated to 85 °C for 6-24 h. The disappearance of the starting material was monitored by TLC and ¹H NMR.



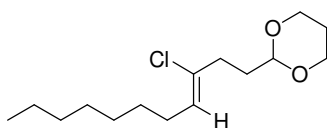
Typical Procedure for *Trans*-selective Cross Coupling. To a 10 mL microwave tube was added *bis*(tri-*tert*-butylphosphine)palladium (0) (11.2 mg, 0.0219 mmol) in a glove

box. This was followed by 1,1-dichloroalkene **4.12** (96.1 mg, 0.492 mmol) as a solution in THF (1.5 mL). Finally zincate derived from 4-bromobutyronitrile (1 M, 1.5 mL) was added to make a dark purple-brown solution. A microwave cap was affixed to the tube and argon was bubbled through the solution to degass for 15 min. The tube was then heated with μ W irradiation for 5 h at 100 °C. After cooling the solution was then quenched with ammonium chloride (2 mL) and extracted with ether (4 X 2 mL). The combined organics were then washed with brine (3 X 1 mL). Finally the organics were dried with MgSO_4 and concentrated. The golden residue was then purified by flash chromatography (1:20, ethyl ether:hexanes) to give **4.13a** as a clear oil (58.1 mg, 52%). R_f 0.24 (5:95 Et_2O /hexanes); IR (thin film) ν_{max} 2248 cm^{-1} ; ^1H NMR (500 MHz, CDCl_3) δ 5.59 (t, $J = 7.0$ Hz, 1H), 2.49 (t, $J = 6.5$ Hz, 2H), 2.34 (t, $J = 6.5$ Hz, 2H), 2.17 (q, $J = 6.5$ Hz, 2H), 1.93 (pentet, $J = 6.5$ Hz, 2H), 1.42-1.35 (m, 2H), 1.32-1.24 (m, 9H), 0.89 (t, $J = 7.0$ Hz, 3H); ^{13}C (125 MHz, CDCl_3) δ 131.7, 128.6, 119.5, 38.0, 32.0, 29.4, 29.3, 28.8(2), 23.1, 22.9, 15.9, 14.3; LRMS (CI) Calcd. for $\text{C}_{13}\text{H}_{22}\text{ClN}$ $[\text{M}+\text{H}]$ 228, found 228.

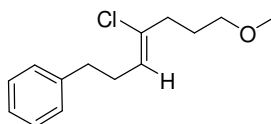


Chloroalkene 4.13b. Chloroalkene **4.13b** was prepared by the general procedure with 1,1-dichloroalkene **4.8** (45.6 mg, 0.227 mmol). Purification by flash chromatography (20:80 ethyl ether:hexanes) gave chloroalkene **4.13b** (42.0 mg, 60%) as a clear oil. R_f 0.37 (5:95 Et_2O /hexanes); IR (thin film) ν_{max} 1730 cm^{-1} ; ^1H NMR (500 MHz, CDCl_3) δ 7.31-7.18 (m, 5H), 5.49 (t, $J = 7.0$ Hz, 1H), 2.70 (t, $J = 8.0$ Hz, 2H), 2.50 (q, $J = 7.0$ Hz, 2H), 2.34 (t, $J = 7.0$ Hz, 2H), 2.18 (t, $J = 7.0$ Hz, 2H), 1.82 (pentet, $J = 7.5\text{Hz}$, 2H), 1.45 (s, 9H); ^{13}C NMR (125 MHz, CDCl_3) δ 172.6, 141.4, 134.3, 128.4, 128.3, 125.9, 125.3,

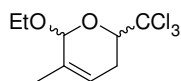
80.2, 38.5, 34.7, 34.0, 30.2, 28.1(3), 22.7; LRMS (CI) Calcd. for $C_{18}H_{25}ClO_2$ $[M+H]$ 309, found 309.



Chloroalkene 4.13c. Chloroalkene **4.13c** was prepared by the general procedure with 1,1-dichloroalkene **4.12** (87.7 mg, 0.450 mmol). Purification by flash chromatography (15:85 ethyl ether:hexanes) gave chloroalkene **4.13c** (48.6 mg, 39%) as a clear oil. IR (thin film) ν_{\max} 1147 cm^{-1} ; ^1H NMR (500 MHz, CDCl_3) δ 5.48 (t, $J = 7.0$ Hz, 1H), 4.52 (t, $J = 5.0$ Hz, 1H), 4.11 (dd, $J = 5.0, 11.0$ Hz, 2H), 3.75 (dt, $J = 2.6, 12.5$ Hz, 2H), 2.41 (app. t, $J = 7.5$ Hz, 2H), 2.15 (q, $J = 7.0$ Hz, 2H), 2.12-2.02 (m, 1H), 1.87-1.82 (m, 2H), 1.40-1.23 (m, 12H), 0.89 (t, $J = 7.0$ Hz, 3H); ^{13}C NMR (125 MHz, CDCl_3) δ 133.8, 126.3, 101.4, 67.1(2), 34.2, 33.3, 32.1, 29.4, 28.9, 28.7, 26.0, 22.9, 14.3; LRMS (CI) Calcd. for $C_{15}H_{27}ClO_2$ $[M+H]$ 275, found 275.



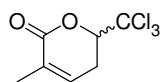
Chloroalkene 4.13d. Chloroalkene **4.13d** was prepared by the general procedure with 1,1-dichloroalkene **4.8** (54.4 mg, 0.27 mmol). Purification by flash chromatography (5:95 ethyl ether:pentane) to give chloroalkene **4.13d** (25.8 mg, 40 %) as a clear oil. IR ν_{\max} 1445 cm^{-1} ; ^1H NMR (300 MHz, CDCl_3) δ 7.34-7.18 (m, 5H), 5.53 (t, $J = 6.6$ Hz, 1H), 3.40-3.30 (m, 5H), 2.73 (t, $J = 6.9$ Hz, 2H), 2.52 (q, $J = 6.6$ Hz, 2H), 2.40 (t, $J = 7.5$ Hz, 2H), 1.82 (pentet, $J = 6.9$ Hz, 2H); ^{13}C NMR (125MHz, CDCl_3) δ 141.7, 134.9, 128.7, 128.6, 126.2, 125.2, 71.5, 58.8, 36.3, 35.0, 30.3, 27.6; LRMS (CI) Calcd. for $C_{14}H_{19}ClO$ 238, found 239 $[M+H]$



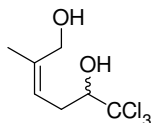
Dihydropyran 4.24. To a solution of ethoxydiene **4.25** (2.249 g, 20 mmol) in toluene (10 mL) was added chloral **4.26** (14.74 g, 100 mmol), which had been distilled and stored over Na_2CO_3 , at 0 °C. The solution was slowly warmed to 23 °C overnight and stirred for 2 days. The reaction mixture was then concentrated by rotary evaporation. The white paste was then purified by flash chromatography (1:9, ether/hexanes) to give a mixture of diastereomeric dihydropyrans **4.24** as a clear oil (2.991g, 58%, dr 1:4) Note: The dr observed in this reaction was variable and ranged from 1:1 to 1:4, the diastereomers could be separated when the diastereomeric ratio was 1:4. R_f 0.68 (1:9 Et_2O /hexanes); IR (thin film) ν_{max} 2974 cm^{-1} ; ^1H NMR (500 MHz, CDCl_3) δ 5.67 (br s, 1H), 5.00 (s, 1H), 4.45 (dd, J = 4.0, 10.5 Hz, 1H), 4.06 (dq, J = 2.5, 7.5 Hz, 1H), 3.65 (dq, J = 2.5, 7.5 Hz, 1H), 2.51-2.39 (m, 2H), 1.77 (br s, 3H), 1.28 (t, J = 7.0 Hz, 3H); ^{13}C (125 MHz, CDCl_3) δ 132.6, 121.1, 100.8, 98.9 (2), 64.3, 27.0, 18.8, 15.3; LRMS (APCI) Calcd. for $\text{C}_9\text{H}_{13}\text{Cl}_3\text{O}_2$ $[\text{M}+\text{H}]$ 259, found 259.

Diol 4.29. To a solution of aldehyde **4.28** (245.3 mg, 1.06 mmol) in EtOH (5 mL) was added a solution of $\text{CeCl}_3 \cdot 7\text{H}_2\text{O}$ (1.21 g, 3.18 mmol) in EtOH (5 mL). This was followed by the addition of NaBH_4 (60.1 mg, 1.59 mmol) at which time the solution fizzed and turned cloudy brown. After stirring for 5 h the reaction was quenched with sat. NH_4Cl (6 mL) and extracted with EtOAc (3 X 5 mL), dried with Na_2SO_4 and concentrated. The residue was purified by flash chromatography (1:1 EtOAc/hexanes) to give diol **4.29** (172.7 mg, 70%) as a white solid. IR ν_{max} 3400 cm^{-1} ; ^1H NMR (500 MHz, CDCl_3) δ 5.59 (t, J = 8.5 Hz, 1H), 4.09-4.05 (m, 2H), 3.59-3.45 (m, 2H), 2.84 (dd, J = 6.5, 14.0 Hz, 1H),

2.77 (d, $J = 5.0$ Hz, 1H) 2.47-2.39 (m, 1H), 1.73 (s, 3H); ^{13}C NMR (125 MHz, CDCl_3) δ 138.9, 120.0, 103.8, 83.1, 68.6, 30.4, 14.2; LRMS (CI) Calcd. for $\text{C}_7\text{H}_{11}\text{Cl}_3\text{O}_2$ 232, found 233 [M+H].

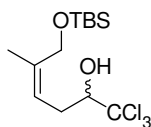


Lactone 4.31. To a solution of dihydropyran **4.24** (204 mg, 0.786 mmol) in acetone (20 mL) was added Jones reagent (2.06 mL, 3 M in H_2O) at 0 $^\circ\text{C}$. The reaction was warmed to 23 $^\circ\text{C}$ and stirred for 3 h. The reaction was quenched with 2-propanol (2 mL) and stirred until the solution had turned from orange to green, and then extracted with EtOAc (3 X 5mL). The combined organics were washed with brine (3 X 2 mL) and dried with MgSO_4 and concentrated. The crude oil was purified by flash chromatography (60:40 Et_2O :hexanes) to give lactone **4.31** as a white solid (95.9 mg, 53%). R_f 0.42 (3:2 Et_2O :hexanes); IR (ATR) ν_{max} 3043, 1732 cm^{-1} ; ^1H NMR (500 MHz, CDCl_3) δ 6.67-6.64 (m, 1H), 4.87 (dd, $J = 4.3, 12.0$ Hz, 1H), 2.90 (br dt, $J = 5.0, 18.0$ Hz, 1H), 2.83-2.75 (m, 1H), 2.0 (app pentet, $J = 1.3$ Hz, 3H); ^{13}C NMR (125 MHz, CDCl_3) δ 163.3, 137.3, 128.7, 97.9, 85.1, 26.2, 17.1; LRMS (CI) Calcd. for $\text{C}_7\text{H}_7\text{Cl}_3\text{O}_2$ [M+H], 229 found 228.9.

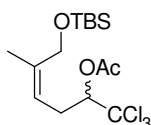


Diol 4.30. To lactone **4.31** (305.4 mg, 1.33 mmol) was added a solution of $\text{CeCl}_3 \cdot 7\text{H}_2\text{O}$ (0.5M, 13.3 mL) in anhydrous MeOH. This was followed by the addition of solid NaBH_4 (252 mg, 6.65 mmol) at 0 $^\circ\text{C}$. The reaction mixture was allowed to warm to 23 $^\circ\text{C}$ overnight. The solution was quenched by the addition of sat. NH_4Cl (2 mL) and extracted repeatedly with Et_2O . The combined organics were dried with Na_2SO_4 and

concentrated. The crude oil was purified by flash chromatography (40:60→50:50 Et₂O:hexanes) to give diol **4.30** as an oil (134 mg, 43%). *R_f* 0.25 (1:1 Et₂O/hexanes); IR (thin film) ν_{\max} 3342 cm⁻¹; ¹H NMR (500 MHz, CDCl₃) δ 5.49 (d of pentets, *J* = 1.4, 8.0 Hz, 1H), 4.36 (d, *J* = 12.0 Hz, 1H), 4.04 (dd, *J* = 2.2, 10.0 Hz, 1H), 3.99 (d, *J* = 12.0 Hz, 1H), 2.78 (dd, *J* = 7.0, 12.0 Hz, 1H), 2.61 (dt, *J* = 10.0, 14.0 Hz, 1H); ¹³C NMR (125 MHz, CDCl₃) δ 139.4, 123.2, 103.9, 81.9, 61.9, 30.7, 22.9; LRMS (CI) Calcd. for C₇H₁₁Cl₃O₂ 232.8 [M+H], found 232.8.

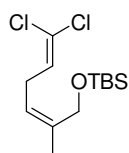


(Z)-6-(*Tert*-butyldimethylsilyloxy)-1,1,1-trichloro-5-methylhex-4-en-2-ol. To a solution of diol **4.30** (133 mg, 0.56 mmol), freshly azeotroped with toluene, in DMF (1 mL) was added imidazole (63.0 mg, 0.93 mmol). Finally TBSCl (108 mg, 0.68 mmol) was added to the reaction mixture and stirred at 23 °C for 42 h. The reaction was quenched with brine (1 mL) and extracted with ether (3 X 1 mL), dried with MgSO₄ and concentrated. The crude oil was purified by flash chromatography (10:90 Et₂O/hexanes) to yield (Z)-6-(*tert*-butyldimethylsilyloxy)-1,1,1-trichloro-5-methylhex-4-en-2-ol (192.4 mg, 97%) as a clear oil. *R_f* 0.30 (2:8 Et₂O/hexanes); IR (thin film) ν_{\max} 3389 cm⁻¹; ¹H NMR (500 MHz, CDCl₃) δ 5.46 (br. t, *J* = 8.0 Hz, 1H), 4.31 (d, *J* = 11.5 Hz, 1H), 4.08 (d, *J* = 5.5 Hz, 1H), 4.01 (d, *J* = 11.5 Hz, 1H), 4.01 (obs., 1H), 2.80 (br. dd, *J* = 6.5, 14.0 Hz, 1H), 2.57 (dt, *J* = 10.0, 14.0 Hz, 1H), 1.84 (s, 3H), 0.94 (s, 9H), 0.14 (s, 6H); ¹³C NMR (125 MHz, CDCl₃) δ 139.3, 122.7, 104.2, 81.9, 62.5, 31.0, 26.2, 22.9, 18.8(3), -5.07, -5.1; LRMS (CI) Calcd. for C₁₃H₂₅Cl₃O₂Si [M+H] 347, found 347.



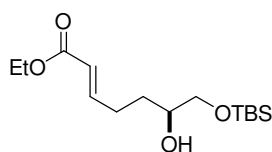
(Z)-5-(*Tert*-butyldimethylsilyloxy)-1,1,1-trichloro-4-methylpent-3-en-2-yl acetate.

To a solution of (Z)-6-(*tert*-butyldimethylsilyloxy)-1,1,1-trichloro-5-methylhex-4-en-2-ol (152 mg, 0.44 mmol) in pyridine (1.5 mL) was added acetic anhydride (89 mg, 0.87 mmol, 0.09 mL) and stirred for 21 h. An additional equivalent of acetic anhydride (45 mg, 0.44 mmol, 0.04 mL) was added and stirred for an additional 2 h. The reaction was concentrated *en vacuo* to give (Z)-6-(*tert*-butyldimethylsilyloxy)-1,1,1-trichloro-5-methylhex-4-en-2-yl acetate (168 mg, 99%) as a pale yellow oil which is of sufficient purity to take on to the next step. IR (thin film) ν_{\max} 1762 cm^{-1} ; ^1H NMR (500 MHz, CDCl_3) δ 5.54 (dd, $J = 2.6, 10$ Hz), 5.38 (br. t, $J = 7.5$ Hz, 1H), 4.01 (s, 2H), 2.88 (dd, $J = 6.5, 15.0$ Hz, 1H), 2.72 (ddd, $J = 8.0, 11.0, 15.0$ Hz, 1H), 2.15 (s, 3H), 1.66 (br. s, 3H), 0.92 (s, 9H), 0.072 (s, 3H), 0.069 (s, 3H); ^{13}C NMR (125 MHz, CDCl_3) δ 169.7, 140.0, 119.0, 99.9, 80.7, 62.0, 29.2, 26.2(3), 21.5, 20.9, 18.6, -5.16, -5.15; LRMS (APCI) Calcd. for $\text{C}_{15}\text{H}_{27}\text{Cl}_3\text{O}_3\text{Si}$ [M+H] 389, found 389.



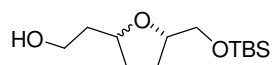
1,1-dichloroolefin 2.52. To (Z)-6-(*tert*-butyldimethylsilyloxy)-1,1,1-trichloro-5-methylhex-4-en-2-yl acetate (17.9 mg, 0.046 mmol) was added degassed THF (0.5 mL). To this solution was added SmI_2 (0.1 M, 1.84 mL) at 0°C and stirred. The reaction mixture was then concentrated and the residue purified by flash chromatography (10:90 Et_2O /hexanes) to give 1,1-dichloroolefin **2.52** (8.1 mg, 60%) as a pale yellow oil. R_f 0.67 (1:9 Et_2O /hexanes); IR (thin film) ν_{\max} 1430 cm^{-1} ; ^1H NMR (500 MHz, CDCl_3) δ 5.82 (t,

$J = 7.5$ Hz, 1H), 5.19 (br. t, $J = 7.5$ Hz, 1H), 4.18 (s, 2H), 2.93 (t, $J = 7.5$ Hz, 2H), 1.77 (br. s, 3H), 0.93 (s, 9H), 0.10 (s, 6H); ^{13}C NMR (125 MHz, CDCl_3) δ 137.8, 128.7, 121.1, 120.3, 62.0, 28.5, 26.2(3), 21.3, 18.6, -5.1(2); LRMS (CI) Calcd. for $\text{C}_{13}\text{H}_{24}\text{Cl}_2\text{OSi}$ [M+H] 295, found 295.

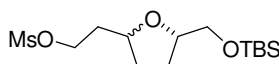


α , β -unsaturated ester 4.34. To a solution of lactone **4.32** (3.01 g, 13.1 mmol) in THF (60 mL) at -78 °C was added DIBAL-H (1.95 g, 13.7 mmol, 2.4 mL) as a neat liquid. This solution was stirred at this temperature for 2 h. In a separate flask, a suspension of NaH (628 mg, 26.2 mmol) in THF (90 mL) was added triethyl phosphonoacetate **4.33** (3.52 g, 15.7 mmol) at 23 °C and stirred at that temperature for 2 h. After stirring the solution of pale yellow sodium phosphonate was added to the lactol at -78 °C. The resulting solution was allowed to warm to 23 °C and stirred overnight. The reaction mixture was carefully quenched with H_2O (2 mL) followed by then a saturated solution of Rochelle's salt (50 mL), and EtOAc (50 mL). The resulting biphasic solution was stirred until both layers were clear. The aqueous phase was then extracted with EtOAc (3 X 10 mL), dried Na_2SO_4 and concentrated. The crude oil was then purified by flash chromatography (20:80 Et_2O :hexanes) to give α , β -unsaturated ester **4.34** (2.57 g, 65%) as a clear oil. IR (thin film) ν_{max} 3474, 1719 cm^{-1} ; ^1H NMR (500 MHz, CDCl_3) δ 7.00 (dt, $J = 7.0, 15.5$ Hz 1H), 5.87 (dt, $J = 1.6, 15.5$ Hz, 1H), 4.21 (q, $J = 7.5$ Hz, 2H), 3.70-3.63 (m, 2H), 3.43 (dd, $J = 7.0, 9.0$ Hz, 1H), 2.43 (d, $J = 4.2$ Hz, 1H), 2.47-2.39 (m, 1H), 2.33 (app. sextet, $J = 7.5$ Hz, 1H), 1.65-1.52 (m, 1H), 1.31 (t, $J = 7.5$ Hz, 3H), 0.92 (s, 9H), 0.10 (s, 6H); ^{13}C NMR (125 MHz, CDCl_3) δ 166.9, 148.9, 121.9, 71.2, 67.3, 60.5,

31.4, 28.6, 26.1, 18.5, 14.5, -5.1, -5.2; LRMS (ESI) Calcd. for $C_{15}H_{30}O_4Si$ [M+Li] 309, found 309.

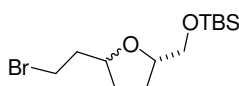


Tetrahydrofuran 4.35. To a solution of α , β -unsaturated ester **4.34** (2.57 g, 8.50 mmol) in THF (120 mL) at 0 °C was added KHMDS (0.85 mmol, 1.7 mL, 0.5M) in toluene. The reaction was warmed to 23 °C over 1 h. Once TLC showed consumption of starting material the reaction solution was concentrated and used in the next step without further purification. The light yellow crude oil was redissolved in CH_2Cl_2 (90 mL) and cooled to 0 °C. To this solution was added neat DIBAL-H (4.23g, 30 mmol, 5.3 mL). After the initial fizzing stopped, the solution became colorless. The reaction mixture was then warmed to 23 °C and stirred for 6 h. The solution was quenched by the addition of a saturated solution of Rochelle's salt (50 mL) and EtOAc (50 mL) and stirred overnight. The solution was then extracted with EtOAc (3 X 10 mL), dried Na_2SO_4 and concentrated to give a colorless oil. The crude oil was then purified by flash chromatography (30:70 EtOAc:hexanes) to give tetrahydrofuran **4.35** (998 mg, 45%) as a colorless oil and a mixture of diastereomers of an indeterminable ratio by 1H NMR due to overlapping peaks. R_f 0.17 (3:7 EtOAc/hexanes); IR (thin film) ν_{max} 3398 cm^{-1} ; 1H NMR (500 MHz, $CDCl_3$) δ 3.88 (ddd, J = 2.5, 4.8, 10.5 Hz, 1H), 3.80-3.75 (m, 2H), 3.65 (app. septet, J = 4.8 Hz, 1H), 3.50-3.44 (m, 1H), 3.12 (app. t, J = 10.5 Hz, 1H), 2.59 (br. s, 1H), 2.03-1.97 (m, 1H), 1.74-1.66 (m, 3H), 1.50-1.40 (m, 2H), 0.89 (s, 9H), 0.07 (s, 3H), 0.06 (s, 3H); ^{13}C NMR (125 MHz, $CDCl_3$) δ 78.0, 73.1, 67.1, 61.7, 37.7, 33.5, 31.1, 26.0(3), 18.4, -4.45, -4.48; LRMS (APCI) Calcd. for $C_{13}H_{28}O_3Si$ [M+H] 261, found 261.



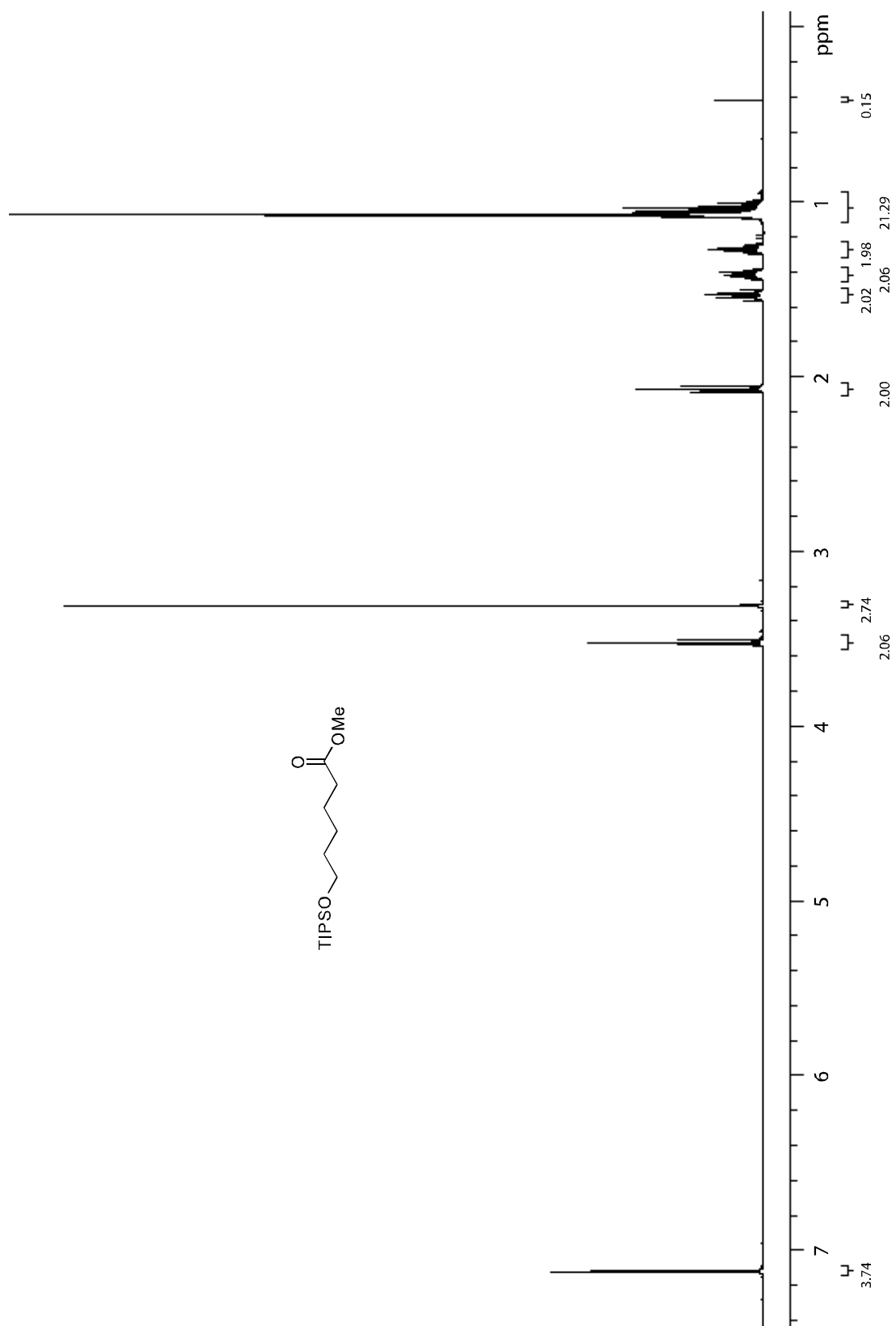
2-(5-((*Tert*-butyldimethylsilyloxy)methyl)tetrahydrofuran-2-yl)ethyl

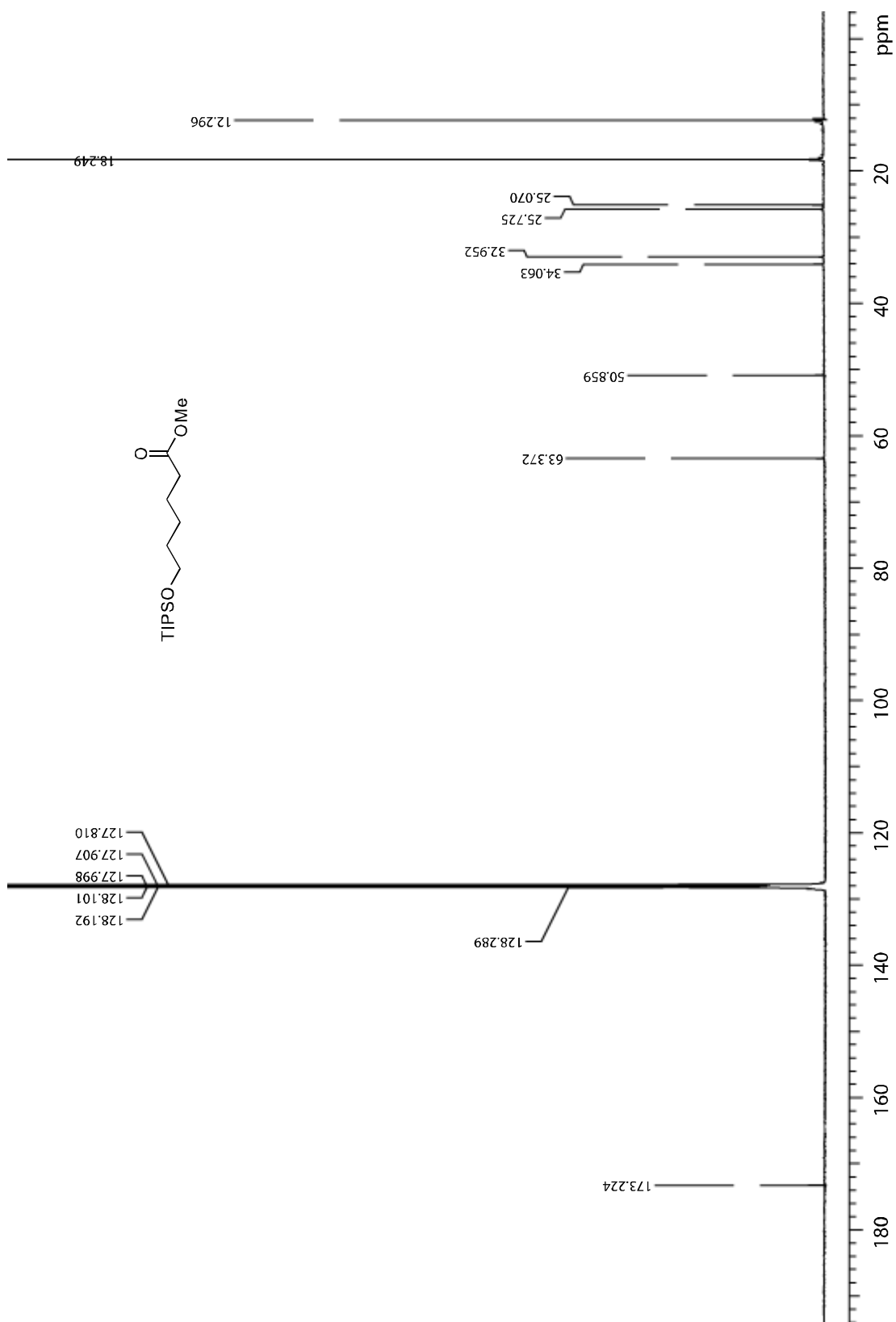
methanesulfonate. To a solution of THF **4.27** in CH₂Cl₂ (10 mL) was added Et₃N (260 μL, 1.86 mmol) at 0 °C. Methanesulfonyl chloride (130 μL, 1.70 mmol) was then added to this solution and stirred at 0 °C. After 24 h starting material was still present methansulfonyl chloride (260 μL, 1.70 mmol) and Et₃N (260 μL, 1.86 mmol) were added. This solution was allowed to slowly warm to 23 °C for 1 h. The reaction was then quenched with pH 7 buffer (2 mL) and extracted with Et₂O (3 X 5 mL) dried with Na₂SO₄ and concentrated. The residue was purified by flash chromatography (4:1 Et₂O/hexanes) to yield 2-(5-((*tert*-butyldimethylsilyloxy)methyl)tetrahydrofuran-2-yl)ethyl methanesulfonate (367 mg, 70%) as a clear oil and a mixture of diastereomers of an indeterminable ratio by ¹H NMR due to overlapping peaks. *R_f* 0.5 (4:1 Et₂O/hexanes); IR (thin film) *v*_{max} 1356 cm⁻¹; ¹H NMR (500 MHz, CDCl₃) δ 4.40 (m, 2H), 3.86 (ddd, *J* = 2.2, 5.0, 11.0 Hz, 1H), 3.80-3.75 (m, 1H), 3.65 (app. septet, *J* = 5.0 Hz, 1H), 3.54-3.44 (m, 1H), 3.41-3.35 (m, 1H), 3.09 (t, *J* = 10.5 Hz, 1H), 3.02 (s, 3H), 2.05-1.67 (m, 4H), 1.52-1.33 (m, 2H), 0.92 (s, 3H), 0.89 (s, 6H), 0.08 (s, 4H), 0.07 (s, 2H); ¹³C NMR (500 MHz, CDCl₃) δ 73.1, 67.6, 67.4, 67.1, 37.3, 35.44, 35.40, 33.5, 31.0, 30.9, 26.2, 26.0, 18.5, 18.4, -4.4, -4.5, -4.6; LRMS (CI) Calcd. for C₁₄H₃₀O₅SSi [M+H] 339, found 339.

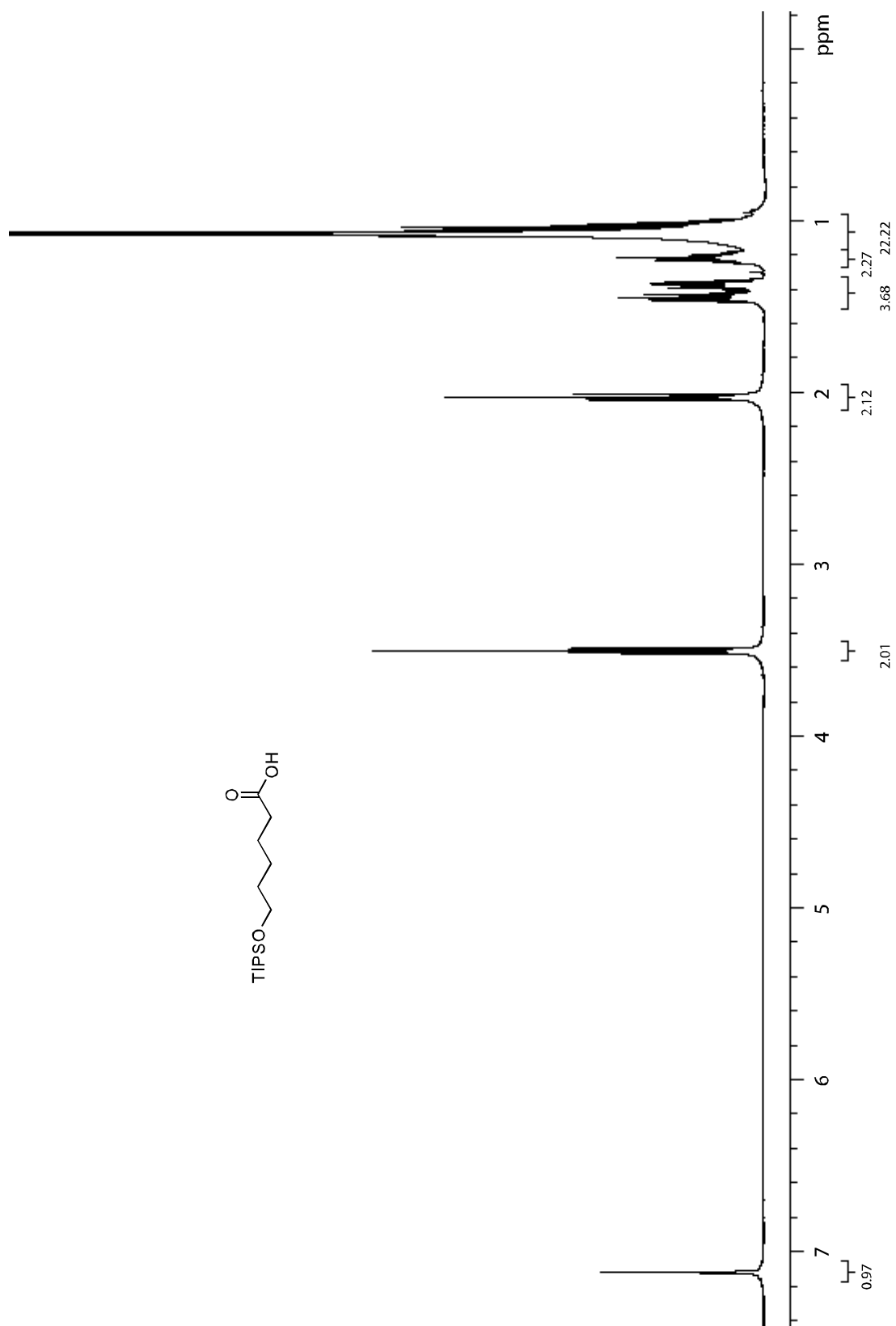


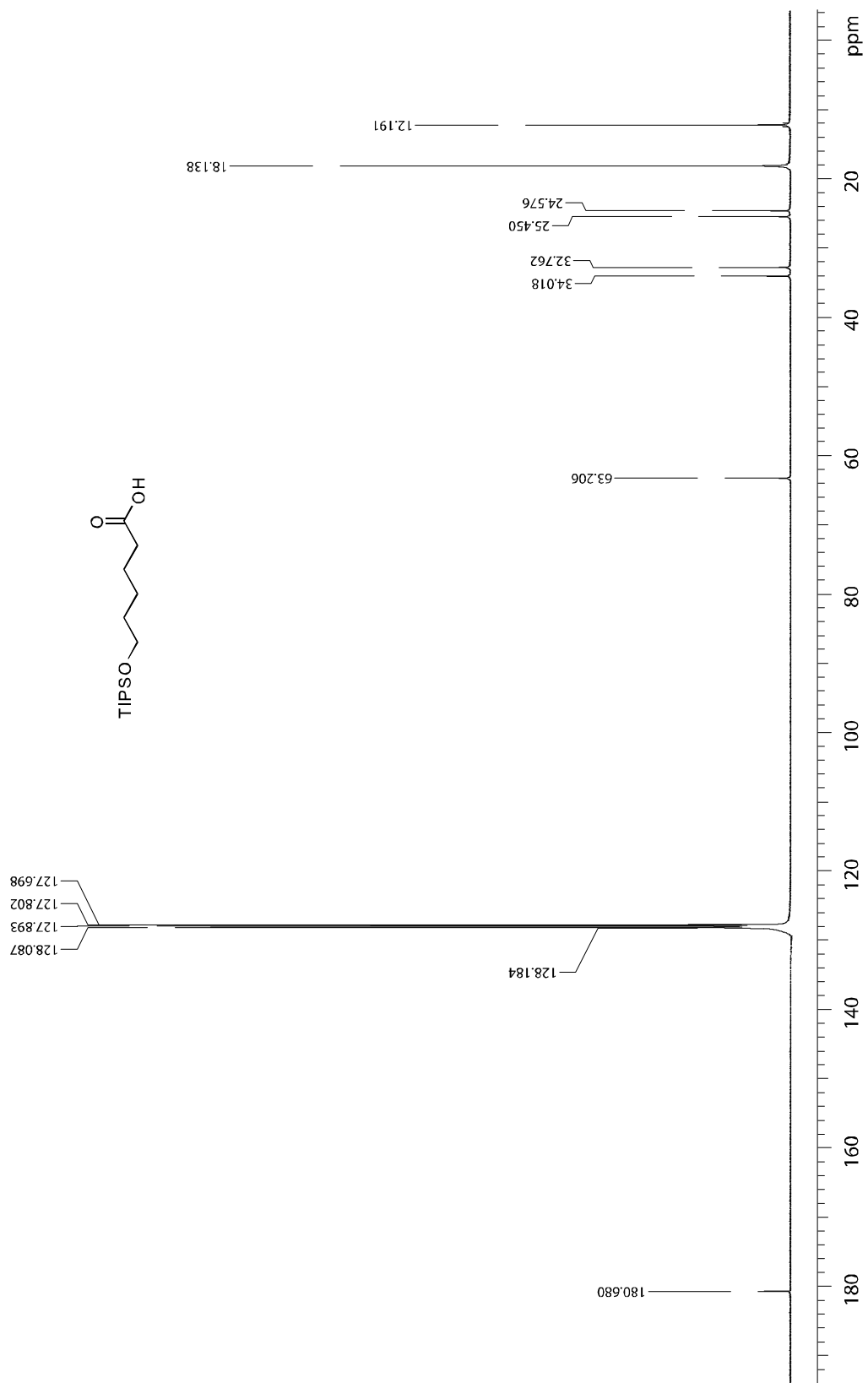
THF Bromide 4.36. To a solution of 2-(5-((*tert*-butyldimethylsilyloxy)methyl)tetrahydrofuran-2-yl)ethyl methanesulfonate (88.4 mg, 0.261 mmol) in acetone (3 mL) as added anhydrous lithium bromide (68.0 mg, 0.783

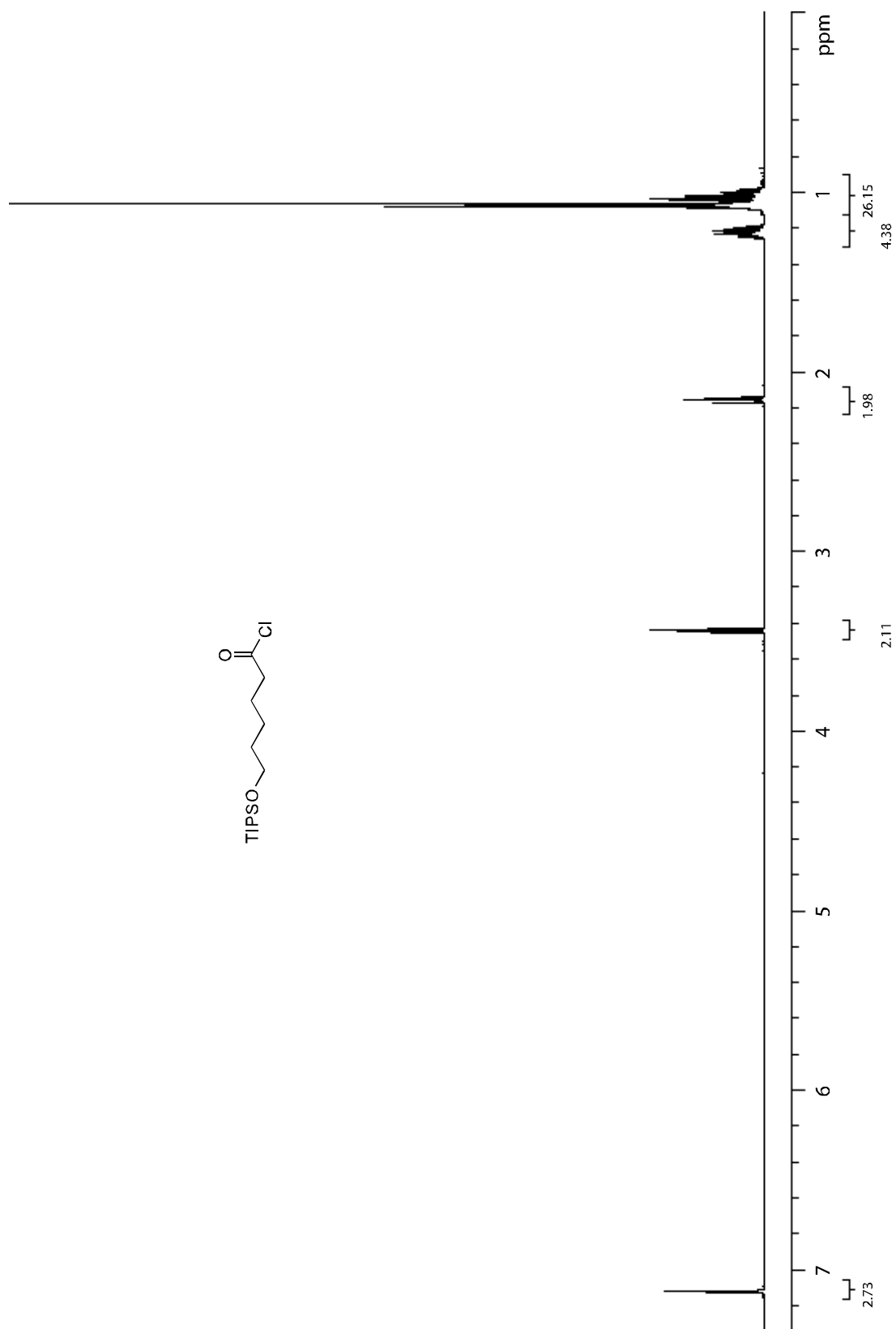
mmol) and refluxed for 4 h. After cooling the salts were dissolved in water and the solution was extracted with CH_2Cl_2 (3 X 5 mL), dried with MgSO_4 and concentrated to give THF bromide **4.36** (58.8 mg, 70%) as a pale yellow oil and a mixture of diastereomers of an indeterminable ratio by ^1H NMR due to overlapping peaks. IR ν_{max} 1249 cm^{-1} ; ^1H NMR (500 MHz, CDCl_3) δ 3.86 (ddd, $J = 0.24, 4.9, 11\text{ Hz}$, 1H), 3.79-3.74 (m, 1H), 3.64 (septet, $J = 5.0\text{ Hz}$, 1H), 3.59-3.46 (m, 3H), (tdd, $J = 2.5, 3.5, 9.5$, 1H), 3.11 (app. t, $J = 10.5$, 1H), 2.19-2.10 (m, 1H), 2.04-1.87 (m, 3H), 1.82-1.65 (m, 2H), 1.51-1.32 (m, 3H), 0.91 (s, H), 0.88 (s, H), 0.70 (s, H), 0.60 (s, H); ^{13}C NMR (125 MHz, CDCl_3) δ 75.0, 74.9, 73.2, 72.6, 67.2, 65.5, 39.1, 33.5, 31.0, 30.7, 30.6, 30.3, 26.2, 26.16, 26.0, 18.5, 18.4, -4.4, -4.46, -4.47, -4.6; LRMS (CI) Calcd. for $\text{C}_{13}\text{H}_{27}\text{BrO}_2\text{Si}$ $[\text{M}+\text{H}]$ 323, found 323.

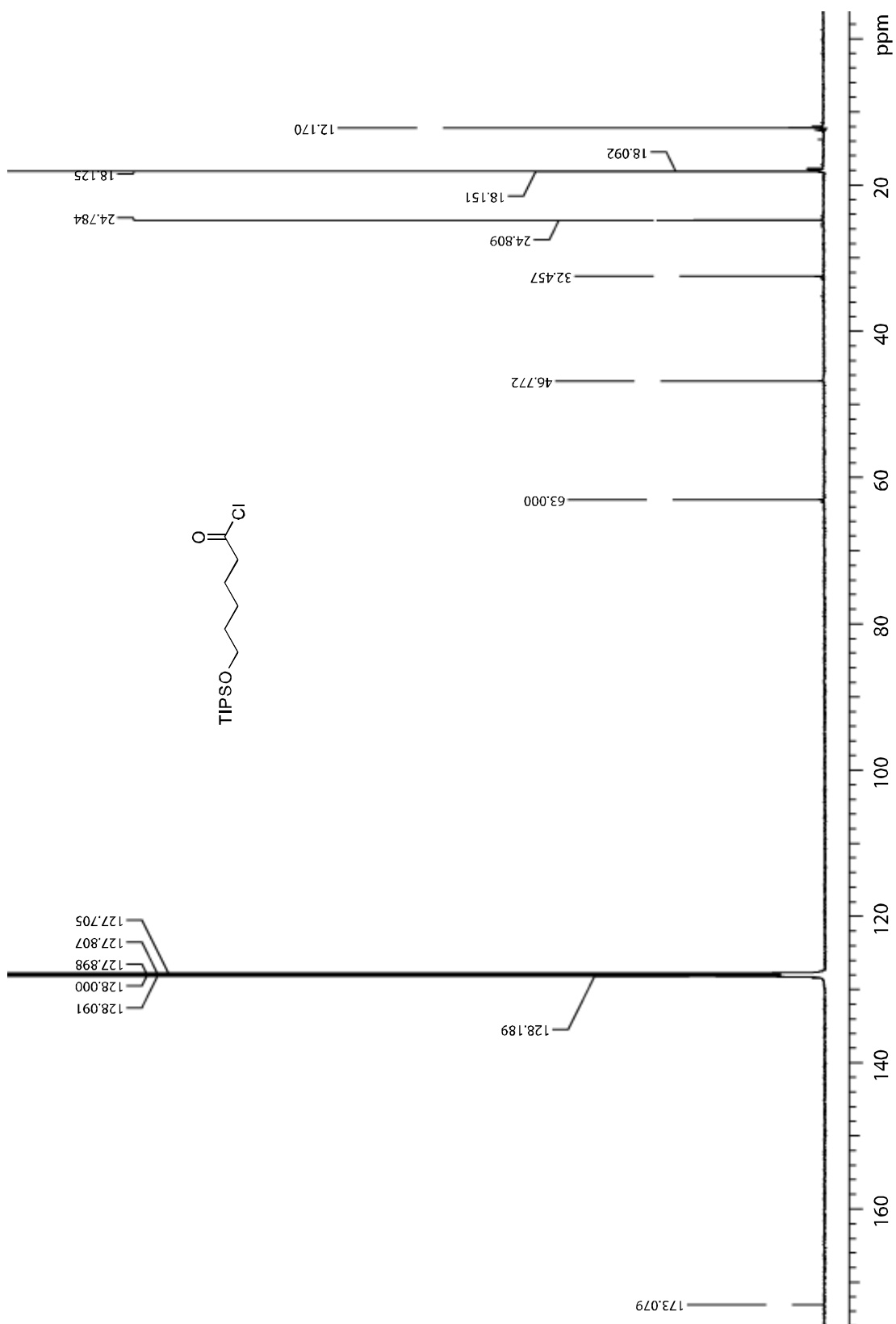


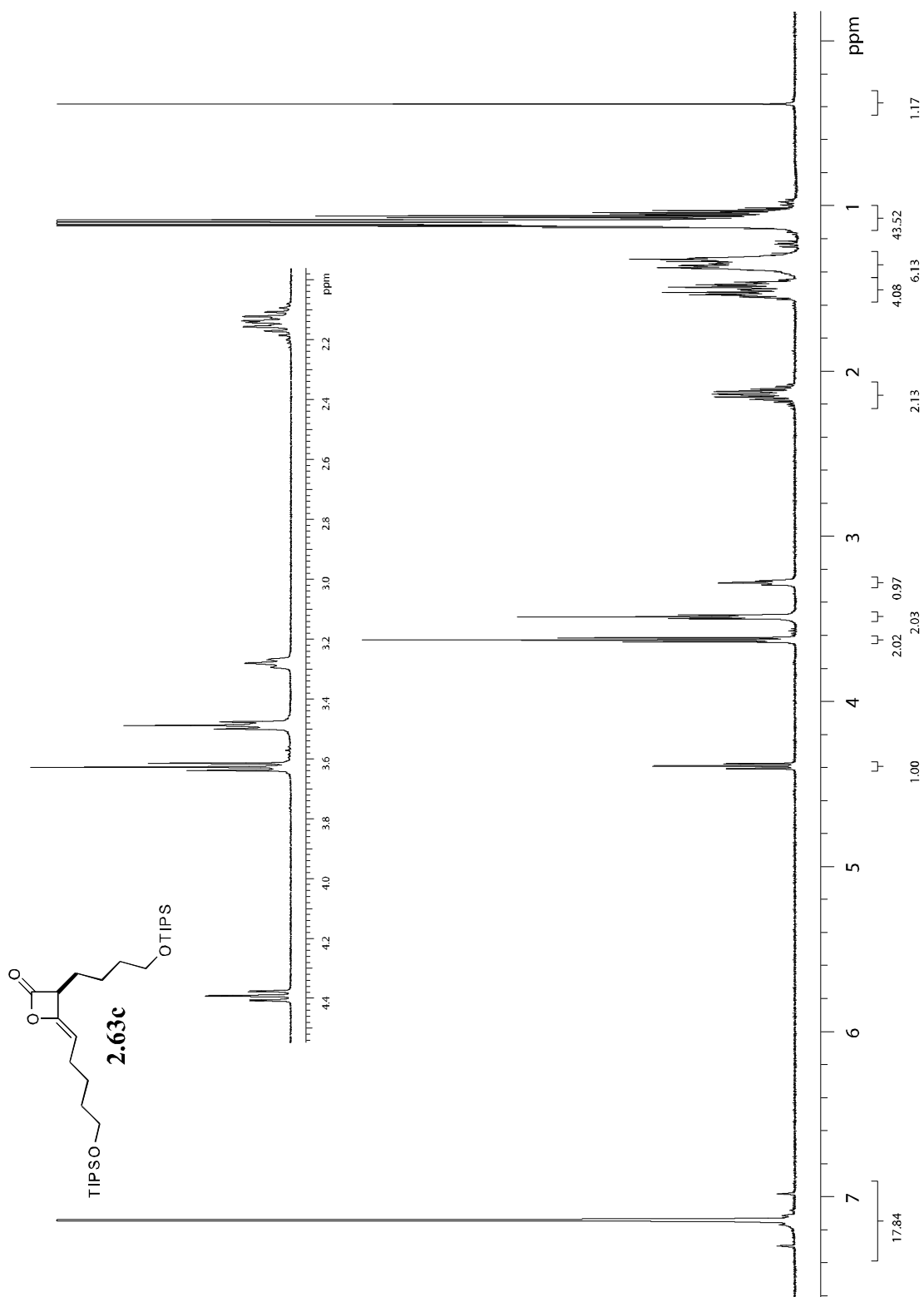


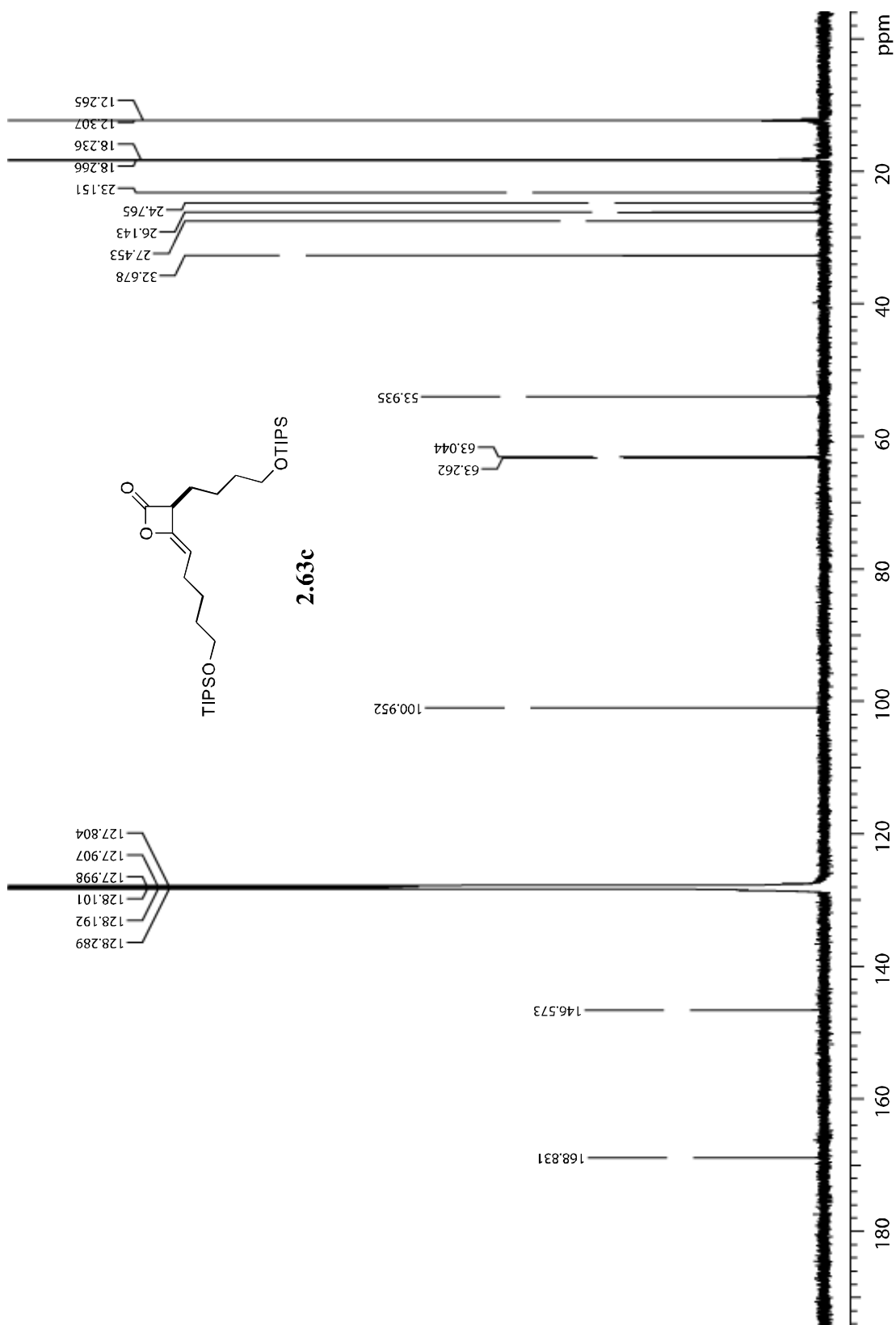


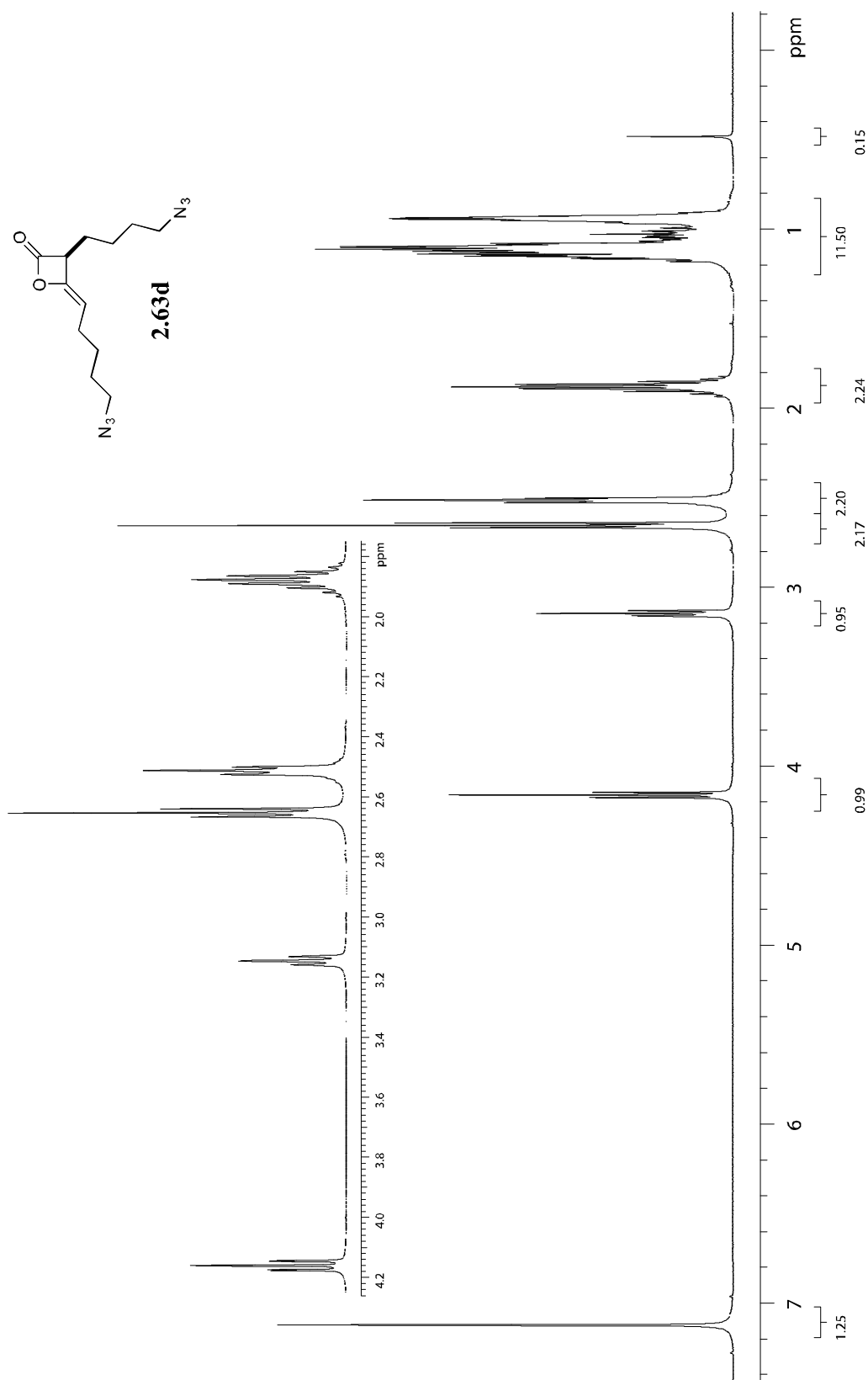


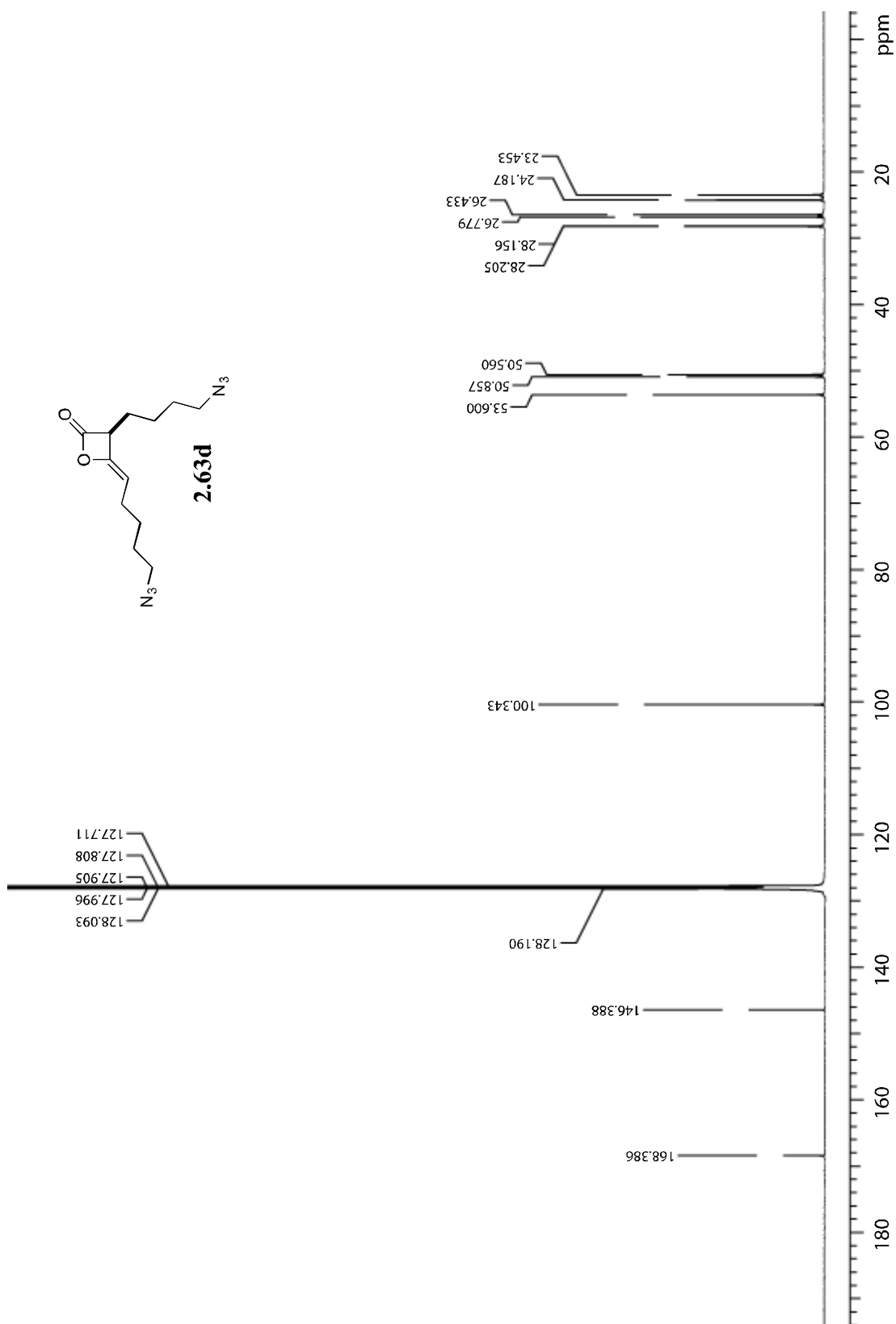


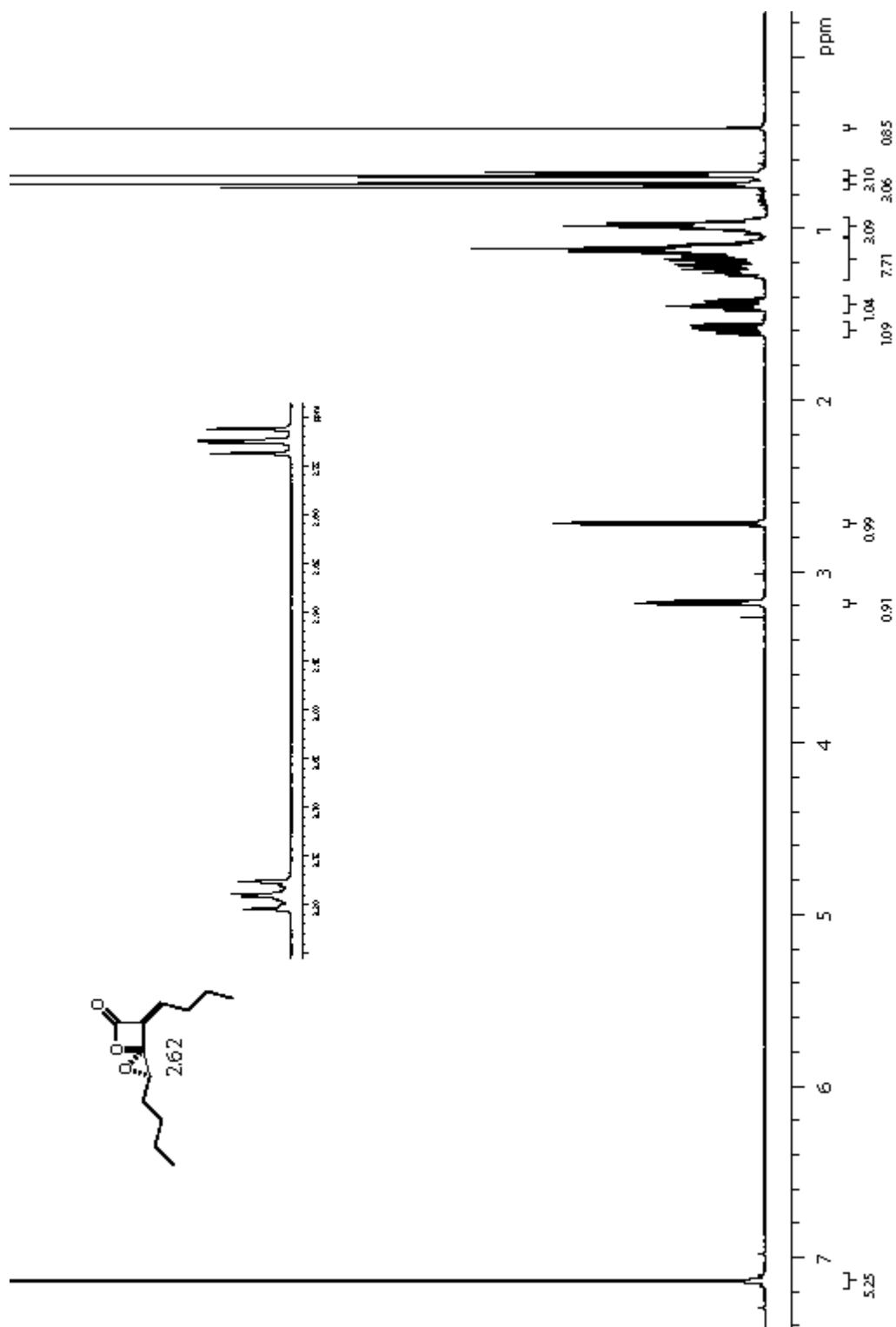


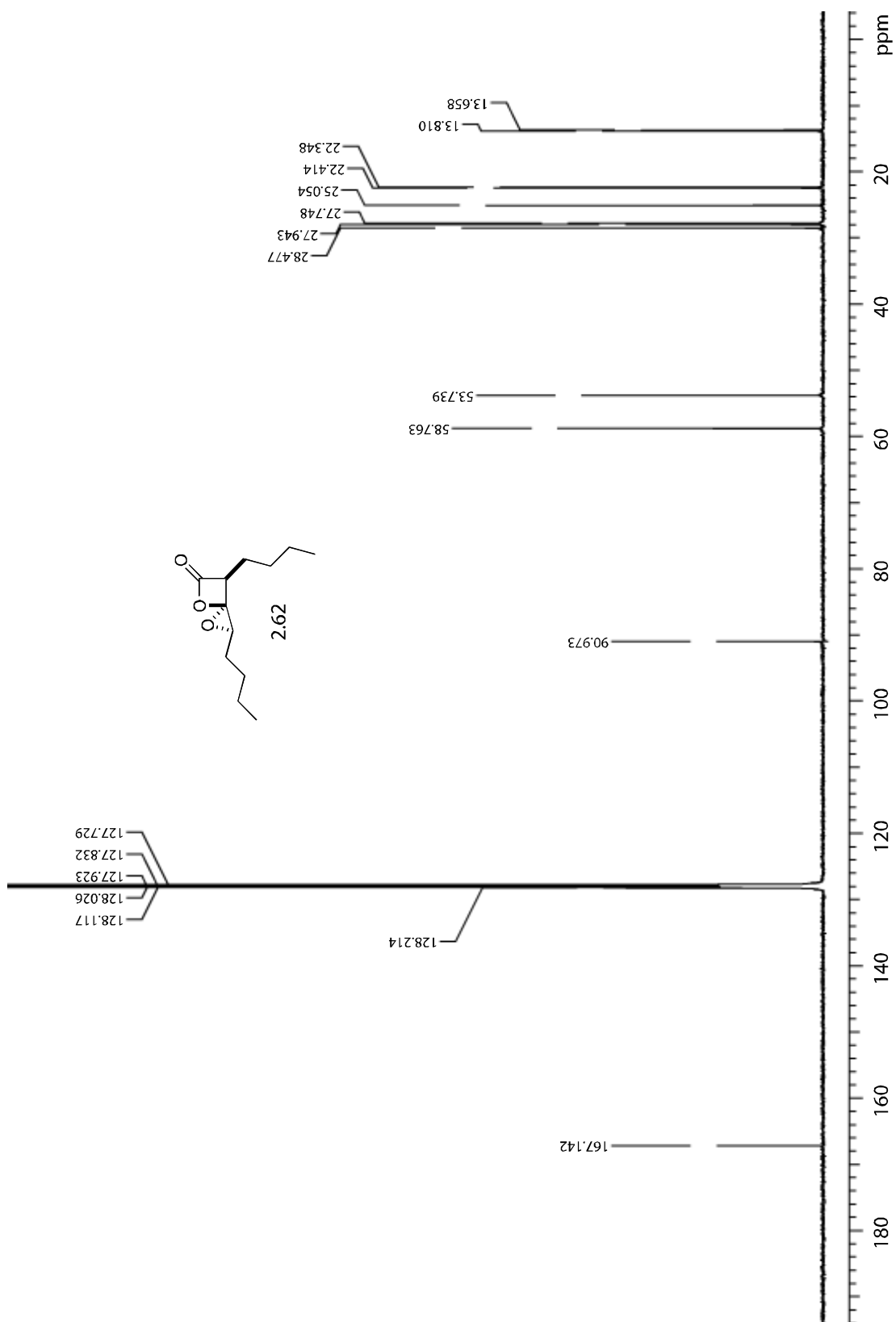


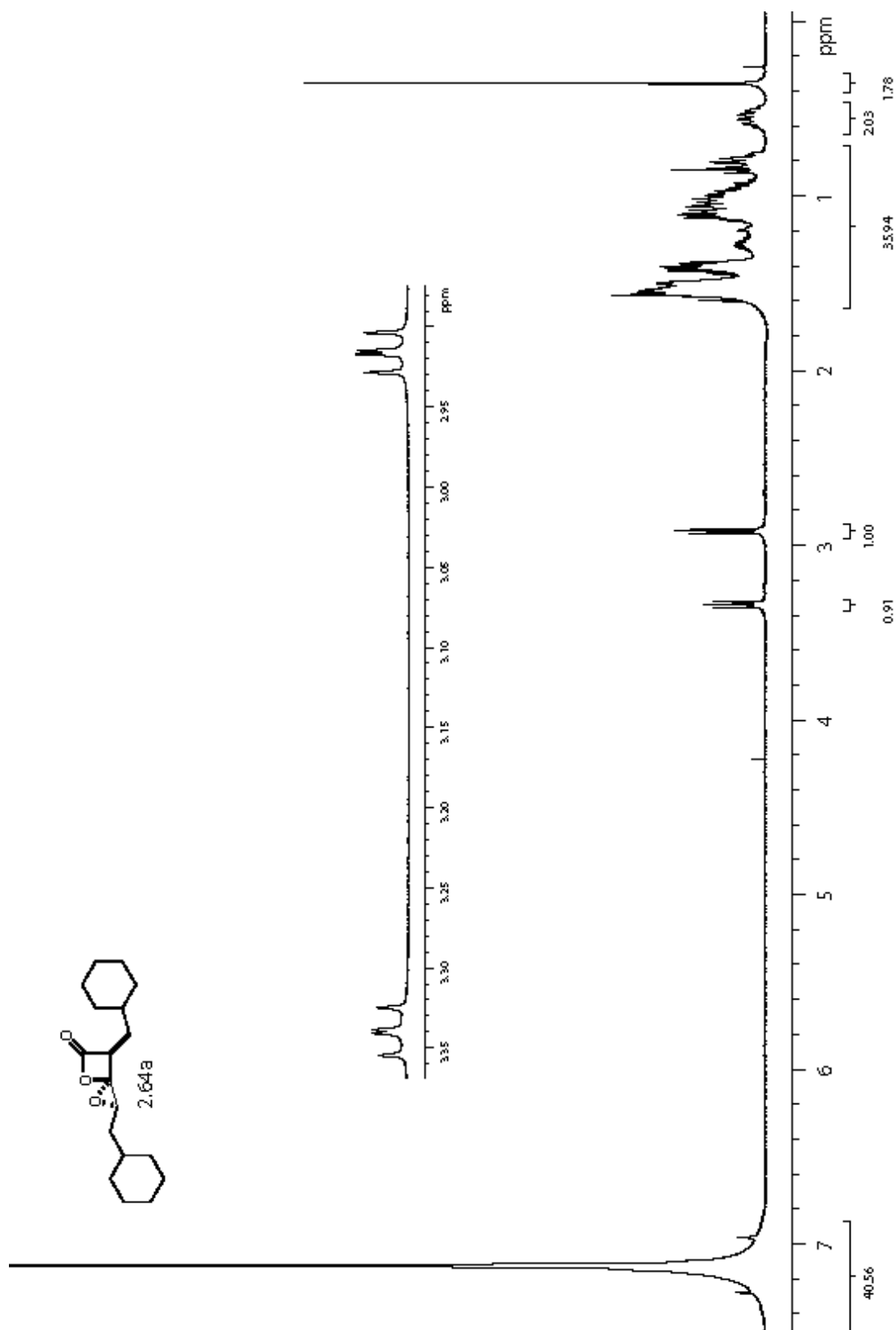


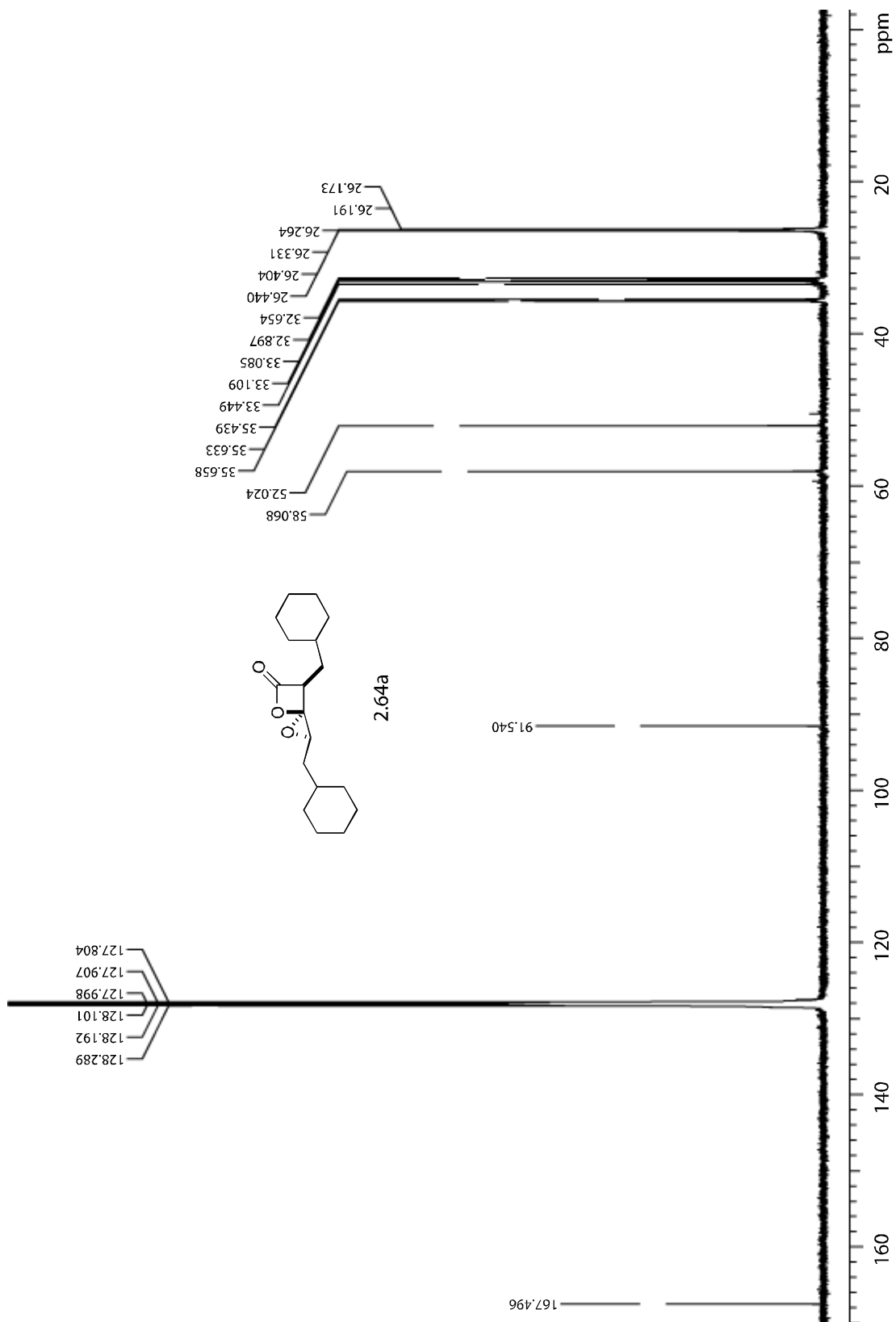


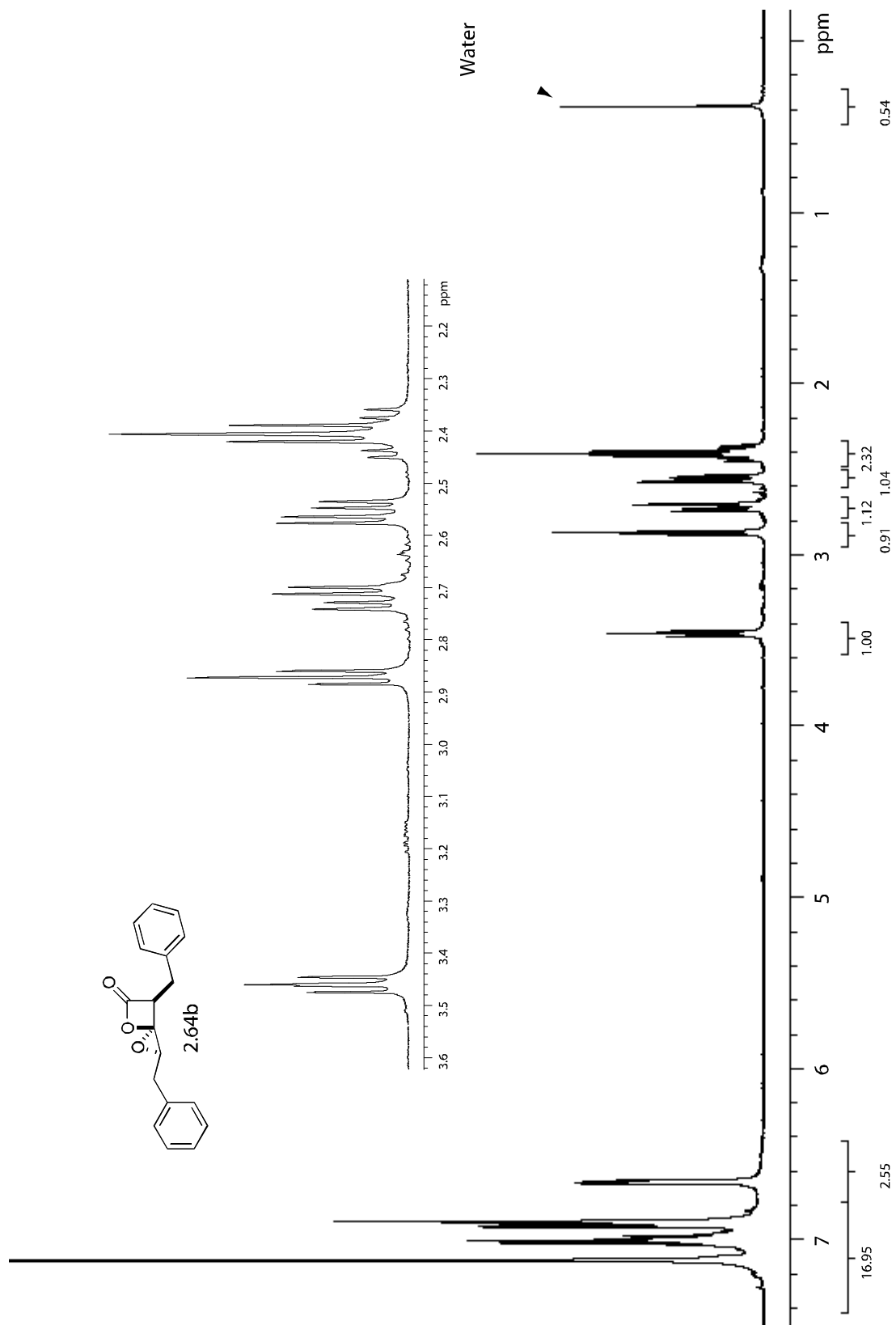


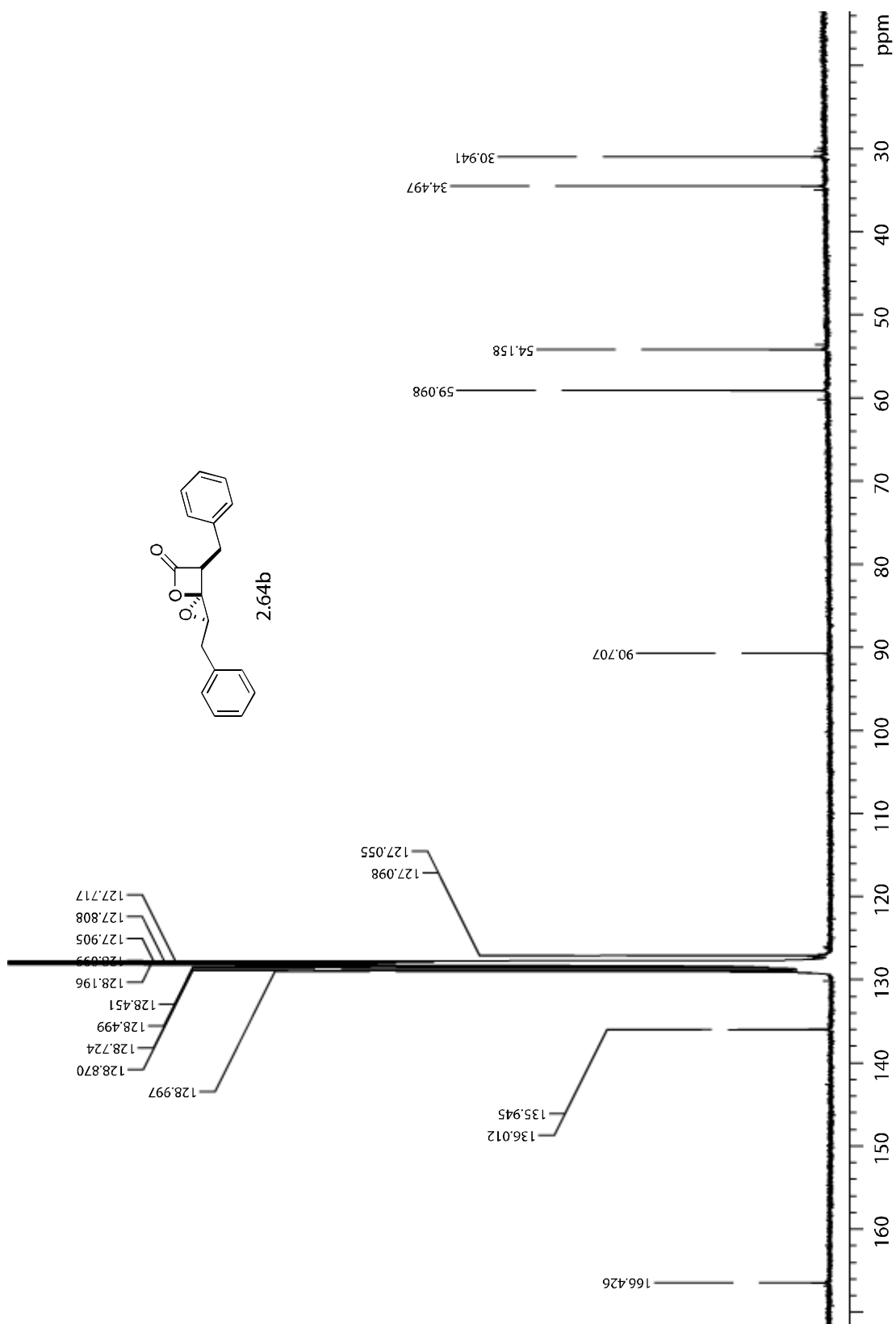


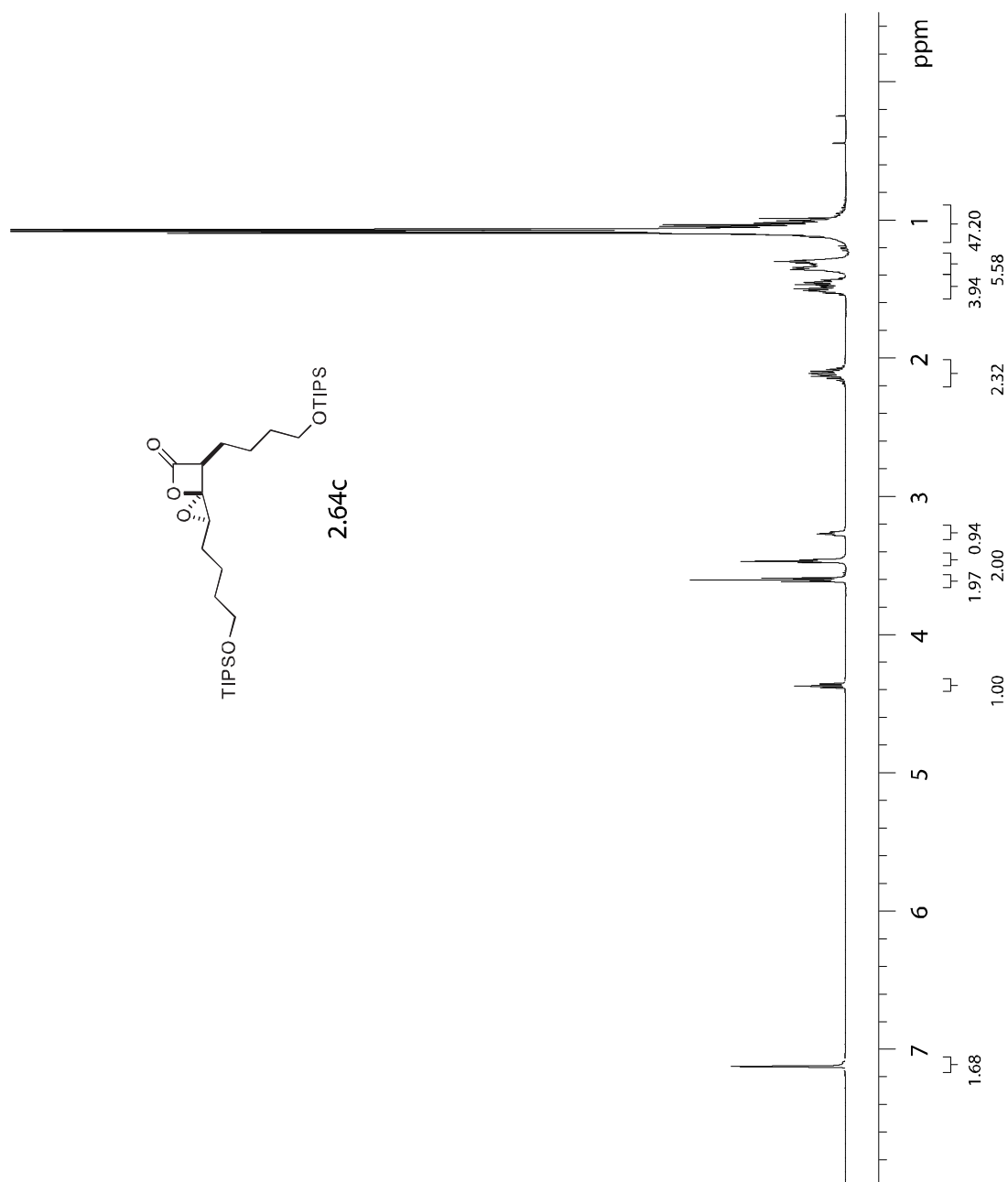


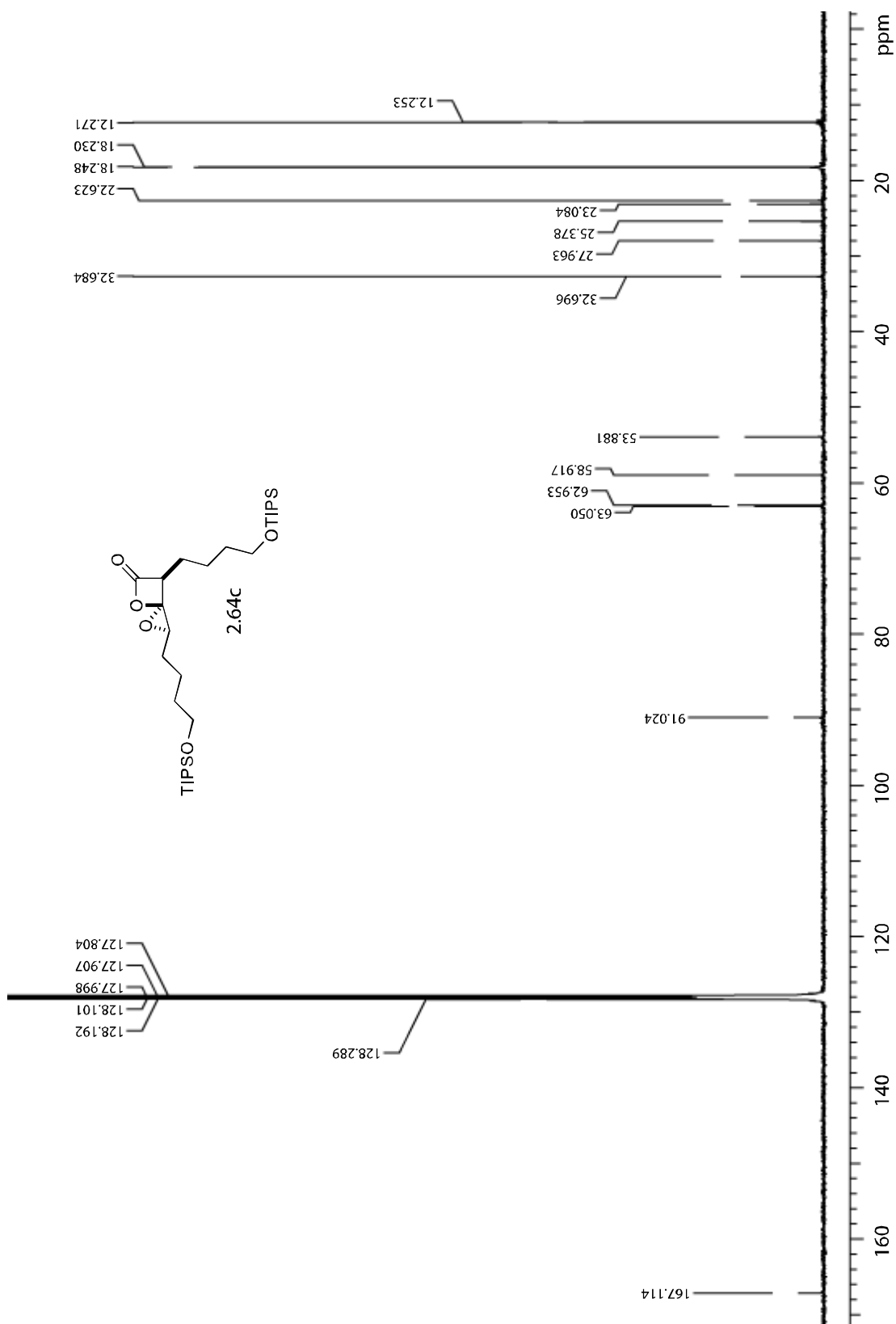


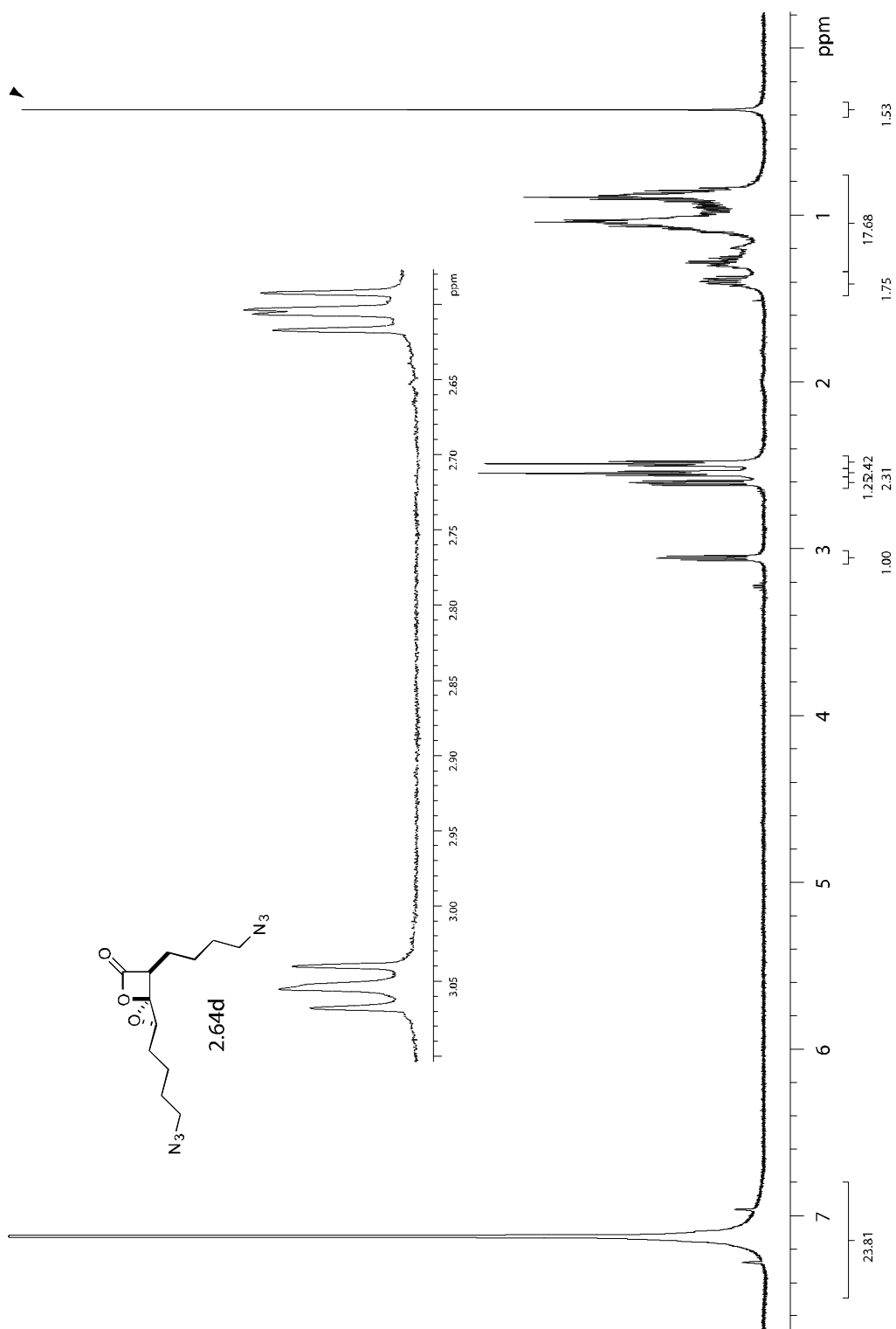


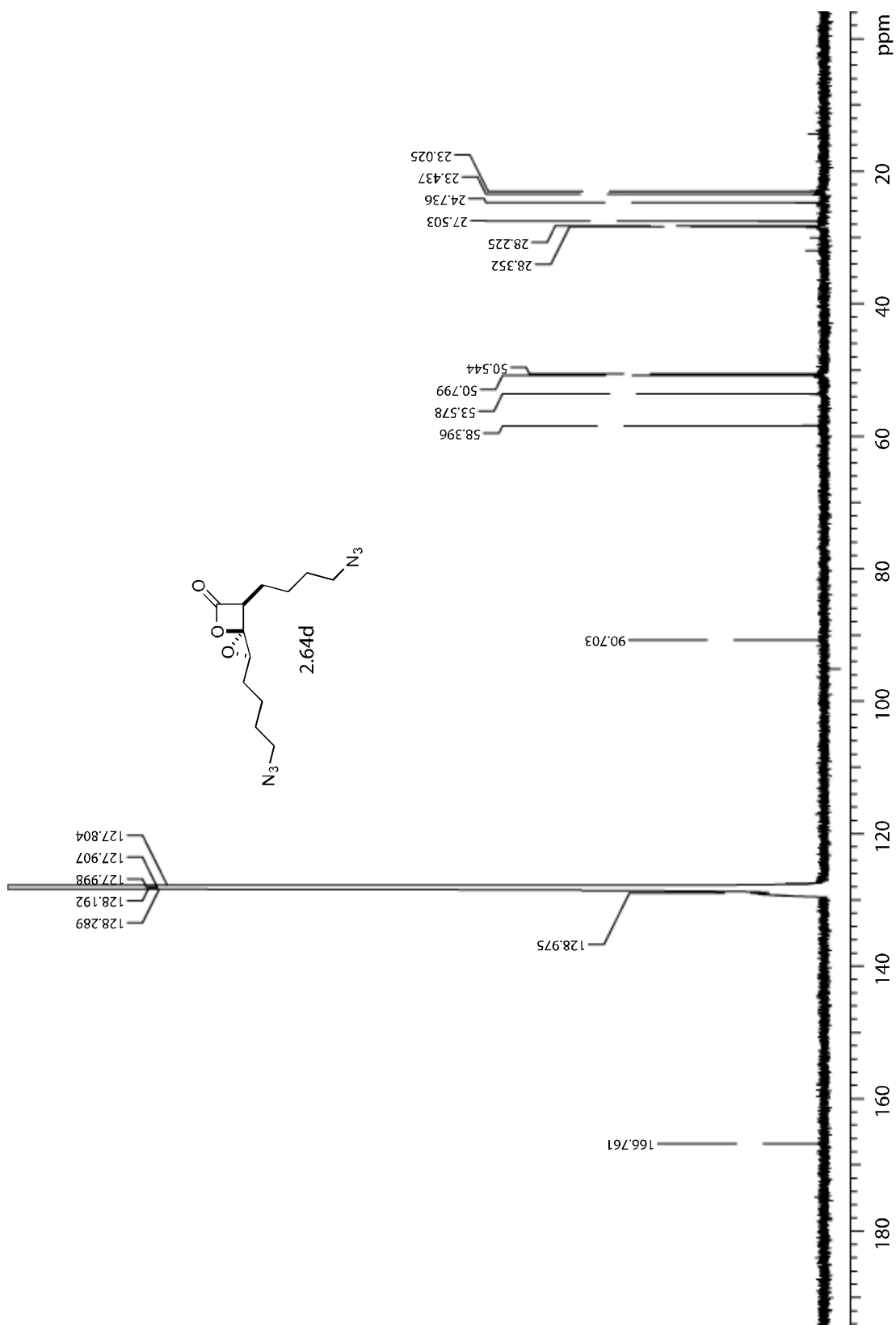


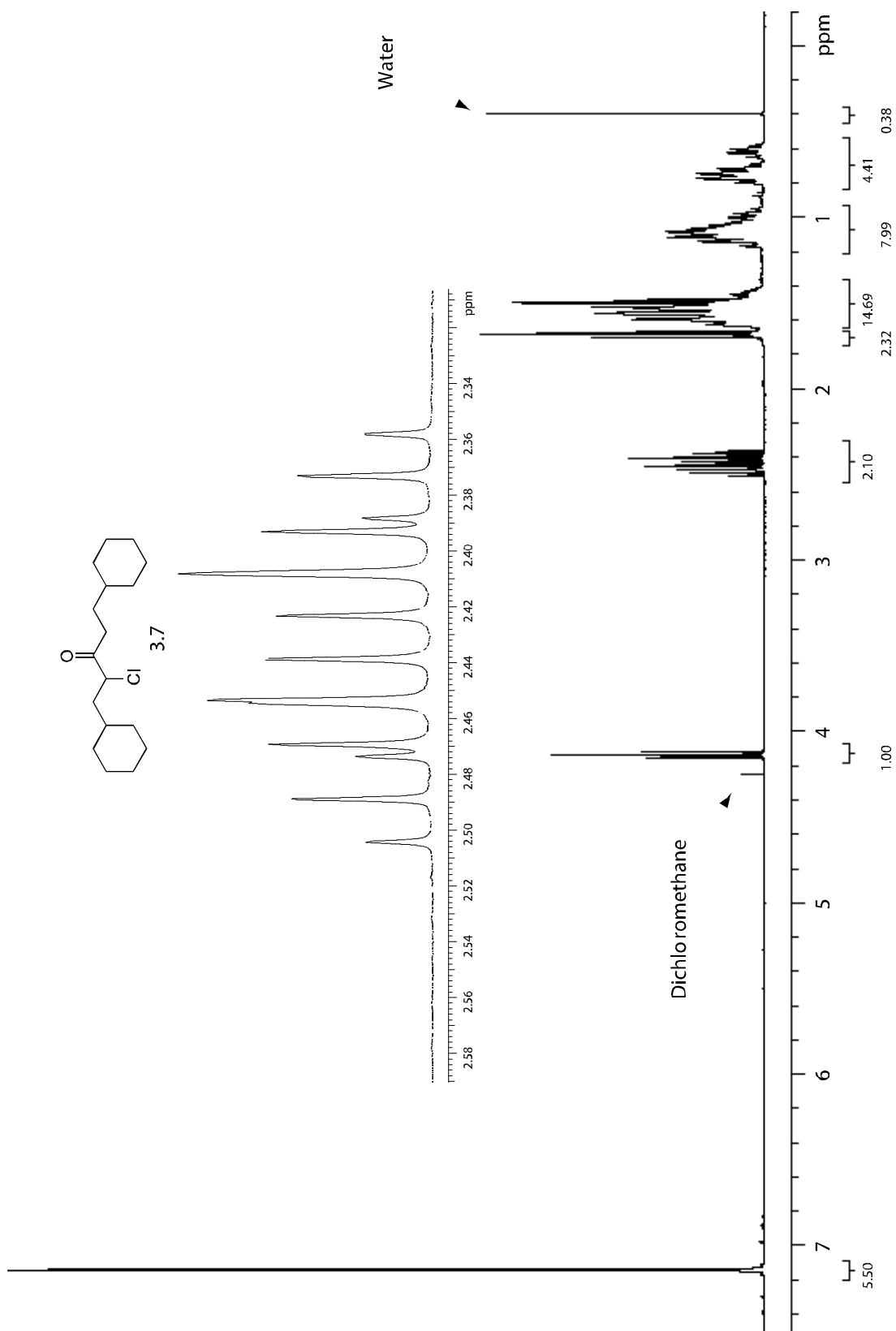


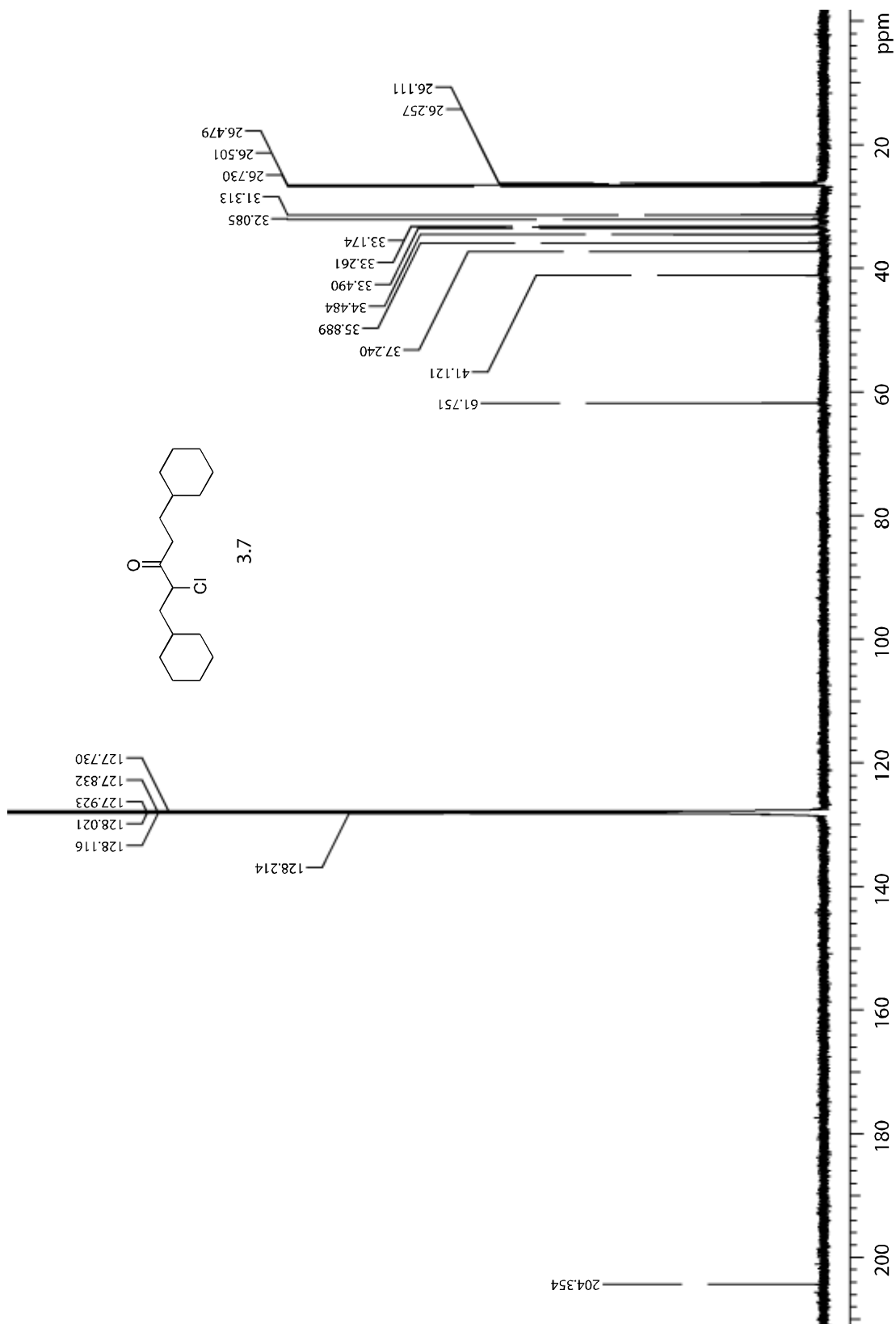


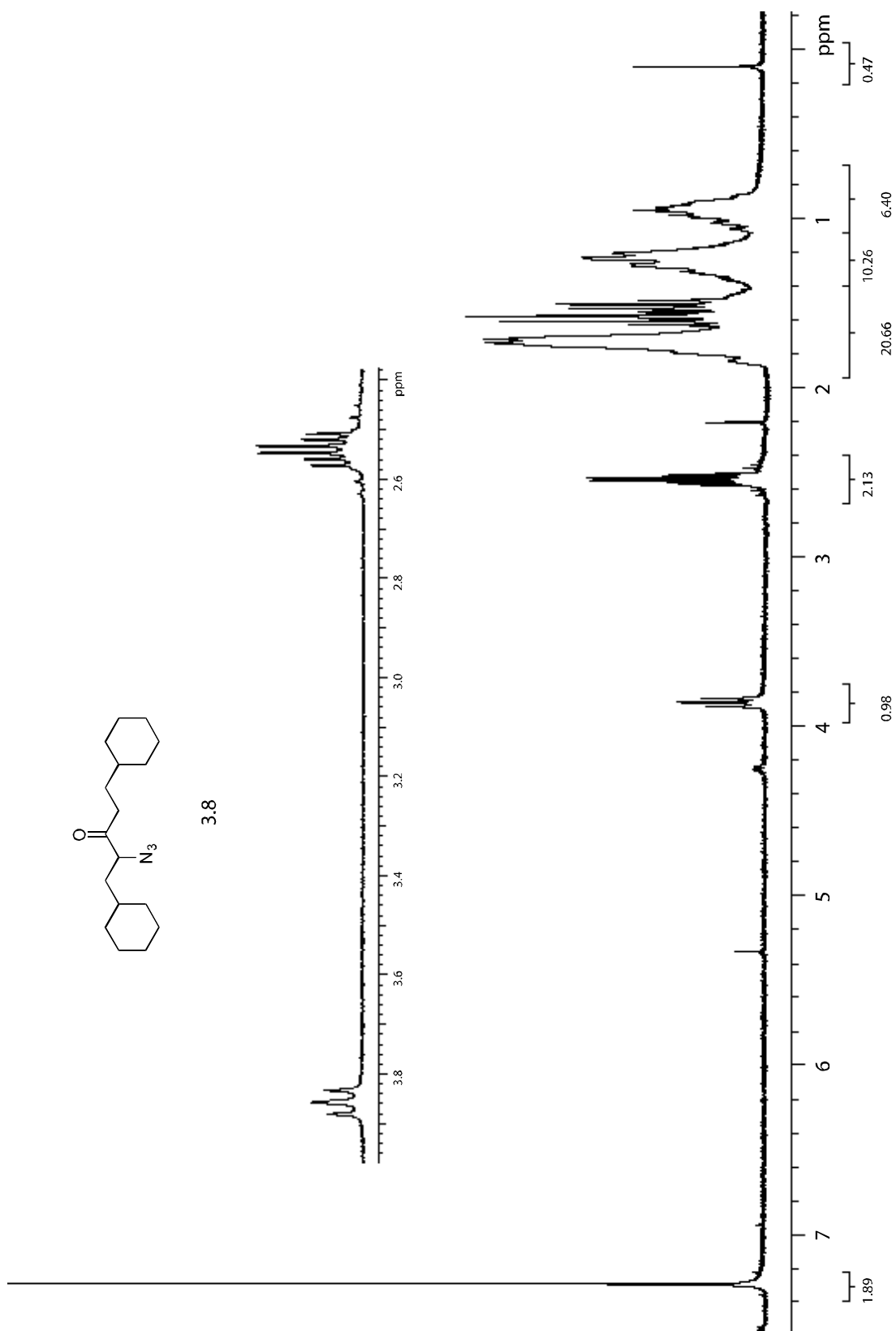


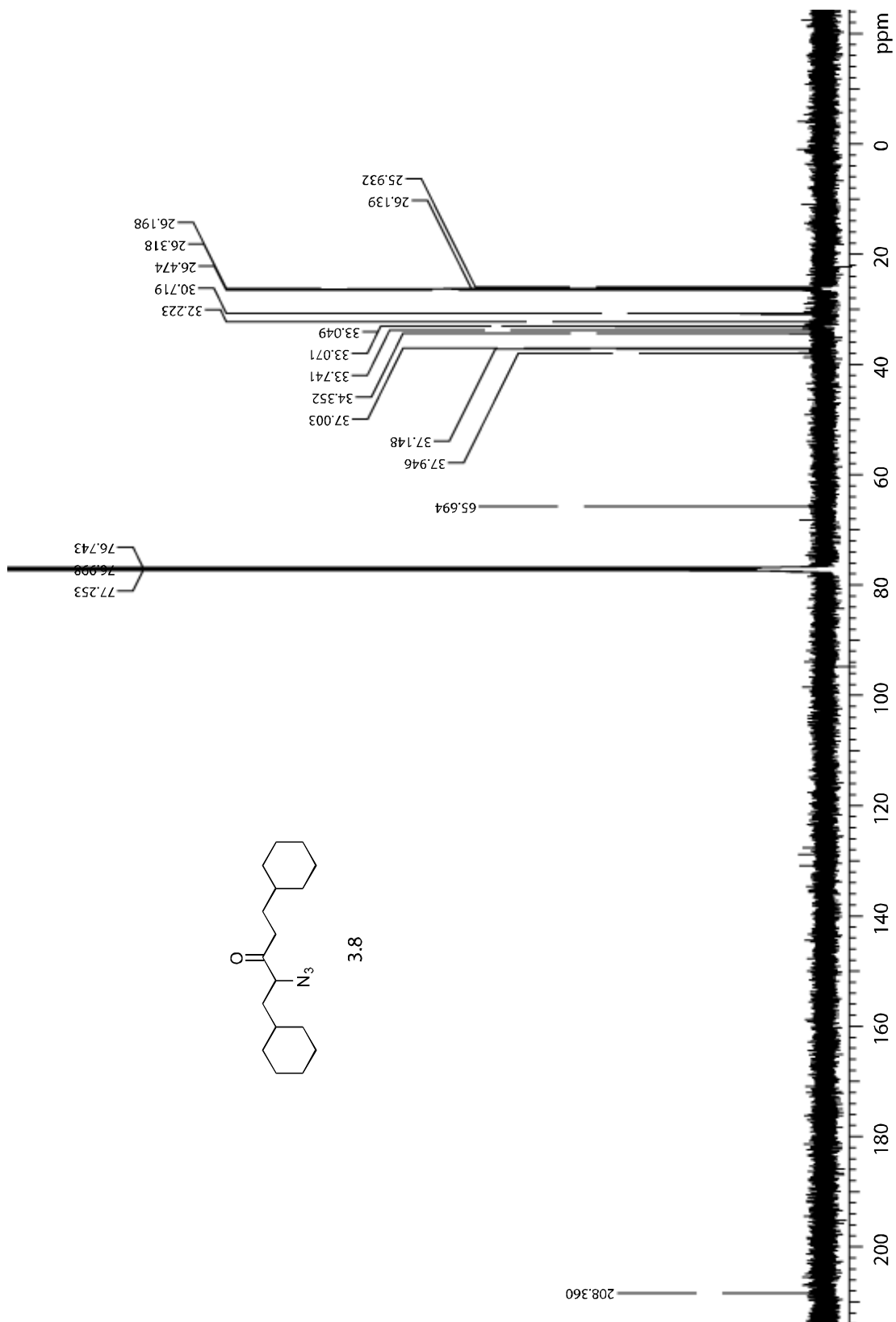


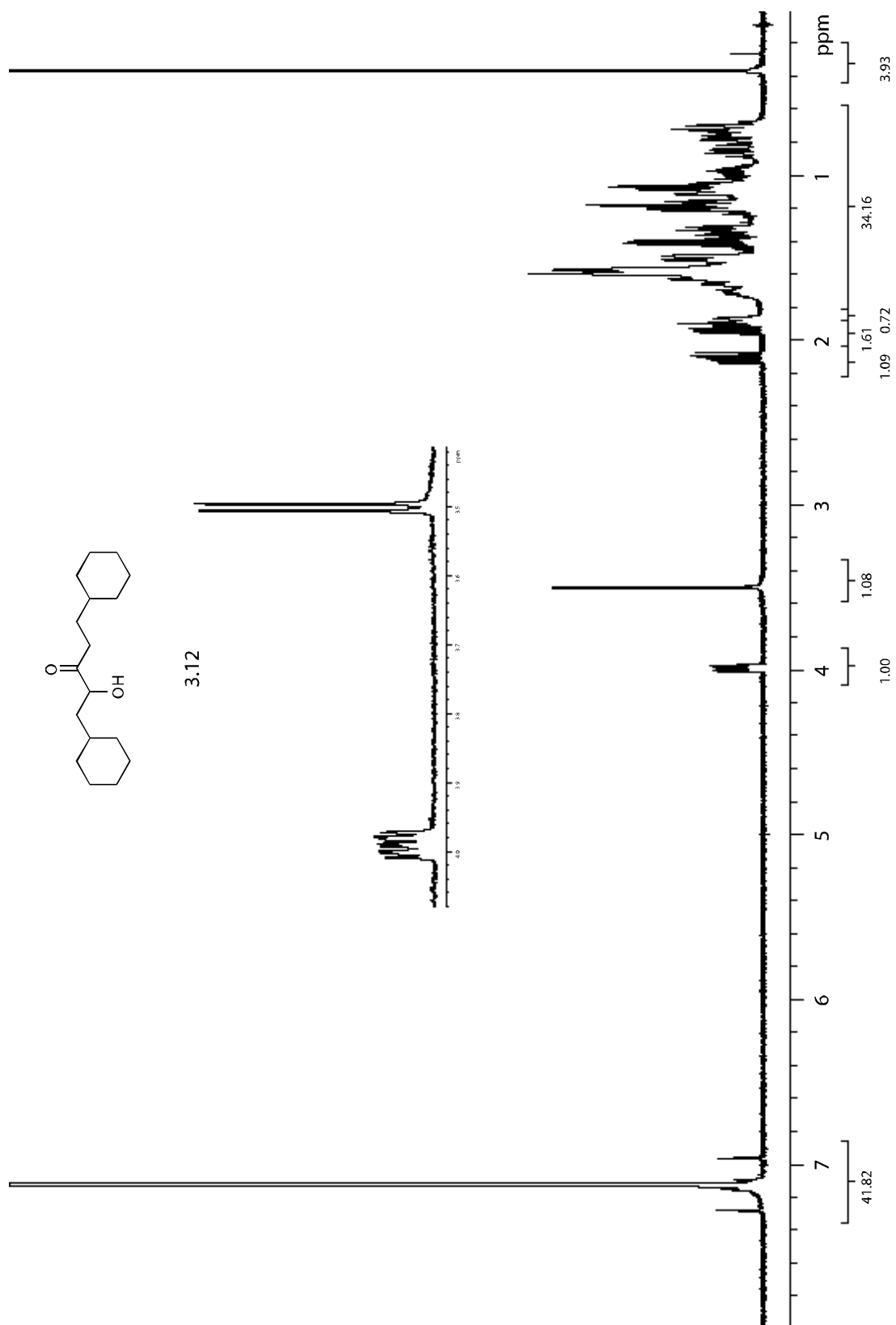


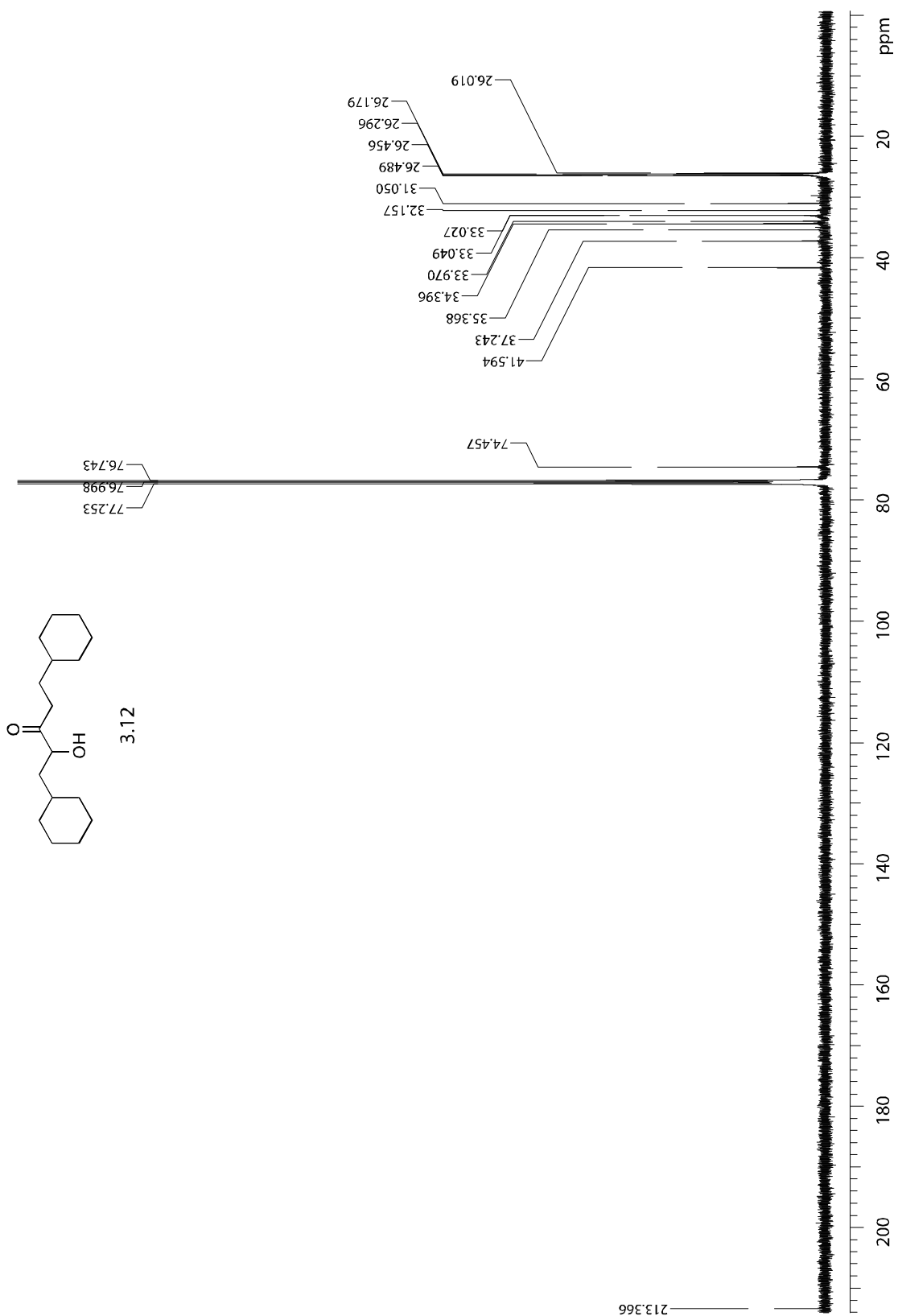


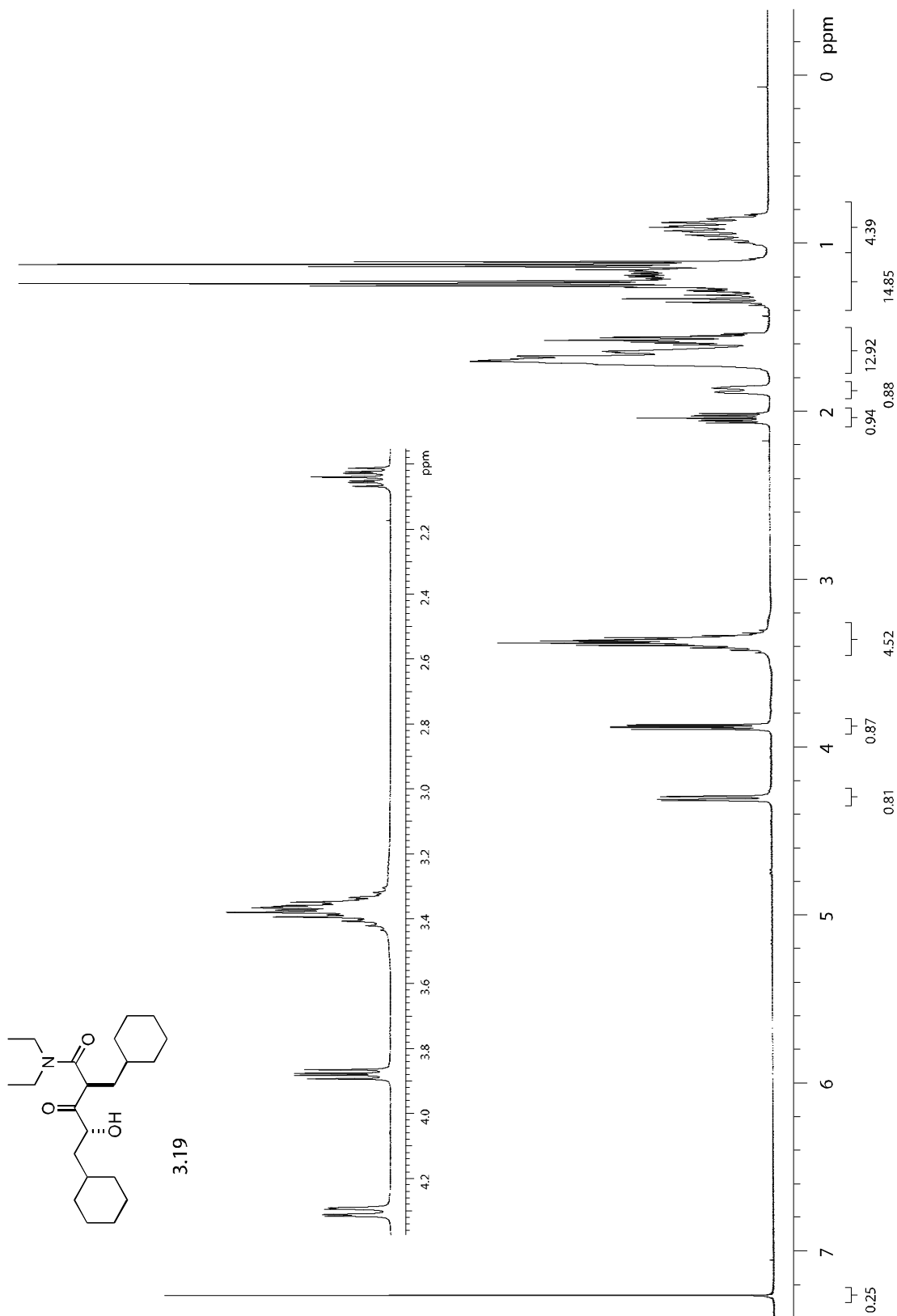


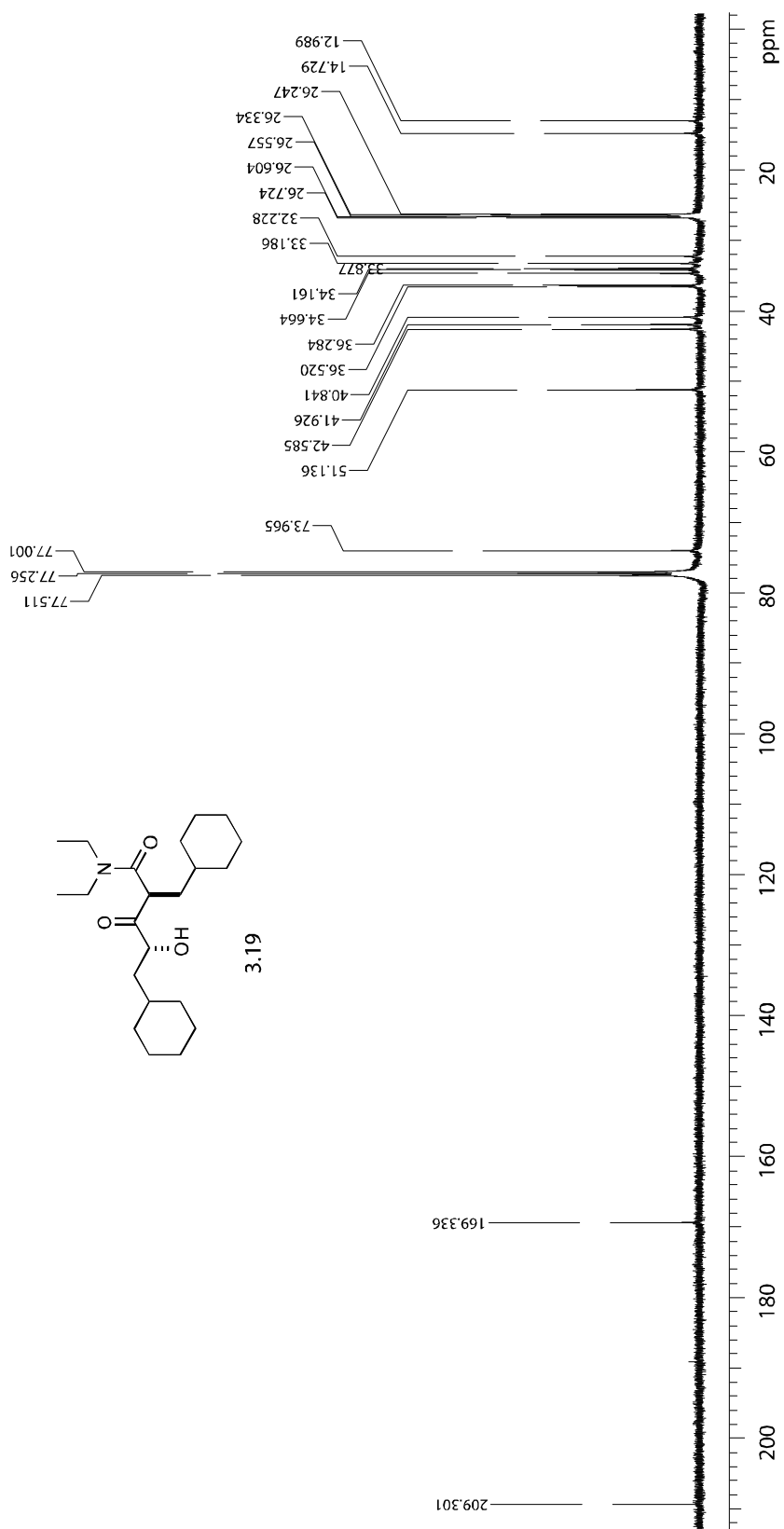


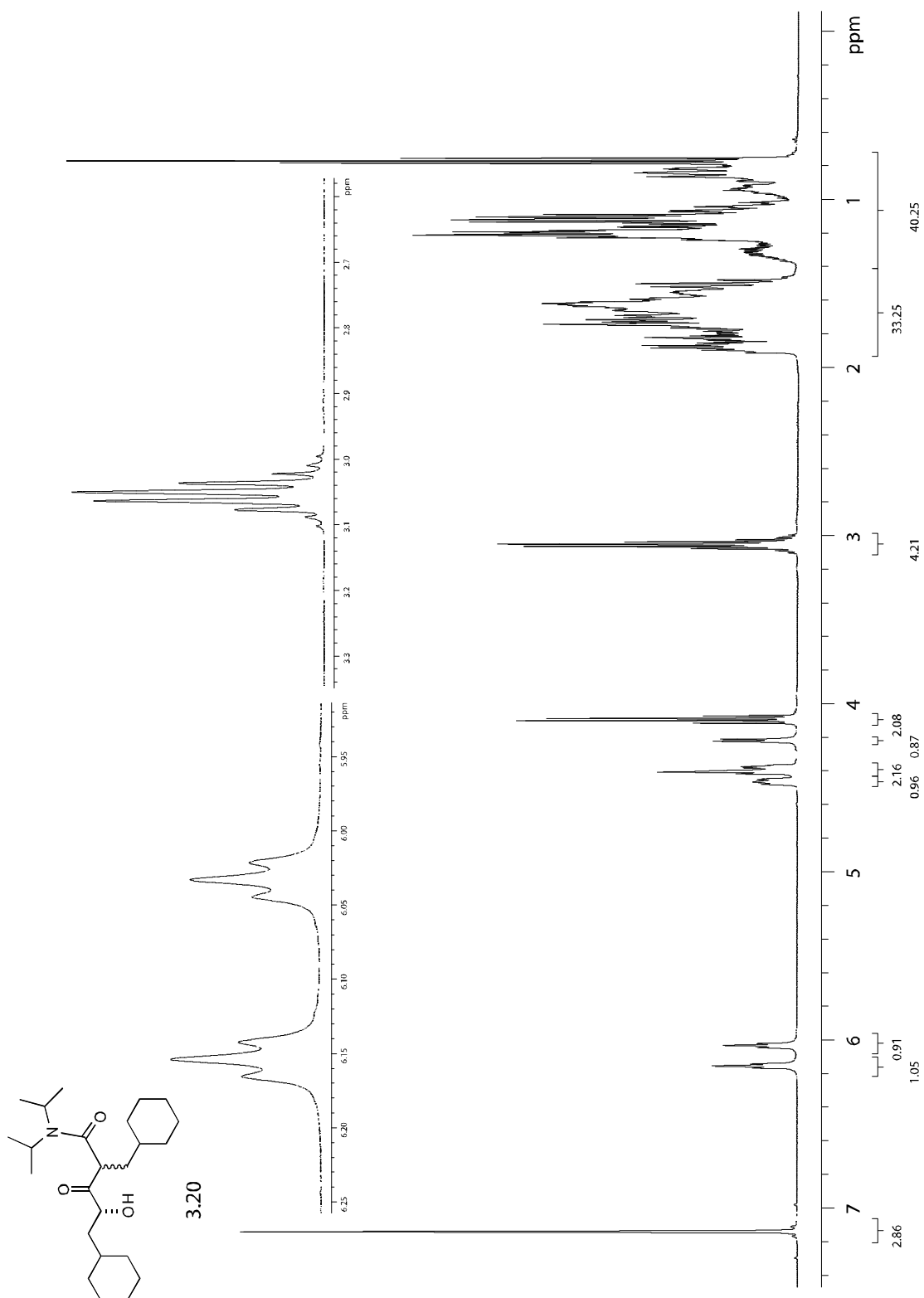


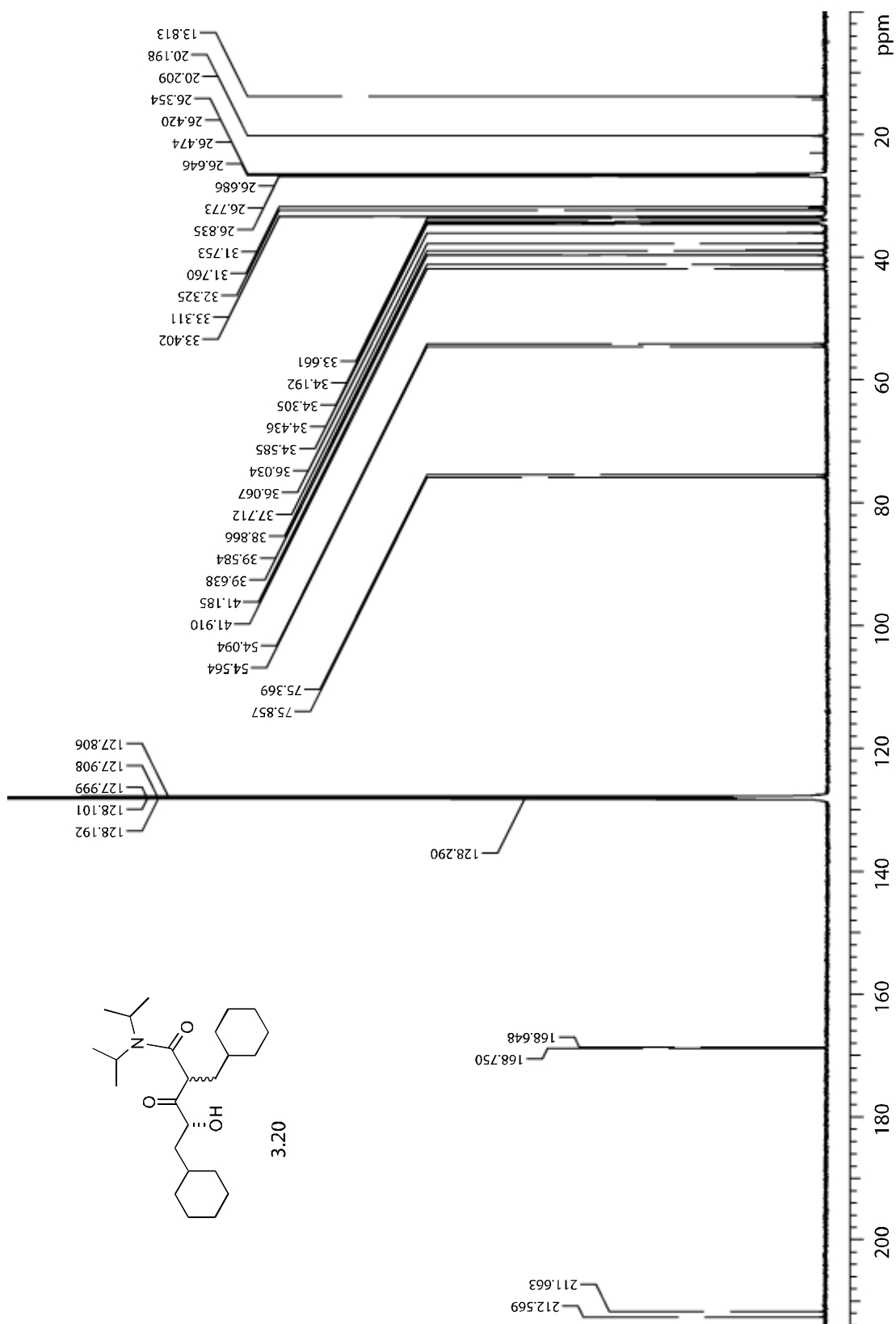


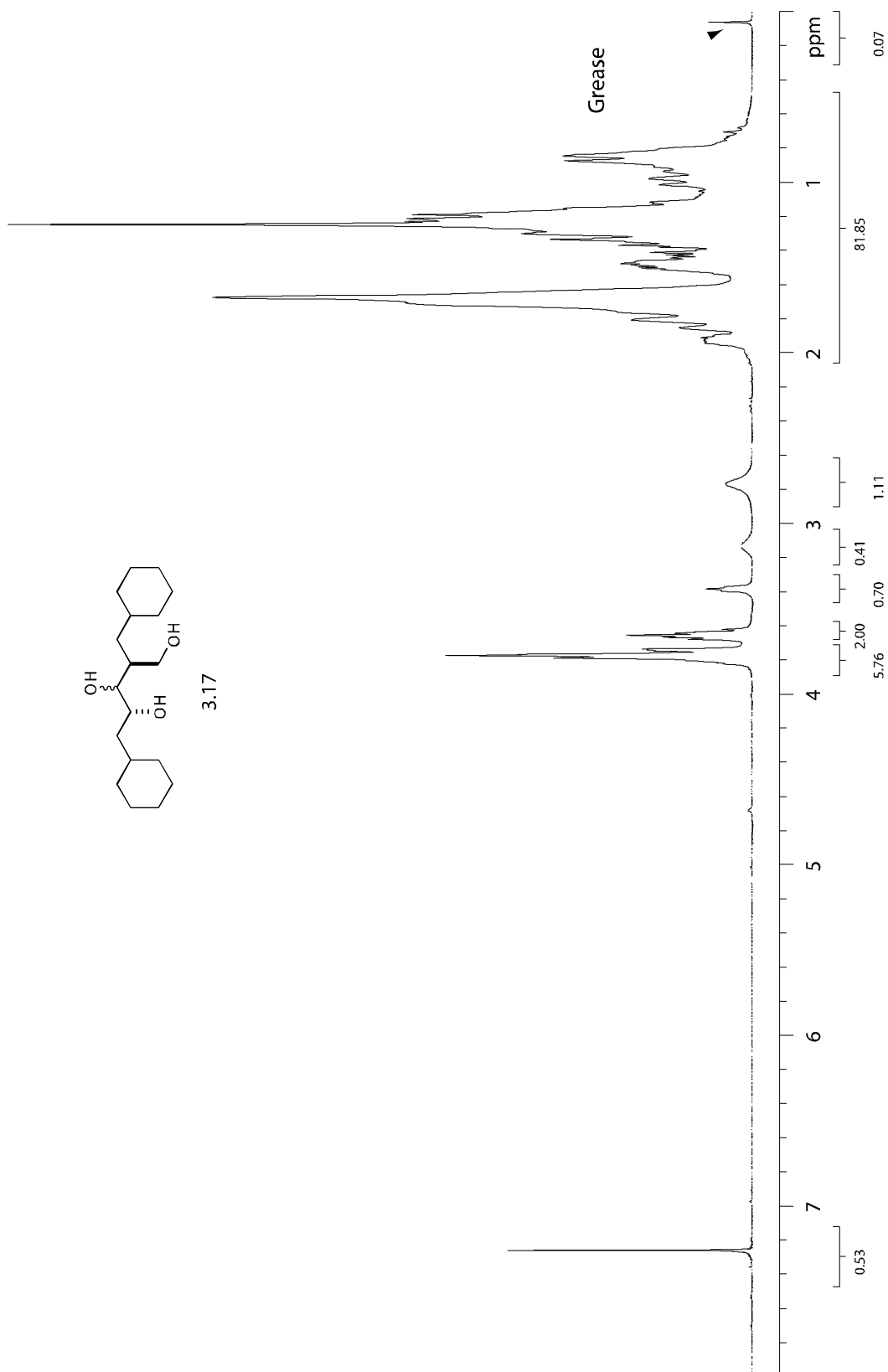


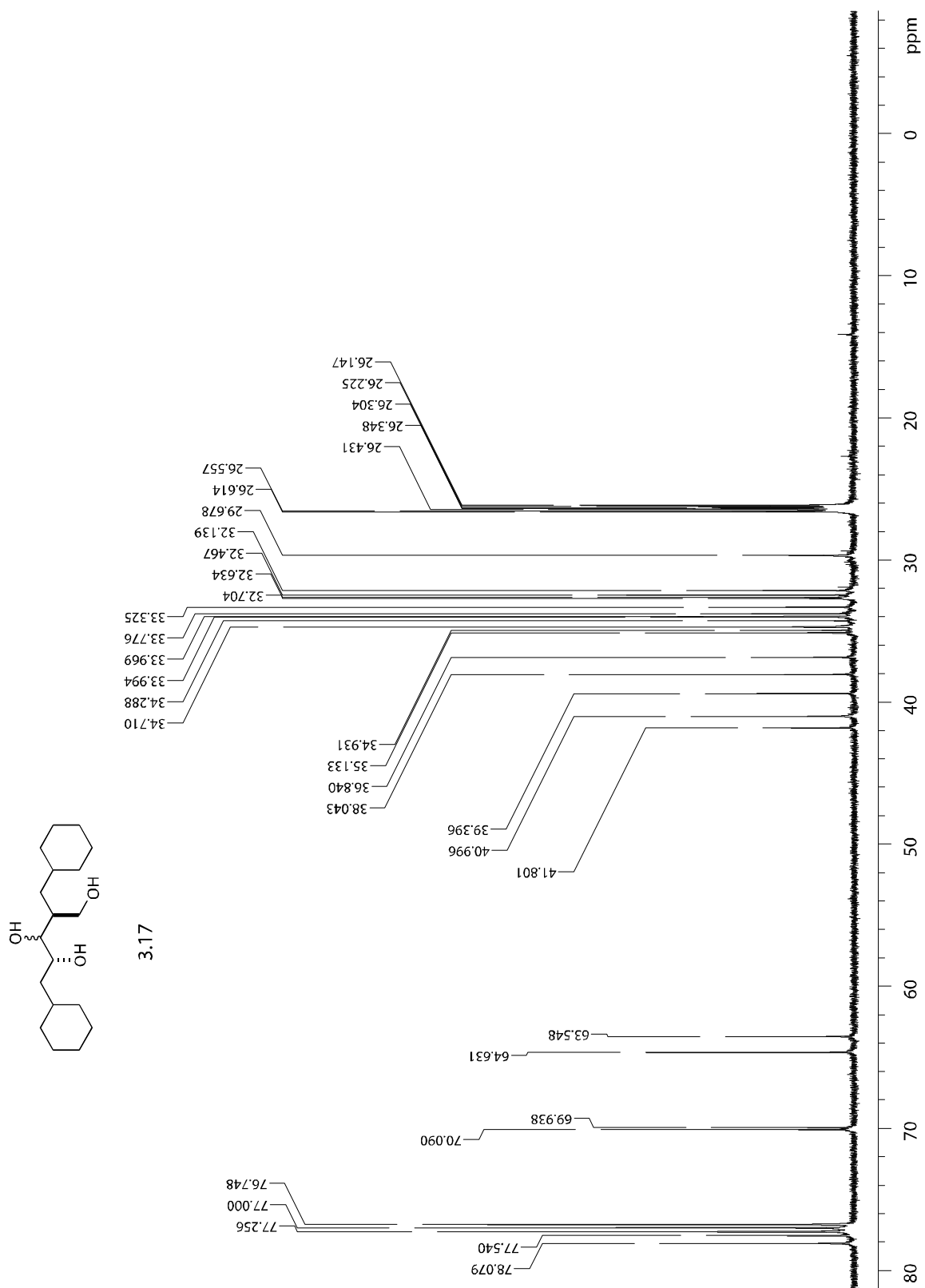


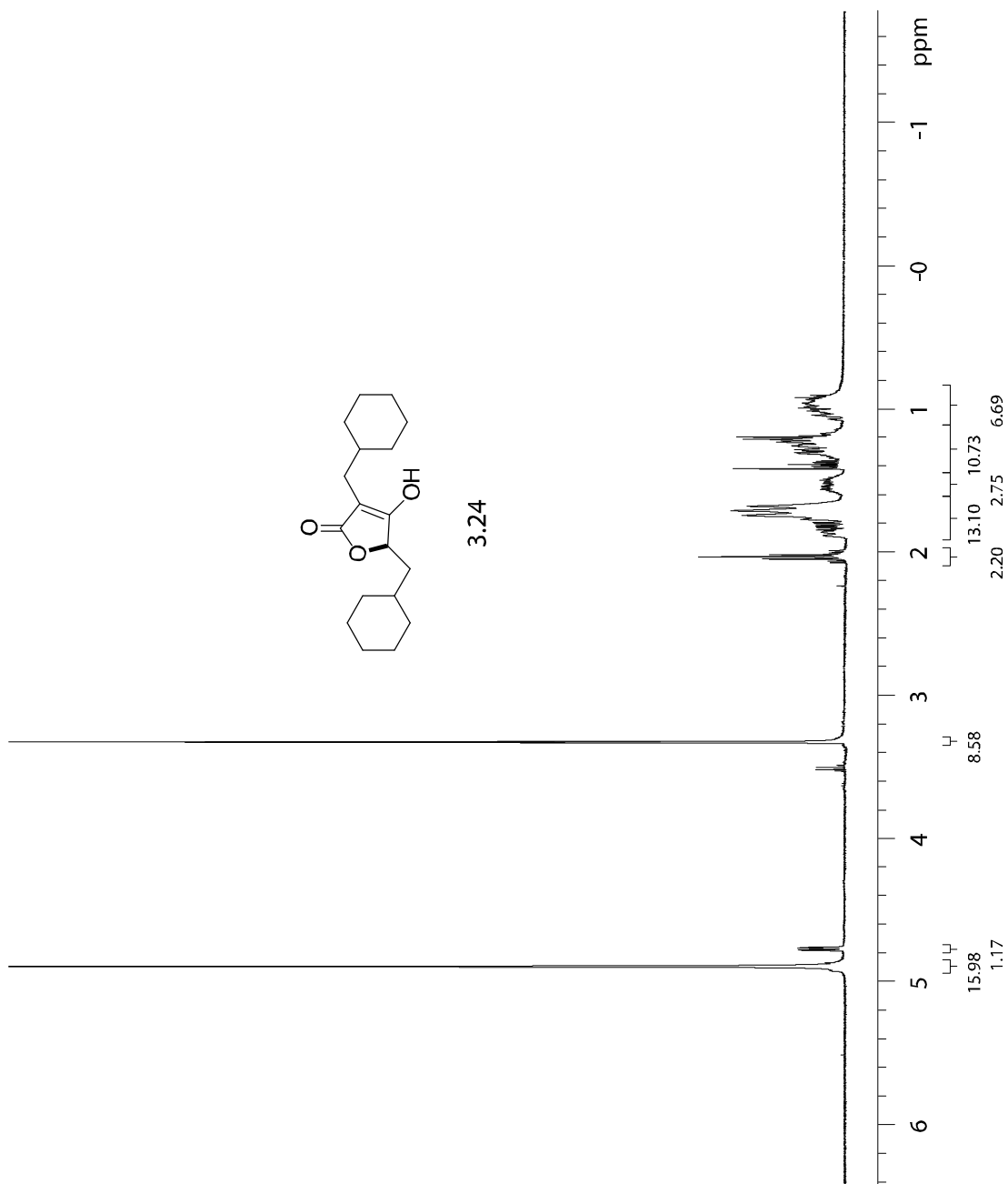


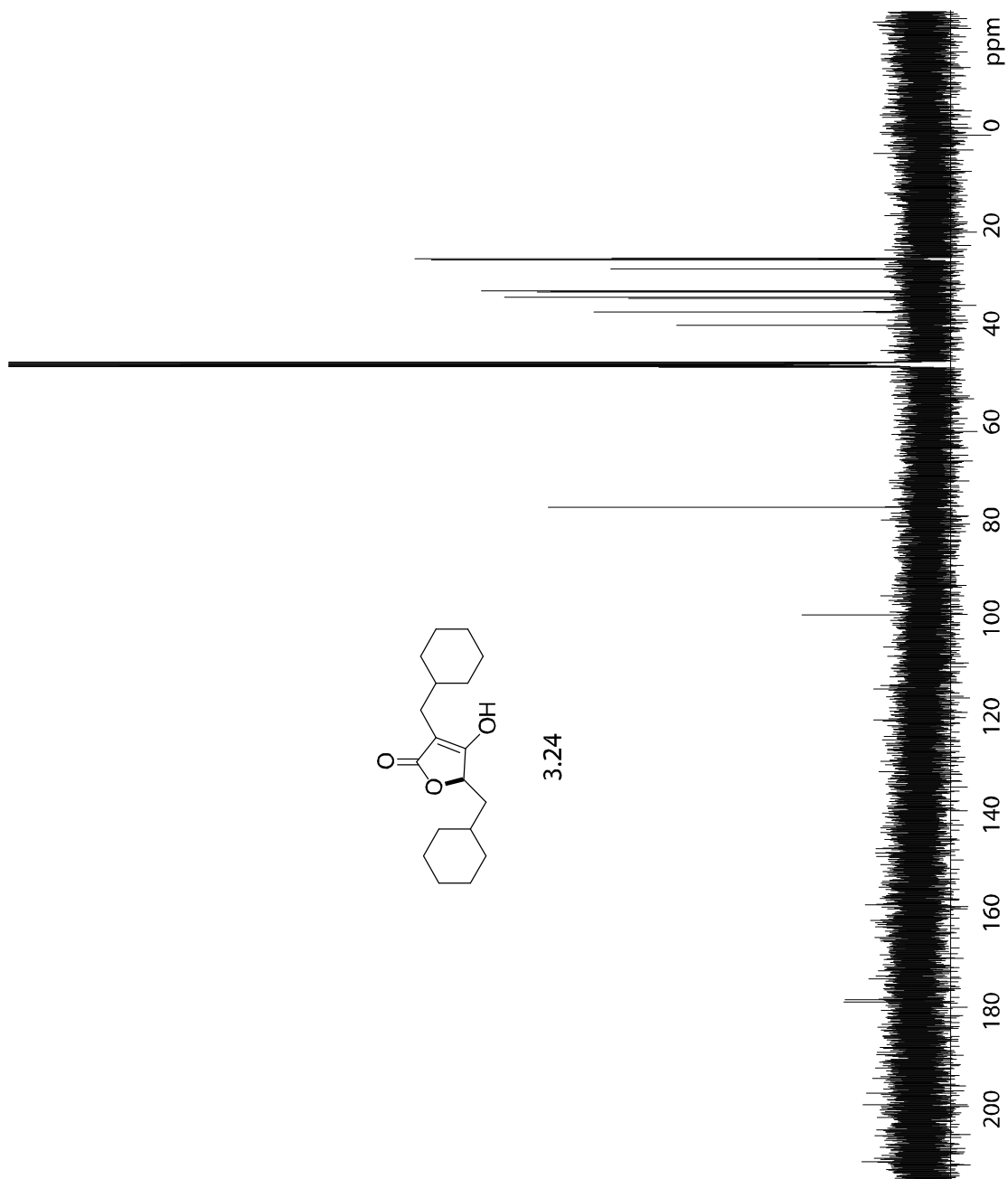


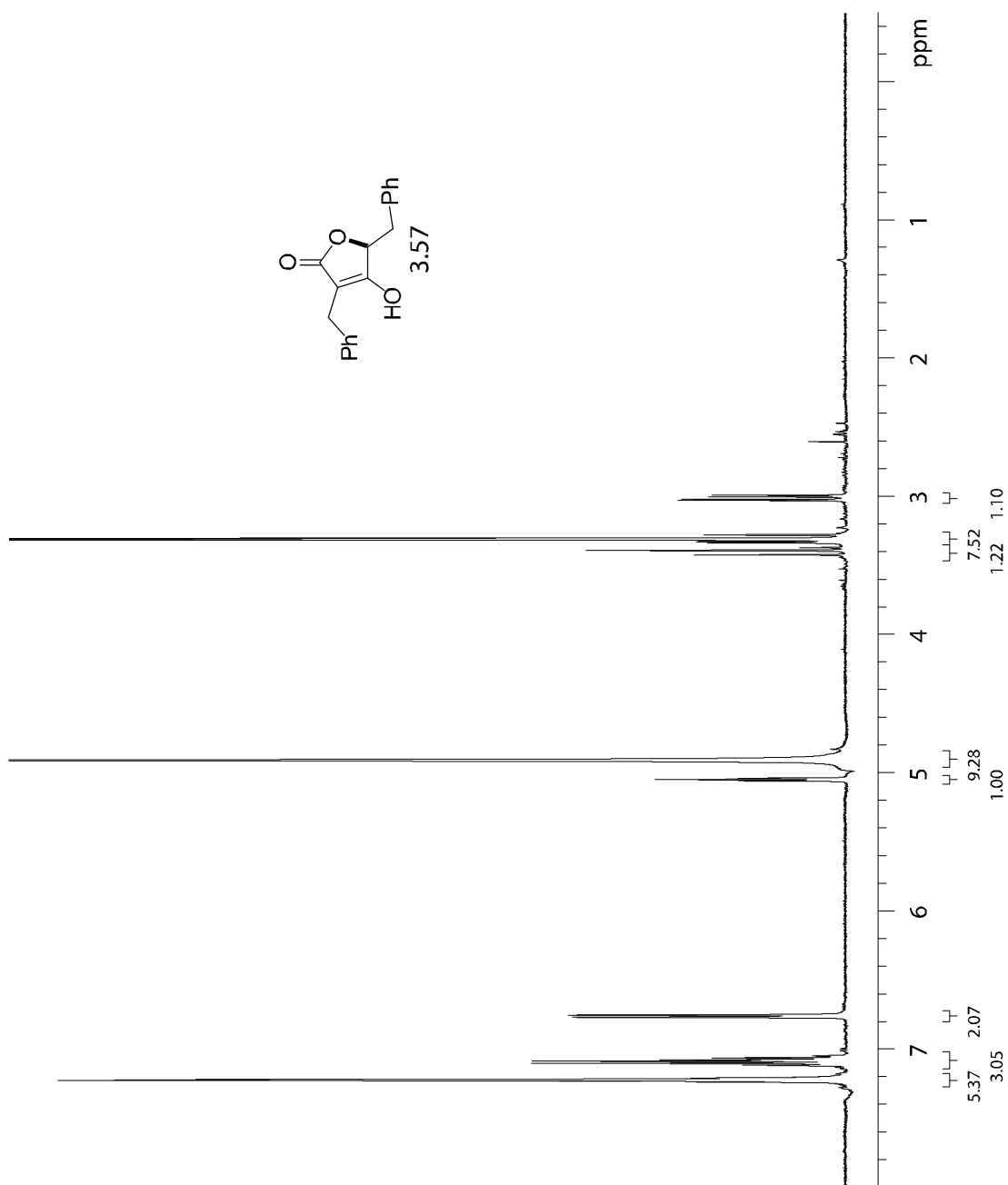


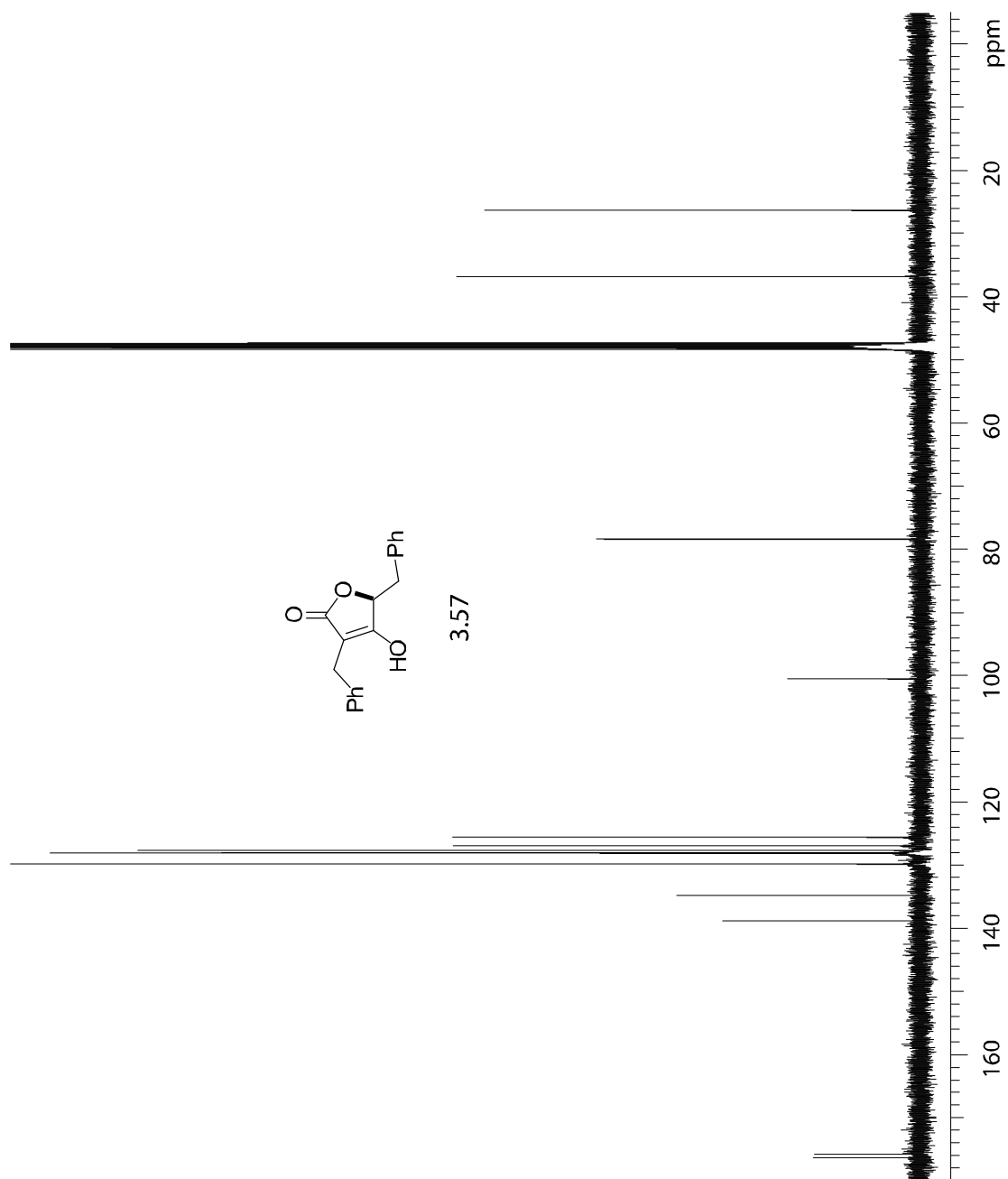


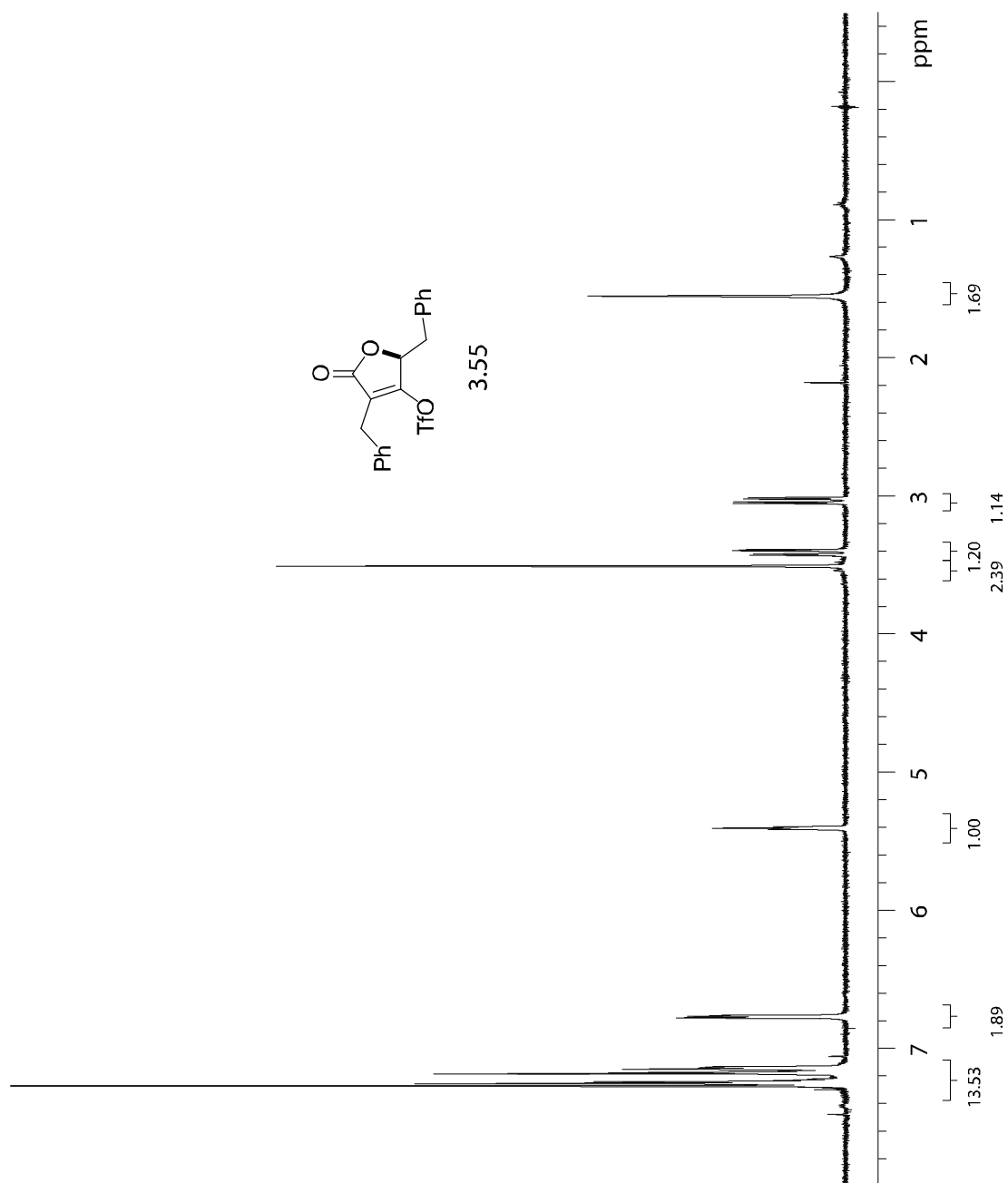


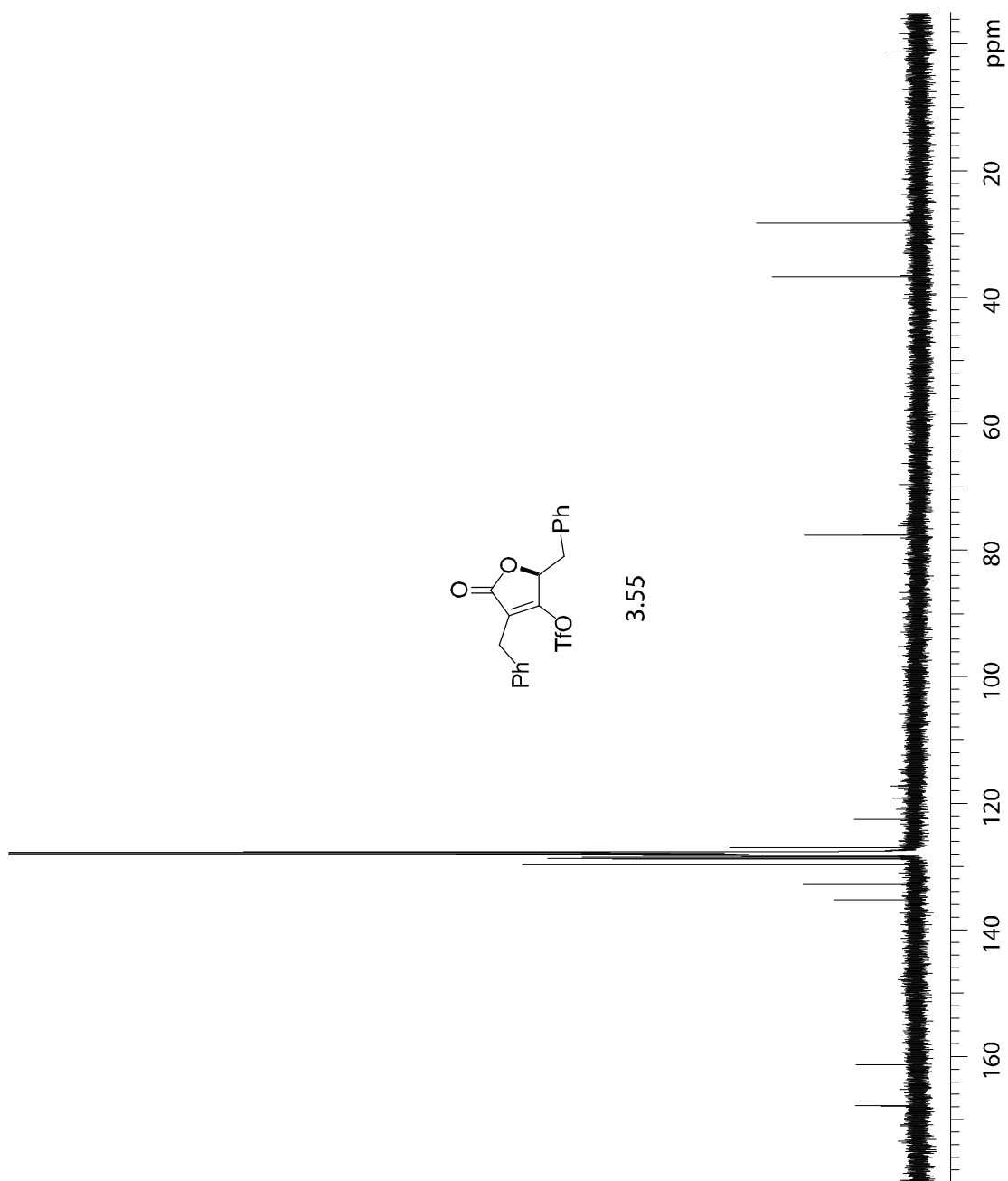


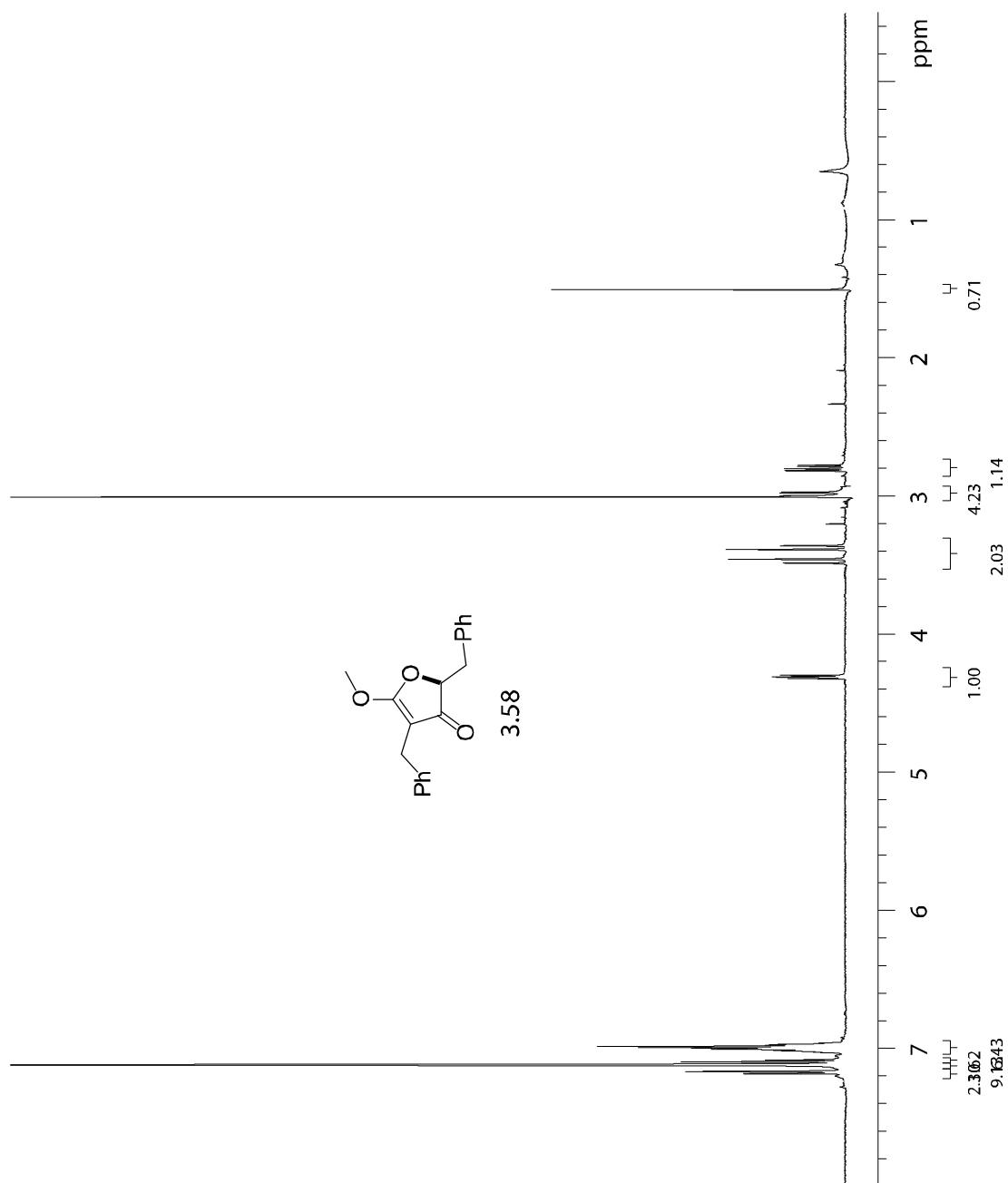


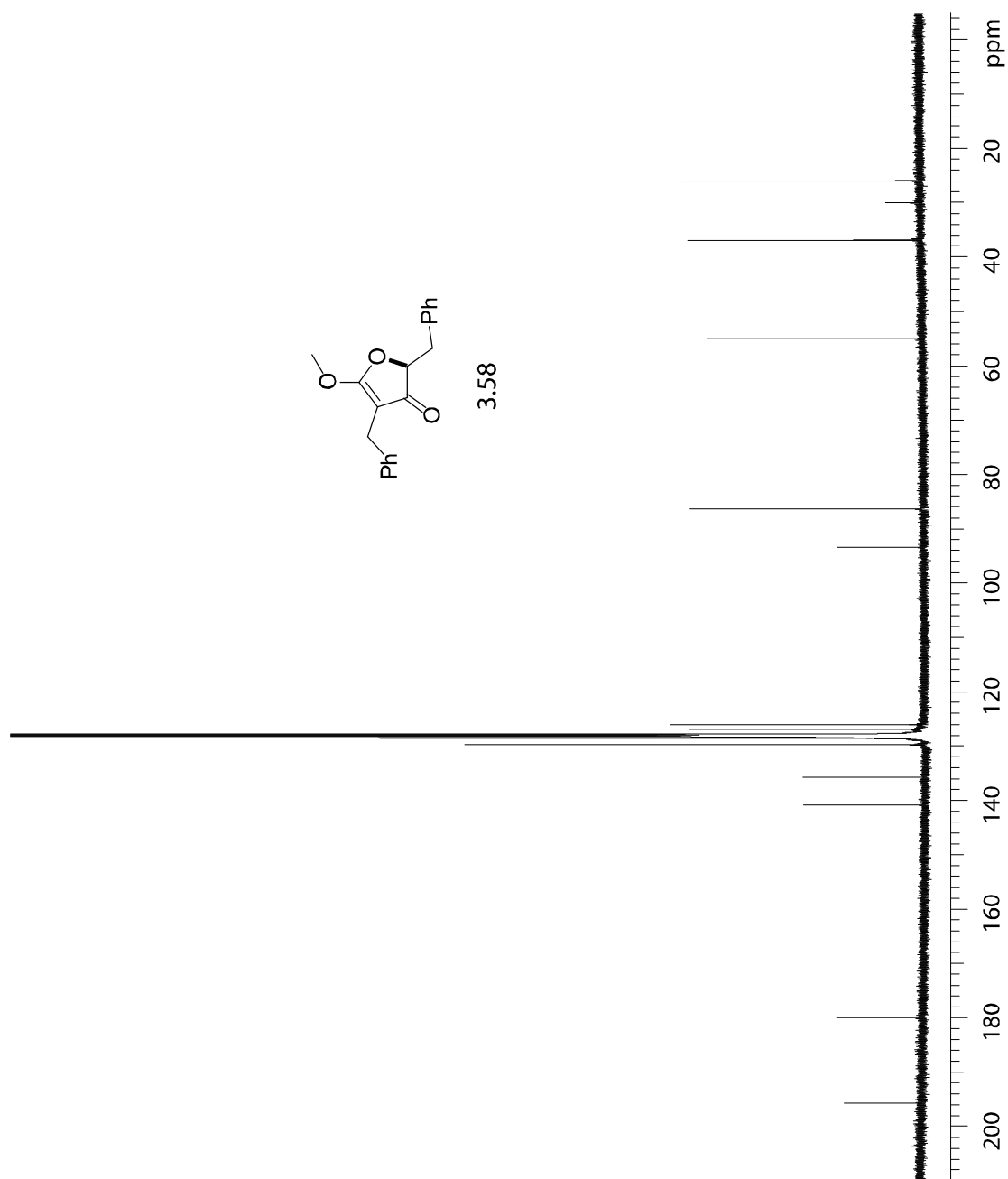


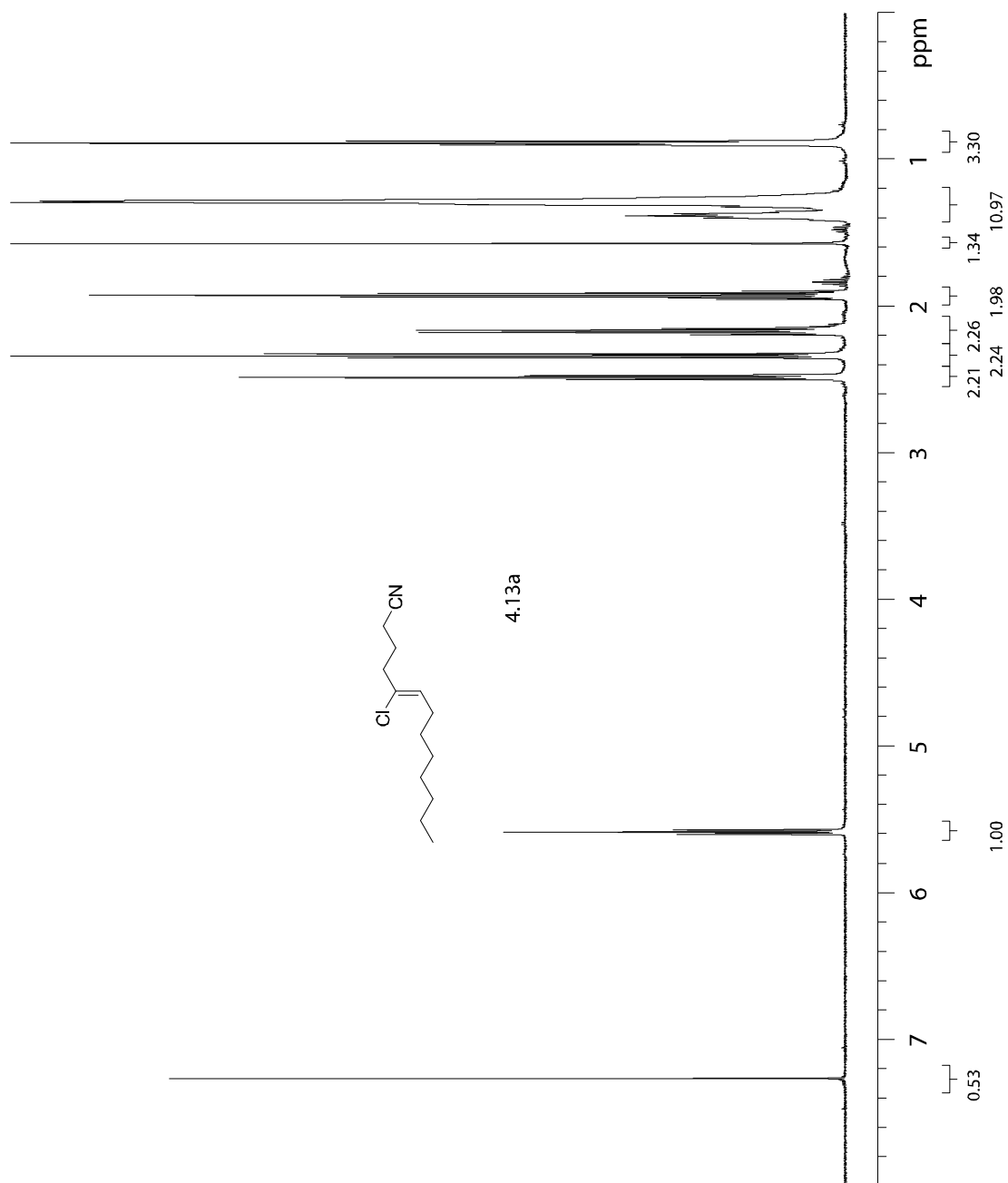


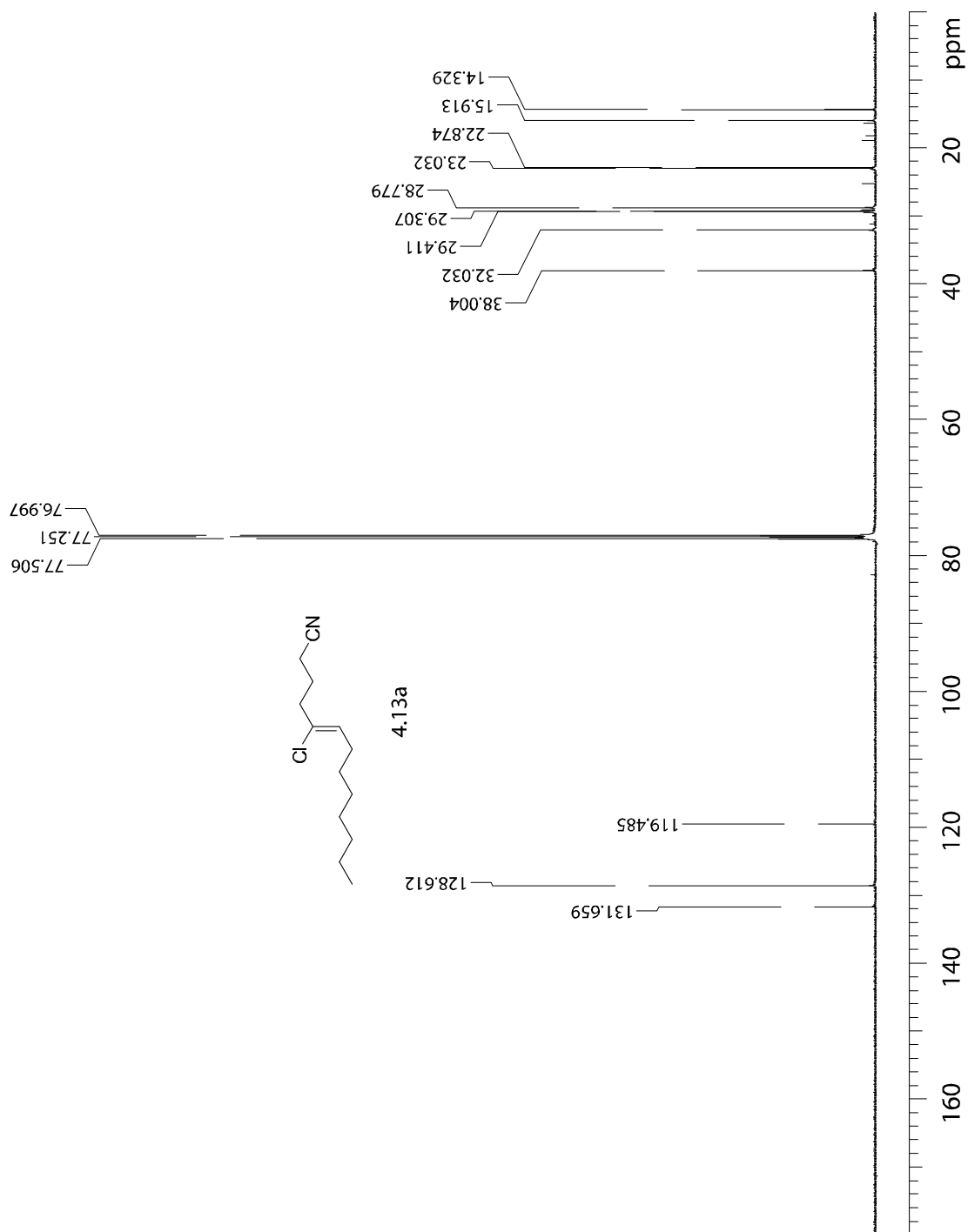


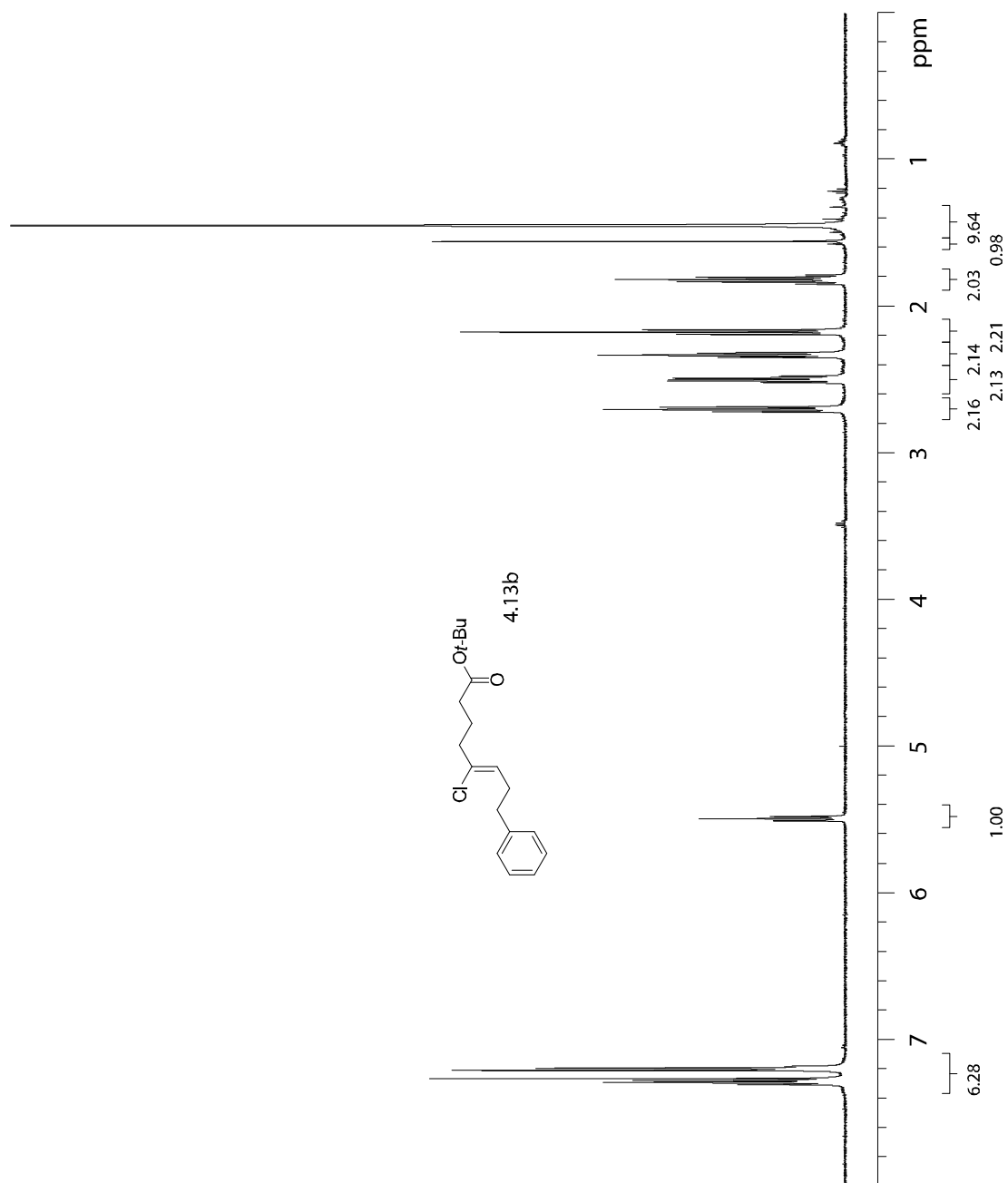


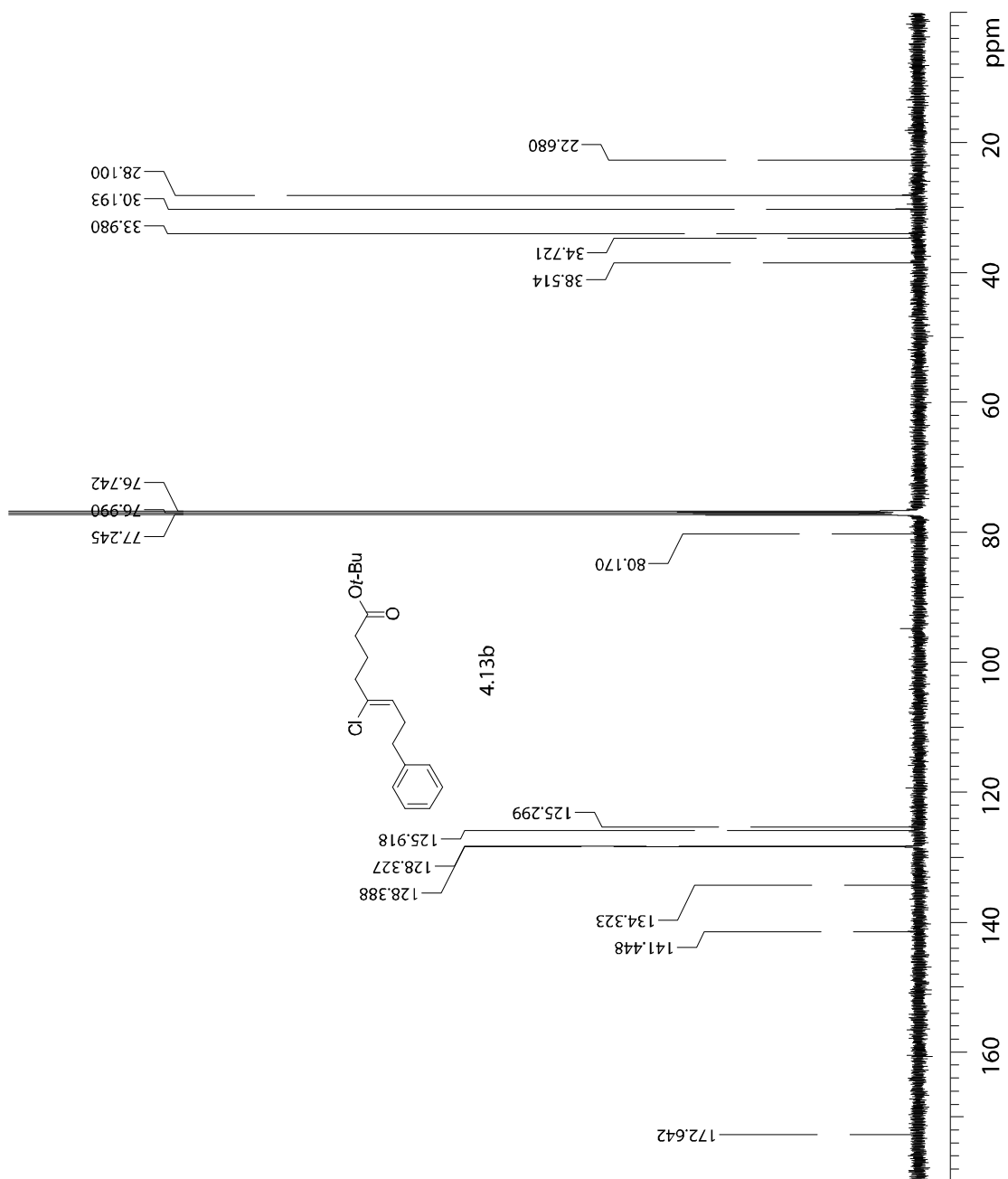


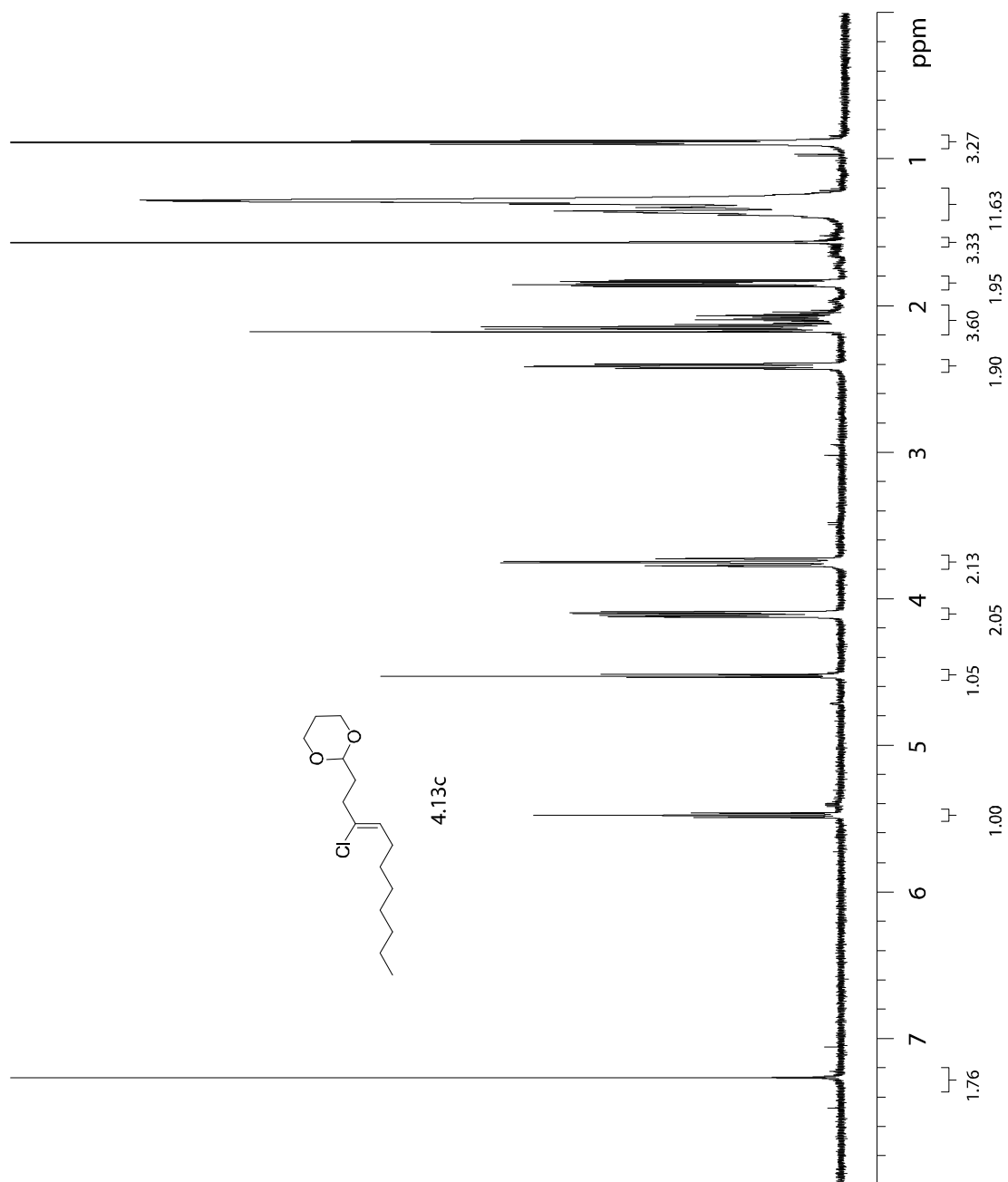


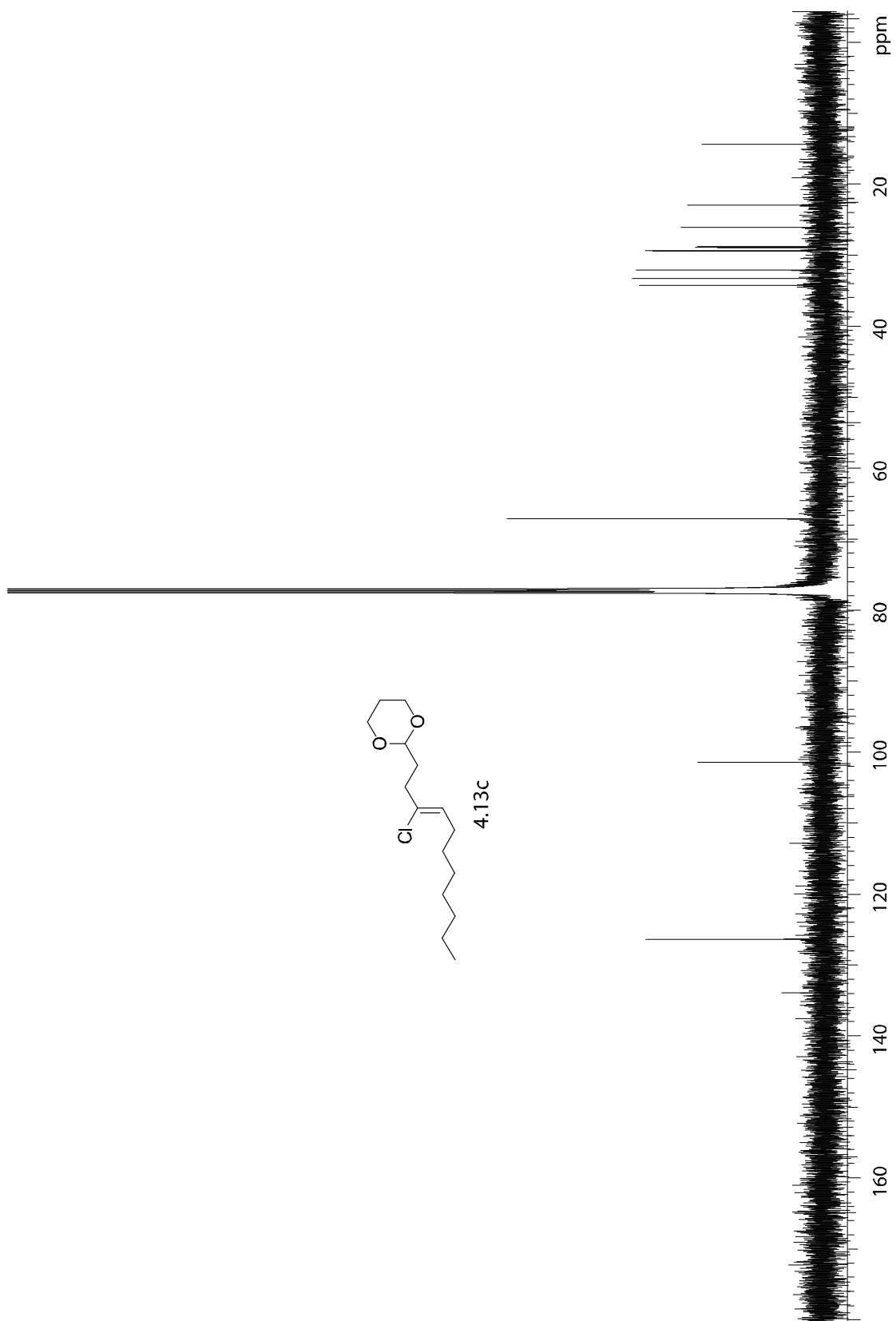


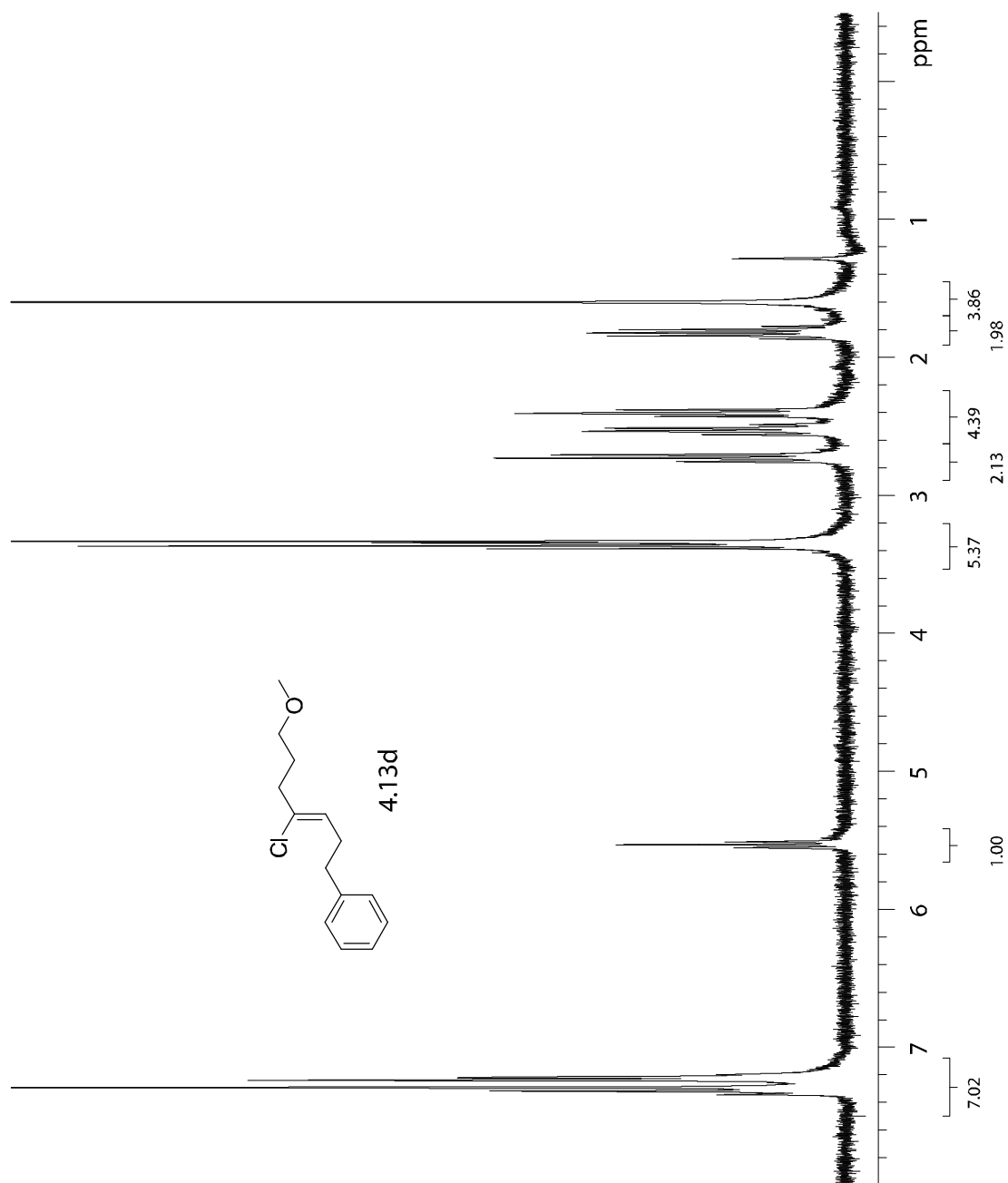


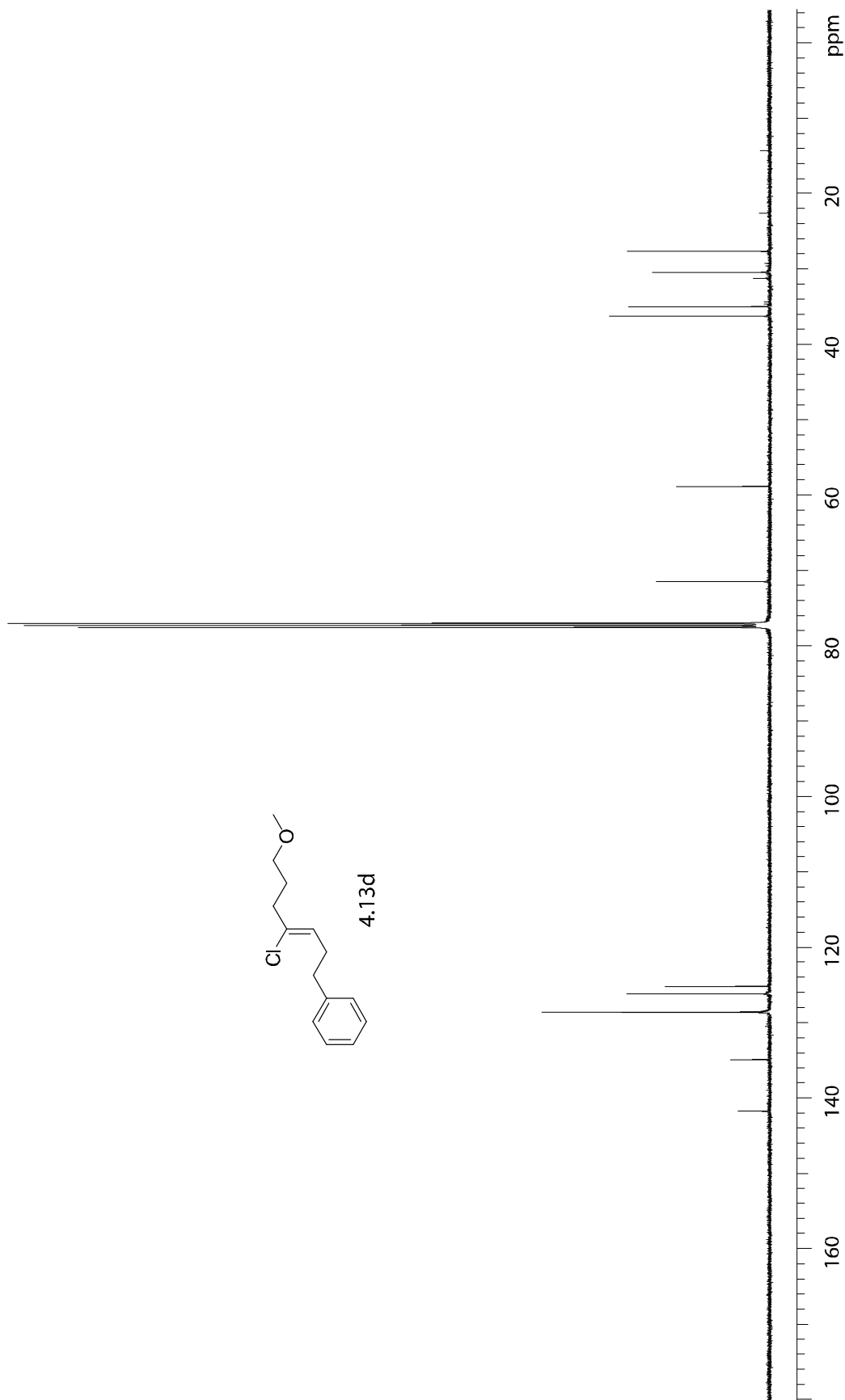


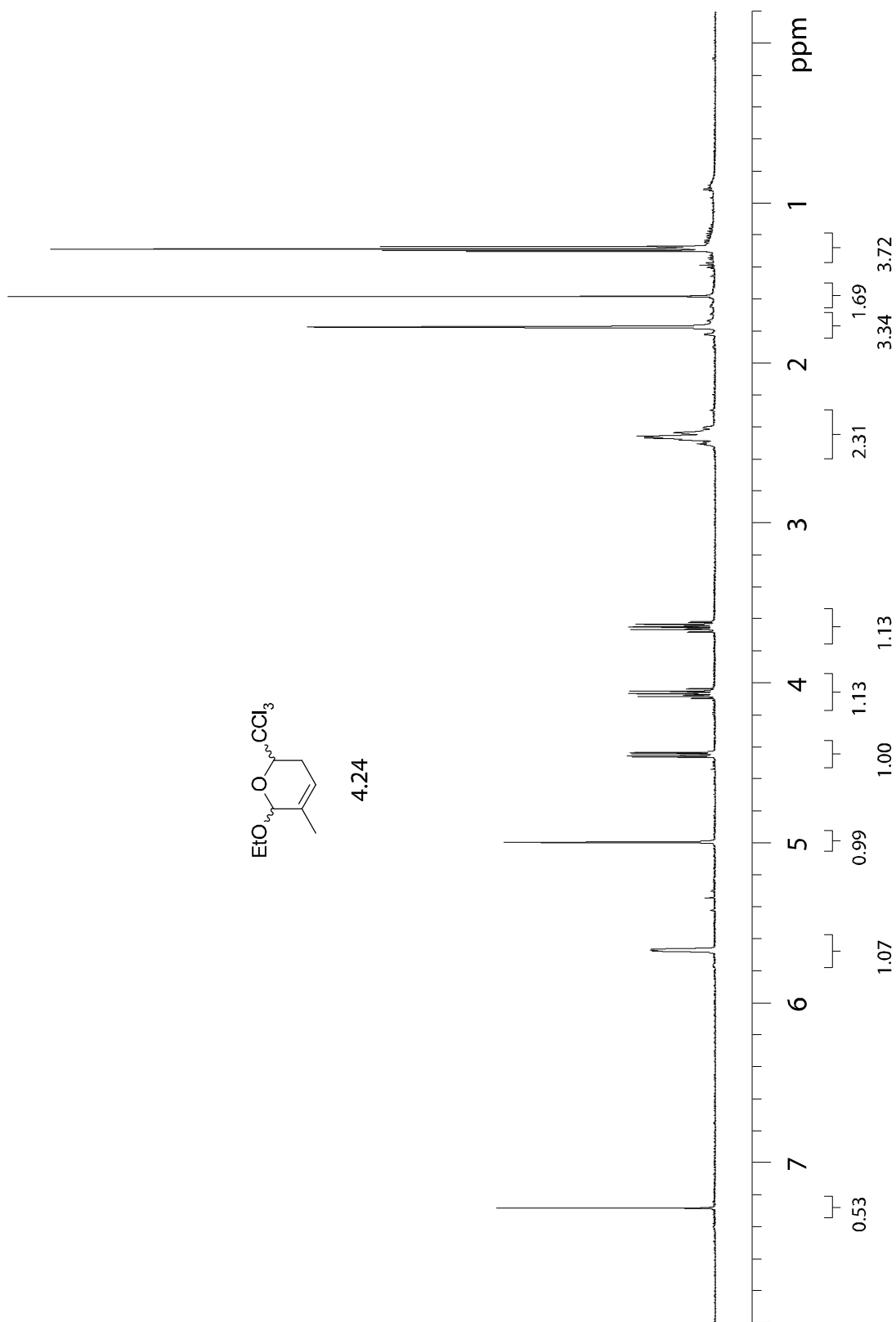


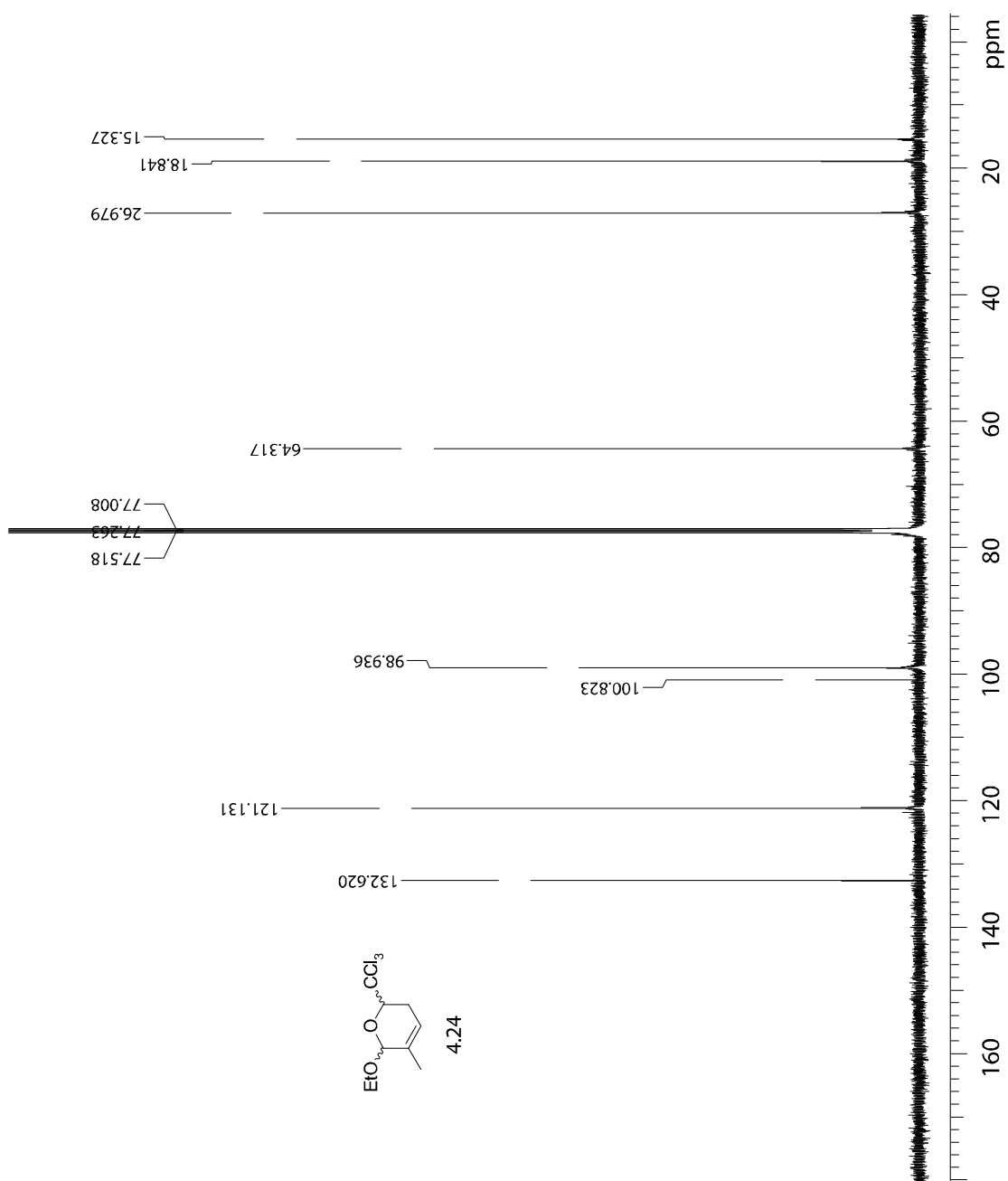


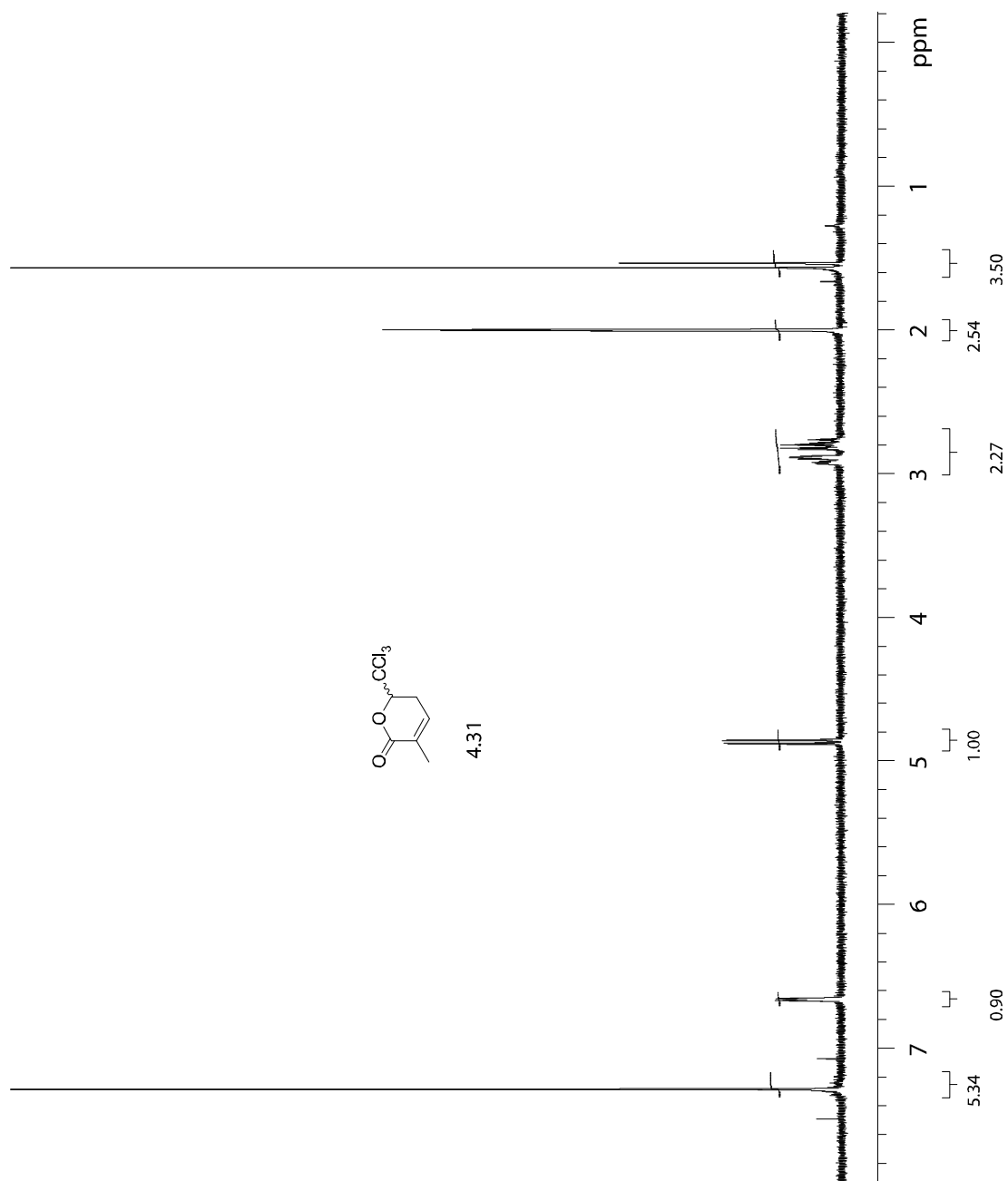


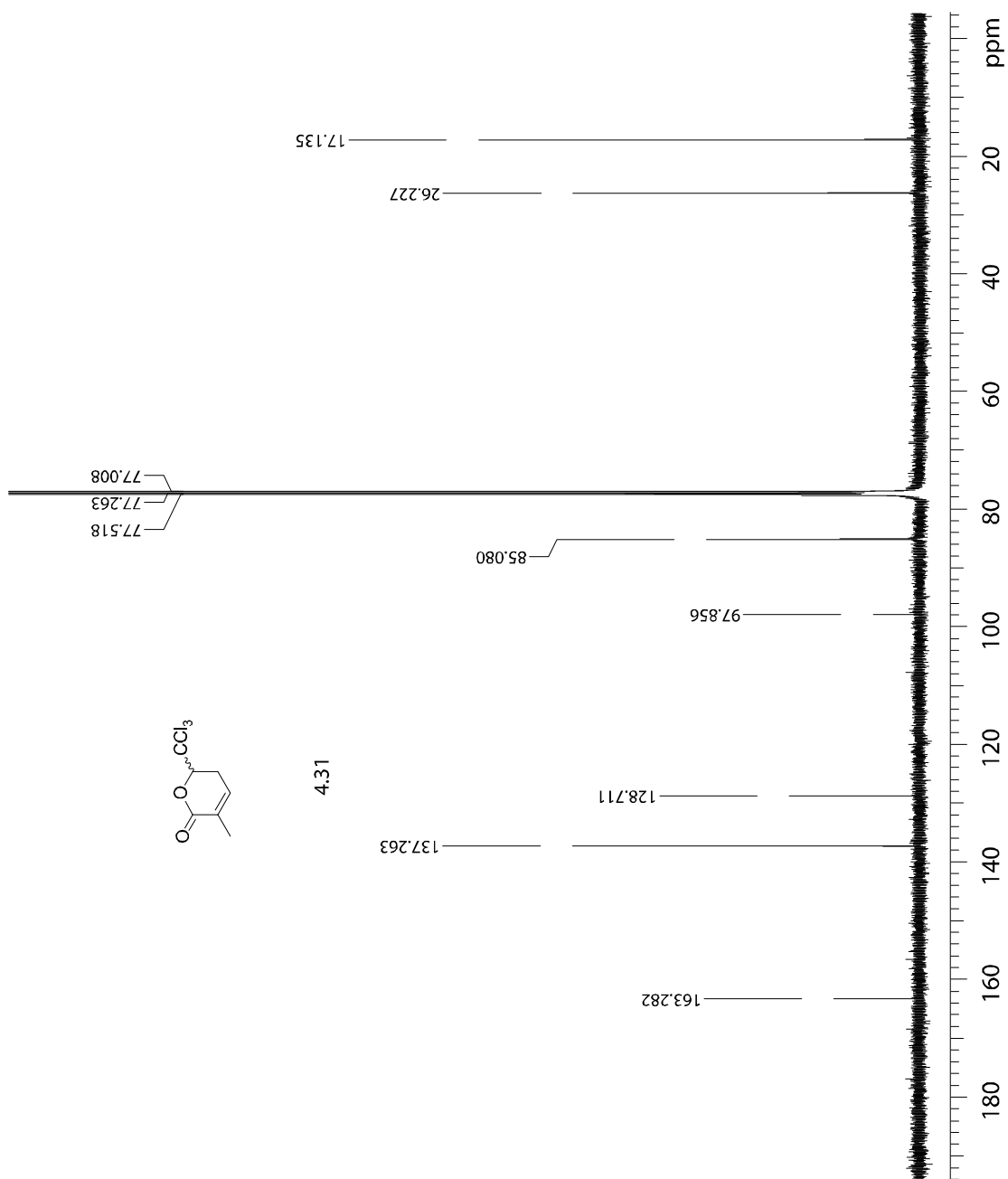


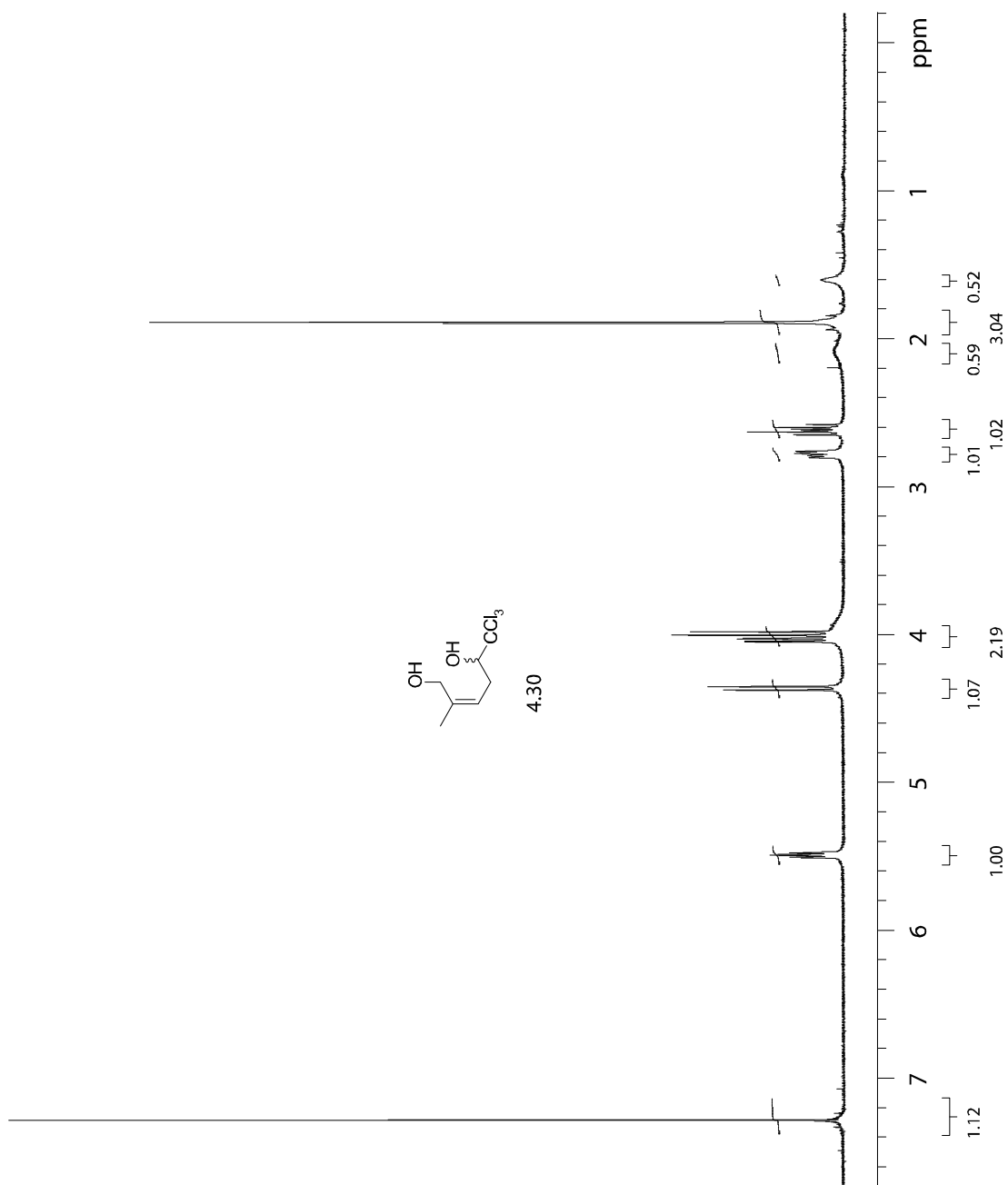


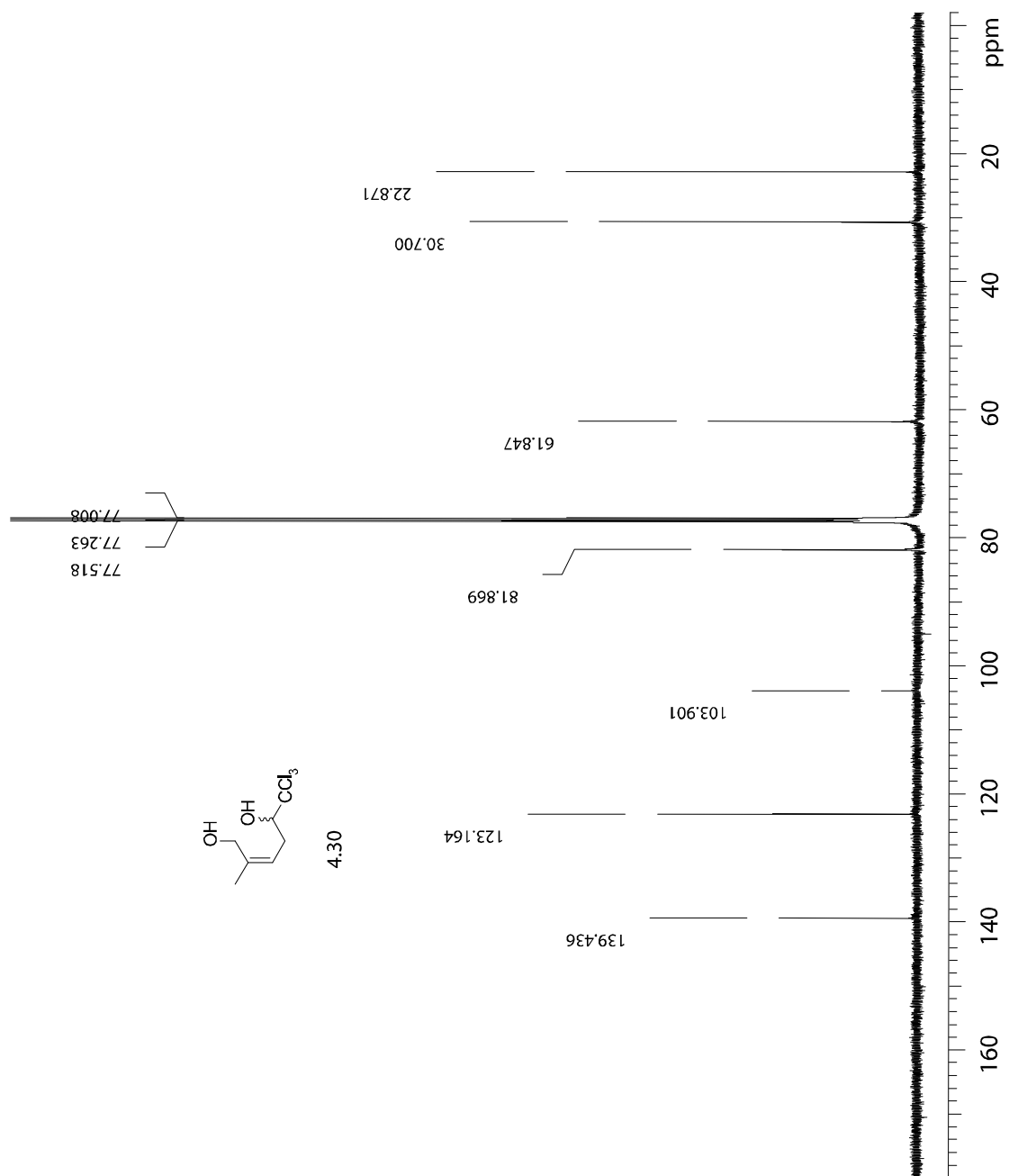


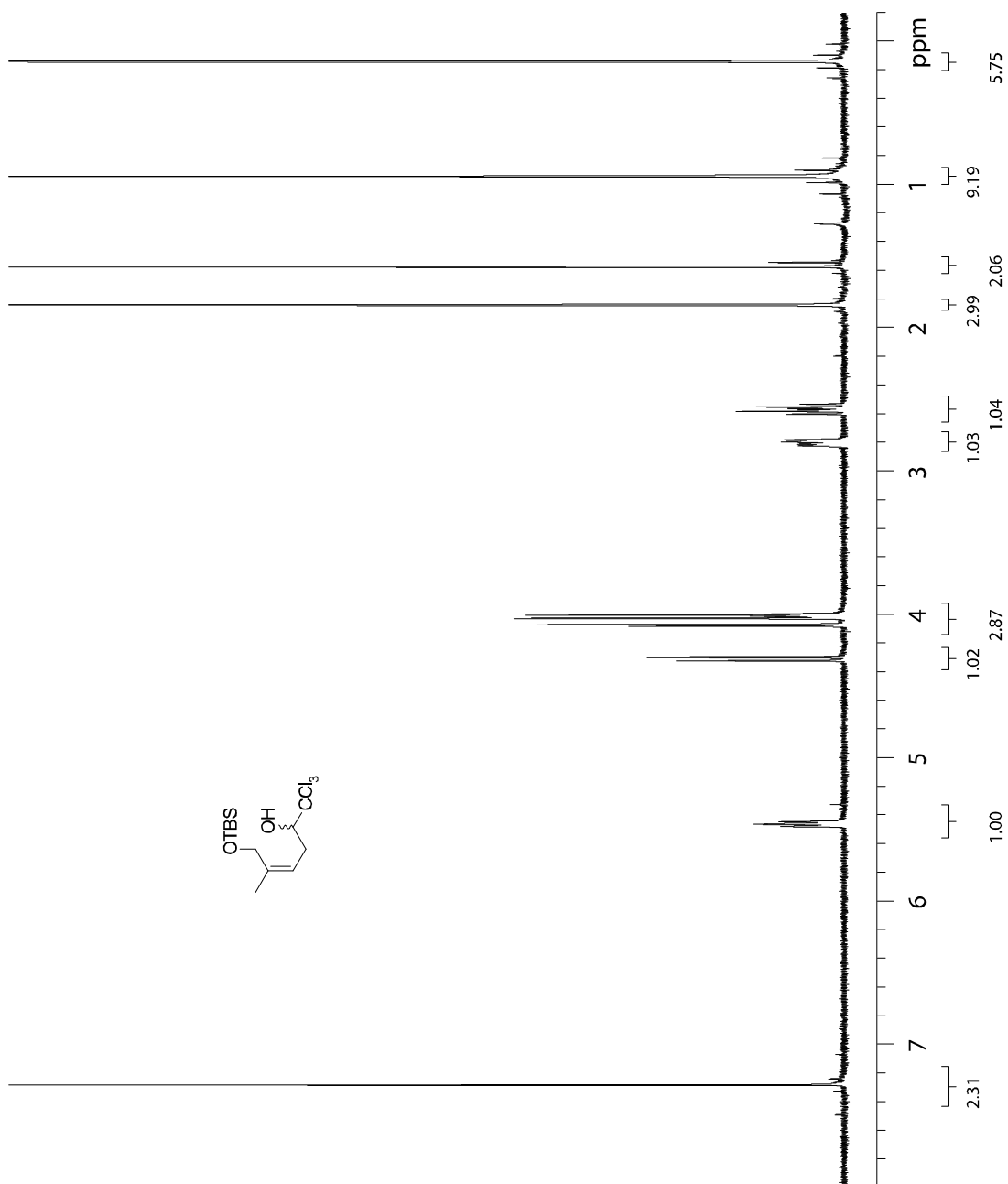


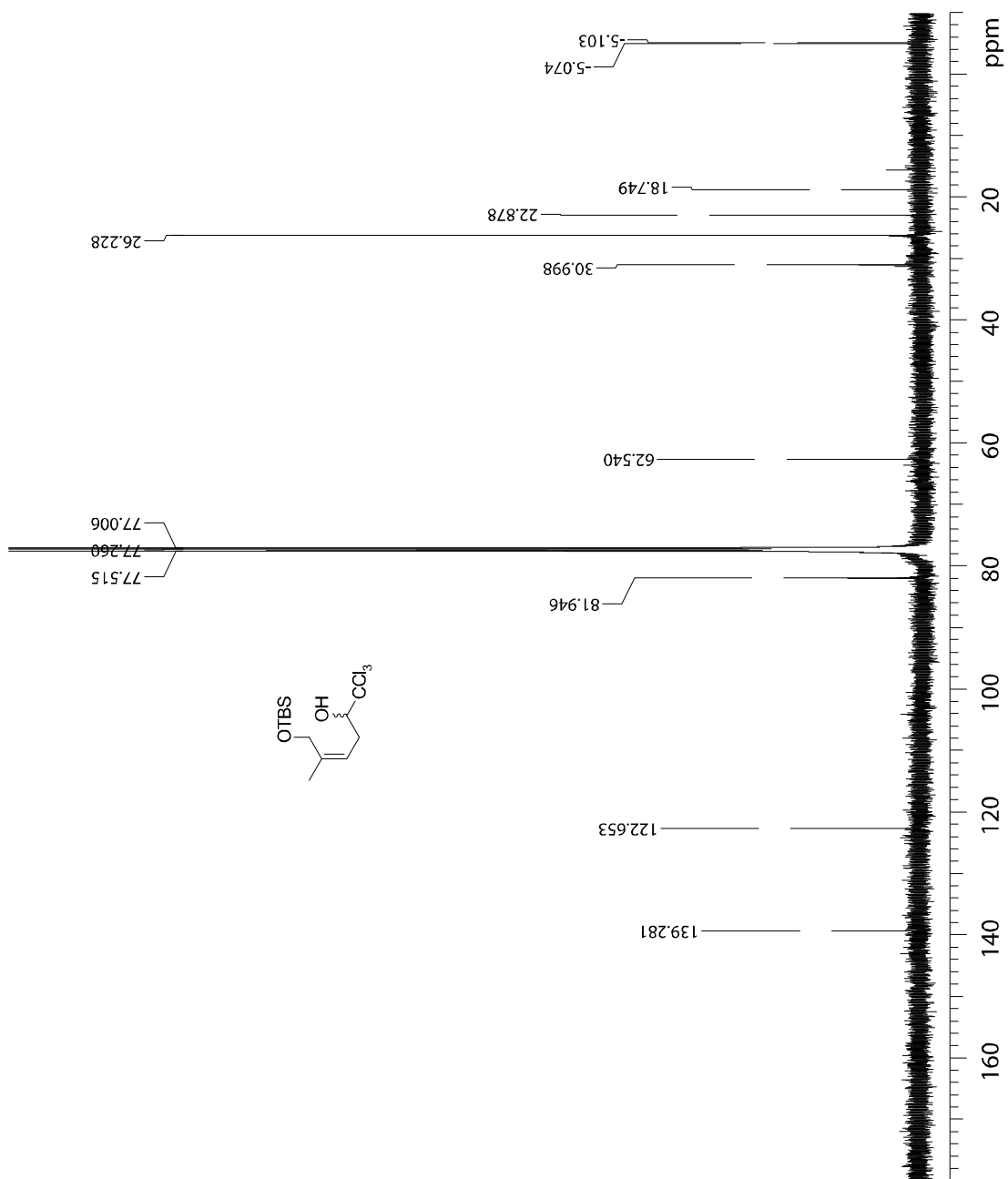


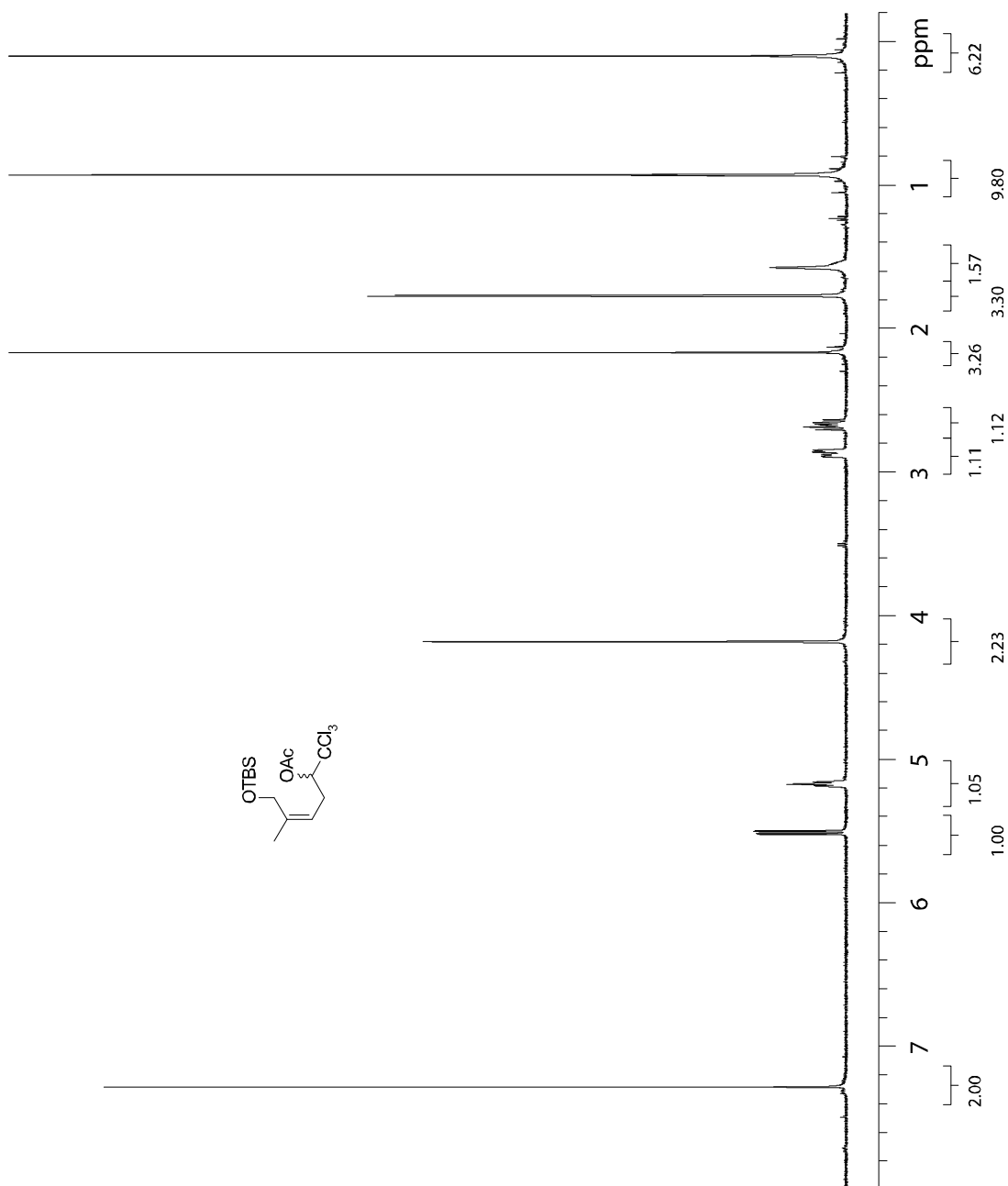


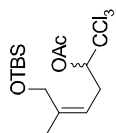


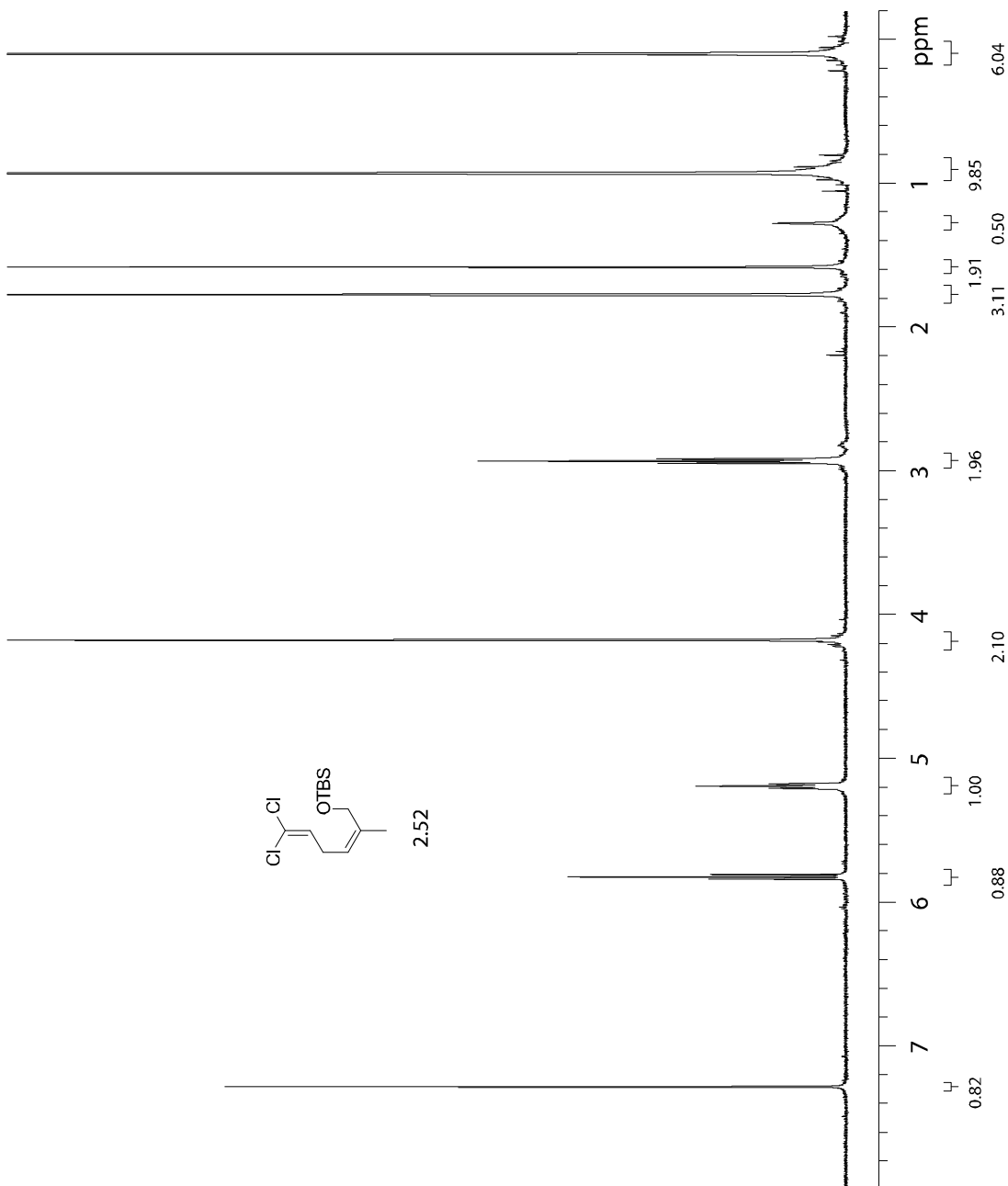


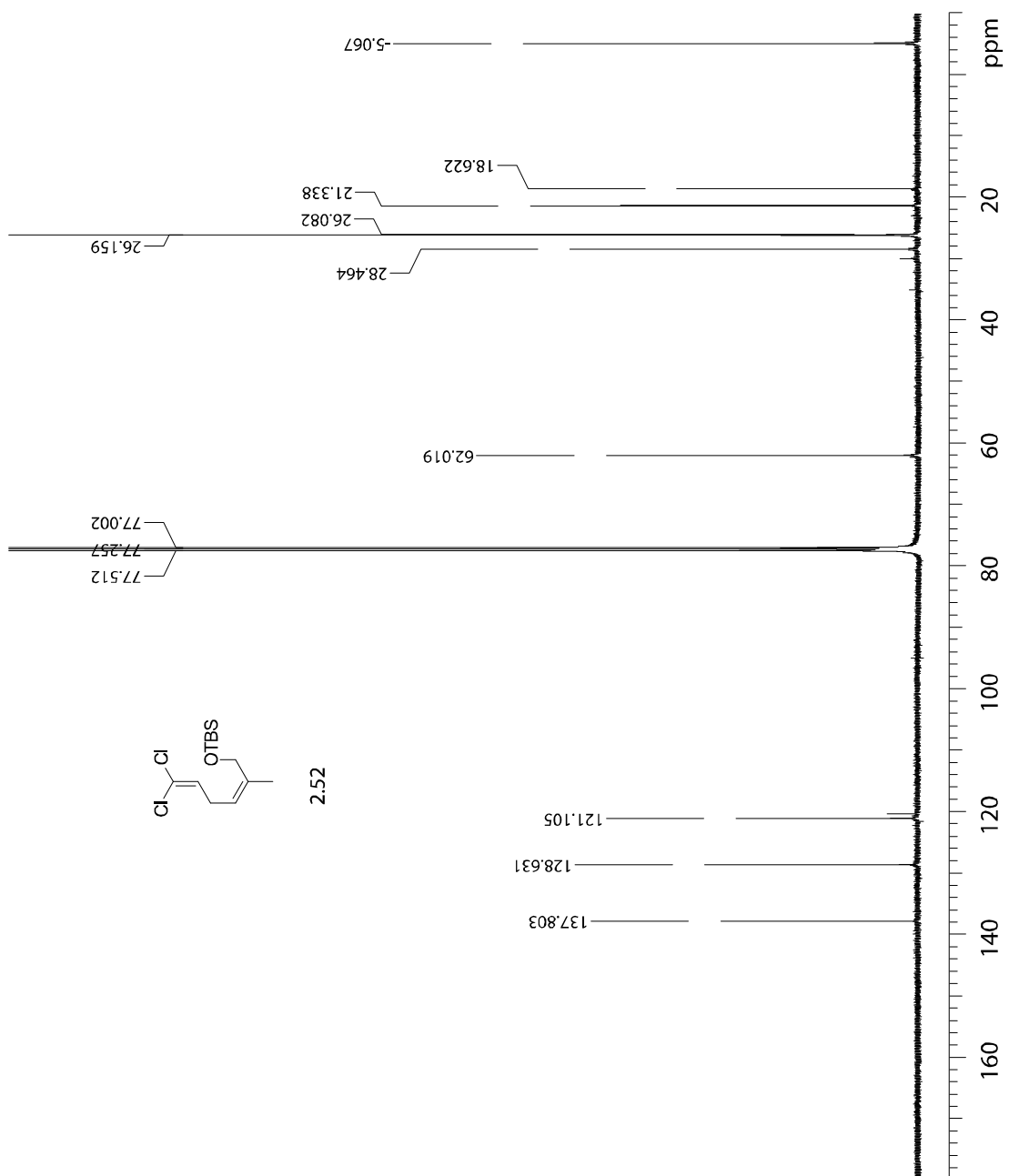


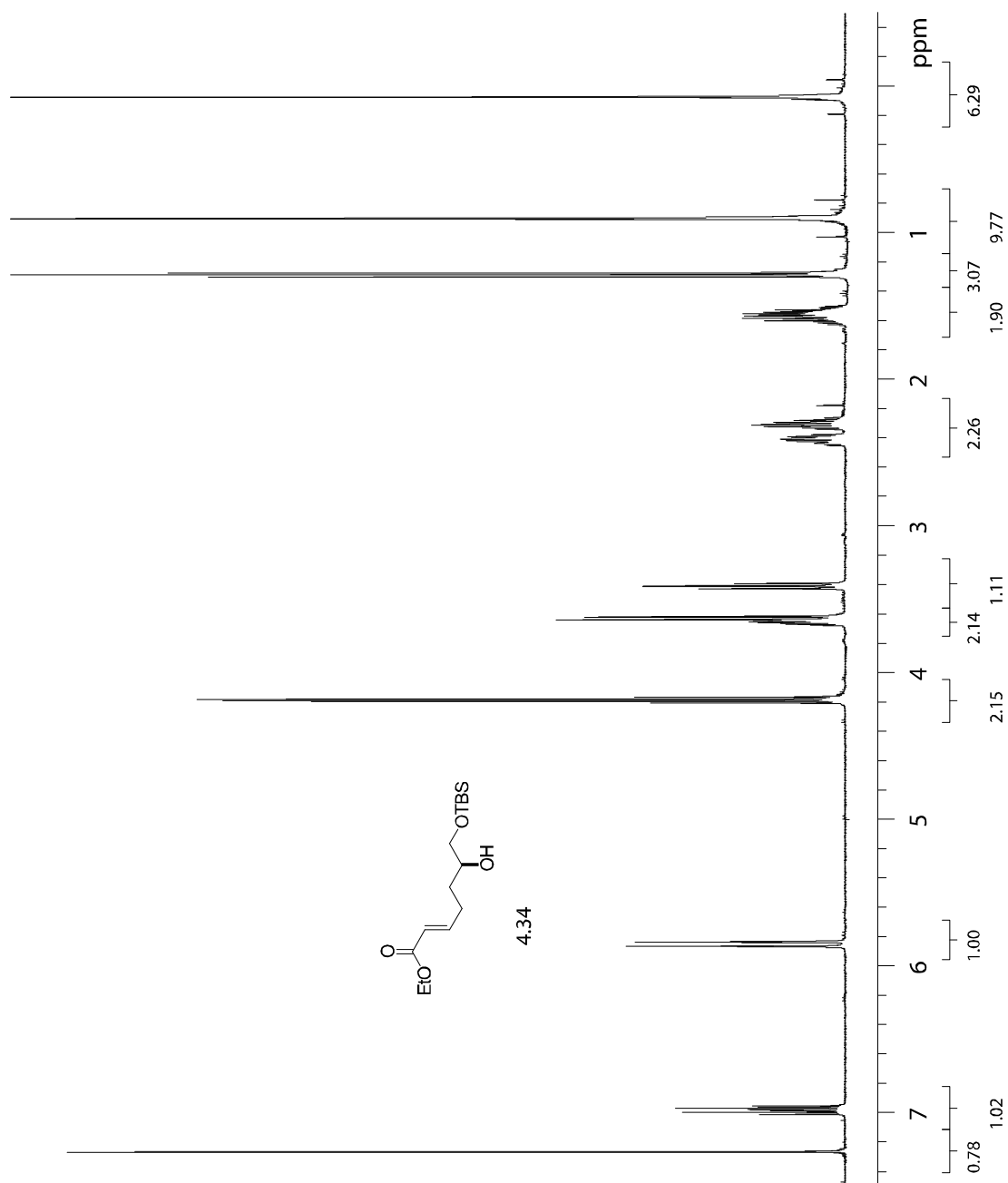


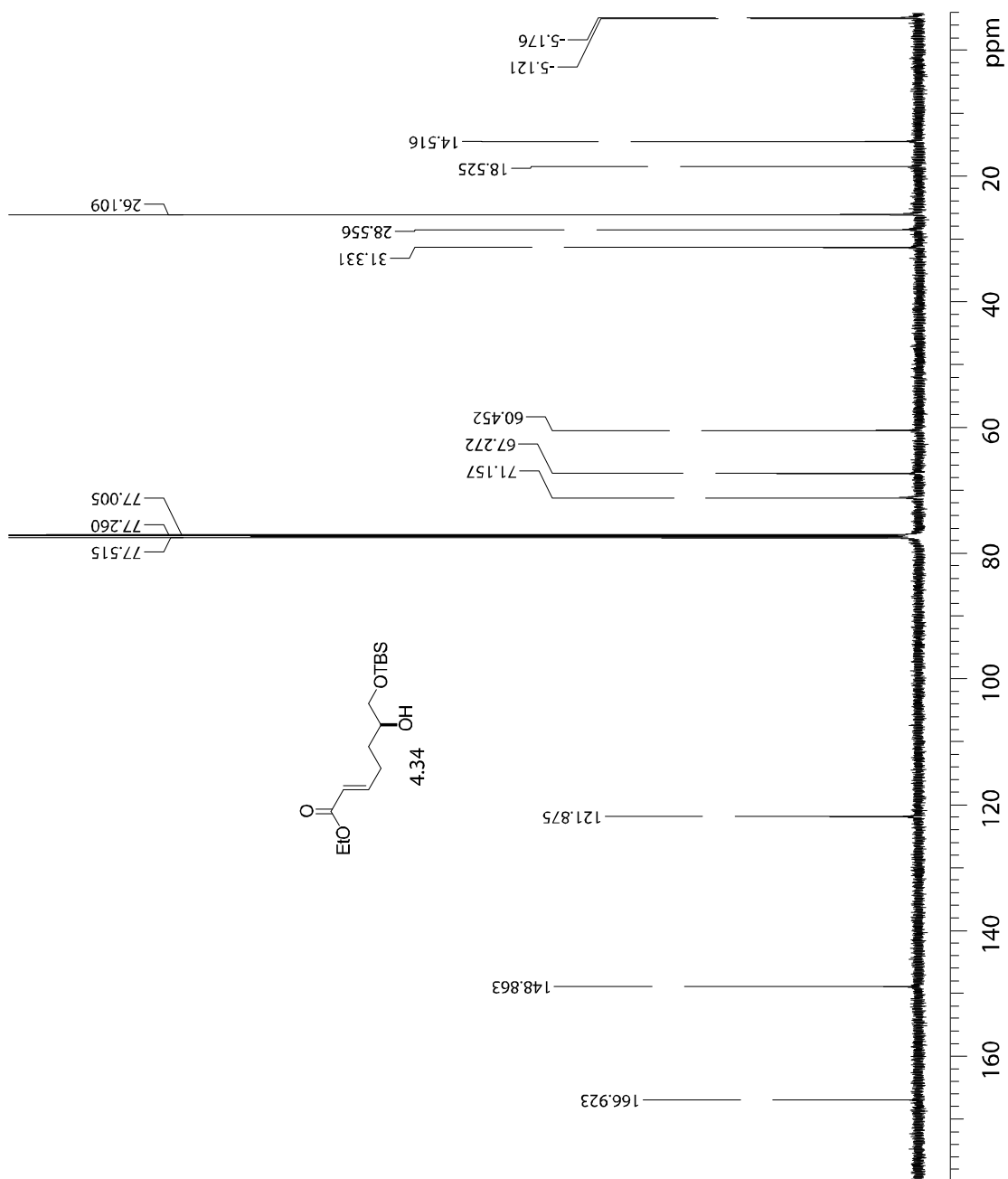


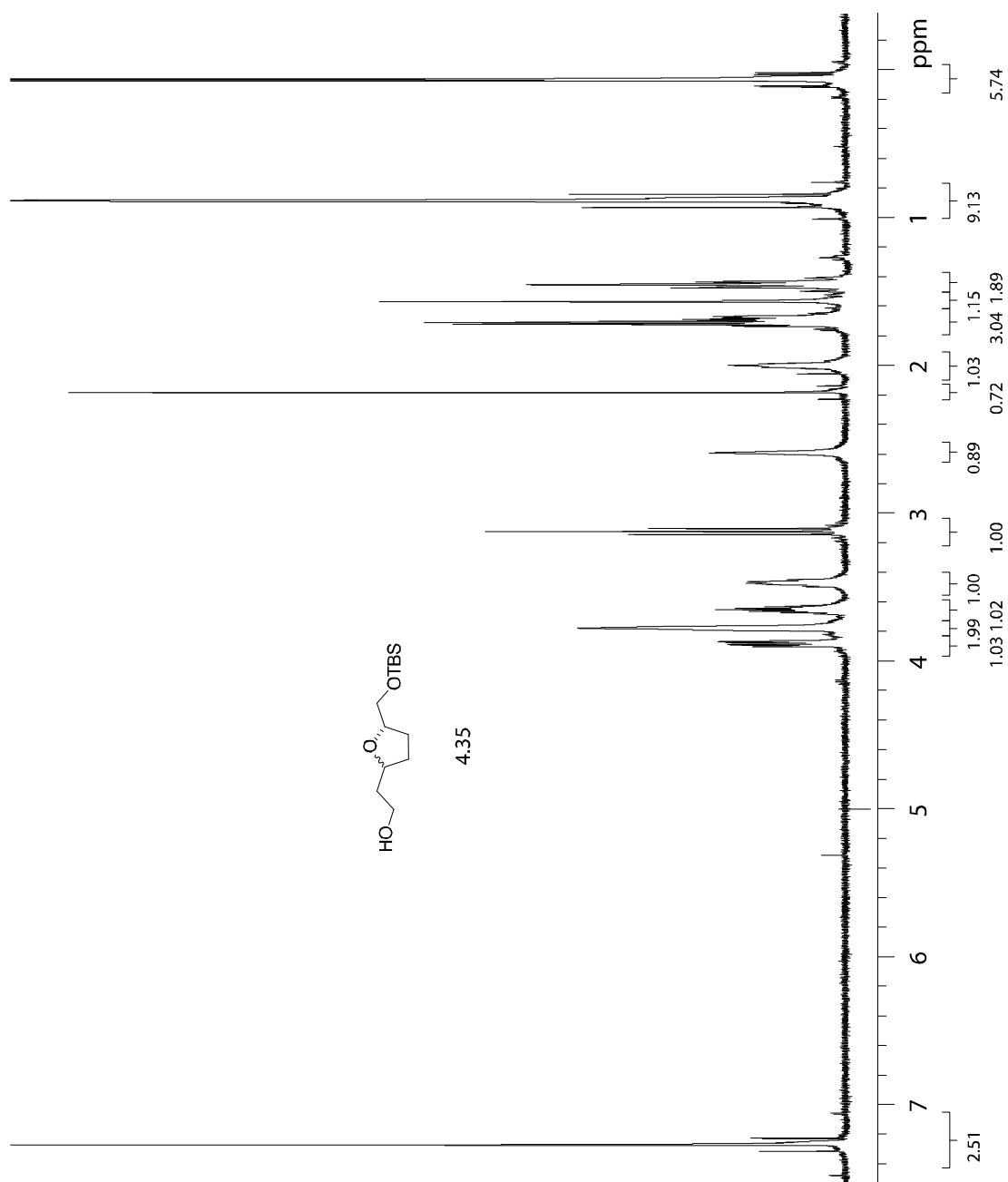


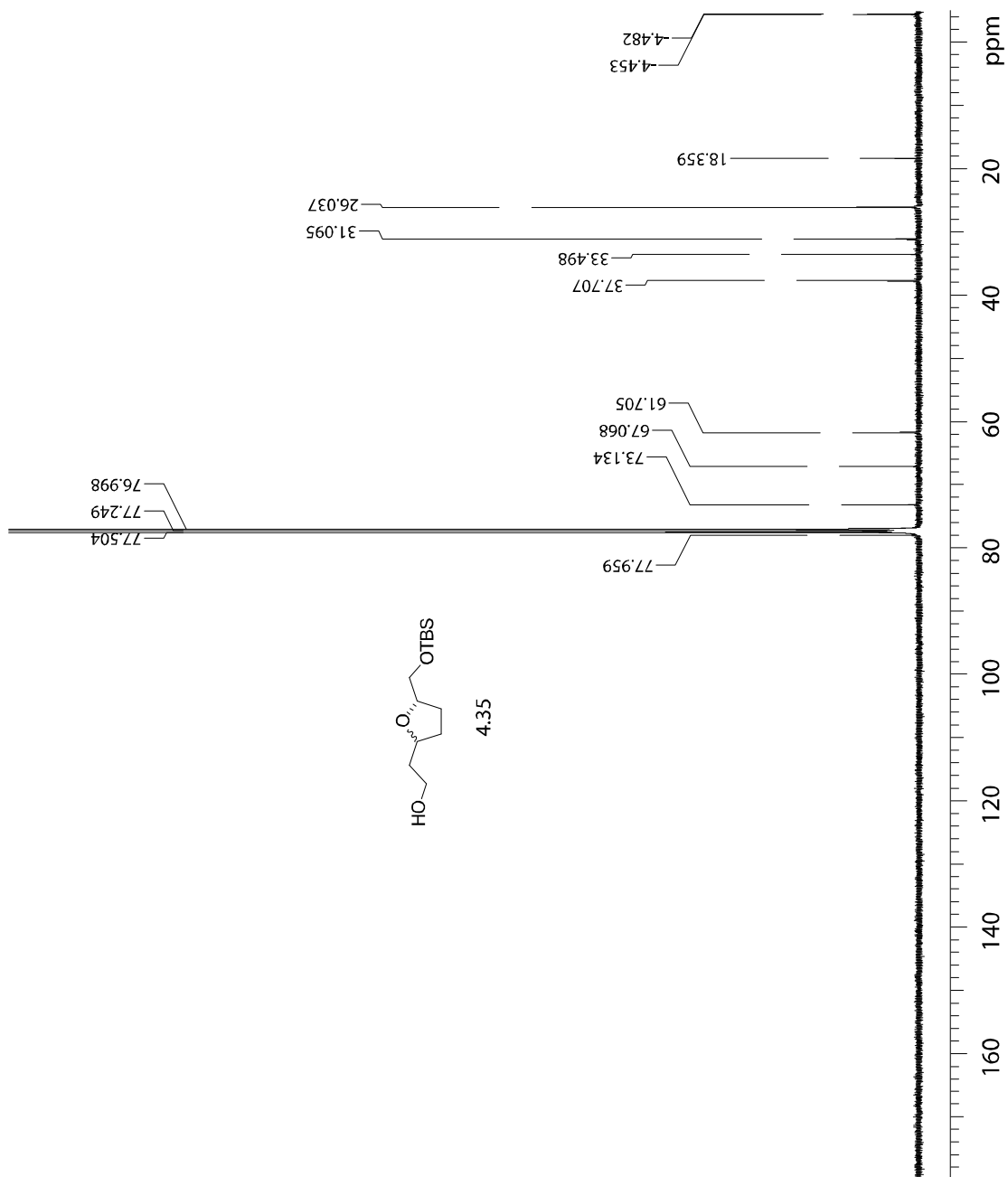


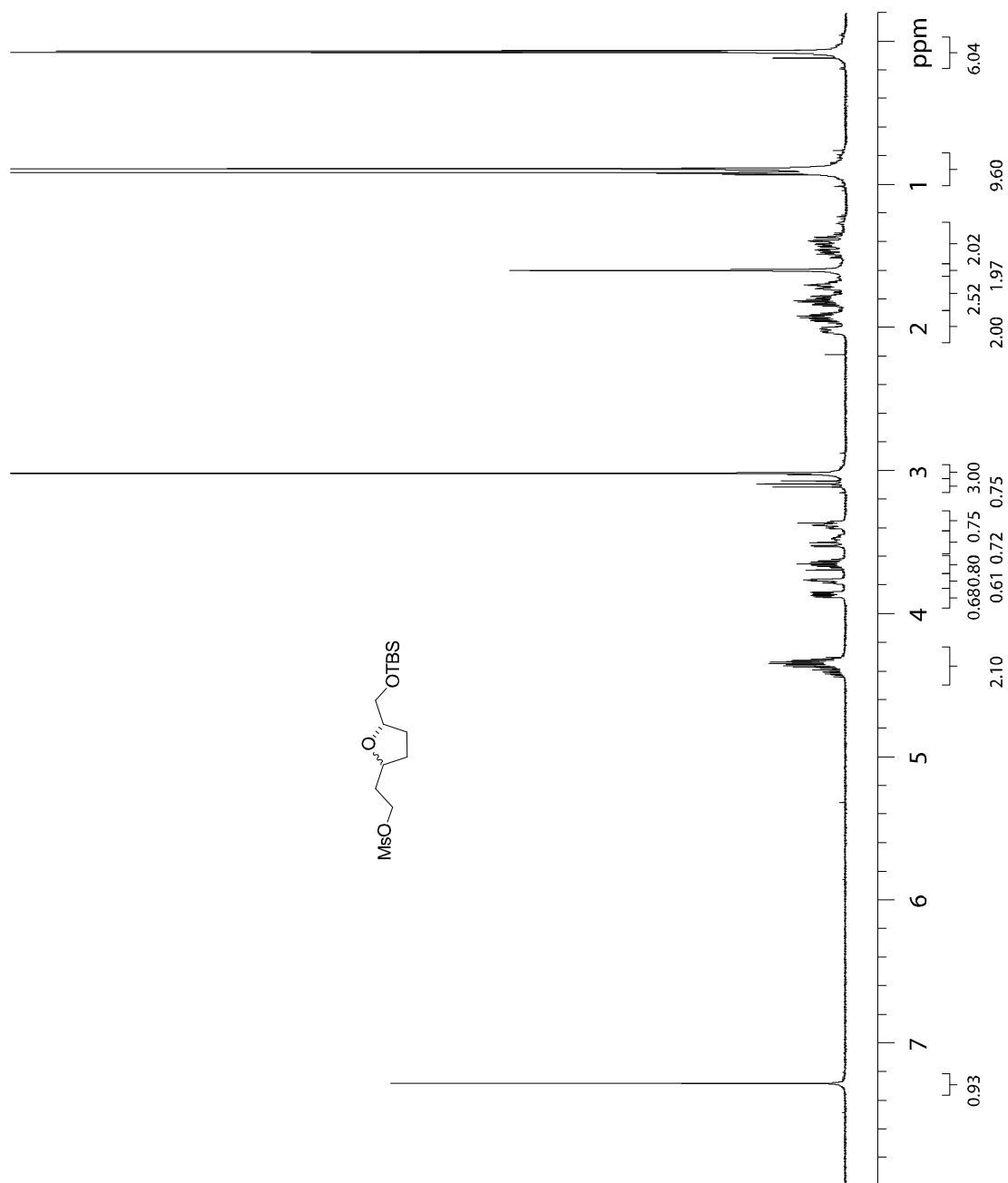


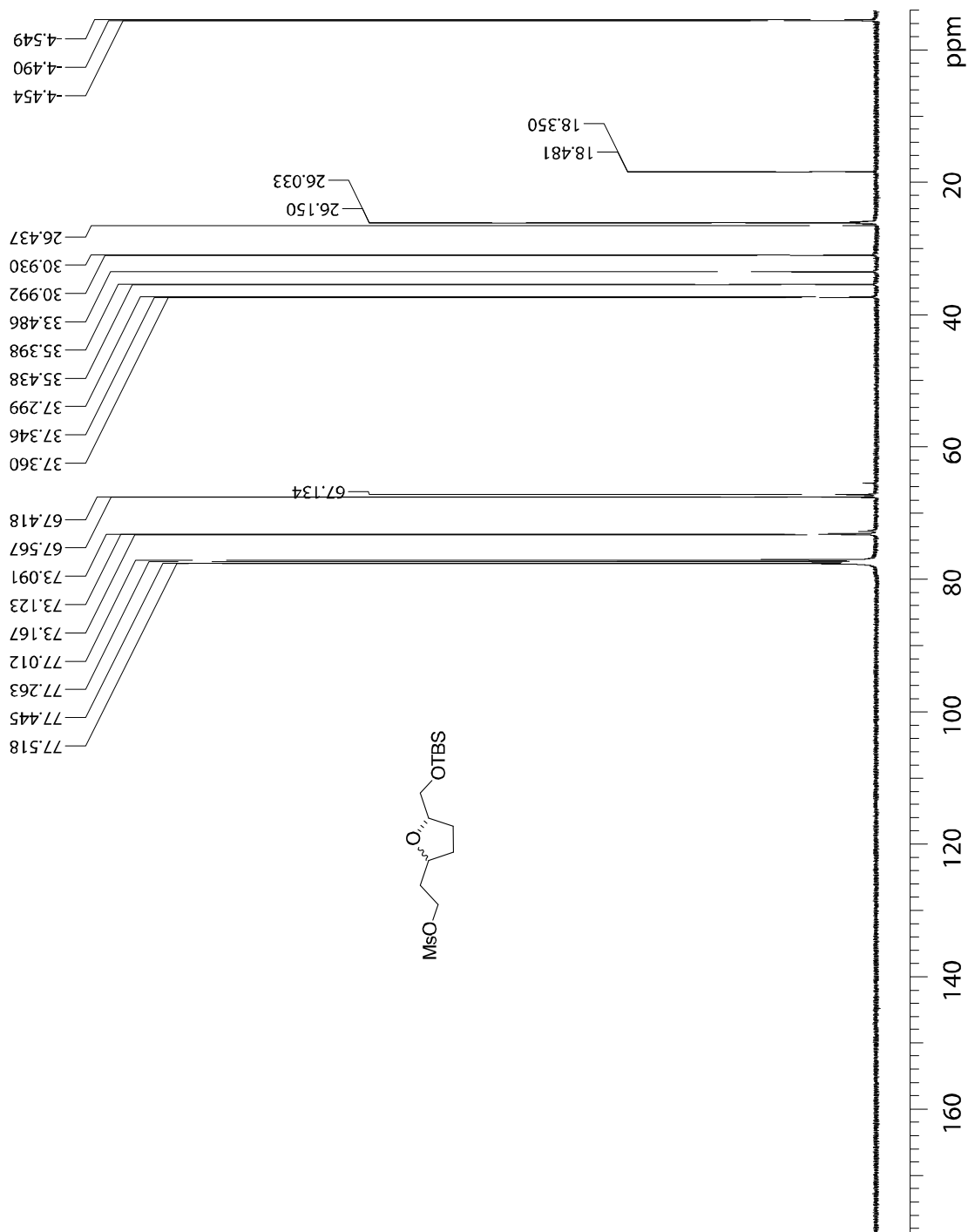


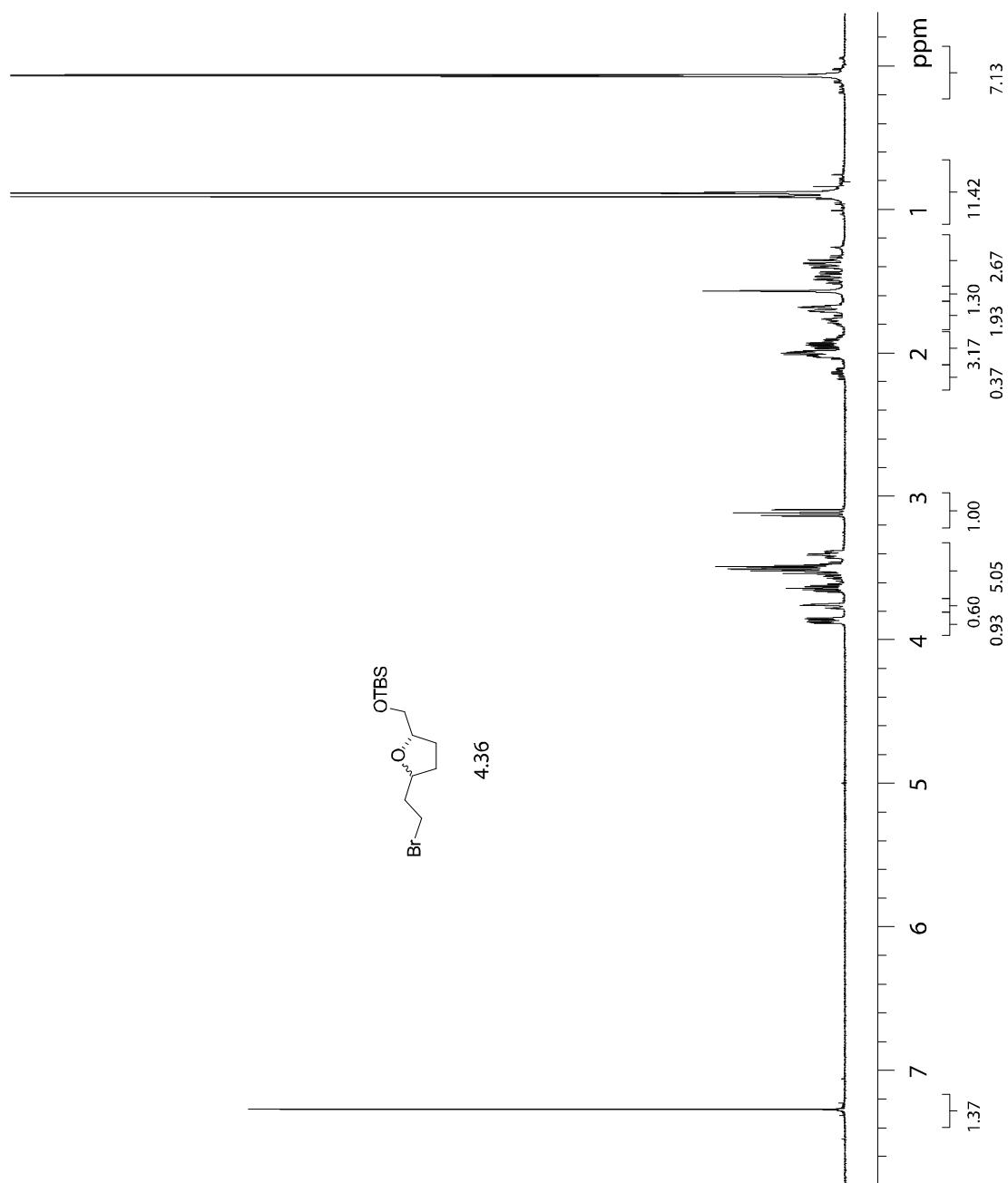


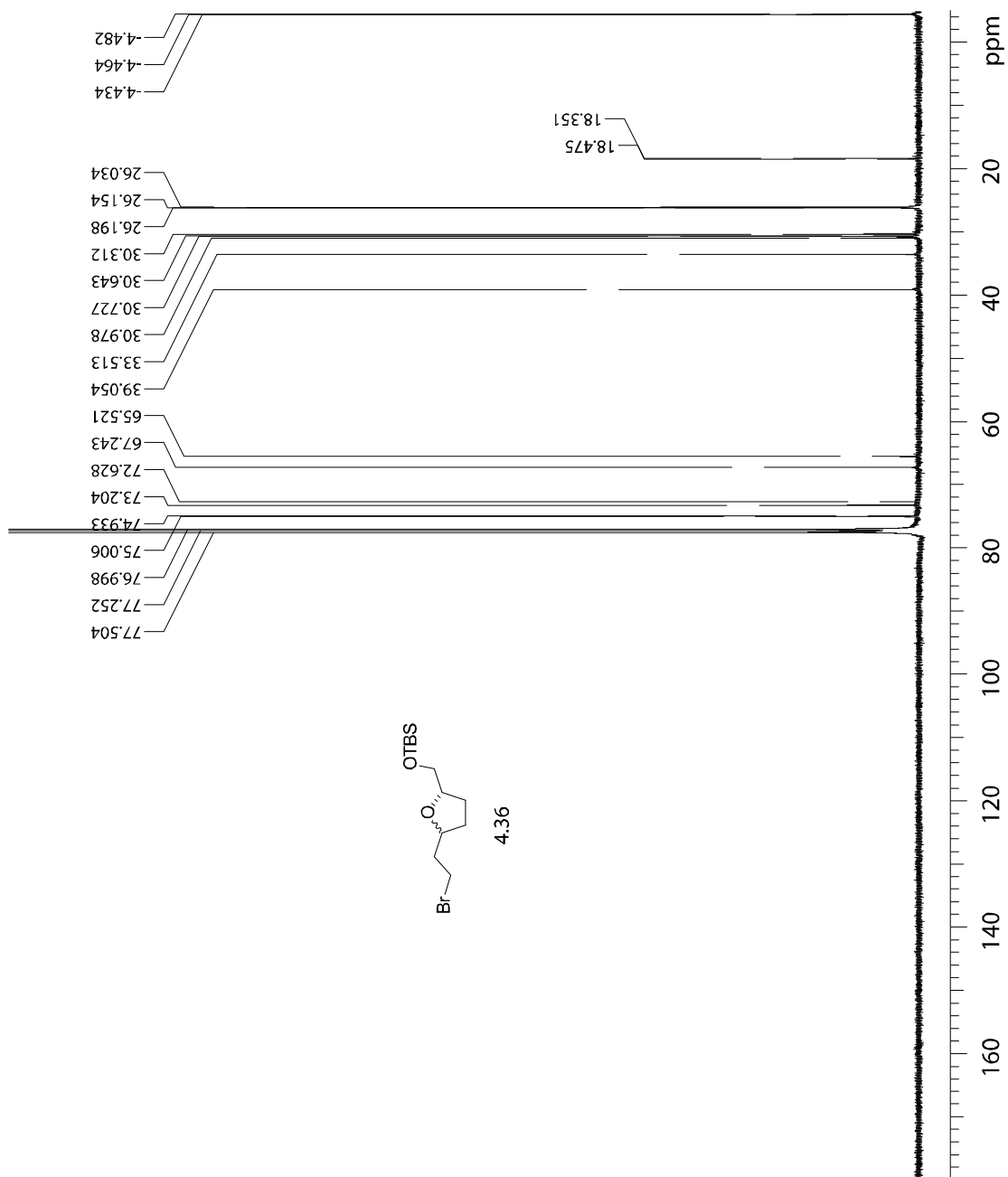












APPENDIX B SINGLE CRYSTAL X-RAY

DATA FOR β -LACTONE 2.64a

Table B.1. Crystal data and structure refinement for 2.64a.

Identification code	dr30a	
Empirical formula	C ₁₈ H ₂₈ O ₃	
Formula weight	292.40	
Temperature	110(2) K	
Wavelength	1.54178 Å	
Crystal system	Monoclinic	
Space group	P2(1)/c	
Unit cell dimensions	a = 15.4756(15) Å	$\alpha = 90^\circ$.
	b = 10.1169(11) Å	$\beta = 94.168(6)^\circ$.
	c = 10.6297(11) Å	$\gamma = 90^\circ$.
Volume	1659.8(3) Å ³	
Z	4	
Density (calculated)	1.170 Mg/m ³	
Absorption coefficient	0.614 mm ⁻¹	
F(000)	640	
Crystal size	0.10 x 0.05 x 0.05 mm ³	
Theta range for data collection	2.86 to 58.94°.	
Index ranges	-17 ≤ h ≤ 17, -11 ≤ k ≤ 11, -11 ≤ l ≤ 10	
Reflections collected	10097	
Independent reflections	2344 [R(int) = 0.0997]	
Completeness to theta = 58.94°	98.2 %	
Absorption correction	Semi-empirical from equivalents	
Max. and min. transmission	0.9699 and 0.9411	
Refinement method	Full-matrix least-squares on F ²	
Data / restraints / parameters	2344 / 0 / 236	
Goodness-of-fit on F ²	1.024	
Final R indices [I > 2σ(I)]	R1 = 0.0575, wR2 = 0.1284	
R indices (all data)	R1 = 0.0861, wR2 = 0.1374	
Largest diff. peak and hole	0.169 and -0.159 e.Å ⁻³	

Table B.2. Atomic coordinates ($\times 10^4$) and equivalent isotropic displacement parameters ($\text{\AA}^2 \times 10^3$) for dr30a. $U(\text{eq})$ is defined as one third of the trace of the orthogonalized U_{ij} tensor.

	x	y	z	U(eq)
O(1)	4039(1)	655(2)	11216(2)	39(1)
O(2)	5426(1)	261(2)	12028(2)	41(1)
O(3)	3147(1)	2597(2)	10871(2)	43(1)
C(1)	6353(1)	2867(2)	10383(2)	29(1)
C(2)	6932(2)	2800(3)	9286(3)	48(1)
C(3)	7876(2)	3023(3)	9689(3)	49(1)
C(4)	8012(2)	4307(3)	10407(3)	41(1)
C(5)	7461(2)	4358(4)	11518(3)	50(1)
C(6)	6507(1)	4145(3)	11102(3)	38(1)
C(7)	5403(2)	2673(3)	9932(2)	34(1)
C(8)	4818(1)	2365(3)	10979(2)	31(1)
C(9)	4893(2)	974(3)	11532(2)	32(1)
C(10)	3894(2)	1932(3)	10623(3)	35(1)
C(11)	3260(2)	2098(3)	9578(3)	37(1)
C(12)	2673(2)	1015(3)	9087(3)	42(1)
C(13)	1778(2)	1455(3)	8601(3)	52(1)
C(14)	1237(6)	2171(10)	9309(10)	48(2)
C(15)	393(4)	2605(8)	8603(10)	62(3)
C(16)	-173(8)	1563(12)	8117(16)	63(3)
C(17)	448(14)	575(17)	7240(20)	74(5)
C(18)	1265(12)	170(17)	7924(18)	63(4)
C(13')	1778(2)	1455(3)	8601(3)	52(1)
C(14')	1243(6)	1586(12)	9887(11)	62(3)
C(15')	311(4)	1989(11)	9578(11)	81(4)
C(16')	-74(9)	947(13)	8477(18)	84(5)
C(17')	366(14)	1154(18)	7380(20)	74(5)
C(18')	1328(11)	663(14)	7754(18)	49(4)

Table B.3. Bond lengths [\AA] and angles [$^\circ$] for **2.64a**.

O(1)-C(9)	1.378(3)
O(1)-C(10)	1.448(3)
O(2)-C(9)	1.190(3)
O(3)-C(10)	1.380(3)
O(3)-C(11)	1.486(3)
C(1)-C(6)	1.513(4)
C(1)-C(2)	1.523(3)
C(1)-C(7)	1.525(3)
C(1)-H(1A)	1.0000
C(2)-C(3)	1.509(4)
C(2)-H(2A)	0.9900
C(2)-H(2B)	0.9900
C(3)-C(4)	1.514(4)
C(3)-H(3C)	0.9900
C(3)-H(3D)	0.9900
C(4)-C(5)	1.507(4)
C(4)-H(4A)	0.9900
C(4)-H(4B)	0.9900
C(5)-C(6)	1.525(3)
C(5)-H(5A)	0.9900
C(5)-H(5B)	0.9900
C(6)-H(6A)	0.9900
C(6)-H(6B)	0.9900
C(7)-C(8)	1.517(3)
C(7)-H(7A)	0.9900
C(7)-H(7B)	0.9900
C(8)-C(10)	1.517(3)
C(8)-C(9)	1.526(4)
C(8)-H(8)	1.0000
C(9)-C(10)	2.012(4)
C(10)-C(11)	1.437(4)

Table B.3. (Continued)

C(11)-C(12)	1.493(4)
C(11)-H(11A)	1.0000
C(12)-C(13)	1.511(4)
C(12)-H(12A)	0.9600
C(12)-H(12B)	0.9599
C(13)-C(14)	1.372(10)
C(13)-C(18)	1.659(16)
C(13)-H(13A)	1.0000
C(14)-C(15)	1.523(11)
C(14)-H(14A)	0.9900
C(14)-H(14B)	0.9900
C(15)-C(16)	1.442(13)
C(15)-H(15A)	0.9900
C(15)-H(15B)	0.9900
C(16)-C(17)	1.71(2)
C(16)-H(16A)	0.9900
C(16)-H(16B)	0.9900
C(17)-C(18)	1.47(3)
C(17)-H(17A)	0.9900
C(17)-H(17B)	0.9900
C(18)-H(18A)	0.9900
C(18)-H(18B)	0.9900
C(14')-C(15')	1.513(13)
C(14')-H(14C)	0.9900
C(14')-H(14D)	0.9900
C(15')-C(16')	1.654(17)
C(15')-H(15C)	0.9900
C(15')-H(15D)	0.9900
C(16')-C(17')	1.41(3)
C(16')-H(16C)	0.9900
C(16')-H(16D)	0.9900

Table B.3. (Continued)

C(17')-C(18')	1.59(3)
C(17')-H(17C)	0.9900
C(17')-H(17D)	0.9900
C(18')-H(18C)	0.9900
C(18')-H(18D)	0.9900
C(9)-O(1)-C(10)	90.73(18)
C(10)-O(3)-C(11)	60.07(16)
C(6)-C(1)-C(2)	110.2(2)
C(6)-C(1)-C(7)	112.4(2)
C(2)-C(1)-C(7)	111.2(2)
C(6)-C(1)-H(1A)	107.6
C(2)-C(1)-H(1A)	107.6
C(7)-C(1)-H(1A)	107.6
C(3)-C(2)-C(1)	112.8(2)
C(3)-C(2)-H(2A)	109.0
C(1)-C(2)-H(2A)	109.0
C(3)-C(2)-H(2B)	109.0
C(1)-C(2)-H(2B)	109.0
H(2A)-C(2)-H(2B)	107.8
C(2)-C(3)-C(4)	111.6(2)
C(2)-C(3)-H(3C)	109.3
C(4)-C(3)-H(3C)	109.3
C(2)-C(3)-H(3D)	109.3
C(4)-C(3)-H(3D)	109.3
H(3C)-C(3)-H(3D)	108.0
C(5)-C(4)-C(3)	111.0(2)
C(5)-C(4)-H(4A)	109.4
C(3)-C(4)-H(4A)	109.4
C(5)-C(4)-H(4B)	109.4
C(3)-C(4)-H(4B)	109.4
H(4A)-C(4)-H(4B)	108.0
C(4)-C(5)-C(6)	111.0(2)
C(4)-C(5)-H(5A)	109.4

Table B.3. (Continued)

C(6)-C(5)-H(5A)	109.4
C(4)-C(5)-H(5B)	109.4
C(6)-C(5)-H(5B)	109.4
H(5A)-C(5)-H(5B)	108.0
C(1)-C(6)-C(5)	112.4(2)
C(1)-C(6)-H(6A)	109.1
C(5)-C(6)-H(6A)	109.1
C(1)-C(6)-H(6B)	109.1
C(5)-C(6)-H(6B)	109.1
H(6A)-C(6)-H(6B)	107.9
C(8)-C(7)-C(1)	114.1(2)
C(8)-C(7)-H(7A)	108.7
C(1)-C(7)-H(7A)	108.7
C(8)-C(7)-H(7B)	108.7
C(1)-C(7)-H(7B)	108.7
H(7A)-C(7)-H(7B)	107.6
C(7)-C(8)-C(10)	118.5(2)
C(7)-C(8)-C(9)	116.0(2)
C(10)-C(8)-C(9)	82.75(18)
C(7)-C(8)-H(8)	112.2
C(10)-C(8)-H(8)	112.2
C(9)-C(8)-H(8)	112.2
O(2)-C(9)-O(1)	126.0(2)
O(2)-C(9)-C(8)	139.5(2)
O(1)-C(9)-C(8)	94.4(2)
O(2)-C(9)-C(10)	171.4(2)
O(1)-C(9)-C(10)	46.03(13)
C(8)-C(9)-C(10)	48.43(14)
O(3)-C(10)-C(11)	63.64(17)

Table B.3. (Continued)

O(3)-C(10)-O(1)	117.2(2)
C(11)-C(10)-O(1)	121.1(2)
O(3)-C(10)-C(8)	126.8(2)
C(11)-C(10)-C(8)	137.5(2)
O(1)-C(10)-C(8)	92.03(18)
O(3)-C(10)-C(9)	140.2(2)
C(11)-C(10)-C(9)	152.3(2)
O(1)-C(10)-C(9)	43.24(12)
C(8)-C(10)-C(9)	48.82(14)
C(10)-C(11)-O(3)	56.29(16)
C(10)-C(11)-C(12)	123.2(3)
O(3)-C(11)-C(12)	117.5(2)
C(10)-C(11)-H(11A)	115.5
O(3)-C(11)-H(11A)	115.5
C(12)-C(11)-H(11A)	115.5
C(11)-C(12)-C(13)	115.0(3)
C(11)-C(12)-H(12A)	107.1
C(13)-C(12)-H(12A)	104.7
C(11)-C(12)-H(12B)	108.3
C(13)-C(12)-H(12B)	113.9
H(12A)-C(12)-H(12B)	107.3
C(14)-C(13)-C(12)	123.3(4)
C(14)-C(13)-C(18)	111.1(8)
C(12)-C(13)-C(18)	108.4(8)
C(14)-C(13)-H(13A)	104.0
C(12)-C(13)-H(13A)	104.0
C(18)-C(13)-H(13A)	104.0
C(13)-C(14)-C(15)	114.6(7)
C(13)-C(14)-H(14A)	108.6
C(15)-C(14)-H(14A)	108.6
C(13)-C(14)-H(14B)	108.6

Table B.3. (Continued)

C(15)-C(14)-H(14B)	108.6
H(14A)-C(14)-H(14B)	107.6
C(16)-C(15)-C(14)	116.3(7)
C(16)-C(15)-H(15A)	108.2
C(14)-C(15)-H(15A)	108.2
C(16)-C(15)-H(15B)	108.2
C(14)-C(15)-H(15B)	108.2
H(15A)-C(15)-H(15B)	107.4
C(15)-C(16)-C(17)	105.8(10)
C(15)-C(16)-H(16A)	110.6
C(17)-C(16)-H(16A)	110.6
C(15)-C(16)-H(16B)	110.6
C(17)-C(16)-H(16B)	110.6
H(16A)-C(16)-H(16B)	108.7
C(18)-C(17)-C(16)	112.8(14)
C(18)-C(17)-H(17A)	109.0
C(16)-C(17)-H(17A)	109.0
C(18)-C(17)-H(17B)	109.0
C(16)-C(17)-H(17B)	109.0
H(17A)-C(17)-H(17B)	107.8
C(17)-C(18)-C(13)	111.3(13)
C(17)-C(18)-H(18A)	109.4
C(13)-C(18)-H(18A)	109.4
C(17)-C(18)-H(18B)	109.4
C(13)-C(18)-H(18B)	109.4
H(18A)-C(18)-H(18B)	108.0
C(15')-C(14')-H(14C)	109.3
C(15')-C(14')-H(14D)	109.3
H(14C)-C(14')-H(14D)	107.9
C(14')-C(15')-C(16')	105.7(8)
C(14')-C(15')-H(15C)	110.6

Table B.3. (Continued)

C(16')-C(15')-H(15C)	110.6
C(14')-C(15')-H(15D)	110.6
C(16')-C(15')-H(15D)	110.6
H(15C)-C(15')-H(15D)	108.7
C(17')-C(16')-C(15')	108.8(11)
C(17')-C(16')-H(16C)	109.9
C(15')-C(16')-H(16C)	109.9
C(17')-C(16')-H(16D)	109.9
C(15')-C(16')-H(16D)	109.9
H(16C)-C(16')-H(16D)	108.3
C(16')-C(17')-C(18')	104.0(17)
C(16')-C(17')-H(17C)	110.9
C(18')-C(17')-H(17C)	110.9
C(16')-C(17')-H(17D)	110.9
C(18')-C(17')-H(17D)	110.9
H(17C)-C(17')-H(17D)	109.0
C(17')-C(18')-H(18C)	108.7
C(17')-C(18')-H(18D)	108.7
H(18C)-C(18')-H(18D)	107.6

Symmetry transformations used to generate equivalent atoms:

Table B.4. Anisotropic displacement parameters ($\text{\AA}^2 \times 10^3$) for **2.64a**. The anisotropic displacement factor exponent takes the form: $-2\pi^2 [h^2 a^{*2} U^{11} + \dots + 2 h k a^* b^* U^{12}]$

	U ¹¹	U ²²	U ³³	U ²³	U ¹³	U ¹²
O(1)	40(1)	40(1)	36(1)	10(1)	-1(1)	-11(1)
O(2)	44(1)	42(1)	37(1)	10(1)	3(1)	-2(1)
O(3)	37(1)	47(1)	47(1)	-15(1)	6(1)	-2(1)
C(1)	33(1)	27(2)	28(2)	6(1)	9(1)	7(1)
C(2)	52(2)	51(2)	44(2)	-9(2)	24(2)	-10(2)
C(3)	47(2)	49(2)	55(2)	8(2)	30(2)	5(2)
C(4)	27(1)	49(2)	46(2)	13(2)	3(1)	0(1)
C(5)	30(1)	76(2)	42(2)	-8(2)	-1(1)	-6(2)
C(6)	30(1)	44(2)	39(2)	-11(1)	4(1)	3(1)
C(7)	40(1)	35(2)	27(2)	0(1)	6(1)	-6(1)
C(8)	33(1)	30(2)	31(2)	-2(1)	2(1)	-2(1)
C(9)	38(2)	36(2)	23(2)	-2(1)	7(1)	-5(1)
C(10)	34(1)	35(2)	36(2)	-1(1)	8(1)	-5(1)
C(11)	32(1)	40(2)	39(2)	7(1)	4(1)	-1(1)
C(12)	39(2)	51(2)	38(2)	-11(2)	6(1)	-4(1)
C(13)	33(2)	60(2)	63(2)	9(2)	-1(2)	-14(2)
C(14)	36(4)	50(6)	57(6)	-25(4)	-3(4)	-14(4)
C(15)	32(3)	93(6)	61(6)	-28(5)	-4(3)	8(4)
C(16)	27(5)	52(8)	107(9)	-44(7)	-8(5)	11(5)
C(17)	42(5)	118(14)	61(6)	-44(11)	1(4)	-4(10)
C(18)	53(6)	79(11)	54(7)	-31(6)	-8(5)	-34(6)
C(13')	33(2)	60(2)	63(2)	9(2)	-1(2)	-14(2)
C(14')	43(4)	82(8)	64(8)	-32(5)	18(5)	-18(5)
C(15')	52(4)	120(8)	73(8)	-60(7)	24(4)	-26(5)
C(16')	19(4)	59(9)	170(15)	-55(9)	-12(6)	12(6)
C(17')	39(8)	94(12)	87(10)	-43(10)	-16(7)	-10(10)
C(18')	34(5)	63(10)	54(6)	-36(7)	17(4)	-11(6)

Table B.5. Hydrogen coordinates ($\times 10^4$) and isotropic displacement parameters ($\text{\AA}^2 \times 10^3$) for **2.64a**.

	x	y	z	U(eq)
H(1A)	6522	2124	10971	35
H(2A)	6866	1922	8879	57
H(2B)	6740	3476	8653	57
H(3C)	8214	3042	8933	59
H(3D)	8093	2279	10229	59
H(4A)	8630	4391	10708	49
H(4B)	7862	5059	9837	49
H(5A)	7534	5227	11940	60
H(5B)	7655	3666	12135	60
H(6A)	6166	4137	11855	45
H(6B)	6299	4893	10561	45
H(7A)	5190	3486	9493	40
H(7B)	5360	1942	9312	40
H(8)	4849	3061	11649	37
H(11A)	3400	2784	8947	44
H(12A)	2578	445	9786	51
H(12B)	2971	506	8491	51
H(13A)	1885	2054	7880	63
H(14A)	1551	2967	9636	57
H(14B)	1097	1631	10044	57
H(15A)	70	3158	9177	75
H(15B)	537	3171	7887	75
H(16A)	-667	1934	7587	75
H(16B)	-401	1055	8816	75
H(17A)	112	-224	6976	89
H(17B)	581	1056	6463	89
H(18A)	1644	-257	7331	75
H(18B)	1141	-485	8579	75

Table B.5. (Continued)

H(13B)	1824	2354	8220	63
H(14C)	1258	726	10333	75
H(14D)	1532	2250	10458	75
H(15C)	278	2910	9261	97
H(15D)	-23	1925	10336	97
H(16C)	13	26	8774	100
H(16D)	-703	1095	8293	100
H(17C)	360	2101	7139	89
H(17D)	99	633	6661	89
H(18C)	1302	-238	8113	59
H(18D)	1647	606	6982	59

APPENDIX C SINGLE CRYSTAL X-RAY

STRUCTURE OF TETRONATE 3.20

Table C.1. Crystal data and structure refinement for 3.20.

Identification code	dr35a	
Empirical formula	C ₁₈ H ₂₈ O ₃	
Formula weight	292.40	
Temperature	110(2) K	
Wavelength	1.54178 Å	
Crystal system	Monoclinic	
Space group	P2(1)/c	
Unit cell dimensions	a = 14.447(3) Å	α = 90°.
	b = 9.549(2) Å	β = 95.406(13)°.
	c = 12.138(3) Å	γ = 90°.
Volume	1667.1(7) Å ³	
Z	4	
Density (calculated)	1.165 Mg/m ³	
Absorption coefficient	0.611 mm ⁻¹	
F(000)	640	
Crystal size	0.10 x 0.01 x 0.01 mm ³	
Theta range for data collection	5.91 to 59.99°.	
Index ranges	-16 ≤ h ≤ 16, -10 ≤ k ≤ 9, -13 ≤ l ≤ 13	
Reflections collected	10030	
Independent reflections	2161 [R(int) = 0.0815]	
Completeness to theta = 59.99°	87.2 %	
Absorption correction	Semi-empirical from equivalents	
Max. and min. transmission	0.9939 and 0.9414	
Refinement method	Full-matrix least-squares on F ²	
Data / restraints / parameters	2161 / 0 / 192	
Goodness-of-fit on F ²	1.034	
Final R indices [I > 2σ(I)]	R1 = 0.0822, wR2 = 0.1805	
R indices (all data)	R1 = 0.1106, wR2 = 0.1973	
Extinction coefficient	0.0023(6)	
Largest diff. peak and hole	0.409 and -0.255 e.Å ⁻³	

Table C.2. Atomic coordinates ($\times 10^4$) and equivalent isotropic displacement parameters ($\text{\AA}^2 \times 10^3$) for **3.20**. $U(\text{eq})$ is defined as one third of the trace of the orthogonalized U^{ij} tensor.

	x	y	z	U(eq)
O(1)	6234(2)	1222(3)	9141(2)	21(1)
O(2)	5675(2)	1033(3)	10812(2)	21(1)
O(3)	4885(2)	3987(3)	7717(2)	25(1)
C(1)	5634(3)	1628(5)	9894(3)	20(1)
C(2)	5019(3)	2757(5)	9453(3)	16(1)
C(3)	5268(3)	3024(5)	8420(3)	17(1)
C(4)	6099(3)	2131(5)	8170(3)	17(1)
C(5)	4291(3)	3426(5)	10087(4)	21(1)
C(6)	3465(3)	2436(5)	10289(3)	18(1)
C(7)	2902(3)	1995(5)	9208(4)	24(1)
C(8)	2071(3)	1039(5)	9407(4)	26(1)
C(9)	1453(3)	1696(6)	10224(4)	27(1)
C(10)	2009(3)	2145(6)	11302(4)	26(1)
C(11)	2823(3)	3128(5)	11071(4)	22(1)
C(12)	6993(3)	2977(5)	8073(4)	20(1)
C(13)	7843(3)	2079(5)	7813(4)	21(1)
C(14)	8748(3)	2953(6)	8019(4)	27(1)
C(15)	9611(3)	2109(6)	7740(4)	33(1)
C(16)	9500(3)	1564(6)	6544(4)	32(1)
C(17)	8609(3)	683(5)	6353(4)	26(1)
C(18)	7744(3)	1524(5)	6618(4)	25(1)

Table C.3. Bond lengths [\AA] and angles [$^\circ$] for **3.20**.

O(1)-C(1)	1.373(5)
O(1)-C(4)	1.462(5)
O(2)-C(1)	1.247(5)
O(3)-C(3)	1.339(5)
C(1)-C(2)	1.466(6)
C(2)-C(3)	1.361(6)
C(2)-C(5)	1.503(6)
C(3)-C(4)	1.525(6)
C(4)-C(12)	1.538(6)
C(5)-C(6)	1.559(6)
C(6)-C(7)	1.536(6)
C(6)-C(11)	1.538(6)
C(7)-C(8)	1.545(7)
C(8)-C(9)	1.530(6)
C(9)-C(10)	1.531(7)
C(10)-C(11)	1.550(6)
C(12)-C(13)	1.554(6)
C(13)-C(18)	1.538(6)
C(13)-C(14)	1.551(6)
C(14)-C(15)	1.548(7)
C(15)-C(16)	1.536(7)
C(16)-C(17)	1.537(6)
C(17)-C(18)	1.545(6)
C(1)-O(1)-C(4)	108.9(3)
O(2)-C(1)-O(1)	119.1(4)
O(2)-C(1)-C(2)	129.6(4)
O(1)-C(1)-C(2)	111.4(4)
C(3)-C(2)-C(1)	105.6(4)
C(3)-C(2)-C(5)	130.6(4)
C(1)-C(2)-C(5)	123.8(4)
O(3)-C(3)-C(2)	126.0(4)

Table C.3. (Continued)

O(3)-C(3)-C(4)	122.8(4)
C(2)-C(3)-C(4)	111.1(4)
O(1)-C(4)-C(3)	102.6(3)
O(1)-C(4)-C(12)	108.9(3)
C(3)-C(4)-C(12)	113.8(4)
C(2)-C(5)-C(6)	113.9(4)
C(7)-C(6)-C(11)	110.1(3)
C(7)-C(6)-C(5)	112.6(4)
C(11)-C(6)-C(5)	110.6(4)
C(6)-C(7)-C(8)	112.7(4)
C(9)-C(8)-C(7)	111.6(4)
C(8)-C(9)-C(10)	112.2(4)
C(9)-C(10)-C(11)	111.1(4)
C(6)-C(11)-C(10)	111.4(4)
C(4)-C(12)-C(13)	114.3(4)
C(18)-C(13)-C(14)	109.8(4)
C(18)-C(13)-C(12)	112.1(4)
C(14)-C(13)-C(12)	109.9(4)
C(15)-C(14)-C(13)	111.6(4)
C(16)-C(15)-C(14)	111.6(4)
C(15)-C(16)-C(17)	109.8(4)
C(16)-C(17)-C(18)	111.5(4)
C(13)-C(18)-C(17)	111.7(4)

Symmetry transformations used to generate equivalent atoms:

Table C.4. Anisotropic displacement parameters ($\text{\AA}^2 \times 10^3$) for dr35a. The anisotropic displacement factor exponent takes the form: $-2\pi^2 [h^2 a^{*2} U^{11} + \dots + 2 h k a^* b^* U^{12}]$

	U ¹¹	U ²²	U ³³	U ²³	U ¹³	U ¹²
O(1)	24(2)	21(2)	20(2)	2(1)	11(1)	5(1)
O(2)	25(2)	20(2)	20(2)	6(1)	7(1)	1(1)
O(3)	28(2)	29(2)	18(2)	3(1)	4(1)	8(2)
C(1)	21(2)	23(3)	15(2)	-5(2)	5(2)	0(2)
C(2)	17(2)	16(2)	17(2)	2(2)	4(2)	1(2)
C(3)	18(2)	18(2)	15(2)	3(2)	1(2)	0(2)
C(4)	15(2)	20(3)	15(2)	5(2)	4(2)	-3(2)
C(5)	24(2)	24(3)	16(2)	1(2)	4(2)	4(2)
C(6)	18(2)	19(3)	18(2)	1(2)	6(2)	0(2)
C(7)	22(2)	27(3)	22(3)	-4(2)	1(2)	7(2)
C(8)	24(2)	30(3)	23(2)	-2(2)	-1(2)	1(2)
C(9)	19(2)	31(3)	33(3)	1(2)	3(2)	-2(2)
C(10)	16(2)	35(3)	29(3)	0(2)	13(2)	-3(2)
C(11)	21(2)	26(3)	19(2)	-2(2)	7(2)	0(2)
C(12)	16(2)	24(3)	20(2)	5(2)	8(2)	-1(2)
C(13)	20(2)	18(3)	24(2)	4(2)	2(2)	3(2)
C(14)	19(2)	35(3)	26(3)	-5(2)	2(2)	-5(2)
C(15)	15(2)	51(4)	34(3)	-4(2)	6(2)	-3(2)
C(16)	22(2)	34(3)	41(3)	-4(2)	12(2)	0(2)
C(17)	22(2)	25(3)	33(3)	-6(2)	11(2)	-4(2)
C(18)	17(2)	32(3)	24(2)	-4(2)	4(2)	0(2)

Table C.5. Hydrogen coordinates ($\times 10^4$) and isotropic displacement parameters ($\text{\AA}^2 \times 10^3$) for **3.20**.

	x	y	z	U(eq)
H(3)	5105	3904	7103	37
H(4)	5942	1561	7486	20
H(5A)	4043	4261	9676	25
H(5B)	4587	3748	10812	25
H(6)	3730	1570	10658	22
H(7A)	3316	1495	8735	28
H(7B)	2667	2844	8805	28
H(8A)	1697	865	8695	31
H(8B)	2307	126	9701	31
H(9A)	972	1011	10395	33
H(9B)	1133	2523	9876	33
H(10A)	2258	1305	11705	31
H(10B)	1592	2636	11778	31
H(11A)	2569	4009	10735	26
H(11B)	3187	3365	11778	26
H(12A)	7153	3483	8777	24
H(12B)	6871	3686	7482	24
H(13)	7890	1258	8327	25
H(14A)	8692	3809	7557	32
H(14B)	8831	3245	8804	32
H(15A)	10169	2713	7845	39
H(15B)	9705	1306	8255	39
H(16A)	10045	986	6404	38
H(16B)	9467	2364	6023	38
H(17A)	8670	-161	6828	31
H(17B)	8528	371	5572	31
H(18A)	7652	2323	6099	29
H(18B)	7187	917	6509	29

APPENDIX D SINGLE CRYSTAL X-RAY

STRUCTURE OF TRIFLATE 3.55

Absolute Configuration :

The absolute configuration (stereochemistry) at position C4 is *S*.

The absolute configuration was determined from the anomalous x-ray scattering from the heavy atom (Sulfur).

The FLACK parameter was $-0.003 \pm .009$ where a value of zero represents the correct structure and a value of one represents the inverted structure. The parameter was determined from the refinement of 7000 Bijvoet pairs (TWIN/BASF, SHELX97). [See Flack, Bernardinelli *J. Applied Crystallography* (2000). **33**, 1143-1148.]

A second crystal was examined and the FLACK parameter of $0.01 \pm .001$ was determined for the structure.

Table D.1. Crystal data and structure refinement for **3.55**.

Identification code	dr37	
Empirical formula	C ₁₉ H ₁₅ F ₃ O ₅ S	
Formula weight	412.37	
Temperature	100(2) K	
Wavelength	1.54178 Å	
Crystal system	Orthorhombic	
Space group	P2(1)2(1)2(1)	
Unit cell dimensions	a = 7.0114(8) Å	α = 90°.
	b = 7.4934(7) Å	β = 90°.
	c = 34.767(3) Å	γ = 90°.
Volume	1826.6(3) Å ³	
Z	4	
Density (calculated)	1.500 Mg/m ³	
Absorption coefficient	2.125 mm ⁻¹	
F(000)	848	
Crystal size	0.20 x 0.04 x 0.01 mm ³	
Theta range for data collection	2.54 to 58.93°.	
Index ranges	-7 ≤ h ≤ 7, -8 ≤ k ≤ 8, -38 ≤ l ≤ 38	
Reflections collected	20057	
Independent reflections	20057 [R(int) = 0.0000]	
Completeness to theta = 58.93°	99.9 %	
Absorption correction	Semi-empirical from equivalents	
Max. and min. transmission	0.9791 and 0.6760	
Refinement method	Full-matrix least-squares on F ²	
Data / restraints / parameters	20057 / 0 / 313	
Goodness-of-fit on F ²	1.068	
Final R indices [I > 2σ(I)]	R1 = 0.0313, wR2 = 0.0802	
R indices (all data)	R1 = 0.0356, wR2 = 0.0847	
Absolute structure parameter	-0.003(9)	
Largest diff. peak and hole	0.176 and -0.271 e.Å ⁻³	

Table D.2. Atomic coordinates ($\times 10^4$) and equivalent isotropic displacement parameters ($\text{\AA}^2 \times 10^3$) for **3.55**. $U(\text{eq})$ is defined as one third of the trace of the orthogonalized U^{ij} tensor.

	x	y	z	U(eq)
S(1)	3586(1)	5481(1)	9664(1)	21(1)
F(1)	2776(1)	3602(1)	10260(1)	27(1)
F(2)	2006(1)	2358(1)	9723(1)	26(1)
F(3)	303(1)	4507(1)	9947(1)	31(1)
O(1)	-1456(1)	8657(1)	9103(1)	18(1)
O(2)	-113(1)	11306(1)	8966(1)	24(1)
O(3)	2486(1)	5628(1)	9268(1)	19(1)
O(4)	3491(2)	7109(1)	9868(1)	30(1)
O(5)	5310(1)	4572(1)	9586(1)	34(1)
C(1)	80(2)	9754(2)	9038(1)	16(1)
C(2)	1865(2)	8721(2)	9087(1)	16(1)
C(3)	1310(2)	7118(2)	9193(1)	16(1)
C(4)	-812(2)	6877(2)	9202(1)	16(1)
C(5)	3791(2)	9501(2)	9022(1)	21(1)
C(6)	4147(2)	10116(2)	8610(1)	17(1)
C(7)	3203(2)	9344(2)	8301(1)	19(1)
C(8)	3616(2)	9862(2)	7927(1)	22(1)
C(9)	4986(2)	11142(2)	7858(1)	26(1)
C(10)	5940(2)	11924(2)	8164(1)	28(1)
C(11)	5508(2)	11413(2)	8538(1)	24(1)
C(13)	2061(2)	3871(2)	9912(1)	20(1)
C(14)	-1592(2)	5498(2)	8921(1)	18(1)
C(15)	-918(2)	5726(2)	8516(1)	16(1)
C(16)	-1835(2)	6909(2)	8270(1)	20(1)
C(17)	-1232(2)	7119(2)	7893(1)	25(1)
C(18)	292(2)	6134(2)	7756(1)	24(1)
C(19)	1227(2)	4968(2)	7998(1)	24(1)
C(20)	623(2)	4756(2)	8375(1)	19(1)

Table D.3. Bond lengths [\AA] and angles [$^\circ$] for **3.55**.

S(1)-O(4)	1.4120(8)
S(1)-O(5)	1.4138(9)
S(1)-O(3)	1.5823(8)
S(1)-C(13)	1.8282(13)
F(1)-C(13)	1.3225(13)
F(2)-C(13)	1.3115(12)
F(3)-C(13)	1.3272(15)
O(1)-C(1)	1.3734(15)
O(1)-C(4)	1.4497(14)
O(2)-C(1)	1.1974(13)
O(3)-C(3)	1.4123(13)
C(1)-C(2)	1.4813(17)
C(2)-C(3)	1.3154(16)
C(2)-C(5)	1.4891(18)
C(3)-C(4)	1.4990(18)
C(4)-C(14)	1.5240(17)
C(5)-C(6)	1.5230(16)
C(6)-C(11)	1.3849(18)
C(6)-C(7)	1.3887(16)
C(7)-C(8)	1.3872(16)
C(8)-C(9)	1.3786(18)
C(9)-C(10)	1.3866(19)
C(10)-C(11)	1.3885(18)
C(14)-C(15)	1.4966(15)
C(15)-C(16)	1.3897(17)
C(15)-C(20)	1.3915(17)
C(16)-C(17)	1.3846(18)
C(17)-C(18)	1.3832(19)
C(18)-C(19)	1.3791(18)
C(19)-C(20)	1.3836(16)
O(4)-S(1)-O(5)	123.53(6)
O(4)-S(1)-O(3)	110.70(5)

Table D.3 (Continued)

O(5)-S(1)-O(3)	106.49(5)
O(4)-S(1)-C(13)	107.80(6)
O(5)-S(1)-C(13)	105.81(6)
O(3)-S(1)-C(13)	99.89(5)
C(1)-O(1)-C(4)	110.22(10)
C(3)-O(3)-S(1)	119.96(7)
O(2)-C(1)-O(1)	121.80(12)
O(2)-C(1)-C(2)	128.84(12)
O(1)-C(1)-C(2)	109.32(9)
C(3)-C(2)-C(1)	105.03(11)
C(3)-C(2)-C(5)	132.03(12)
C(1)-C(2)-C(5)	122.94(10)
C(2)-C(3)-O(3)	126.93(12)
C(2)-C(3)-C(4)	114.18(11)
O(3)-C(3)-C(4)	118.71(10)
O(1)-C(4)-C(3)	101.13(10)
O(1)-C(4)-C(14)	111.01(10)
C(3)-C(4)-C(14)	115.14(11)
C(2)-C(5)-C(6)	114.27(11)
C(11)-C(6)-C(7)	118.70(11)
C(11)-C(6)-C(5)	119.67(11)
C(7)-C(6)-C(5)	121.55(12)
C(8)-C(7)-C(6)	120.64(13)
C(9)-C(8)-C(7)	120.18(12)
C(8)-C(9)-C(10)	119.80(12)
C(9)-C(10)-C(11)	119.76(14)
C(6)-C(11)-C(10)	120.91(12)
F(2)-C(13)-F(1)	109.73(9)
F(2)-C(13)-F(3)	109.12(10)
F(1)-C(13)-F(3)	108.96(10)
F(2)-C(13)-S(1)	110.53(8)
F(1)-C(13)-S(1)	108.06(9)
F(3)-C(13)-S(1)	110.41(8)

Table D.3 (Continued)

C(15)-C(14)-C(4)	114.43(11)
C(16)-C(15)-C(20)	118.37(11)
C(16)-C(15)-C(14)	120.43(12)
C(20)-C(15)-C(14)	121.19(11)
C(17)-C(16)-C(15)	120.88(13)
C(18)-C(17)-C(16)	120.02(13)
C(19)-C(18)-C(17)	119.70(12)
C(18)-C(19)-C(20)	120.26(13)
C(19)-C(20)-C(15)	120.75(12)

Symmetry transformations used to generate equivalent atoms:

Table D.4. Anisotropic displacement parameters ($\text{\AA}^2 \times 10^3$) for **3.55**. The anisotropic displacement factor exponent takes the form: $-2\pi^2 [h^2 a^{*2} U^{11} + \dots + 2 h k a^* b^* U^{12}]$

	U ¹¹	U ²²	U ³³	U ²³	U ¹³	U ¹²
S(1)	17(1)	26(1)	19(1)	8(1)	-2(1)	-2(1)
F(1)	37(1)	32(1)	14(1)	7(1)	-3(1)	-7(1)
F(2)	33(1)	20(1)	25(1)	-2(1)	-1(1)	-1(1)
F(3)	24(1)	30(1)	40(1)	9(1)	13(1)	6(1)
O(1)	14(1)	17(1)	22(1)	0(1)	1(1)	1(1)
O(2)	25(1)	18(1)	28(1)	2(1)	-2(1)	3(1)
O(3)	20(1)	23(1)	13(1)	1(1)	-3(1)	8(1)
O(4)	43(1)	24(1)	22(1)	3(1)	-12(1)	-11(1)
O(5)	14(1)	50(1)	38(1)	22(1)	5(1)	12(1)
C(1)	17(1)	18(1)	12(1)	-1(1)	-1(1)	-1(1)
C(2)	16(1)	20(1)	11(1)	-2(1)	-2(1)	1(1)
C(3)	15(1)	19(1)	13(1)	-2(1)	-2(1)	6(1)
C(4)	16(1)	16(1)	16(1)	3(1)	3(1)	3(1)
C(5)	16(1)	25(1)	21(1)	-2(1)	-2(1)	0(1)
C(6)	12(1)	18(1)	23(1)	-1(1)	0(1)	3(1)
C(7)	14(1)	19(1)	24(1)	-1(1)	0(1)	-3(1)
C(8)	18(1)	25(1)	23(1)	-2(1)	-3(1)	0(1)
C(9)	23(1)	29(1)	25(1)	6(1)	2(1)	0(1)
C(10)	20(1)	27(1)	38(1)	5(1)	2(1)	-6(1)
C(11)	21(1)	24(1)	27(1)	-3(1)	-5(1)	-3(1)
C(13)	23(1)	21(1)	16(1)	-2(1)	0(1)	3(1)
C(14)	18(1)	15(1)	22(1)	1(1)	3(1)	-3(1)
C(15)	15(1)	15(1)	17(1)	-2(1)	-1(1)	-5(1)
C(16)	16(1)	21(1)	22(1)	-3(1)	-2(1)	2(1)
C(17)	28(1)	25(1)	21(1)	2(1)	-5(1)	-2(1)
C(18)	28(1)	31(1)	13(1)	-3(1)	2(1)	-6(1)
C(19)	20(1)	27(1)	25(1)	-9(1)	5(1)	2(1)
C(20)	22(1)	17(1)	19(1)	-2(1)	-5(1)	5(1)

Table D.5. Hydrogen coordinates ($\times 10^4$) and isotropic displacement parameters ($\text{\AA}^2 \times 10^3$) for **3.55**.

	x	y	z	U(eq)
H(4)	-1306(17)	6650(12)	9455(3)	10(3)
H(5A)	3917(18)	10476(16)	9204(3)	34(4)
H(5B)	4790(20)	8661(17)	9100(3)	33(4)
H(7)	2261(18)	8488(15)	8339(3)	22(4)
H(8)	2946(16)	9333(13)	7724(3)	13(3)
H(9)	5210(20)	11484(17)	7603(3)	39(4)
H(10)	6820(20)	12801(18)	8131(4)	42(4)
H(11)	6105(19)	11943(15)	8745(3)	25(4)
H(14A)	-1294(18)	4359(15)	9010(3)	25(3)
H(14B)	-2990(18)	5539(15)	8932(3)	22(4)
H(16)	-2860(20)	7581(15)	8357(3)	28(4)
H(17)	-1894(19)	7977(15)	7721(4)	31(4)
H(18)	730(18)	6258(15)	7495(3)	22(3)
H(19)	2190(20)	4315(16)	7905(3)	35(4)
H(20)	1169(17)	3962(14)	8523(3)	12(3)

Table D.6. Crystal data and structure refinement for **3.55** (xtal 1) and **3.55_2** (xtal2)

Identification code	dr37	dr37_2nd xtal
Empirical formula	C ₁₉ H ₁₅ F ₃ O ₅ S	
Formula weight	412.37	
Temperature	100(2) K	
Wavelength	1.54178 Å	
Crystal system	Orthorhombic	
Space group	P2(1)2(1)2(1)	
Unit cell dimensions	a = 7.0114(8) Å b = 7.4934(7) Å c = 34.767(3) Å	a = 7.0153(5) Å b = 7.4932(6) Å c = 34.774(3) Å
Volume	1828.0(2) Å ³	1826.6(3) Å ³
Z	4	
Density (calculated)	1.500 Mg/m ³	1.498 Mg/m ³
Absorption coefficient	2.125 mm ⁻¹	2.123 mm ⁻¹
F(000)	848	
Crystal size	0.20 x 0.04 x 0.01 mm ³	0.04 x 0.04 x 0.01 mm ³
Theta range for data collection	2.54 to 58.93°.	2.54 to 58.93°.
Index ranges	-7<= <i>h</i> <=7, -8<= <i>k</i> <=8, -38<= <i>l</i> <=38 -7<= <i>h</i> <=7, -8<= <i>k</i> <=8, -38<= <i>l</i> <=38	
Reflections collected	20057	19215
Independent reflections	20057 [R(int) = 0.0000]	19215 [R(int) = 0.0000]
Completeness to theta = 58.93°	99.9 %	99.6 %
Absorption correction	Semi-empirical from equivalents	
Max. and min. transmission	0.9791 and 0.6760	0.9791 and 0.9199
Refinement method	Full-matrix least-squares on F ²	
Data / restraints / parameters	20057 / 0 / 313	19215 / 0 / 314
Goodness-of-fit on F ²	1.068	1.037
Final R indices [I>2sigma(I)]	R1 = 0.0313, wR2 = 0.0802	R1 = 0.0414, wR2 = 0.1027
R indices (all data)	R1 = 0.0356, wR2 = 0.0847	R1 = 0.0537, wR2 = 0.1141
Absolute structure parameter	-0.003(9)	0.01(1)
Largest diff. peak and hole	0.176 and -0.271 e.Å ⁻³	0.251 and -0.374 e.Å ⁻³

APPENDIX E SINGLE CRYSTAL X-RAY

STRUCTURE OF DIOL 4.23.

Table E.1. Crystal data and structure refinement for 4.23.

Identification code	dr60a	
Empirical formula	C ₇ H ₁₁ Cl ₃ O ₂	
Formula weight	233.51	
Temperature	110(2) K	
Wavelength	0.71073 Å	
Crystal system	Tetragonal	
Space group	I-4	
Unit cell dimensions	a = 18.6042(4) Å	α = 90°.
	b = 18.6042(4) Å	β = 90°.
	c = 11.8256(3) Å	γ = 90°.
Volume	4093.03(16) Å ³	
Z	16	
Density (calculated)	1.516 Mg/m ³	
Absorption coefficient	0.855 mm ⁻¹	
F(000)	1920	
Crystal size	0.25 x 0.25 x 0.18 mm ³	
Theta range for data collection	2.99 to 28.31°.	
Index ranges	-24 ≤ h ≤ 24, -24 ≤ k ≤ 24, -15 ≤ l ≤ 15	
Reflections collected	29227	
Independent reflections	4181 [R(int) = 0.0353]	
Completeness to theta = 28.31°	84.0 %	
Absorption correction	Semi-empirical from equivalents	
Max. and min. transmission	0.8614 and 0.8147	
Refinement method	Full-matrix least-squares on F ²	
Data / restraints / parameters	4181 / 0 / 217	
Goodness-of-fit on F ²	1.028	
Final R indices [I > 2σ(I)]	R1 = 0.0467, wR2 = 0.1114	
R indices (all data)	R1 = 0.0508, wR2 = 0.1149	
Absolute structure parameter	-0.05(7)	
Largest diff. peak and hole	0.934 and -0.300 e.Å ⁻³	

Table E.2. Atomic coordinates ($\times 10^4$) and equivalent isotropic displacement parameters ($\text{\AA}^2 \times 10^3$) for **4.23**. $U(\text{eq})$ is defined as one third of the trace of the orthogonalized U^{ij} tensor.

	x	y	z	$U(\text{eq})$
Cl(1A)	8874(1)	999(1)	344(1)	35(1)
Cl(2A)	8098(1)	1682(1)	2181(1)	32(1)
Cl(3A)	7983(1)	148(1)	1820(1)	31(1)
O(1A)	11557(1)	578(1)	4528(2)	28(1)
O(2A)	8982(1)	686(1)	3679(2)	28(1)
C(1A)	11690(2)	1226(2)	3913(3)	29(1)
C(2A)	11069(2)	1478(2)	3200(3)	25(1)
C(3A)	10433(2)	1148(2)	3209(3)	26(1)
C(4A)	9786(2)	1365(2)	2530(3)	25(1)
C(5A)	9219(2)	760(2)	2553(3)	24(1)
C(6A)	8570(2)	906(2)	1766(3)	25(1)
C(7A)	11237(2)	2140(2)	2506(3)	32(1)
Cl(1B)	9355(1)	7129(1)	5462(1)	37(1)
Cl(2B)	7909(1)	6581(1)	5341(1)	46(1)
Cl(3B)	8882(1)	6065(1)	7073(1)	47(1)
O(1B)	9716(1)	3386(1)	2997(2)	26(1)
O(2B)	9079(1)	5985(1)	3718(2)	28(1)
C(1B)	9116(2)	3177(2)	3676(3)	27(1)
C(2B)	8771(2)	3772(2)	4349(3)	24(1)
C(3B)	8978(2)	4457(2)	4275(3)	25(1)
C(4B)	8628(2)	5064(2)	4927(3)	27(1)
C(5B)	9085(2)	5748(2)	4850(3)	24(1)
C(6B)	8813(2)	6354(2)	5631(3)	28(1)
C(7B)	8169(2)	3523(2)	5096(3)	29(1)

Table E.3. Bond lengths [\AA] and angles [$^\circ$] for **4.23**.

Cl(1A)-C(6A)	1.783(3)
Cl(2A)-C(6A)	1.759(3)
Cl(3A)-C(6A)	1.784(3)
O(1A)-C(1A)	1.430(4)
O(1A)-H(1AA)	0.8499
O(2A)-C(5A)	1.409(4)
O(2A)-H(2AA)	0.8500
C(1A)-C(2A)	1.505(4)
C(1A)-H(1AB)	0.9900
C(1A)-H(1AC)	0.9900
C(2A)-C(3A)	1.333(4)
C(2A)-C(7A)	1.512(4)
C(3A)-C(4A)	1.502(4)
C(3A)-H(3AA)	0.9500
C(4A)-C(5A)	1.542(4)
C(4A)-H(4AA)	0.9900
C(4A)-H(4AB)	0.9900
C(5A)-C(6A)	1.548(4)
C(5A)-H(5AA)	1.0000
C(7A)-H(7AA)	0.9800
C(7A)-H(7AB)	0.9800
C(7A)-H(7AC)	0.9800
Cl(1B)-C(6B)	1.771(3)
Cl(2B)-C(6B)	1.767(4)
Cl(3B)-C(6B)	1.792(4)
O(1B)-C(1B)	1.430(4)
O(1B)-H(1B)	0.8500
O(2B)-C(5B)	1.409(4)
O(2B)-H(2BA)	0.8499
C(1B)-C(2B)	1.506(4)
C(1B)-H(1BB)	0.9900
C(1B)-H(1BC)	0.9900

Table E.3 (Continued)

C(2B)-C(3B)	1.334(4)
C(2B)-C(7B)	1.499(4)
C(3B)-C(4B)	1.514(4)
C(3B)-H(3BA)	0.9500
C(4B)-C(5B)	1.533(4)
C(4B)-H(4BA)	0.9900
C(4B)-H(4BB)	0.9900
C(5B)-C(6B)	1.544(4)
C(5B)-H(5BA)	1.0000
C(7B)-H(7BA)	0.9800
C(7B)-H(7BB)	0.9800
C(7B)-H(7BC)	0.9800
C(1A)-O(1A)-H(1AA)	110.5
C(5A)-O(2A)-H(2AA)	102.7
O(1A)-C(1A)-C(2A)	114.5(3)
O(1A)-C(1A)-H(1AB)	108.6
C(2A)-C(1A)-H(1AB)	108.6
O(1A)-C(1A)-H(1AC)	108.6
C(2A)-C(1A)-H(1AC)	108.6
H(1AB)-C(1A)-H(1AC)	107.6
C(3A)-C(2A)-C(1A)	122.2(3)
C(3A)-C(2A)-C(7A)	124.2(3)
C(1A)-C(2A)-C(7A)	113.6(3)
C(2A)-C(3A)-C(4A)	125.7(3)
C(2A)-C(3A)-H(3AA)	117.1
C(4A)-C(3A)-H(3AA)	117.1
C(3A)-C(4A)-C(5A)	110.1(3)
C(3A)-C(4A)-H(4AA)	109.6
C(5A)-C(4A)-H(4AA)	109.6
C(3A)-C(4A)-H(4AB)	109.6
C(5A)-C(4A)-H(4AB)	109.6

Table E.3 (Continued)

H(4AA)-C(4A)-H(4AB)	108.2
O(2A)-C(5A)-C(4A)	107.6(2)
O(2A)-C(5A)-C(6A)	110.0(2)
C(4A)-C(5A)-C(6A)	113.2(2)
O(2A)-C(5A)-H(5AA)	108.6
C(4A)-C(5A)-H(5AA)	108.6
C(6A)-C(5A)-H(5AA)	108.6
C(5A)-C(6A)-Cl(2A)	111.4(2)
C(5A)-C(6A)-Cl(1A)	109.7(2)
Cl(2A)-C(6A)-Cl(1A)	109.95(17)
C(5A)-C(6A)-Cl(3A)	108.5(2)
Cl(2A)-C(6A)-Cl(3A)	109.47(17)
Cl(1A)-C(6A)-Cl(3A)	107.69(16)
C(2A)-C(7A)-H(7AA)	109.5
C(2A)-C(7A)-H(7AB)	109.5
H(7AA)-C(7A)-H(7AB)	109.5
C(2A)-C(7A)-H(7AC)	109.5
H(7AA)-C(7A)-H(7AC)	109.5
H(7AB)-C(7A)-H(7AC)	109.5
C(1B)-O(1B)-H(1B)	100.5
C(5B)-O(2B)-H(2BA)	109.3
O(1B)-C(1B)-C(2B)	115.5(3)
O(1B)-C(1B)-H(1BB)	108.4
C(2B)-C(1B)-H(1BB)	108.4
O(1B)-C(1B)-H(1BC)	108.4
C(2B)-C(1B)-H(1BC)	108.4
H(1BB)-C(1B)-H(1BC)	107.5
C(3B)-C(2B)-C(7B)	123.3(3)
C(3B)-C(2B)-C(1B)	123.0(3)
C(7B)-C(2B)-C(1B)	113.7(3)
C(2B)-C(3B)-C(4B)	123.8(3)

Table E.3 (Continued)

C(2B)-C(3B)-H(3BA)	118.1
C(4B)-C(3B)-H(3BA)	118.1
C(3B)-C(4B)-C(5B)	110.6(3)
C(3B)-C(4B)-H(4BA)	109.5
C(5B)-C(4B)-H(4BA)	109.5
C(3B)-C(4B)-H(4BB)	109.5
C(5B)-C(4B)-H(4BB)	109.5
H(4BA)-C(4B)-H(4BB)	108.1
O(2B)-C(5B)-C(4B)	108.1(2)
O(2B)-C(5B)-C(6B)	109.8(3)
C(4B)-C(5B)-C(6B)	112.9(3)
O(2B)-C(5B)-H(5BA)	108.7
C(4B)-C(5B)-H(5BA)	108.7
C(6B)-C(5B)-H(5BA)	108.7
C(5B)-C(6B)-Cl(2B)	111.8(2)
C(5B)-C(6B)-Cl(1B)	109.8(2)
Cl(2B)-C(6B)-Cl(1B)	109.02(18)
C(5B)-C(6B)-Cl(3B)	109.1(2)
Cl(2B)-C(6B)-Cl(3B)	108.99(18)
Cl(1B)-C(6B)-Cl(3B)	108.10(17)
C(2B)-C(7B)-H(7BA)	109.5
C(2B)-C(7B)-H(7BB)	109.5
H(7BA)-C(7B)-H(7BB)	109.5
C(2B)-C(7B)-H(7BC)	109.5
H(7BA)-C(7B)-H(7BC)	109.5
H(7BB)-C(7B)-H(7BC)	109.5

Symmetry transformations used to generate equivalent atoms:

Table E.4. Anisotropic displacement parameters ($\text{\AA}^2 \times 10^3$) for **4.23**. The anisotropic displacement factor exponent takes the form: $-2\pi^2 [h^2 a^{*2} U^{11} + \dots + 2 h k a^* b^* U^{12}]$

	U11	U22	U33	U23	U13	U12
Cl(1A)	36(1)	43(1)	25(1)	2(1)	-2(1)	-1(1)
Cl(2A)	28(1)	27(1)	40(1)	-6(1)	-7(1)	4(1)
Cl(3A)	30(1)	28(1)	35(1)	-1(1)	-7(1)	-3(1)
O(1A)	25(1)	32(1)	27(1)	1(1)	2(1)	2(1)
O(2A)	27(1)	31(1)	27(1)	2(1)	0(1)	-4(1)
C(1A)	21(1)	31(2)	35(2)	-3(1)	-1(1)	-4(1)
C(2A)	24(1)	26(1)	24(1)	0(1)	3(1)	1(1)
C(3A)	23(1)	28(1)	27(1)	2(1)	-1(1)	2(1)
C(4A)	22(1)	25(1)	29(1)	1(1)	-2(1)	-2(1)
C(5A)	24(1)	22(1)	25(1)	-1(1)	-5(1)	2(1)
C(6A)	25(1)	26(1)	24(1)	-2(1)	-3(1)	-5(1)
C(7A)	29(2)	35(2)	32(2)	2(1)	5(1)	-5(1)
Cl(1B)	43(1)	28(1)	40(1)	-9(1)	6(1)	-6(1)
Cl(2B)	31(1)	37(1)	68(1)	-9(1)	6(1)	7(1)
Cl(3B)	74(1)	43(1)	24(1)	-5(1)	6(1)	-5(1)
O(1B)	24(1)	29(1)	25(1)	0(1)	-1(1)	4(1)
O(2B)	34(1)	29(1)	23(1)	-4(1)	0(1)	-7(1)
C(1B)	28(2)	24(1)	30(2)	-1(1)	-2(1)	-1(1)
C(2B)	26(1)	22(1)	24(1)	3(1)	-2(1)	-1(1)
C(3B)	23(1)	24(1)	28(1)	-1(1)	1(1)	0(1)
C(4B)	30(2)	22(1)	29(2)	-5(1)	3(1)	2(1)
C(5B)	27(1)	22(1)	23(1)	-6(1)	2(1)	1(1)
C(6B)	33(2)	24(1)	28(2)	-7(1)	1(1)	-4(1)
C(7B)	31(2)	25(1)	31(2)	3(1)	6(1)	-2(1)

Table E.5. Hydrogen coordinates ($\times 10^4$) and isotropic displacement parameters ($\text{\AA}^2 \times 10^3$) for **4.23**.

	x	y	z	U(eq)
H(1AA)	11232	645	5023	34
H(2AA)	8849	250	3706	42
H(1AB)	12111	1151	3416	35
H(1AC)	11815	1611	4458	35
H(3AA)	10385	740	3687	31
H(4AA)	9931	1461	1739	30
H(4AB)	9577	1811	2847	30
H(5AA)	9453	301	2314	29
H(7AA)	10813	2275	2062	48
H(7AB)	11639	2038	1996	48
H(7AC)	11367	2537	3012	48
H(1B)	9500	3565	2429	39
H(2BA)	9481	6177	3562	42
H(1BB)	9275	2798	4207	33
H(1BC)	8746	2963	3176	33
H(3BA)	9366	4570	3785	30
H(4BA)	8574	4923	5729	32
H(4BB)	8144	5159	4615	32
H(5BA)	9591	5627	5065	29
H(7BA)	7970	3935	5507	44
H(7BB)	8352	3168	5637	44
H(7BC)	7792	3303	4632	44

VITA

Richard Jeffrey Duffy received his Bachelor of Science degrees in chemistry and botany from the University of Oklahoma at Norman in May 2001. He entered the chemistry program at Texas A&M University in September of 2001 and received his Doctor of Philosophy degree in December 2007. His research interests are focused on the development of methodologies that exploit small rings in synthesis and application of palladium catalyzed cross couplings to natural products.

Name: Richard Jeffrey Duffy

Address: University of Maryland

Department of Chemistry & Biochemistry

0107 Chemistry Building

College Park, MD 20742-4454